Integration of 3D Feedback Control Systems for Fabrication of Engineered Assemblies for Industrial Construction Projects

by

Mohammad Mahdi Sharif

A thesis
presented to the University of Waterloo
in fulfillment of the
thesis requirement for the degree of
Doctor of Philosophy
in
Civil Engineering

Waterloo, Ontario, Canada, 2022

Examining Committee

The following served on the Examining Committee for this thesis. The decision of the Examining Committee is by majority vote.

External Examiner	PINGBO TANG Associate Professor, Carnegie Mellon University
Supervisor	CARL HAAS Professor, Department Chair, University of Waterloo
Internal Member	SCOTT WALBRIDGE Professor, Director (ArchE), University of Waterloo
Internal Member	ARASH SHAHI Adjunct Professor, University of Waterloo
Internal External	WILLIAM MALEK Professor, University of Waterloo

AUTHOR'S DECLARATION

I hereby declare that I am the sole author of this thesis. This is a true copy of the thesis, including any required final revisions, as accepted by my examiners.

I understand that my thesis may be made electronically available to the public.

Abstract

A framework and methods are presented in this thesis to support integration of 3D feedback control systems to improve dimensional conformance during fabrication of engineered assemblies such as process piping, structural steel, vessels, tanks, and associated instrumentation for industrial construction projects. Fabrication includes processes such as cutting, bending, fitting, welding, and connecting. Companies specializing in these processes are known as fabricators, fabrication shops or fab shops. Typically, fab shops do not use 3D feedback control systems in their measurement and quality control processes. Instead, most measurements are done using manual tools such as tape measures, callipers, bubble levels, straight edges, squares, and templates. Inefficiency and errors ensue, costing the industry tens of billions of dollars per year globally. Improvement is impeded by a complex fabrication industry system dependent on deeply embedded existing processes, inflexible supply chains, and siloed information environments. The goal of this thesis is to address these impediments by developing and validating a new implementation framework including several specific methods.

To accomplish this goal, several research objectives must be met:

1. Determine if 3D dimensional control methods are possible for fab shops that do not have access to 3D models corresponding to shop drawings, thus serving as a step toward deploying more integrated, sophisticated and higher performing control systems.
2. Discover ways to solve incompatibility between requested information from fabrication workers and the output information delivered by state-of-the-art 3D inspection systems.
3. Conduct a credible cost-benefit analysis to understand the benefits required to justify the implementation costs, such as training, process change management, and capital expenditures for 3D data acquisition units for fab shops.
4. Investigate ways to compare quality and accuracy of dimensional control data sourced from modern point cloud processing methods, conventional surveying methods, and hand tools.

Methodologies used in this research include: (1) an initial literature review to understand the knowledge gaps coupled with informal interviews of practitioners from industrial research partners, which was revisited throughout the development of the dissertation, (2) development of a

conceptual framework for 3D fabrication control based on 3D imaging, (3) development and validation of algorithms to address key impediments to implementation of the framework, (4) experiments in the fab shop environment to validate elements of the framework, and (5) analysis to develop conclusions, identify weaknesses in the research, understand its contributions, and make recommendations.

By developing and testing the preceding framework, it was discovered that three stages of evolution are necessary for implementation. These stages are:

1. Utilization of 3D digital templates to enable simple scan-vs-3D-model workflows for shops without access to 3D design models.
2. Development of a new language and framework for dimensional control through current ways of thinking and communication of quality control information.
3. Redefining quality control processes based on state-of-the-art tools and technologies, including automated dimensional control systems.

With respect to the first stage, and to address the lack of access to 3D models, a framework for developing 3D digital template models was developed for inspecting received parts. The framework was used for developing a library of 600 3D models of piping parts. The library was leveraged to deploy a 3D quality control system that was then tested in an industrial-scale case study. The results of the case study were used to develop a discrete event simulation model. The simulation results from the model and subsequent cost-benefit analysis show that investment in integrating the scan-vs-3D-model quality control systems can have significant cost savings and provide a payback period of less than two years.

With respect to the second stage and to bridge the gap between what 3D inspection systems can offer and what is expected by the fabrication workers, the concept of Termination Points was further defined and a framework for measuring and classifying them was developed. The framework was used to developed applications and tools based on the provided set of definitions. Those applications and tools were further analyzed, and the results are reported in each chapter. It is concluded that the methods developed based on the framework can have sufficient accuracy and can add significant value for fabrication quality control.

The last stage in transitioning fabrication shops from manual and 2-dimensional processes to automated and advanced control processes is discussed in Chapter 8. Four main areas for improvement and advancements are identified. These areas include: (1) Collaboration through cloud technology, (2) Advanced control systems, (3) Measurement and comparison technologies, and (4) Improved visualization. Advanced Visualization tools are further explored as an example area for future development and advanced quality control of fabricated assemblies.

Acknowledgements

I would like to thank Stacey Jenson Rose, Scott Waters, and Chas Williams from Aecon Group for supporting this research by providing valuable industrial input, facilitating access to fabrication shops, and providing data that was used in this research.

This research was supported by NSERC and Mitacs, I would like to acknowledge and thank both of these institutions for their investment in our research group and the body of knowledge.

Here I have listed and provided a personal note to some of the most important people in my life, without whom I wouldn't have been able to finish my Ph.D.

To Professor Haas,

Phil Knight, the co-founder of Nike, writes in his memoir:

> "But it's not just the young people within the company who honour the history. I (Phil) think back to July 2005. In the middle of some event, I can't recall which, LeBron James asks for a private word.
>
> "Phil, can I see you a moment?"
>
> "Of course."
>
> "When I first signed with you," he says, "I didn't know all that much about the history of Nike. So I've been studying up."
>
> "Oh?"
>
> "You're the founder."
>
> "Well. Cofounder. Yes. It surprises a lot of people."
>
> "And Nike was born in 1972."
>
> "Well. Born—? Yes. I suppose."
>
> "Right. So I went to my jeweler and had them find a Rolex watch from 1972." He hands me the watch. It's engraved: **With thanks for taking a chance on me**."

I am not as successful as LeBron James, but I do want to thank you for taking a chance on me. With your guidance, I have been able to grow as a person as well as a member of the scientific community, for that, I thank you.

To my wife Fatemeh,

Thank you for supporting me throughout the past several years. Your company has allowed me to push myself and grow. I am happy to be co-authoring this amazing experience that is life with you, and I am looking forward to the rest of it.

To my parents,

The world can be disorienting at times. Your presence in my life has always allowed me to align myself with you and continue moving forward without getting overwhelmed. Thank you Dad, for always listening to me and passionately giving your perspective. Thank you Mom, for dedicating your entire life to our well-being and education.

To my friends and colleagues,

I would like to thank Ray Simonson, Rob Payne, Dan Liebster, Wilson Li, Vishvam Mazumdar, Hamed Shahrokhi, Ali Sarhadi, Steve Chuo, Caroline Kwiatek, Nicolas Jeanclos, Ekin Eray, Chris Rausch, and Mohammad Nahangi for all their support and input in this research.

To my committee,

I want to immensely thank you for your time to read and provide feedback on this research.

Dedication

I would like to dedicate this work to Mansour Esnaashari Esfahani and all perished passengers of Ukraine Flight 752. Many of the passengers were active members of the scientific community with great potential that will now never be realized.

Table of Contents

List of Figures

List of Tables

Chapter 1
Introduction

1.1 Problem Context

Globally, industrial infrastructure construction is a $1.6T per year industry that includes a variety of markets, such as construction of power plants, pharmaceutical facilities, shipbuilding, and defense-related structures [1]. To address budget and schedule overrun issues in these projects, many construction companies and asset owners are increasingly leveraging prefabrication and modularization. A study by FMI shows that prefabrication has been increasing at a compound annual growth rate of 12% in the past four years, and it is expected to continue its growth [2].

Prefabrication allows for more activities to be done in controlled fabrication shop environments and for optimization of workflows to reduce rework and increase efficiency [3,4]. The adoption of prefabrication and modularization have provided many benefits, such as higher product quality [5-8] and increased worker safety [9,10]. However, fabrication shops and fabrication workers are still struggling with high rework rates in performing their tasks. Reviewing the literature shows that documented rework can have a cost impact ranging from 5% to 10% of projects' costs [11-14]. A significant body of knowledge exists, which identifies the root causes of rework. In a study carried out by the Construction Industry Institute (CII), 359 projects were analyzed, and it was found that owner changes in the design that were not properly communicated to the contractors acted as the main driver of rework [15]. Other studies have found inadequate planning, poor communication of quality control data, low spatial cognition for design interpretation, and ineffective use of technology to be other major contributing factors in project rework [11,16,17]. Out of all root causes identified in the literature, geometric misalignment plays a significant role. In their recent research, Chuo et al. investigated more than 1000 Non-Compliance Reports (NCRs) on a prefabrication project and identified that more than half of the reported issues were related to incorrect geometry of components [18]. This is because, with increased prefabrication, workers are asked to build more complex assemblies with tighter tolerances, and the visualization, measurement and comparison tools that fabrication workers use have not changed over time. One reason for the lack of advanced measurement and comparison tools is the difficulty of implementing automated

measurement tools for projects with radically different geometric requirements (everything is custom made). For example, the partner fabrication shop in the research related to this thesis fabricates complex nuclear pipe assemblies with 2'' to 6'' diameter pipes that are 10 to 12 ft long. They also fabricate large volumetric modules, complex ring grinders, and other complex assemblies. The configuration of the equipment and workforce in this shop is always changing to accommodate each project's specific requirements. The other reason is the transition between 3D to 2D and back to 3D. In other words, designs are made in 3D that are then translated into 2D drawings with termination point information. These termination points have to be then identified by the fabrication workers in 3D and translated back to a 2D QC document. This back and forth causes workers to incur errors in design visualization, termination point identification, and information transcription. A more streamlined QC process can eliminate these errors.

With respect to measurement and comparison, currently, fabrication shops have two primary options: (1) utilization of manual hand measurement tools such as tape measures, calipers, bubble levels, squares, straight edges, and templates, or (2) utilization of advanced surveying grade equipment such as laser trackers and/or total stations. The utilization of manual measurement tools can be error-prone and highly complex, as explained in Chapters 5, 6 & 7. Moreover, the utilization of surveying grade equipment is too complex for a typical fabrication worker (fabrication workers are highly skilled in fitting and welding). As such, fabrication shops must hire expensive 3rd party surveying crews to perform tasks related to accurate measurement. As explained in Chapters 5 & 7, due to their cost and high turnaround time between data acquisition and the final report, surveying crews are seldom used, leaving fabrication shops with no option but the manual measurement tools for the majority of their measurement needs.

Three-dimensional (3D) image acquisition tools coupled with 3D design models can potentially offer a 3rd measurement approach for fabrication shops. These systems are palatable due to their high level of automation, sufficient accuracy, and superior visualization support. In order to perform an inspection after acquiring a 3D image (i.e. point cloud), two primary methods exist: (1) Scan-to-BIM and (2) Scan-vs-BIM. As explained in Chapter 2, Scan-to-BIM methods are primarily used to transform the raw 3D scan data into a semantically rich point cloud and then typically into a building information model (BIM) including objects defined by Industry Foundation Classes (IFCs) [19]. On the

other hand, Scan-vs-BIM methods and algorithms have been widely adopted by the industry and academia to perform various types of geometric inspections. Nahangi et al. used forward kinematics for dimensional variability quantification of complex assemblies, and Rausch et al. used 3D laser scanning and a digital twining approach for geometric inspection during fabrication and assembly in offsite construction environments [20,21].

Furthermore, the adoption of 3D inspection systems is becoming more feasible due to the decline in the capital cost of acquisition units (a laser scanner can be bought for as low as $25K in 2021). The decline in cost, increased automation in acquiring the data, and the increased geometric complexity of assemblies, have provided an unprecedented opportunity for development and implementation of 3D feedback control systems in fabrication shops as part of the fabrication workflow. The implementation of such systems has the potential to reduce the risk of geometric rework. While the benefits of the adoption of these systems are well documented, there is still little to no adoption by fabrication shops [18,20-23]. Understanding this paradox requires further understanding of the available technologies as well as existing requirements, processes, supply chains, and information environments within fabrication shops.

There are several barriers to the adoption of 3D feedback control systems for fabrication shops. The root cause of all these barriers lies in the fact that fabrication shops and fabrication workers have been working with 2D data for centuries. For example, currently, fabrication workers are provided design drawings in the format of printed line drawings that are distributed to the shop, even though the original design is done in a 3D CAD environment and there is proven productivity improvement by simply visualizing the 3D model [24]. Furthermore, as explained in Chapters 5 & 7, all required quality control reporting is still expected in a 2D format. Figure 1-1 shows an example document used by a fabrication worker to measure and validate the geometric compliance of a pressure vessel. As such, implementation and integration of 3D tools require frameworks, language, and tools that would allow all stakeholders, including fabrication workers, to transition from 2D data into 3D data capture and communication (Figure 1-4).

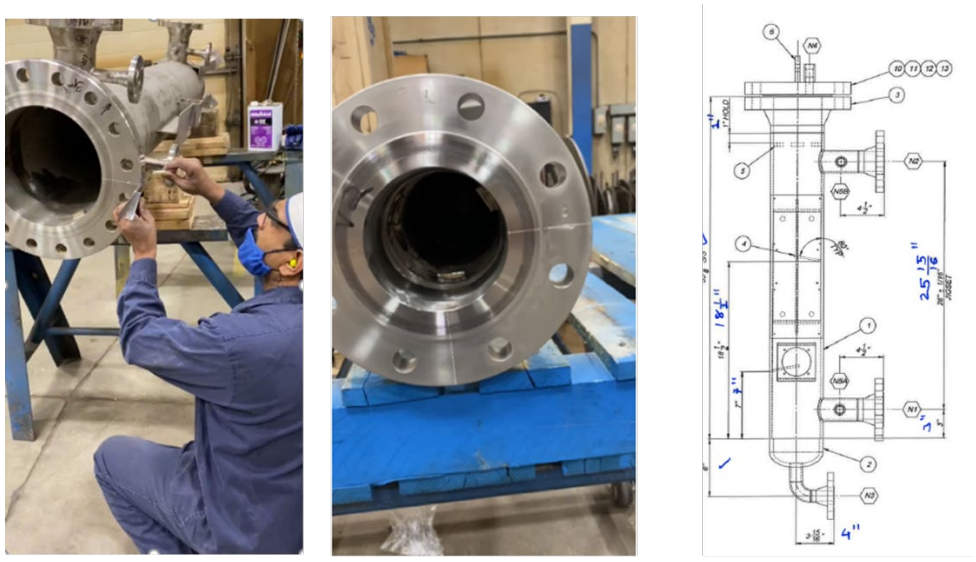

(a) (b) (c)

Figure 1-1. (a) Utilization of manual measurement tools. (b) Centerline is drawn onto the assembly using chalk and a calibrated caliper. (c) Manual transcription and communication of information on a paper drawing in a fabrication shop.

To enable this transition, this thesis defines three stages of evolution for fabrication shops, and experiments are conducted to validate the efficacy of this definition. In the first stage, primitive scan-vs-BIM workflows are enabled by developing a framework for the utilization of 3D digital templates. The developed workflow can be used for situations where fabrication shops are not provided with a 3D design model of their incoming parts. In the second stage, which constitutes the majority of the work done in this thesis, a new language and framework are developed to allow the derived 3D information to conform with existing 2D-based processes and requirements. Using the developed framework, an application and a physical tool are developed and tested at partners' fabrication shops. Finally, a third stage is envisioned where a complete paradigm shift allows fabrication shops to utilize automated dimensional control systems in potentially the most effective way.

1.2 Control Theory and 3D Feedback Control in Fabrication

In control theory, when dealing with a dynamic system, the goal of a controller is to develop models and algorithms governing the inputs in a way that a system's status is maintained closest to the desired state (the total system error is nearing zero). This is done in parallel with minimizing other system characteristics, such as delay, overshoot, and/or steady-state error.

To achieve the desired state, a controller monitors the difference between the controlled process variable (PV) and the set point (SP). By comparing PV and SP, the controller establishes an error signal. The error signal is used to generate feedback action.

A similar analogy can be made for building complex assemblies using Scan-vs-BIM for measurement and comparison. In this analogy, the desired state (SP) is determined by the BIM (building information model) or a 3D design model, and the process variable is determined using the 3D as-built data. The difference between SP and PV can be calculated using various methods and tools, such as general discrepancy analysis or using termination points (termination points are defined as the coordinate system points where assemblies connect or are constrained as described in Chapters 5,6,&7). Once the SP-PV is calculated, the data can be visualized by a fabrication worker for remedial actions, assuming an adequate visualization system exists. In this analogy, the human operator is still the controller but is assisted in determining and understanding SP-PV. Figure 1-2 (b) shows the integration of 3D feedback control loop systems in the fabrication workflows.

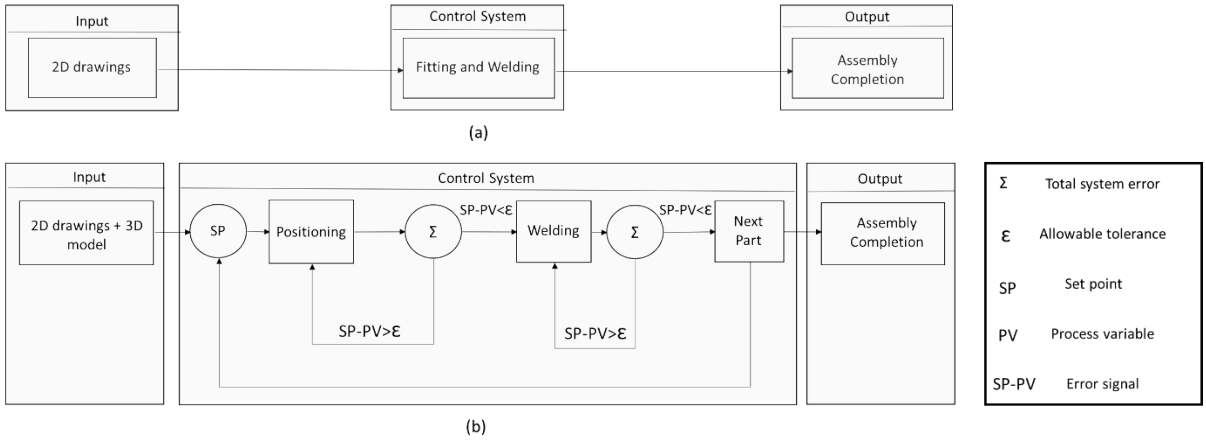

Figure 1-2. Different types of fabrication models. (a) The traditional model. (b) 3D feedback control enabled

1.3 Research Scope

The developed frameworks and algorithms in this research are generalized and can ultimately be applied and used for the fabrication of a variety of assembly types. However, this thesis mainly targets fabrication of industrial assemblies. Most important are piping assemblies, colloquially termed “pipe spools” in the industry. Piping accounts typically for 50% of the installed cost of many industrial plants. Thus, due to their cost impact and high complexity, piping assemblies are the main focus of experiments in this research.

Additionally, while three stages of evolution are defined, the majority of the focus of this thesis is on the first and second stages. New and novel frameworks are defined, and related experiments are carried out. The last stage has been discussed in Chapter 8; most of that discussion is conceptual with some preliminary work for improved visualization using Augmented Reality headsets.

1.4 Research Objectives

To accomplish the integration of 3D feedback control systems for fabrication of engineered assemblies for industrial construction projects, several research objectives must be met:

1. Determine if 3D dimensional control methods are possible for fab shops that do not have access to 3D models corresponding to shop drawings, thus serving as a step toward deploying more integrated, sophisticated and higher performing control systems.
2. Discover ways to solve incompatibility between requested information from fabrication workers and the output information delivered by state-of-the-art 3D inspection systems.
3. Conduct a credible cost-benefit analysis to understand the benefits required to justify the implementation costs, such as training, process change management, and capital expenditures for 3D data acquisition units for fab shops.
4. Investigate ways to compare quality and accuracy of dimensional control data sourced from modern point cloud processing methods, conventional surveying methods, and hand tools.

1.5 Research Methodology

Methodologies used in this research include (outlined in Figure 1-3):

(1) An initial literature review to understand the knowledge gaps coupled with informal interviews of practitioners from industrial research partners, and this was revisited throughout the development of the dissertation. In fact, more than 500 hours of onsite presence over the course of this research informed the state-of-the-art investigation. The literature review covered:
    a. Existing processes and workflows in fabrication shop environments,
    b. Recent trends in 3D modeling and data acquisition,
    c. Increased prefabrication in the industry,
    d. The advent of Digital Twins. Knowledge gaps were thereby identified

(2) Development of a conceptual framework for 3D fabrication control based on 3D imaging. The definition of termination point framework allows for the transition between existing quality control requirements in fabrication shops that are predicated on 2D transcription and acquisition of data into 3D feedback control systems.

(3) Development and validation of algorithms to address key impediments to implementation of the framework.

(4) Experiments in the fab shop environment to validate elements of the framework. Data acquisition in this research was primarily based on laser scanners, and some data collection was done via a SLAM (Simultaneous Localization and Mapping) scanner that is described in Chapter 7. Most of the findings of this research were tested and validated using fabrication data acquired at the partner's facility (Aecon Industrial Group).

(5) Analysis to develop conclusions, identify weaknesses in the research, understand its contributions, and make recommendations.

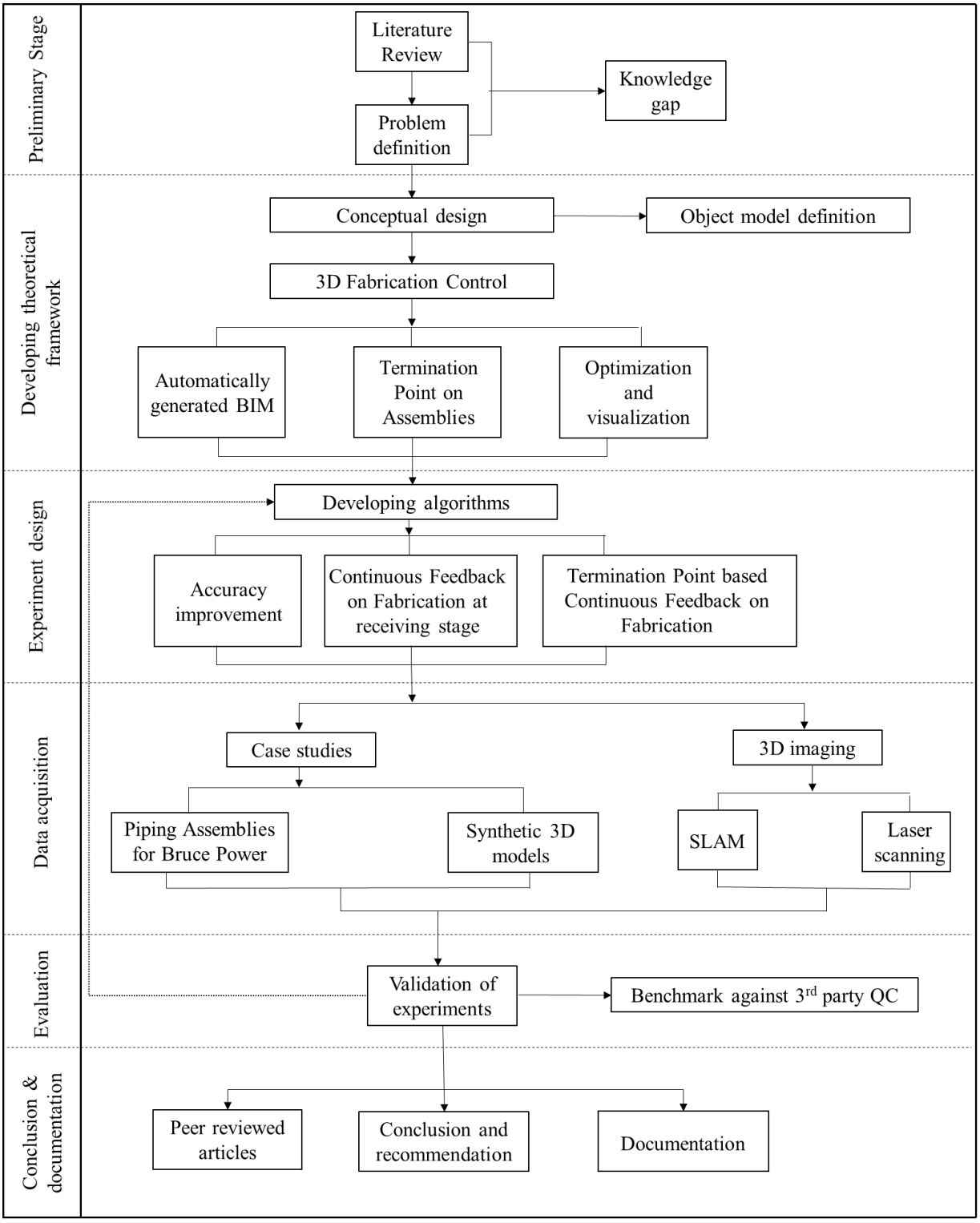

Figure 1-3. Research methodology of this thesis

1.6 Thesis Organization

As described earlier, this thesis offers a methodology for the implementation of 3D feedback control systems in fabrication shops. As such, Chapters in this thesis are organized based on their contribution in transitioning fabrication shops from fully 2D-based processes to fully 3D-based processes. Figure 1-4 summarizes the organization of chapters and their relationship with the defined evolution stages.

Chapters 1 and 2 focus on defining the problem, context, and existing tools and processes. Chapter 3 investigates an approach that can enable fabrication shops to take advantage of 3D data, even if they do not have a 3D model. Chapter 4 describes two case studies where implementing simple scan-vs-BIM analysis provided significant value to the fabricator and the project owner. Chapter 5 looks at how and why existing 3D data workflows are inconsistent with how quality control is done today. A new conceptual framework is developed to address the gap between existing QC requirements and the data provided by 3D acquisition units. Using the defined framework, a physical fixture was designed and manufactured for the detection of termination points that is described in Chapter 6. Chapter 7 then builds a Scan-vs-BIM approach that leverages the developed framework in Chapter 5. Chapter 8 explores the new possibilities enabled by a complete paradigm shift in measurement and control processes. Future research opportunities and a summary of the thesis are then described in the last Chapter.

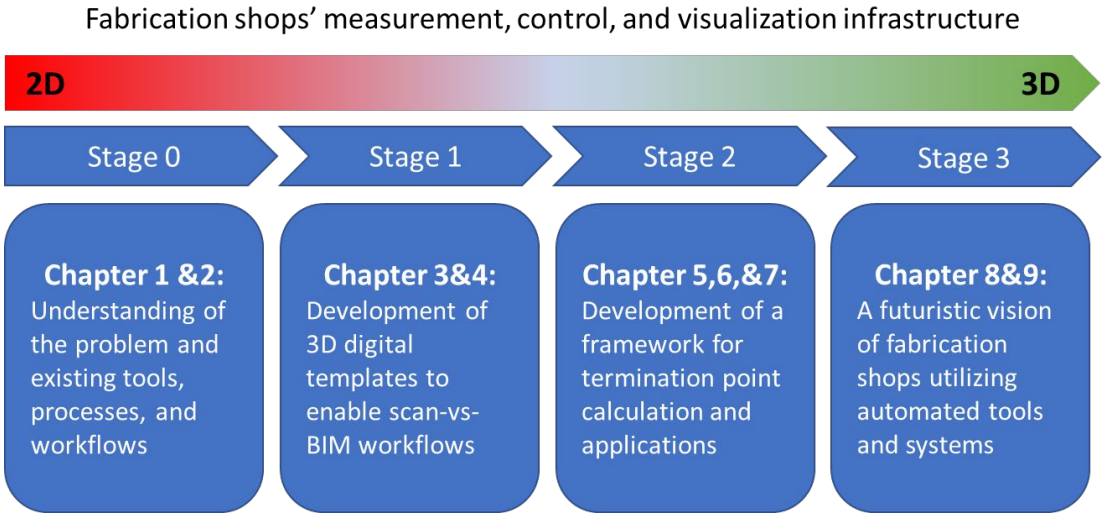

Figure 1-4. Summary of thesis organization

Chapter 2
Literature Review and Background

This chapter is broken into two major sections. Initially, a detailed literature review is carried out. The review covers the state-of-the-art in the industrial fabrication sector, increased prefabrication in the industry, existing processes and workflows in fabrication shop environments, recent trends in 3D modeling and data acquisition, and the advent of Digital Twins.

The second part of this chapter provides background information regarding an application software that was prototyped as part of a larger research initiative. The components of the application are explained, and existing research carried out using the prototype is reviewed. Finally, considering the shortcomings of the application software along with literature review and provided background information, the knowledge gap that motivated this research is explained.

2.1 Modular fabrication in industrial construction

The dream of industrially produced homes, buildings, and industrial facilities has inspired architects and engineers for a long time. This desire was first reflected in Buckminster Fuller's Dymaxion house. The Dymaxion House was developed to address several perceived shortcomings with existing homebuilding techniques. All designed components were factory manufactured kits assembled onsite, intended to be suitable for any site or environment and to use resources efficiently. A key design consideration was the ease of shipment and assembly. This was the first step towards modularization [25,26].

For decades, researchers have investigated the merits of utilizing modular and off-site construction. These benefits include shorter project schedule, lower costs, and increased safety [7,27-29]. Modular construction allows for a greater proportion of the construction to be moved from the construction site to controlled environments. With the shift towards modularization, managing the geometric variabilities of the fabricated components has become a more critical task in these projects [30]. This is because the traditional "custom-cut and fit at the job site" approach used in stick-built construction will no longer be effective [31].

While the production processes in modular construction have seen significant progress, the risk management strategies for controlling tolerances have remained manual (using shim plates, cut-off lengths, and trimming) and error-prone [31-33]. Furthermore, the cumulation of deviations from design can eventually become problematic in the erection phase of these projects [6]. The refurbishment project at Ontario Power Generation and Bruce Power's nuclear reactor core are examples where utilization of cut-lengths has substantially increased the cost in the erection phase of refurbishment projects.

Implementation of systematic tolerance checking mechanisms is more complicated in modular and prefabricated construction projects compared to manufacturing [34,35]. This is due to the custom-made nature of construction projects. Many researchers have looked at the design phase of these modular projects for addressing tolerance management [31,36,37]. Rausch et al. have investigated improving the design through DVA (Dimensional Variation Analysis); the approach is based on kinematics theory in robotics. Shahtaheri et al. have investigated a framework for the optimal design of dimensional and geometric variability using comprehensive tolerance strategies by jointly minimizing both fabrication costs and project risks. In addition to design requirements, Rausch et al. have proposed a framework for optimally planning the order and arrangement of components in order to optimize the assembly plan [38]. The developed method is applied to components with similar design geometry and different as-builts. As such, the proposed framework cannot be applied to custom-made components such as pipe spools.

2.2 Pipe fabrication

A segment to which prefabrication is being explored is pipe fabrication. Pipe spools are components of larger piping networks intended to carry water, steam, fluids, chemical gases, or fuel for industrial processes. Pipe spools are normally made in fabrication facilities or fabrication shops, away from the construction site in a process that involves cutting, bending, forming, and fitting individual piping components and finally welding them together. After conducting the final quality check on the pipe spools, they will then be shipped to the site [39].

Typically, 30% to 50% of the industrial construction work involves pipe spool fabrication [40]. Each piping component is part of a larger assembly. A module consists of several assemblies which will be welded or bolted together at specific coordinates dictated by design. Tight tolerances are usually

stipulated to ensure that each pipe will fit within an assembly and assemblies meet each other at the designed location in modules. Developing automated and systematic control mechanisms is difficult in the pipe spool fabrication industry due to complicated design and complex geometry [36].

2.3 3D BIM

Building Information Models (BIM) are digital representations of facilities and structures that include information about the asset's life cycle. Available information in a BIM can include 3D design information, project schedule, material, costs, and safety specifications. With increased computation power, the utilization of these models has become prevalent. The prevalence of BIM is a critical enabler of the research proposed in this thesis. Researchers have shown that the utilization of BIM on construction projects can increase productivity up to 30% while reducing the request for information and change orders by a factor of 10 [41]. In addition to improved productivity, BIMs are great visualization tools to improve design communication between different project stakeholders [42]. Steven et al. have used BIMs in VR (Virtual Reality) environments for improved project delivery in AEC (Architectural, Engineering and Construction) projects [43]. Park et al. have used Augmented Reality in conjunction with BIMs for defect management [44]. In the context of fabrication and dimensional control, utilization of BIM is divided into two major applications, which are discussed hereinafter.

2.4 Dimensional Quality Assurance Without a Design Model (Scan-to-BIM)

When an existing model is not available, feature detection algorithms are often used to extract or identify parametric shapes, surfaces, and curvature-based features in a point cloud; these methods are often categorized under "scan-to-BIM." For instance, Ahmed et al. [45] used a Hough Transform on cross-sectional slices of pipe assemblies to extract pipe radii of known sizes. A major shortcoming of the method described by Ahmed is that it assumes the orientation of the pipe spools is parallel or perpendicular to the scanner's Z-axis. Son et al. [46] used curvature feature extraction from local surface patches at known locations prescribed on piping and instrumentation diagrams (P&IDs) and subsequently fit non-uniform rational basis spline (NURBS) geometry to generate pipe spool model elements. Wang et al. [47] used Density-Based Spatial Clustering of Applications with Noise (DBScan) to help generate complete pipe spool assembly models from 3D point clouds. While these

algorithms may rely on a set of pre-existing parametric objects (oftentimes of set sizes) to fit to a segmented point cloud, other methods have also been developed which reconstruct model elements using more granular geometric techniques to minimize discrepancies with the as-built conditions. For instance, Dimitrov et al. [48] developed a generalizable technique that fits NURBS geometry to constructed elements which do not need to conform to strict parametric assumptions (e.g., a pipe must be perfectly straight). The significance of techniques like this avoids the errors accrued by trying to best-fit straight pipe elements to as-built features which may have non-negligible deformation, such as from welding distortion. However, the downside of these approaches is that inferring discrete errors between as-built and as-designed states is still not obvious, and relies on tedious, timely analyses. Across existing scan-to-BIM methods for pipe spool fabrication, perhaps the most useful (and recent) technique has been developed by Maalek et al. [49] Their method extracts the center and orientation of key pipe flanges on assemblies using algorithms such as the Pratt's circle fitting algorithm and the squared Mahalanobis distance computation. While the most conducive to industrial fabrication DQA (Dimensional Quality Assurance), this method still requires a subsequent comparison of as-built features (i.e., flange centers and plane orientations) with as-designed information, which can be tedious and time-consuming. Additionally, many commercially available software packages rely on human operators to manually find objects and then semi-automatically best-fit parametric objects into point clouds. In their recent work, Essnashary et al.[50] have investigated fundamental imprecisions when manual processes are used for scan-to-BIM methods.

2.5 Dimensional Quality Assurance with a Design Model (Scan-vs-BIM)

While notable works have emerged to help conduct DQA (Dimensional Quality Assurance), when an existing model is not available or developed to a suitable level of detail, far more suitable methods have been developed for directly comparing 3D point clouds with existing as-designed models (i.e., “scan-vs-BIM”). Not only does this approach circumvent extensive subsequent evaluations to understand and abstract information for DQA, but these processes do not strictly require a semantically rich BIM for engendering full automation. Often, a “semantically sparse” CAD model (e.g., stereolithography format) is suitable, as is posited later in Chapter 7 of this thesis. Upon surveying existing methods for DQA within scan-vs-BIM, there are three distinct sub-categories: (1)

direct dataset comparisons, (2) extracted feature-based comparisons, and (3) analytical system comparisons.

2.5.1 Direct dataset comparisons

The most basic yet perhaps pervasive scan-vs-BIM method is directly overlaying a scan on a model and depicting deviations using a heat-map. This method can be used to visualize overall Euclidean distance-based deviations between an as-built and as-designed state. However, the challenge of using this method for DQA (Dimensional Quality Assurance) in industrial fabrication is that not all deviations can be directly inferred by Euclidean distances, and the best overlay fit is subject to underlying premises, such as whether anchor points and surfaces should be used. For instance, if a pipe is shifted along its principal axis, deviations may not be appropriately displayed (in contrast to a case where a pipe is rotated about that same axis, whereby a linear propagation in a heat-map would be displayed). Given the limitations of direct heat-map comparison, researchers have adopted more advanced methods such as the use of random sample consensus (RANSAC) to extract pipe segments and perform deviation analysis using orientation comparisons of pipes [51].

2.5.2 Extracted feature-based comparisons

Since direct dataset comparisons do not capture all of the types of discrepancies that can exist for industrial fabrication, researchers have used extracted feature-based comparisons for improved DQA. The most basic form of this involves extracting the centerline of cylindrical objects such as pipes, pressure vessels, and tanks (including start and end nodes) and comparing this data with similar features from an as-designed model. Since the model does not need to be semantically rich, this method is efficient and robust. In their work, Guo et al. [8] use this form of centerline comparison after extracting straight pipe segments in MEP modules. While their method achieves a suitable accuracy (3.78 mm), it cannot be directly used for more complex assemblies which have various angles and joints. This is where other techniques such as comparing skeleton networks as posited by Nahangi et al. [52] may be more suitable. In this method, the point cloud is converted into a skeletal model by extracting cross-sections of objects and fitting lines through the center of each cross-section. An input BIM is also used to instantiate the skeletal candidates (i.e., radius of pipe at key locations) and to infer the deviation of the as-built status to the design intent. This is then carried out for an entire pipe assembly. In general, the use of extracted feature-based

comparison may be useful for understanding potential realignment measures, these methods involve more computation than strictly required for an initial DQA assessment of termination points on pipe spool assemblies. Furthermore, occlusions introduced during acquisition of point cloud data lead to challenges when generating centerlines through an assembly.

2.5.3 Analytical system comparison

A final way to utilize an as-designed model for DQA in industrial fabrication is the use of advanced analytical system comparisons. Such techniques are related to extracted features yet assume or represent assemblies as analogous analytical systems. In their work, Nahangi et al. [53] use the analogy of kinematic chains to identify errors and posit realignment measures. First, forward kinematics is used to compute the discrepancy between as-built and as-planned pipe spool segments. Such computation relies on the assumption that pipes can be modelled and behave similar to joints in robotics systems (i.e., rotations and translations about joints). This method, while powerful for potentially providing near real-time feedback on how to correct defective assemblies, relies on having sufficient point cloud coverage of pipe spools. Furthermore, the results of this method are not conducive for quick termination point (we earlier defined termination points as the coordinate system points where assemblies connect or are constrained) checking (i.e., center points and alignment of pipe flanges). Other analytical systems comparisons have involved the use of graph theory to abstract and track the accumulation of error in pipes. This technique, as outlined by Kalasapudi et al. [54], requires establishing a comprehensive tolerance network associated with each pipe element and subsequently quantifying and comparing the errors of each associated pipe element. In summary, while several innovative techniques can be used to abstract errors in pipe spool assemblies, oftentimes, these approaches are far too comprehensive to adopt for DQA practices that can be integrated as part of the fabrication process of critical assemblies. Due to their sophistication, these approaches end up being too complicated to use and navigate for an ordinary fabrication worker, rendering them impractical to use in the fabrication shops workflows. In summary, existing methods for DQA of industrial assemblies are presented in Figure 2-1.

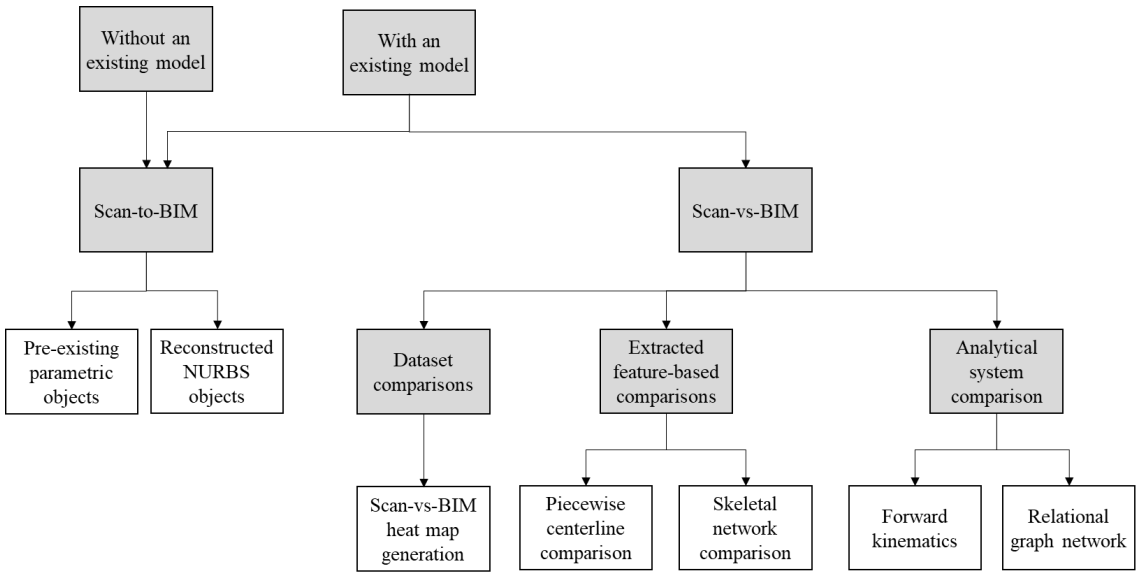

Figure 2-1. Overview of existing methods for dimensional quality assurance for prefabricated industrial assemblies using 3D point cloud data.

2.6 Digital Twin

The need for developing 3D-scanning measurement systems is further accelerated by the adoption of Digital Twins in the industry. From [55] :

> "A Digital Twin (DT) can be defined as a digital replica of a real-world asset. This asset can be a building, a tunnel, a bridge, or any other man-made asset of the built environment. A DT differs from traditional computer-aided design (CAD) and is not merely an Internet of Things (IoT) solution. It is based on massive, cumulative, real-time, real-world data measurements in multiple dimensions and uses information of a digital model across the entire life cycle of an infrastructure."

Implementation of 3D-scanning measurement systems would allow the fabrication shops to participate and contribute to the life cycle of a Digital Twin. The updated 3D design model is utilized in the measurement process, and the measurement and the information on the as-built assemblies are captured and reflected as an attribute in the Digital Twin. In their recent work, Rausch et al. have demonstrated an approach for automatic geometric digital twinning using laser scanned data [56].

Other researchers have been looking at enriching the digital twin with visual data capture, various analysis and reporting [57].

2.7 Prototyped Software Application for Dimensional Quality Assurance (named SfM)

Four years of research and development were conducted (2016-2020) to write a software application facilitating a continuous feedback control system named "SfM." The goal in developing SfM was to increase the control over the geometric compliance of the as-built state of an assembly and to create a guidance mechanism for the fabrication workers by employing 3D imaging and augmented reality tools in a preventative way that avoids rework and improves assembly efficiency. Beyond detecting and preventing further design misinterpretations during fabrication or assembly, the goal was to offer an effective and efficient alignment feedback control loop for direct work. These feedback loops, while adding time up-front, resulted in significant time and cost savings.

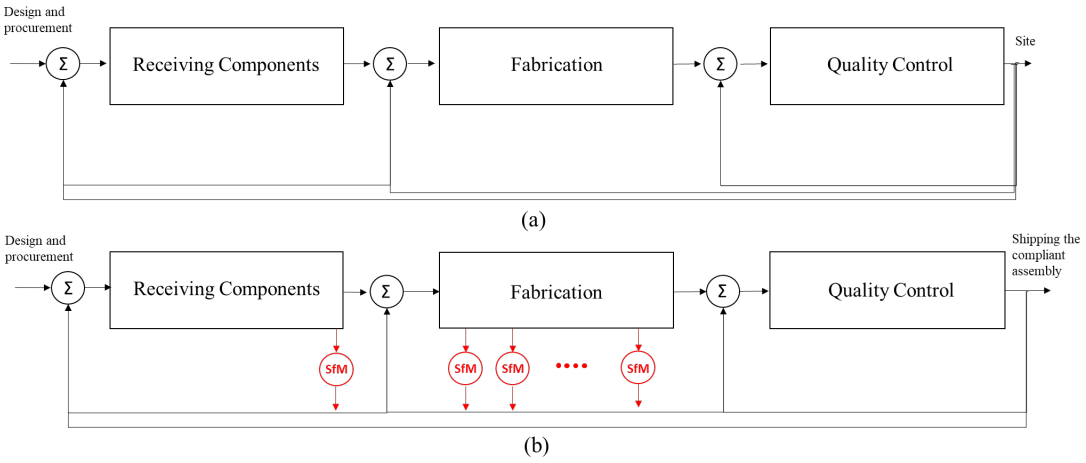

Figure 2-2. (a) Current fabrication model. (b) Proposed fabrication model with 3D feedback loops.

The research objective was broken down into 4 sub-objectives. The objectives were developed and fulfilled to obtain a functional prototype software. Each sub-objective is discussed; the results of the preliminary deployment of the system are then investigated and reported.

The first of these objectives was to develop a systematic tolerance checking and correction planning method. One effective way to control rework during pipe spool installation in modules is with the

control and checking of tolerances. Rework in industrial fabrication is extensively dependent on ease of assembly and erection alignment processes. Industrial modules are prone to allowable distortion and deviation tolerances during fabrication, assembly, and transportation; however, the accumulation of such tolerances should be controlled systematically, and corrective plans are required in a timely manner.

The work done was heavily focused on developing a software application for step-by-step fabrication and checking of industrial assemblies (to facilitate the continuous feedback control model). The developed software can partition the design files (BIM) associated with an assembly, allowing a fitter or welder to verify that each component has been fabricated and installed correctly. By allowing a craft worker to partition the model into smaller models that can be grown by adding the next piece to be installed, the software gives the craft worker greater ability to plan the work being undertaken and provides a visual 3D model that can be manipulated to reaffirm the planned work sequence.

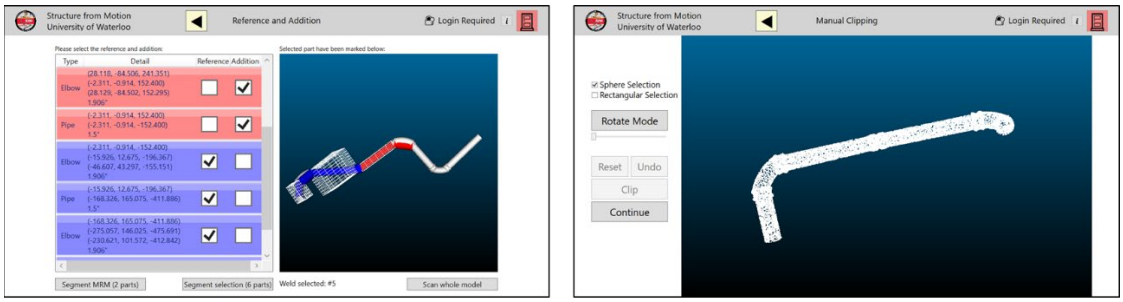

(a) (b)

Figure 2-3. Part segmentation for assembly planning and control. (a) Referenced components are coloured in blue, and components to be added are coloured in red. (b) Segmented model point cloud automatically generated.

The second sub-objective was to develop real-time fitting strategies. Once two assemblies are being erected and placed together, real-time feedback of the assemblies' plumbness and conformance facilitates the fitting process. A real-time fitting strategy algorithm and workflow were designed and implemented. The algorithm compares the scanned data with the designed BIM model. The algorithm would then overlay in a best-fit way the obtained as-built point cloud onto the as-designed model in 3D, in a rotatable 3D rendering, augmenting workers' visualization to detect discrepancies (and planning rectification actions, if necessary) [58].

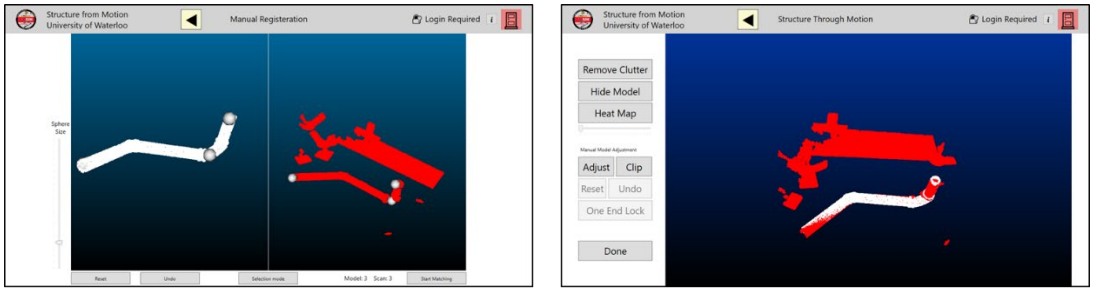

(a) (b)

Figure 2-4. Developed algorithm to overlay the model point cloud on the as-built point cloud. (a) Three approximately corresponding points are selected by the user. (b) the model point cloud overlaid in a best-fit on the scan point cloud.

The third sub-objective that was worked on was to develop metrics for evaluating the quality of corrective actions, realignment, plumbing, and fitting strategies. The strategy developed to evaluate the as-built assembly for correctness involves using a 3D scanner to acquire the 3D geometric data for the built assembly and overlay it on the 3D model for the design. The as-built scan has been colourized to show the deviations between points on the scan and points on the model (Figure **2**-**5**). This is referred to as a heat map. The colours used in the heat map are on a spectrum from green, showing compliant assembly parts, to red, indicating non-compliant assembly parts and/or locations.

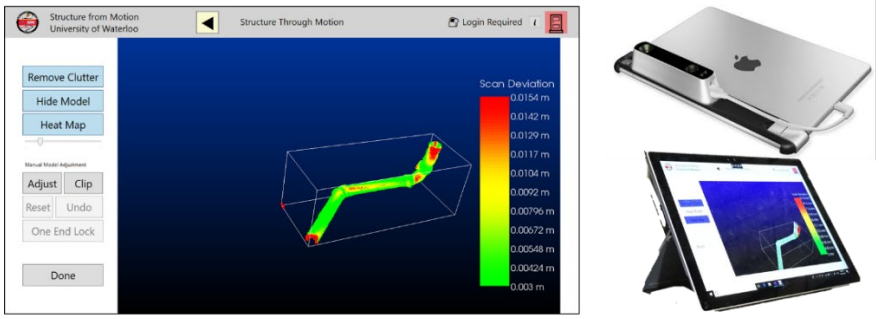

(a) (b)

Figure 2-5. Calculating the discrepancy between the model point cloud and as-built point cloud. (a) Visualizing the discrepancy between the as-built and design. (b) the current prototype uses a SLAM-based sensor connected to a windows-based computing station.

To overlay the scan point cloud over the model point cloud, an investigation was completed to develop an object finding algorithm that would retrieve the object of interest in the scan from the model [59].

The fourth and final sub-objective outlined as part of the research project was to measure expected resulting rework reduction and productivity improvement**.** Controlled experiments were conducted to compare typical fabrication work packages based on the metrics defined in the previous objective, with and without the developed prototype software.

To evaluate the impact of the software, an experiment was conducted where participants assembled a PVC pipe assembly using the developed software, and their productivity was compared against participants completing the same assembly using a two-sided isometric drawing (paper-based). This experiment was run on both engineering students (40 participants) and on welders and pipefitters (21 participants) to see how experience with creating pipe assemblies will affect the participants' productivity. Significant productivity improvement and rework reduction was recorded. The results of this study were then published [22].

(a) (b) (c)

Figure 2-6. Experiment setup. (a) The first used conventional tools to build the assembly. (b) The second group used conventional tools in addition to SfM. (c) An experienced pipe fitter using manual hand tools to assemble the designed pipe spool

The results of the carried-out experiment were then used as a basis to build a simulation model to investigate the economic and workflow impact of the implementation of such a system [18]. The investigation was based on various project types with varying levels of geometric complexities. In all cases, it was shown that investment in the implementation of such a system can have a payback period of less than a year.

2.8 Knowledge gap

Fabrication shops do not use 3D feedback control systems in their measurement and quality control processes. This is despite clearly demonstratable benefits of the adoption of 3D control feedback systems. After extensive review of the academic literature, as well as investigation of available commercial products at the disposal of fabricators, it is evident that existing measurement technologies, methods, and frameworks have the following limitations, which this thesis aims to address:

- All current scan-vs-BIM methods are rendered impractical, if fabrication shops cannot access the original 3D design models (as is often the case). Also, utilization of existing scan-to-BIM approaches is too time-consuming and complicated as a feedforward solution to this problem. There is no known solution to scan-vs-BIM, when the BIM is unavailable.
- There is a fundamental difference in how the design-vs-as-built discrepancy is reported today in fabrication shops and how it is communicated in existing and prototype scan-vs-BIM methods. This difference creates confusion on the shop floor, challenges in modifying processes, and emotional resistance to potentially positive change. All scan-vs-BIM analysis results need to be communicated in a way that is consistent with the existing requirement, supply chains, and information environments. The solution to this problem is not known.
- There is no known method for expressing current scan-vs-BIM accuracy and data quality results for pipe spools, modules and related assemblies in a way that is consistent with current measures of accuracy, which are the language of the shop floor and the construction site
- No models exist for managing change and bridging the paradigms gap from current fabrication dimensional quality control processes in industrial construction and fabrication to potentially better performing (in terms of productivity and risk reduction) processes relying on 3D imaging and models.

The remaining chapter of this thesis attempt to address these knowledge gaps.

Chapter 3
Rapid 3D Feedback Quality Control in Prefabrication Using a 3D Digital Templates Framework

3.1 Chapter Summary and Contribution Statement

This Chapter includes a method and a framework for building a library of 3D design models (i.e. Digital Templates). The 3D generated templates can be used to use scan-vs-3D-model at the receiving stage in fabrication shops. The built framework is in the first stage of the fabrication evolution as defined in Chapter 1, and it addresses the first knowledge gap identified in the previous chapter.

This chapter is based on the work submitted to the journal of Construction Engineering and Management on August 14, 2021, with the same title. The article was revised and resubmitted on January 15th, 2022 based on received reviews from the journal on December 7th, 2021. Minor changes are made to some parts of the article to be more consistent with the body of the thesis. Thus, the content of this chapter is not exactly the same as the paper.

In this Chapter, I have written the manuscript and performed the analysis. Steve Chuo has assisted with editing the manuscript for clarity as well as helping in building the simulation model. Dr. Haas reviewed the manuscript and has provided editorial input to the manuscript in this Chapter.

3.2 Abstract

With increased prefabrication in the construction industry, fabrication workers are tasked to assemble more complicated assemblies with tighter tolerances. However, the existing measurement tools and processes have not changed to accommodate this shift. Lack of advanced measurement tools and existing processes results in increased risk of late detection of geometric errors. To reduce these risks, 3D quality control systems leveraging scan-vs-BIM methods can be adopted as part of the fabrication process. However, these systems have not been widely adopted yet by fabrication shops, because: (1) fabrication shops often do not have 3D models corresponding to shop drawings, and (2) the cost of integrating accurate 3D scanning equipment into fabrication workflows is assumed to be too high. To remove the first barrier, in this article, a framework for developing 3D

digital templates is developed for inspecting received parts. The framework is used for developing a library of 600 3D-models of piping parts. The library is leveraged to deploy a 3D quality control system that was then tested in an industrial scale case study. The results of the case study are used to develop a discrete event simulation model. The simulation results from the model and subsequent cost benefit analysis show that investment in integrating the scan-vs-3D-model quality control systems can have significant cost savings and provide a payback period of less than two years.

3.3 Introduction

Construction labor productivity has increased by less than 10% in Canada since 1997, while productivity in the manufacturing industry improved by almost 50% in the same period [60]. Though both industries produce goods, their production methods are divergent: traditional construction projects are unique, craft-based, and typically done on-site, while manufacturing can mass-produce standardized products on automated assembly lines in a controlled environment off-site. Inspired by manufacturing's labor productivity growth, and to increase control and allow for automation, use of prefabrication methods is increasing in the construction industry. In fact, the global modular and prefabricated building market accounted for US$ 149.7 billion in 2019 according to one study [2]. Furthermore, the same study has anticipated the modular and prefabrication market will register a Compound Annual Growth Rate (CAGR) of 6.8% over the next decade, making the industry worth US$ 287.2 billion by 2029. Rework reduction and improved productivity are well documented improvements related to adoption of prefabrication and modularization [4,61-67]. These improvements have helped projects to reach their schedule and budget targets [68]. However, in general, reported rework still accounts for 6% to 12% of the cost of a typical construction project [69,70].

The lack of an integrated 3D quality control system for detection and verification of geometric compliance of assemblies has resulted in fabrication shops relying on highly skilled craftsman using hand measurement tools during the fabrication process, and implementation of quality control personnel for inspection after fabrication. The existing measurement method results in project risks (rework events) by: (1) relying on error-prone measurement tools, and (2) leaving the detection of errors to the end of the fabrication process; even if they are detected, these errors can still have a

significant impact on the project schedule and budget. Researchers have proposed scan-vs-BIM frameworks to be integrated as part of the fabrication process for accurate and rapid feedback on the geometric conditions of assemblies. Existing frameworks rely on the designed 3D model as an input parameter. However, many fabrication shops do not have or receive 3D models corresponding to the assemblies that they are building or receiving, rendering existing scan-vs-BIM approaches impractical to implement. Furthermore, the perceived high cost of purchasing and integrating 3D scan-vs-BIM solutions also remains a barrier for fabrication shops to decide on refining and changing their existing measurement processes.

3.3.1 Measurement Risks using Existing Tools

Currently, two methods are commonly used to verify the geometry of assemblies in fabrication shops. The first method uses an optical instrument as a discrete-point-based acquisition unit (e.g., a "total station" and a laser tracker). Total stations can read slope and distances from the instrument to a point (target or reflector). Total stations can measure the distance to a point on an object that is reasonably light in color, up to a few hundreds of meters away without a reflector. A high-quality total station is typically claimed by its maker to be able to measure distances with an accuracy of about 1.5 millimeters over a distance of 1,500 meters [71].

Overall, the acquisition process with a total station is highly complex and has manual elements that make it prone to errors, and it has a high turnaround time to process the data. As such, these tools are rarely used in fabrication shops, since highly experienced surveying crews are needed to operate this equipment, which would increase costs and can delay the fabrication schedule.

The second most commonly used method in fabrication shops and by fabrication workers, is the use of manual hand measurement tools. To complete a manual measurement, a kit of measuring tools is typically required, such as levels, squares, rulers, offset jigs, and tape measures. Lack of automation and dependence on human craftsmanship in using manual tools is the root cause of many measurement errors. Furthermore, utilization of manual tools can be complex, even for deceptively simple objects. For example, elbows are assumed to be simple objects. However, elbow manufacturing processes, including the Mandrel method, the Extrusion method, the UO method, and the Hot Forming method can each introduce a specific type of error on any given pipe elbow

[72]. To verify the curvature on a large diameter pipe elbow that has been received by a fabrication shop from a third-party supplier, four workers are required (this is highly inefficient). The process starts with operating the crane and adjusting the pipe stands until both sides of the bend are leveled. Once the elbow is leveled, a bubble level is then used to find the centerlines on the two ends of the bend. Points A and B can then be determined by the tangent of the elbow's cross section and the drawn center line (Figure 3-1-(a)). Once the centerlines are drawn, two workers are tasked to each hold a square such that one face is laying on the centerline and perpendicular to the face and the other face of the square flush to the end surface of the bend. The goal is to find the intersecting lines between the on a manually maintained level plane centerlines in 3D space, point O in Figure 3-1. Once the intersecting point is determined, the distance between the intersection and the center of each face is verified against the design (L_1 and L_2 are verified).

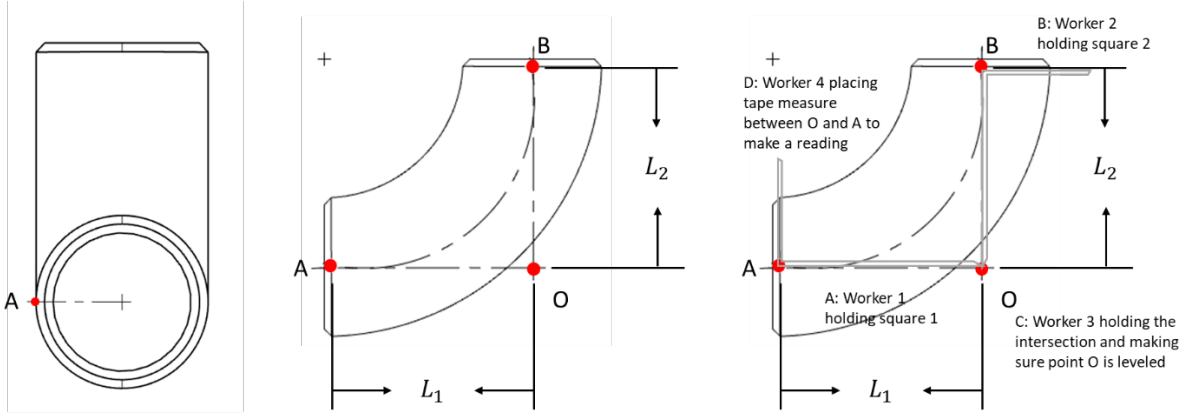

Figure 3-1. An example elbow and its critical dimensions for checking curvature.

3.3.2 Scan-vs-3D-Model

Deployment of scan-vs-3D-model methods potentially offers solutions to the problems described in the previous section. These methods are most commonly referred to as scan-vs-BIM in the literature. However, in this study they are referred to as scan-vs-3D-model since only the geometric characteristics of the model are of interest. Superimposing point clouds of as-built assemblies onto their 3D design model can provide valuable information with respect to geometric quality.

While there are several advantages in using scan-vs-3D-model methods, and they may present a preferable long-term solution, fabrication shops have been slow to adopt them. The slow adoption rate can be attributed to challenges identified earlier in this paper: (1) fabrication shops often do not have 3D models corresponding to shop drawings, and (2) the cost of integrating accurate 3D scanning equipment into fabrication workflows is assumed to be too high. Existing scan-vs-3D-model methods and frameworks in the literature require the 3D model as input data for quality control and analysis. Unfortunately, fabrication shops are often not provided with the 3D model, which precludes them from leveraging scan-vs-3D-model methods. To understand the main reason why fabrication shops do not have 3D models, it is important to first understand the difference between isometric drawings and cutsheets (shop drawings).

Isometric drawings are not-to-scale symbolic line drawings that use isometric projection to represent the three-dimensional shape of an assembly (i.e. a pipe spool) on a two-dimensional surface. Used in the context of industrial prefabrication and assembly, an “isometric” refers to the drawing itself, and not just the method of representation. Isometric drawings are used in the module assembly yard or the project site to assemble subassemblies into larger sections.

Cutsheets are similar to isometrics in that they, too, are not-to-scale symbolic line drawings that use isometric projection to represent the three-dimensional shape of an assembly on a two-dimensional drawing. However, cutsheets provide limited information for fabrication of sub-assemblies and do not provide the information found in isometrics for the assembly of sub-assemblies into larger sections and their installation into a module or plant. As such, information required for assembly and installation, such as bolting, and support material and location information are omitted from cutsheets. Instead, information that is useful to fabrication (typically in the shop), such as cut lengths, and labelling of welds (used for tracking and identification) are added just prior to release to the shop floor. A single isometric may not necessarily correspond to a single cutsheet. These terms are broadly used throughout North America and in much of the world in industrial fabrication shops.

On projects where fabrication shops do receive 3D models from project owners and designers, models will correspond to isometric drawings not the cutsheet drawings. Typically, in such cases,

fabrication shops do not have sufficient resources to translate the 3D model into the subsets of information corresponding to cutsheets. Other reasons fabrication shops may not have access to 3D models include: (1) lack of contractual obligation to transfer 3D models (design firms are usually obligated to provide 2D isometric drawings and consider the 3D model proprietary information), and (2) data format compatibility issues between various software packages.

3.3.3 Problem Definition

Implementation of existing scan-vs-3D-model methods are often impractical, because fabrication shops do not have access to the 3D design models corresponding to their shop drawings. Furthermore, the existing measurement methods are complicated and require measurement expertise and skill, manual dexterity, human observation, application of geometry and mathematics, use of defined workflows, and manual transcription of information, all of which can be subject to complexity and error. Despite knowing this, fabrication shops typically have no geometric verification and quality control step at the receiving stage and rely on their expert fitters and welders to perform the measurement and verification, once a part is in the fabrication shop. However, detection of issues by fitters, welders, or quality control personnel as part of the fabrication process can be too late and will have a significant impact on lean shop floor flow and thus on project budget and schedule.

3.3.4 Research Contribution and Scope

The main contribution of this research is developing a framework for generating and using 3D digital templates of parts used in fabrication projects for improved quality control and rework reduction. Utilization of the developed framework eliminates the need for the 3D design model by creating and effectively utilizing a comprehensive library of parts.

To evaluate the usefulness of the developed framework, piping parts were chosen since 30% to 50% of industrial construction work involves pipe spool fabrication [73], and reducing rework in pipe spool fabrication is a particularly important problem. Reducing rework in piping projects is difficult since it requires tight tolerances and rigorous geometric verification processes. The problem becomes even more difficult due to the subtle but distinct differences in the geometries and volumes of pipe spools. Furthermore, existing measurement tools are flawed, including conventional methods and many

methods using surveying grade systems to accurately control fabrication. They tend to be ad hoc, not well formalized, or not well integrated with fabrication shops' workflows.

3.4 Background

Rework root causes have been the subject of many subsequent research efforts for rework reduction. In a study that analyzed 359 projects with varying project characteristics from the Construction Industry Institute (CII) database, it was found that heavy industrial projects for contractors were most affected by rework, and the most important root causes of rework are owner change and design error/omission for both owner and contractor reported projects [74]. These issues may result from inadequate planning and poor communication among owners, designers and constructors, thus they highlight the need for a comprehensive rework management system that involves all the stakeholders and different organizational and technological measures at every stage of the project [16]. This recommendation echoed the findings from a survey of 115 civil infrastructure projects by [11] where they identified the ineffective use of information technology to communicate as the primary factor contributing to rework. Therefore, rework reduction requires the need to better plan and manage the design, documentation, and fabrication process.

To mitigate the impact of rework, preventative methods must be applied in order to reduce the probability of errors occurring throughout a project lifecycle, and appraisal measures should be implemented to detect defects and assess conformance to the required tolerance level. This is part of a broader change to an organization's management practices and strategies to mitigate risk, which necessitates a continuous improvement loop, similar to a model of a rework reduction program that supports the Total Quality Management (TQM) framework [75].

3.4.1 3D scanning

A point-cloud is a 3D virtual representation of a scene. The terms "point cloud" and "3D image" are often used interchangeably. In its simplest form, a point cloud is a $3 \times n$ matrix where the 3D surrounding is represented by coordinate values expressed in a global Cartesian coordinate system. 3D images can be obtained through numerous techniques with Laser Scanning, 2D image reconstruction [76-78], and SLAM (Simultaneous Localization and Mapping) being the most prominent ones [79,80] . A terrestrial laser scanner is an optical 3D data acquisition technology that

is able to directly capture 3D as-built information. 3D data acquisition is conducted by surveying the 3D coordinates of the points on objects' surfaces, which are within the scanner's view range [79,81-83]. Time-of-flight (TOF) and phase-based are two technologies used by terrestrial laser scanners to calculate the coordinates of points. TOF scanners calculate their distance to a point by shooting a pulse of laser light to the point and recording the duration of the pulse's round trip. In phase-based scanners, distance is measured by calculating the phase shift of a continuously emitted sinusoidal wave, when it is returned to the scanner. Phase-based scanners provide more accurate information and are faster (up to a million points per second) than TOF scanners, while TOF scanners have longer measurement range (up to a kilometre). Regardless of their technology, several studies have shown that laser scanners can reliably acquire coordinates up to a few hundred meters within a few millimeters accuracy range [83]. While accurate, the major shortcoming of laser scanners is the capital cost of purchasing one and the computational challenges posed by the dense data produced [84].

SLAM (Simultaneous Localization and Mapping) based scanners can map the trajectory of the scanner in real-time. These scanners do this by employing methods such as GraphSLAM [85], particle filter [86], and extended Kalman filter [87]. Once the trajectory is mapped, the acquired point clouds from each frame are then registered together to create a unified point cloud [88]. For localizing, structured lighting is one of the most commonly used methods [89]. An infrared (IR) projector and one sensor within a certain distance of the projector are combined. The projector projects speckle patterns on the objects, and the sensor calculates the distance of a point to itself. In order to use triangulation, two separate images must be captured. The major advantage of this technology is automating the registration step, allowing for a moving target to map the environment [90]. The accuracy of point clouds obtained by SLAM scanners can vary radically based on the path taken for mapping, size of the scanned object (the bigger the less accurate), and the environment's circumstances such as lighting.

3.4.2 Scan-vs-BIM

Superimposing point clouds of as-built assemblies onto their 3D design model can provide valuable information with respect to geometric quality. Another important advantage of scan-vs-BIM methods is that the data acquisition step is more automated and less time consuming compared to

total stations and laser trackers, and the output is visually easy to understand and interpret [91]. As such, many research studies have focused on scan-vs-BIM methods as a tool for geometric compliance verification [92,93]. Tang et al. used and formalized scan-vs-BIM methods as a deviation analysis method for quality control and demonstrated its functionality in large civil projects [94]. Further, Turkan and Bosche focused on both quality control and progress tracking for MEP components in large infrastructure projects [92,95]. Malek et al. proposed a framework that utilizes geometric primitives as well as relationship-based reasoning as a preprocessing step to automate the scan-vs-BIM process for inspection of common structural elements such as columns [96]. Bassier et al. have developed a novel scan-vs-BIM method that is robust to noise, clutter, and gross positioning errors [97].

While there are several advantages in using scan-vs-BIM methods, and they may present a preferable long-term solution, fabrication shops have been slow to adopt them. Kwiatek et al. investigated a framework to integrate 3D scan-vs-BIM based feedback control systems in fabrication shops as part of the fabrication process [91]. The framework was developed to increase the control over the geometric compliance of the as-built state of assemblies and to create a guidance mechanism for the fabrication workers by employing 3D imaging and augmented reality tools in a preventative way that avoids rework and improves assembly efficiency. In their experiments they found professional pipe fitters had a 53% reduction in time to absorb information and 57% reduction in time to complete rework. However, the investigated model workflow is predicated on having 3D design models and is focused on in-process checking during fabrication.

3.4.3 Augmented Reality

There has been a resurgence in various immersive Augmented Reality (also referred to as Mixed Reality) visualization tools. Big tech companies such as Amazon, Microsoft, Google, and Meta (Facebook) have all invested in their own version of these devices. In addition to their application and use cases in the general consumer market [98], medical [99,100], and gaming [101], these tools can be utilized in the context of construction and fabrication applications. Various user assistance systems have been developed using AR headsets. For example, Zhou et al. have developed a system to show important segments displacement inspection for tunnel construction [102], and, Mitterberger et al. have developed an advanced system for bricklaying that helps

construction workers to be more productive [103]. Augmented Reality has also been extensively explored for immersive design and data sharing, where researchers have been able to gain productivity improvements through better visualization of the design across various shareholders [101,104]. Other efforts include developing simplified human-robotic user interfaces (UI) to allow non-programmer users to use and operate robots [105].

Most relevant to this research are the efforts to use AR systems as guidance and visualization tools as part of the fabrication and assembly process. These research efforts attempt to enable unskilled workers with low visualization abilities to become as effective as expert fitters and craftsman and craftswomen [106]. Jahn et al. demonstrate the feasibility of creating AR holographic instruction systems to build highly complex forms [107]. However, this is only done on small frames to maintain the required precision. In their study they have shown that using AR manufacturers can avoid using expensive molds.

While Augmented Reality opens new avenues of communication and collaboration between architects, designers, craftspeople and engineers, their use was not investigated in this research. This was due to accuracy and precision requirements in the context of industrial QA/QC. Song et al. concluded (after reviewing more than 80 recent publications in the domain of AR) that the holographic deviation of location and virtual project drift in headset devices remains an issue to be solved by technology providers [108].

3.4.4 Fabrication Workflow for Receiving Incoming Parts and Assemblies

When materials arrive in a fabrication shop, they are offloaded onto the receiving bay. Receivers would then confirm the materials match the order; this entails documenting the purchase order number, quantity of order, as well as types and grades of materials. This step of quality control is commonly referred to as “OSD” (over/short/damage) in the industry, and it is intended to make sure sufficient materials exist (the over or short part of OSD) for the project, and that the materials are up to standards (the damage part of OSD). If there are not enough materials, or if certain materials are flawed and not fit for use, then they will be sent back to the vendor, and the new batch of materials will go through the same process of quality control when they arrive.

Once materials are received, they are then stored in the warehouse for future project use. A barcode tag may be attached to each material, and information such as project number, heat number (source of batch material) and material description (type, grade, and nominal dimensions) are then uploaded onto the partner's internal information system.

When materials are needed for fittings in an industrial fabrication shop, the warehouse receives a pick list, and the cutting table receives a cut list. After fitters pick up the materials, they measure their length and diameter, and record the "heat number" to keep track of the components that make up an assembly. As such, there is a duplicated effort where the receiver conducts a visual inspection of the materials, and the fitters perform another quality control step before fittings. There is a potential for the warehouse to 3D-scan incoming materials when they are being stored, so their associated dimensions can be confirmed and uploaded onto the information system. In this workflow, the fitters would simply pick up the materials, and they would not have to spend time checking their geometry. More importantly, enabling checkers to detect errors earlier in the process can greatly reduce risk of schedule delays due to incorrect parts delivery.

3.5 Methodology

The methodology section of this paper starts with developing a framework to generate 3D digital template libraries of various fabrication components. While the developed framework is intended for general fabrication, in this chapter the scope of investigation is limited to piping parts. To demonstrate the usefulness and application of the developed framework, a comprehensive library of four of the most commonly used part categories is created. Then, a process for using a 3D quality control system is defined, and its integration at the receiving stage is investigated. The process takes advantage of scan-vs-3D-model quality control methods and utilizes the developed library for generating corresponding 3D models. The developed framework does not require the 3D model as an input, rather the corresponding 3D model of a received part can be easily parsed and selected from the developed library as part of the processing step (Figure 3-3). Using the process, an application software is developed, and tested at a fabrication shop. Finally, using the results of the experiment, a discrete event simulation model is defined to analyze the economic benefits of

utilizing the 3D quality control system. The proposed methodology is compared against existing traditional workflows. The steps involved are summarized in Figure 3-2.

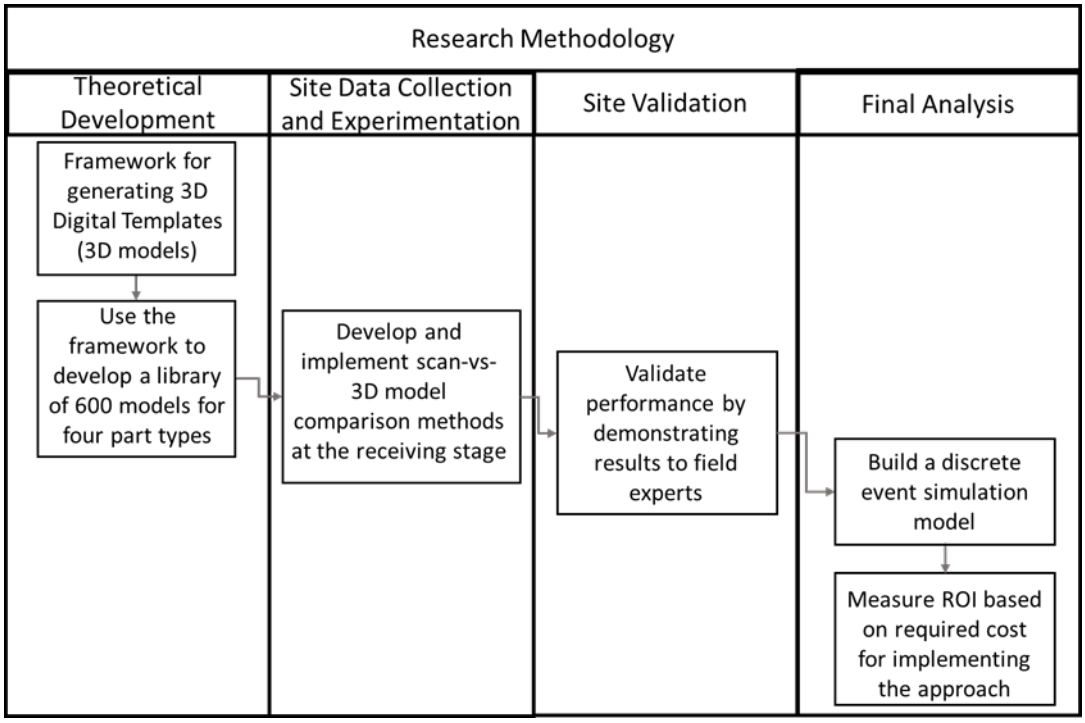

Figure 3-2. Steps involved in this research methodology

Additionally, Figure 3-3 shows the input and output along with the processing steps required for implementing 3D scan-vs-3D-model quality control systems for geometric verification of assemblies. Unlike Kwiatek et al. the model does not need a 3D model from the supplier as an input and rather, it can be generated as part of the processing steps [36]. The model is also focused on the receiving stage of the fabrication process.

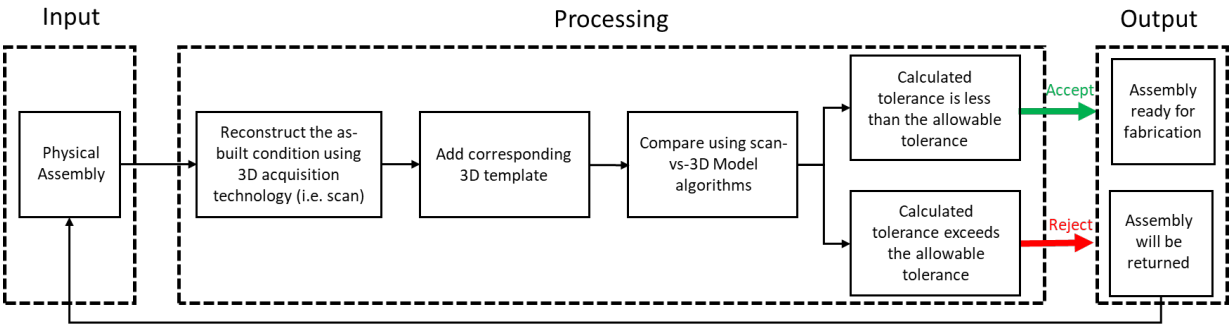

Figure 3-3. 3D Digital Templates used for scan-vs-3D-model comparison for 3D dimensional inspection

3.5.1 Generation of 3D Templates

Figure 3-4 shows the developed framework for developing 3D digital templates of piping components. Each component of the framework is explained in this section. The framework is developed using piping components because of their geometric complexity and variety.

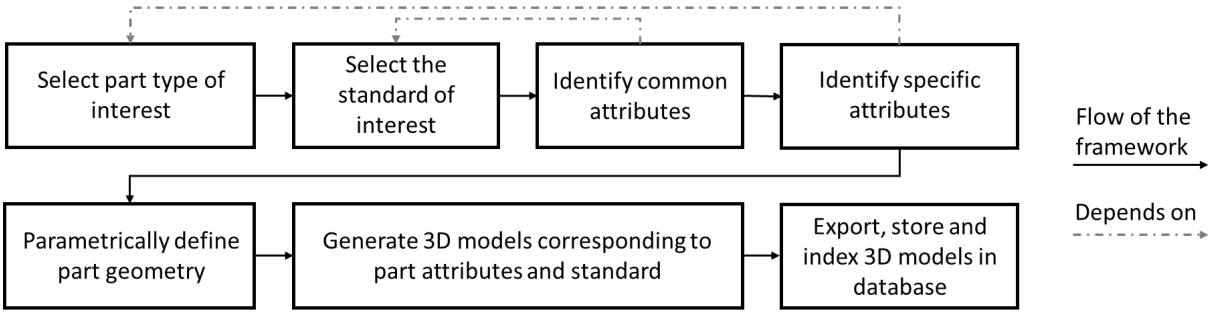

Figure 3-4. Developed framework for generation of 3D digital templates for model library

3.5.2 Select Part of Interest

In order to develop the 3D model library and geometrically characterize a component, the first step is to identify the part type that is of interest. In the context of piping projects, some of the most used parts that fabricators need to order from other contractors include Caps, Flanges, Elbows, and Tees. An example of each part type is shown in Figure 3-5.

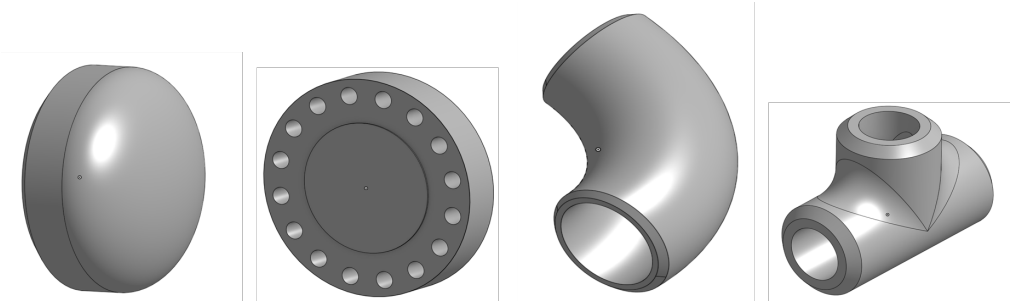

Figure 3-5. Example part types in piping projects.

3.5.3 Select the Standard of Interest

The various attributes and the geometric characteristics of different parts are dictated by the standard to which they are manufactured. Once the part of interest is identified, the next step is to select a standard to which the part adheres. ANSI/ASME-B16, and DIN EN 1092-1 are some of the most commonly used standards with which North American manufacturers and fabricators order parts.

3.5.4 Identify Common Attributes

With respect to geometric characterization of different part types, there are several attributes that are common regardless of the selected part type. These attributes are:

- Connection type
- Nominal size
- Wall schedule and pressure class

3.5.4.1 Connection type

In the context of piping projects, commonly used connection types are: (1) Butt Weld, (2) Socket Weld, and (3) Threaded.

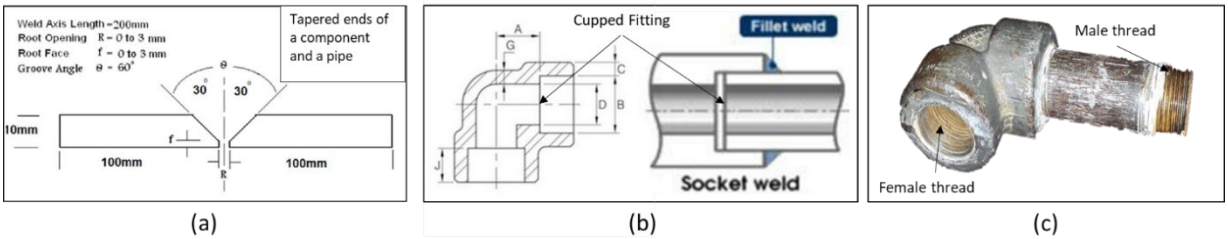

Figure 3-6. Common connection types across piping components. (a) Butt Weld connection [109]. (b) Socket weld connection [110]. (c) Threaded connection [111].

BW (Butt Weld)

In butt welding the two components that are being welded together have tapered ends. These ends are brought together and welded at their meeting point.

SW (Socket Weld)

In socket welded fittings the component will have a cupped end where it connects to the pipe. The pipe's end is placed in this socket and welded.

TD (Threaded Ends)

Threaded fittings will have threaded ends. These ends will then screw onto each other.

3.5.4.2 Nominal Size

Indicates the nominal pipe size (NPS) of the pipe that will be connected to the part. Note that the nominal size is not the actual outer diameter or inner diameter.

3.5.4.3 Wall schedule and pressure class

Both pressure class and wall schedule indicate the thickness of the part's walls. Pressure class is mostly used for threaded components while wall schedule is used for butt welded components. Note that socket welded components can have both a schedule and pressure class. The pressure class refers to the actual pressure the fitting can hold (in psi) while the wall schedule more directly references the wall thickness. By using a pipe chart, fabricators and manufacturers can get the outer diameter and wall thickness of a certain schedule of a part [112].

3.5.5 Identify Specific Attributes

To geometrically model each part, there may be several attributes that will only pertain to a specific part. In this section we have investigated specific attributes related to four different part types that are more commonly used. However, the framework is not limited to these four types.

3.5.5.1 Caps

Unlike flanges, tees, and elbows, caps can be characterized with the common attributes discussed earlier and do not need specific attributes. For example, a cap with nominal pipe size of ½ inch and wall schedule of 0.18 can be characterized by determining the outer diameter and the "E" value based on the nominal pipe size and wall schedule as shown in Figure 3-7 [113]. The general shape of Caps is ellipsoidal and conforms with the requirements in the ASME and ANSI code.

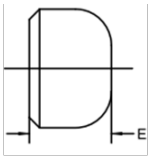

Figure 3-7. Characterization of Caps based on nominal pipe size and wall schedule.

3.5.5.2 Elbows

In addition to the common attributes, Elbows require three additional attributes to be characterized: (1) Reduced type, (2) Angle, and (3) Radius type. Elbows can be reducing or non-reducing. In cases where an elbow is reducing, the nominal reduced pipe size needs to be determined. The second specific attribute is the elbow's angle. While any elbow angle can be custom made, stock elbows come in two variations: 45° and 90°. Elbows come in two radius types, Long Radius (LR) and Short Radius (SR). In the case of LR, the centre to end dimension is 1.5x the nominal pipe size while in the case of SR, the centre to end dimension is 1x the nominal pipe size.

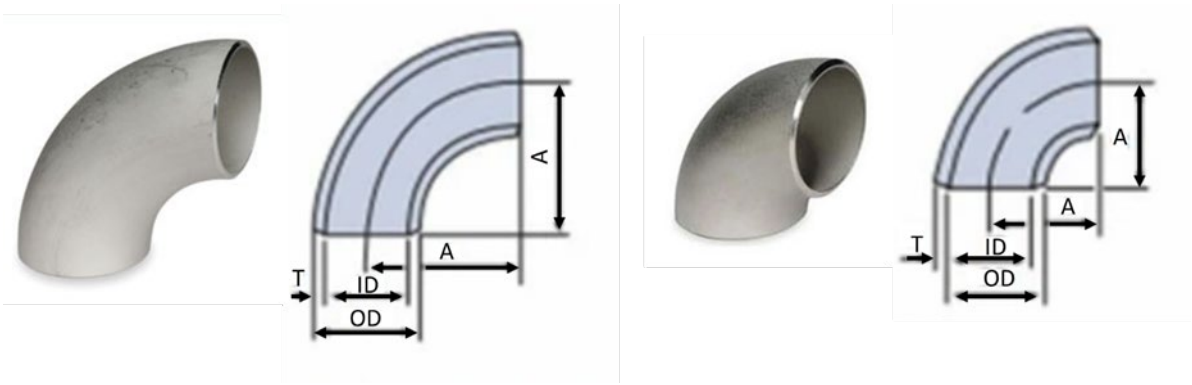

Figure 3-8. Representations of a long radius and short radius elbows [114-117]. (a) Long Radius elbow. (b) Short Radius elbow.

3.5.5.3 Tees

Tees are comprised of three limbs. The two limbs that are parallel are called the run and the limb perpendicular to the run is called the branch. To geometrically characterize a Tee, in addition to the common attributes, three pipe sizes are required for the three limbs. Once the nominal pipe sizes are determined, a Tee can be geometrically modeled (Figure 3-9).

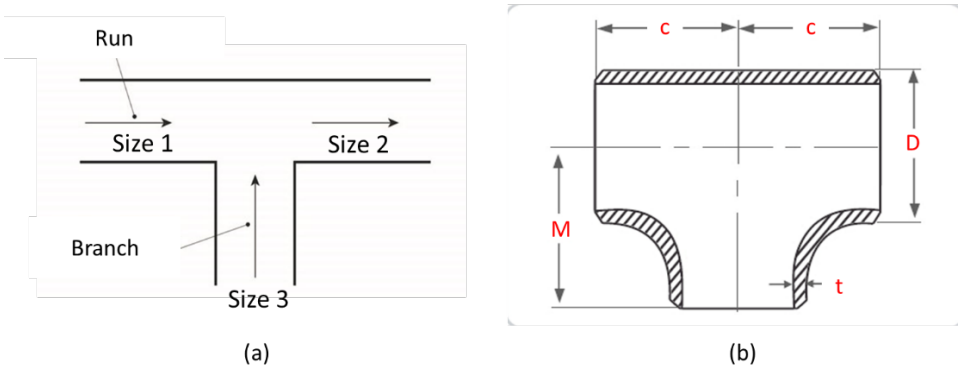

Figure 3-9. An example Tee [118]. (a) Top view of a Tee outlining the run and the branch. (b) different geometric characteristics of a Tee.

3.5.5.4 Flanges

Amongst piping parts, flanges are by far the most diverse in their standard geometric shapes. In addition to the common attributes, there are three additional attributes to consider when modeling

flanges: (1) reduced type, (2) face type, and (3) connection type. Reduced type relates to the flanges where the two connecting pipes are of different diameters. Furthermore, flanges come in various face types. Some of the most common face types and their descriptions are provided in Table 3-1 and Figure 3-10.

Table 3-1. various types of flange face and their descriptions

Name	Meaning	Description
OG	O-ring Groove	The O-ring sits in the channel of the flanges
FF	Flat Face	The face of the flange is completely flat
RF	Raised Face	The face of the flange has a raised portion around the bore at the center of the flange.
TG	Tongue	The face of the flange has a lip that fits into the groove of a groove faced flange
GR	Groove	The face of the flange has a groove that the lip of the matching tongue flange fits into

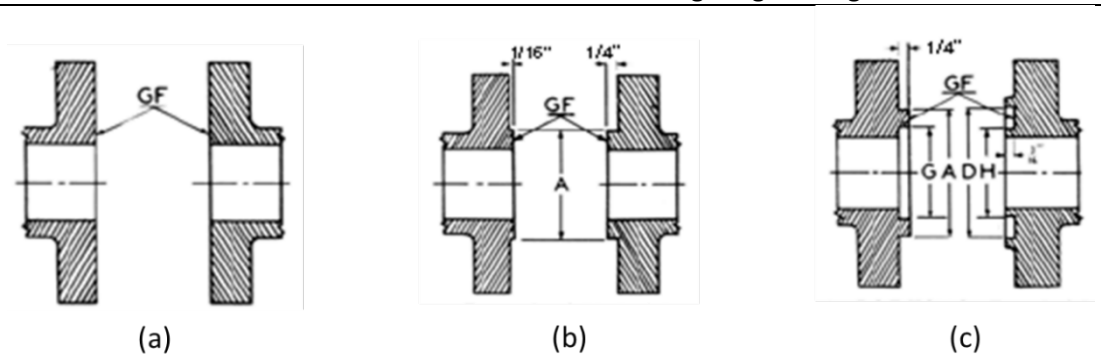

Figure 3-10. Example flange face types [119]. (a) Flat Face. (b) Raised Face. (c) Tongue and Groove face.

The final specific value for flanges is the connection type. In addition to the common connection types discussed earlier, there are other common connection types specific to flanges. Table 3-2 and Figure 3-11 summarize these connection types.

Table 3-2. Additional connection types.

Name	Meaning	Description
BL	Blind	This is a cap for flanges where it completely covers the front and prevents any further connections.

SO	Slip On	In a slip on connection, the flange has a ring that is placed onto the end of a pipe. The flange is then welded into place.
WN	Weld Neck	This is another name for a butt-welded flange.
LJ	Lap Joint	The flange is a ring that is mounted to a stub end hub. The stub end hub is similar in shape to the end of a brass instrument like a tuba except that the flared part of the stub end is much smaller. The flange is placed on the stub end hub and that hub is then welded to the pipe spool.
FW	Flat Weld	Flat weld flanges are the DIN (European) equivalent of slip on flanges in North America
LS	Loose	Loose flanges are the DIN (European) equivalent to lap joint flanges in North America.

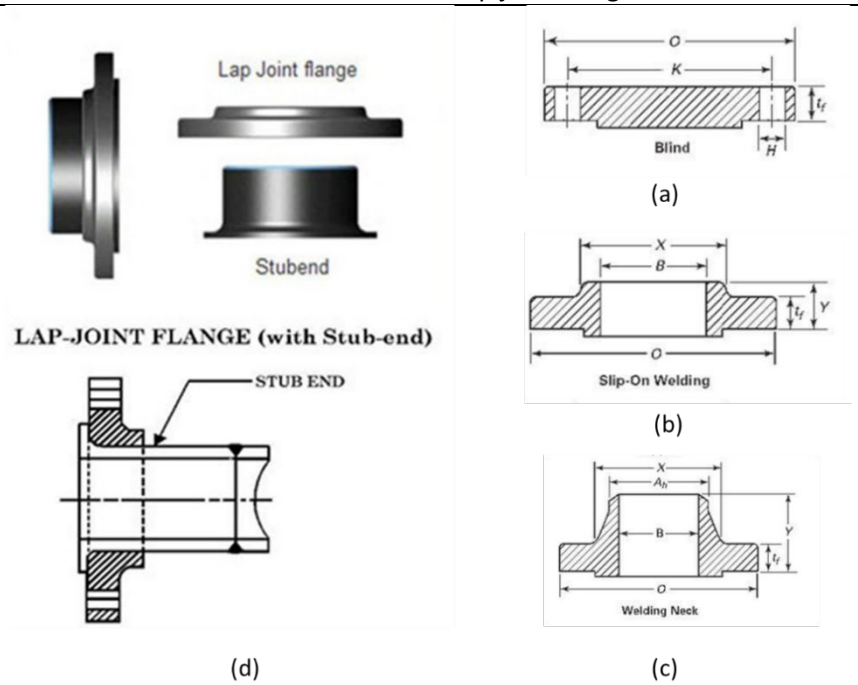

Figure 3-11. Additional connection types. (a) Blind connection. (b) Slip on connection. (c) weld neck connection. (d) Lap joint connection.

3.5.6 Parametric Modeling

To speed up the generation of 3D digital templates for each part category, the part is initially parametrically modeled. This is done by defining an object along with its required dimensions manually in a CAD software. For example, in Figure 3-12-(a) an object has been defined such that dimensions d1 and d2 are parametric (variable). Once the initial CAD model along with its variable dimensions are defined (this would be different for different part types) a macro script (code that runs inside of a CAD package) can be linked to an excel spreadsheet. The excel spreadsheet contains the table of available parameter combinations (parsed from available standards and catalogs). The design software can then use the table to permutate between different parameter configurations and generate a 3D model for each set of parameters (this part is done automatically). This process can be done in most commercially available design packages in the market, including Autodesk Inventor and SolidWorks (Figure 3-12).

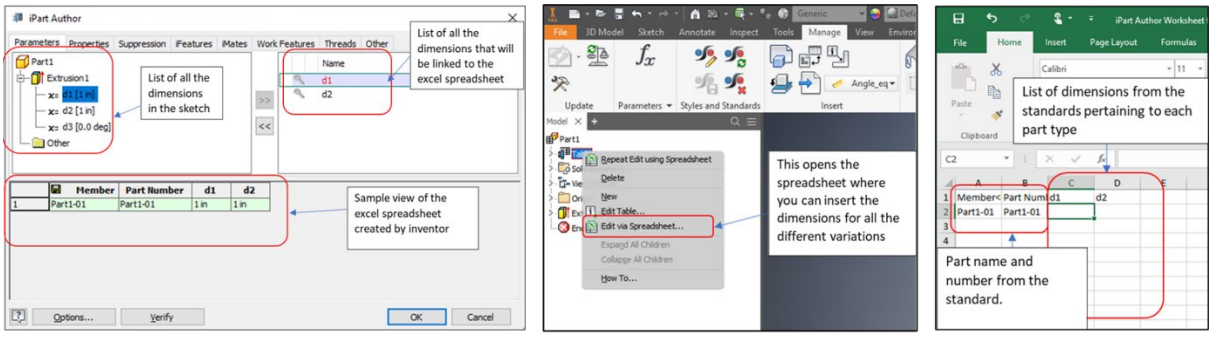

Figure 3-12. Steps involved in parametric generation of digital templates. (a) Parametric definition of an example object. (b) linking the parametric object to an excel spreadsheet with desired dimensions. (c) Excel spreadsheet containing all available dimensions from various codes and standards.

3.5.7 3D Scan-vs-3D-Model Feedback Control Loop (3D Quality Control System)

With the developed 3D digital template library, a 3D scan-vs-3D-model quality control system can be developed and integrated as part of the material receipt workflow (Figure 3-3). The proposed model can be advantageous, since it instead enables the checkers to quickly and reliably verify the dimensional compliance of arrived parts. The integration of a 3D scan-vs-3D-model QC system

allows for earlier detection of geometric errors and lowers risk to the overall project. Figure 3-13 demonstrates the integration of the 3D scan-vs-3D-model QC system as part of the fabrication receipt workflow. As shown in Figure 3-13, the main difference between the proposed model and the traditional model is to allow the checkers to dimensionally verify parts as they arrive with an automated and accurate tool. This will in-turn reduce the workload of the fitters to a simple review of the 3D scan-vs-3D-model analysis results and make sure that arrived parts are within compliance.

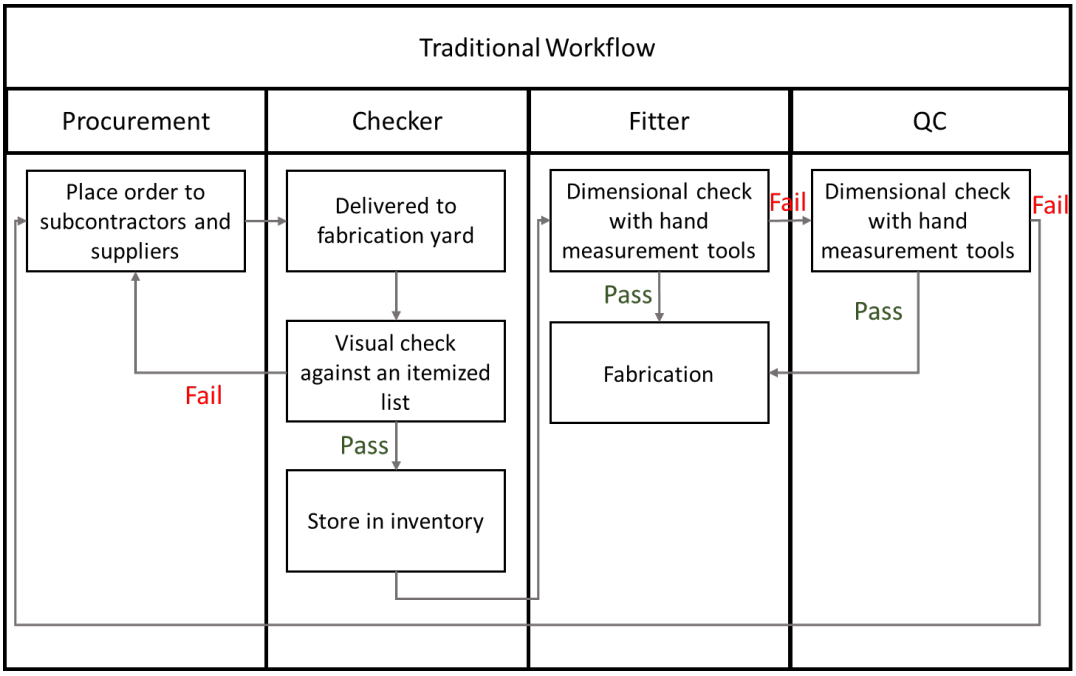

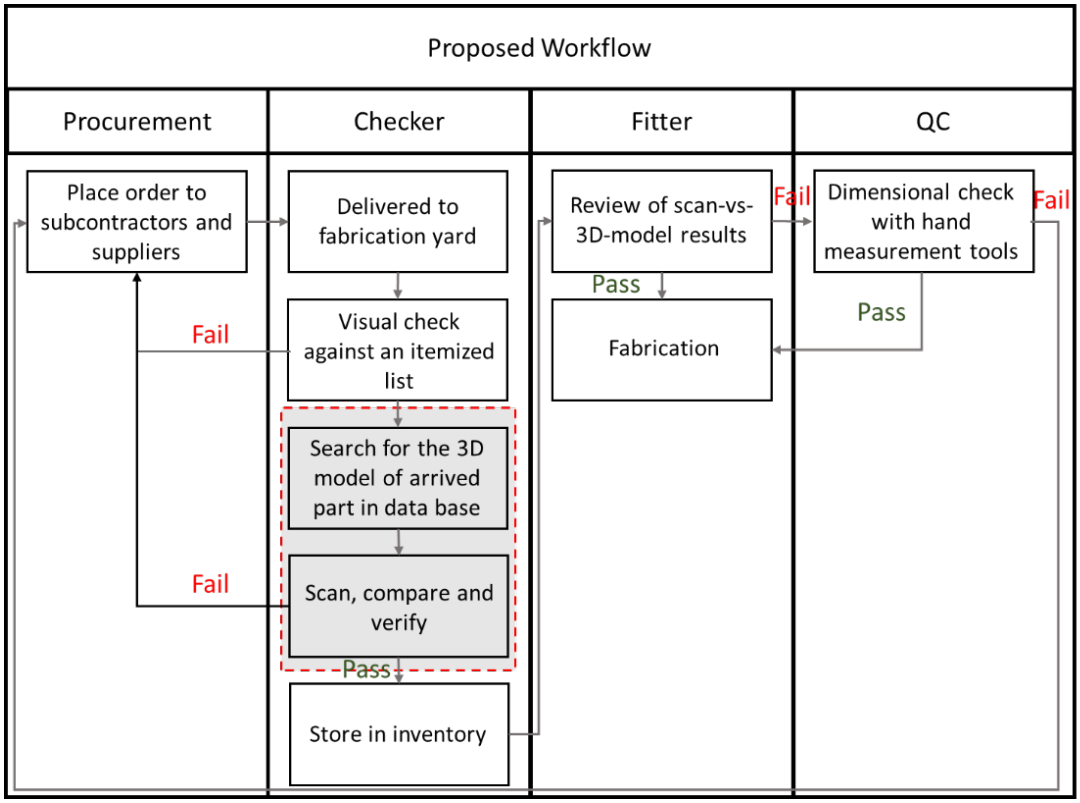

Figure 3-13. Traditional workflow of receiving parts vs the proposed workflow. The steps integrating the proposed 3D QC system are grayed out.

As shown in Figure 3-13, the main difference between the proposed model and the traditional model is to allow the checkers to dimensionally verify parts as they arrive with an automated and accurate tool. This will in-turn reduce the workload of the fitters to a simple review of the 3D scan-vs-3D-model analysis results and make sure that arrived parts are within compliance. It should be noted that the only case where the fitter can fail an assembly would be if the accuracy for the particular inspection was not enough (user induced errors in the scanning process) as well as general operator error.

3.6 Industrial Experimentation

An industrial scale experimental study was conducted to examine the usefulness of the developed digital templates along with the 3D scan-vs-3D-model QC system at the receiving stage of fabrication shops. In this study, to emulate a checker using the developed framework, one researcher was stationed at a fabrication shop's site for three months. The researcher was tasked to scan batches of piping parts as they arrived and provide the compliance report to the checker. To further investigate

the impact of the framework, two scanners were used. One scanner utilized laser scanning technology, and the other scanner utilized SLAM and Structure from Motion. The details of the scanners are provided in Table 3-3 and Table 3-4.

Table 3-3. FARO Focus M70 Laser Scanner specifications

Factor	Value
Range error	± 3 mm at 25 m
Scanning range	0.6 m – 70 m
Acquisition speed	488,000 points/sec
Weight	4.2 KG

Table 3-4. DPI-8S specification

Factor	Value
Accuracy	99% between 2 to 3.3 m
Accuracy	Not specified for more than 3 m
Scanning range	0.6 m – 3.7 m
Weight	1.4 KG

In the piping industry, from a size perspective, parts are broken down to two groups, large-bore and small-bore. For each group, different equipment and processes apply, so for estimating, planning and control purposes, the two groups are defined. A typical nominal outer diameter of large-bore parts is greater than 12''. In this study, laser scanners were chosen because of their accuracy. Laser scanners can easily and accurately scan large-bore parts, however the scanning time and the capital expenditure for purchasing them impedes their adoption by fabricators. Laser scanners do struggle with shiny surfaces; however this limitation can mostly be solved for industrial parts by using higher resolution settings on the scanner. On the other hand, SLAM-based scanners are considerably less expensive, easier-to-use, and faster to acquire data. These scanners, while having several advantages over laser scanners, are normally less reliable and less accurate on larger parts. The accuracy declines with the size of the part being scanned. This is because the accuracy in these devices is highly dependent on the scanner's tracking system. As such, as the path and the scanning time increases, the accuracy of the final point cloud decreases. After initial experimentation, it was deemed that the accuracy of SLAM-based scanners was not high enough for scanning and inspection of large-bore parts. Their accuracy was deemed sufficient for small-bore piping parts.

To geometrically verify the compliance of incoming parts (this is limited to the exterior geometry, as both scanner technologies are limited in their ability to scan the inner walls of the components), an application software was developed [22]. The generated digital template library was stored in a database and connected to the application's user interface. To use the application, the user follows the steps outlined in Section 4.1 of the framework. Initially, the user selects the part type of interest, then the common and specific attributes of that part are entered, and then the corresponding part is populated. Once the 3D digital template is populated, the user can take or add a scan of the as-built condition, and then, having the 3D model and the 3D scan, the two-point clouds are compared and verified. The comparison is achieved by measuring the Euclidean distance of each point on the scan point cloud to the nearest corresponding plane on the 3D model. Depending on the tolerance value and calculated distance, the point would be colored in red (the calculated distance exceeds the allowable tolerance) or green (the calculated distance is less than the allowable tolerance). Figure 3-14 shows the workflow for using the application onsite. In this study, to validate whether a part was out of alignment, two steps were involved. First, the researcher would evaluate the heatmap analysis with respect to the acceptable tolerance for each part (step 4 in Figure 3-14). The acceptable tolerance (inspection criteria) were communicated by the site superintendent. If all areas of the comparison were green (deviation below the acceptable tolerance), the part would be considered as compliant. However, if there were areas where there were red points (out of tolerance), then the issue would have been raised with the site supervisor. After that point, the supervisor could decide to mark the deviation as unimportant and accept the part (not all red areas are critical) or to further investigate and potentially flag the part as non-compliant and proceed with a return and replacement.

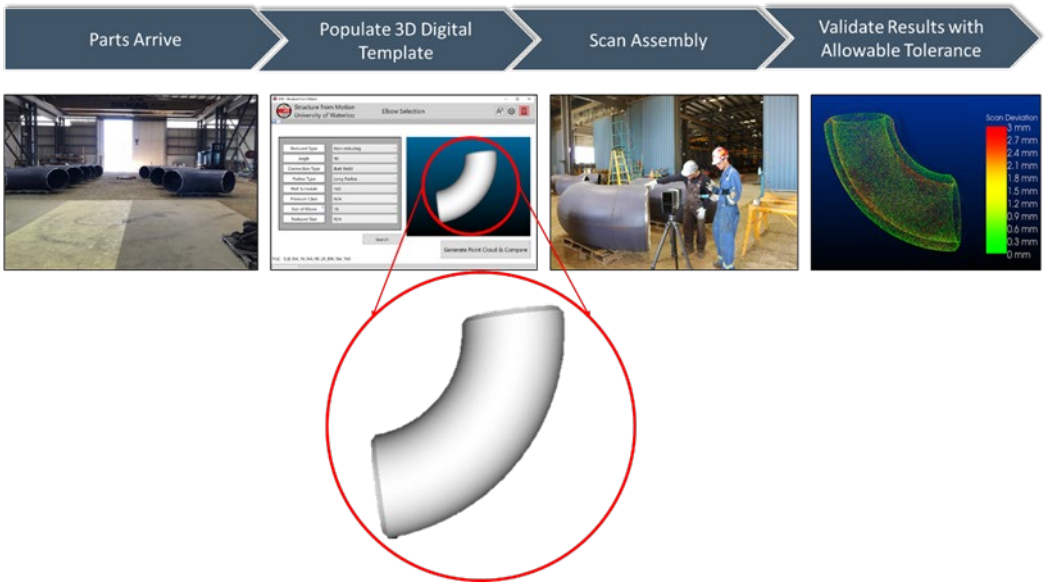

Figure 3-14. Workflow for using scan-vs-BIM at the receiving stage

In this case study, a total of 63 parts were scanned using the laser scanner, and 48 parts were scanned using the SLAM scanner. The distribution of different parts and the scanner used for inspection is outlined in Table 3-5.

Table 3-5. Inspected part type with the laser scanner and the SLAM scanner

	Flange		Cap		Elbow		Tee	
	Number	Percent	Number	Percent	Number	Percent	Number	Percent
Laser Scanner	37	60%	0	0%	15	22%	11	17%
SLAM Scanner	25	52%	3	6%	7	15%	10	21%

After reviewing all inspection results, 5 parts were determined to be incorrect (out of tolerance). The distribution of the errors between large-bore and small-bore assemblies along with the scanner used for detection is outlined in **Error! Reference source not found.**.

Error! Reference source not found.

The distinction between small-bore and large-bore is important, since manual measurement and verification on large-bore parts takes longer than small-bore parts. Large-bore items may require two

to five people for inspection and verification. Additionally, because of logistical challenges, later detection of issues on large-bore parts has a higher schedule impact, thus it is more costly.

As outlined in , 43.2% of all inspected parts were large-bore and 4.2% of them had a geometric issue. Similarly, 56.8% of all inspected parts were small-bore where 4.8% of them had a geometric issue. During this case study, it was determined that the inspection time for large-bore assemblies using the laser scanner on average takes 30 minutes (scanning and comparison) and 15 minutes for small-bore. The 3D scan-vs-3D-model verification takes a shorter time on small-bore parts, since on the same scan file multiple parts can be scanned, and on average fewer scans are required to capture a complete 3D point cloud. Finally, during this study, the manual inspection times for large-bore and small-bore parts were observed and cross checked with the checker and the fabrication manager. As mentioned earlier, the manual inspection of large-bore parts takes significantly longer, since usually two persons are required, and due to safety issues, all maneuvers should be done with the crane (Figure 3-15).

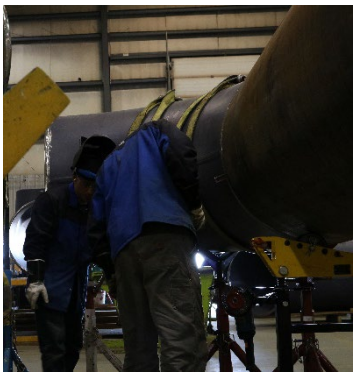

Figure 3-15. Two workers measuring a large-bore elbow

3.6.1 Simulation Scenarios

The numbers achieved in the experiments are leveraged to investigate the time and cost impact of integrating digital templates and 3D scan-vs-BIM verification at the receiving stage over a span of a year for a fabrication shop. A discrete event simulation model is developed and calibrated using the preceding shop-floor experiments to model different integration workflows and benchmark the results against the traditional workflow for receiving piping parts, while accounting for uncertainties and probability distributions in process parameters. The modeled workflows are as follows:

- Workflow A: The traditional workflow. The existing workflow of receiving parts in fabrication shops as described in Section 4 is modeled.
- Workflow B: In this workflow laser scanners are used in conjunction with the 3D scan-vs-BIM application at the receiving stage for all arrived parts (large-bore and small-bore).
- Workflow C: In this workflow the SLAM-based scanner is used for small-bore parts and the laser scanner is used for large-bore parts.
- Workflow D: In this workflow the SLAM scanner is used for small-bore parts and the traditional workflow is used for large-bore parts.

Figure 3-16 shows the simulation model developed to model defined workflows. Table 3-6 has the information on time assumptions for different activities, with normal distribution derived from site observed mean time and estimated standard deviation. Path 1 and 2 in Table 3-6 refers to Traditional Workflow and Proposed Workflow as shown in Figure 3-16, respectively.

Table 3-6. Simulation Modelling Parameters

	Workflow A	Workflow B	Workflow C	Workflow D
Path	1	2	2	1&2
Inspection Time Large-bore (min)	Normal (60,7)	Normal (30,5)	Normal (30,5)	Normal (60,7)
Inspection Time Small-bore (min)	Normal (10,1.5)	Normal (15,2)	Normal (5,1)	Normal (5,1)
Store Time Large-bore (min)	Normal (30,5)	Normal (30,5)	Normal (30,5)	Normal (30,5)
Store Time Small-bore (min)	Normal (5,1)	Normal (5,1)	Normal (5,1)	Normal (5,1)
OSD Time Large-bore (min)	Normal (120,10)	Normal (30,5)	Normal (30,5)	Normal(120,10)
OSD Time Small-bore (min)	Normal (60,7)	Normal (20,3)	Normal (20,3)	Normal (20,3)
Number of Received Large-bore (per year)	2200	2200	2200	2200
Number of Received Small-bore (per year)	2800	2800	2800	2800
Large-bore Failure Probability	4.2%	4.2%	4.2%	4.2%
Small-bore Failure Probability	4.8%	4.8%	4.8%	4.8%

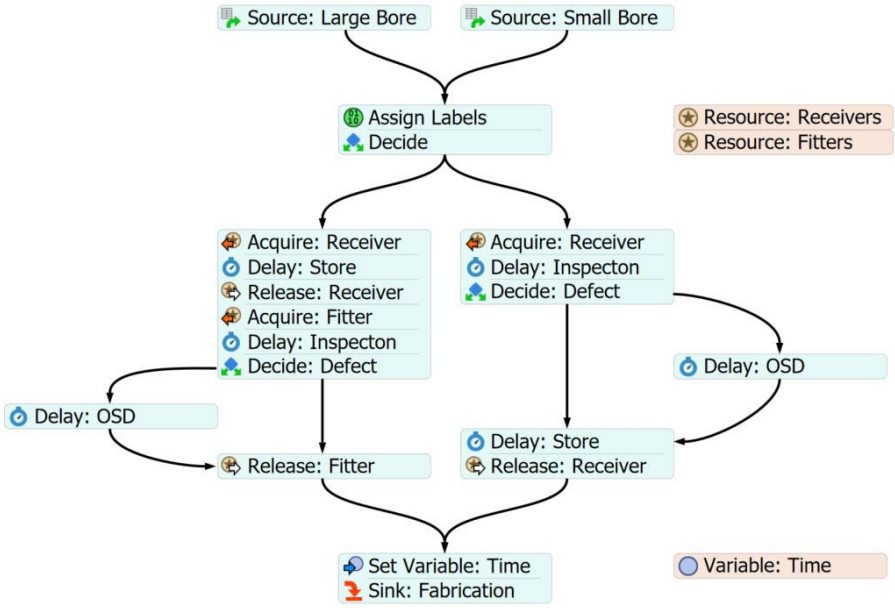

Figure 3-16. Simulation Modelling of Traditional and Proposed Workflow. FlexSim software version 21.1.4 was used to build the simulation model [120]

In Figure 3-16, the left path represents the activities that occur during traditional workflow, and the right path represents the activities that take place with proposed workflow utilizing 3D scanning during receiving for various products. In this model, Workflow A takes the left path, Workflow B and C take the right path, and Workflow D takes both paths. The fabrication shop in this study (on track to receive 5,000 parts in the year of this study) had 25 fitters and 3 receivers. It is also important to note the receiving task and the fitting task are serial activities not sequential. This means that there is typically a significant time gap between the time that a part is received and stored, and the time that the part is moved to the shop for fabrication. It should be noted that in Figure 3-16 additional OSD (over/short/damage) time will be to review the component and place the order again added for assemblies that failed inspection in. The model does not cycle back to earlier activities like “Acquire: Receiver” because a designated distribution of fail and no fail is assigned to components right at the beginning of the simulation.

An OSD (over/short/damage) delay would be added whenever there is an issue with a part. Earlier detection of errors has a significantly lower impact on the project schedule, since the logistics of

return and replacement is easier. Furthermore, fabrication shops do not carry inventory and always build to order, thus, if some critical parts are incorrect, that can cause significant damage to project schedule. The assumed time for detection of issues in this model was reviewed by industry experts and was approved as a reasonable average number in case if a large-bore or small-bore part has an issue.

To perform the analysis, a total of 5,000 parts were assumed to be required for a fabrication shop over a year. This number can radically vary from shop to shop (depends on the amount of work secured in any given year), and it is used as a conservative estimate in this study. After running the simulation model 1,000 times to investigate the time impact of different workflows over a year, the simulated project time for each workflow is summarized in Table 3-7.

Table 3-7. Simulation results for the case study

Scenario	Mean (99% Confidence) Simulated Project Time (Minutes)	Sample Standard Deviation	Minimum (Minutes)	Maximum (Minutes)
Workflow A	7,235 < 7,239 < 7,244	55.25	7,077	7,408
Workflow B	3,890 < 3,891 < 3,892	12.40	3,851	3,934
Workflow C	3,328 < 3,329 < 3,330	11.27	3,287	3,366
Workflow D	5,837 < 5,842 < 5,847	61.26	5,664	6,470

To validate the results of the model, the results of the workflow A specifically was reviewed by the shop manager. Additionally, to further validate the results, sensitivity analysis was carried out on some of the more critical parameters of the model.

3.7 Results

To further investigate the impact of large and small-bore distribution on time savings of the four defined workflows, three scenarios are considered in the sensitivity analysis, as summarized in Table 3-8.

Table 3-8. Large-bore and small-bore distribution assumptions in the model for sensitivity analysis

	Large-bore	Small-bore	Note
Scenario 1	50%	50%	To show impact of equal distribution
Scenario 2	80%	20%	To show the impact if large-bore parts are in majority
Scenario 3	20%	80%	To show the impact if small-bore parts are in majority

After discussion with fabrication managers, it was determined that error rate probability can vary depending on the supplier and volume of work. As such, to thoroughly investigate the impact of the error rate on the model, the simulation analysis was done with the following scenarios as well, as summarized in Table 3-9.

Table 3-9. Error probability analysis

	Large-bore	Small-bore
Scenario 1	1%	1%
Scenario 2	2%	2%
Scenario 3	3%	3%
Scenario 4	4%	4%
Scenario 5	5%	5%

The results are organized based on bore composition: (1) large-bore 50%, small-bore 50%, (2) large-bore 80%, small-bore 20%, and (3) large-bore 20%, small-bore 80%. Within each bore composition, each workflow is assigned the same increase in error probability from 1% to 5%. Therefore, for each figure, the total project completion time is outlined for each error probability and the workflow of interest. Figure 3-17 to Figure 3-19 summarizes the results of the sensitivity analysis.

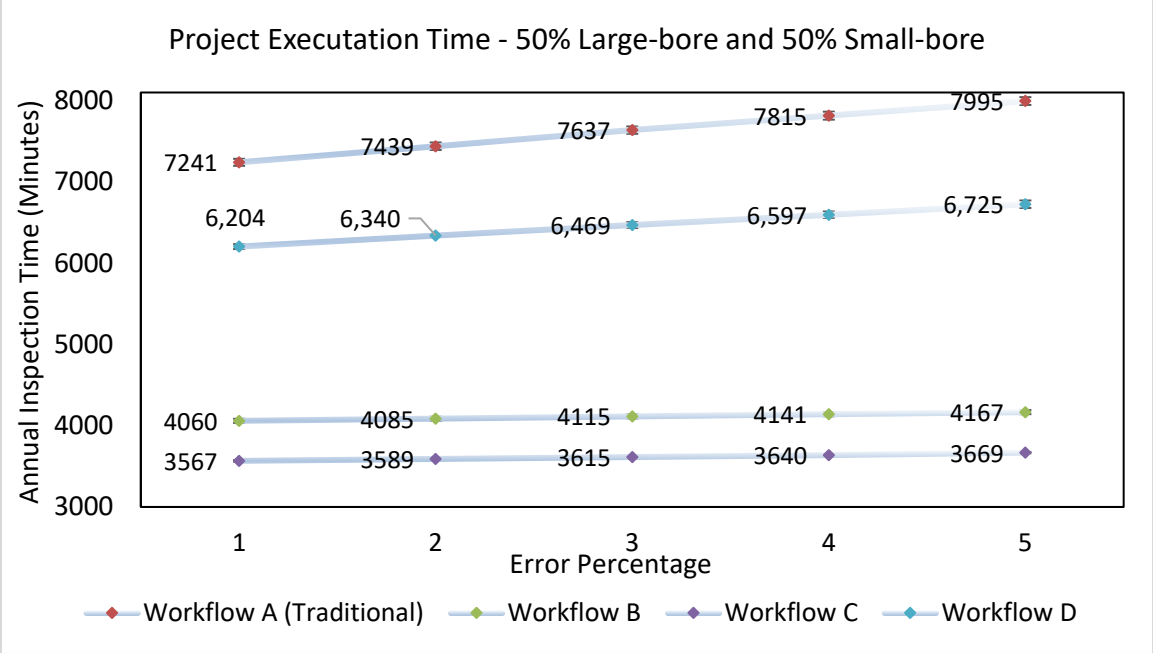

Figure 3-17. Simulated project execution time - 50% Large-bore and 50% Small-bore

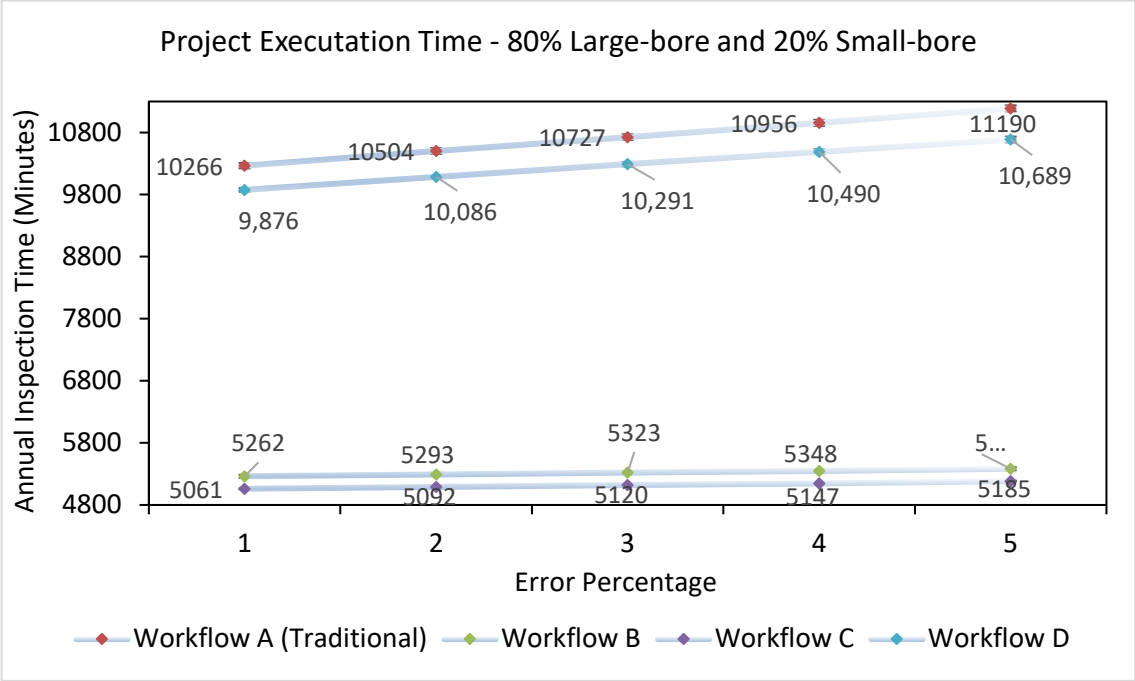

Figure 3-18. Simulated project execution time - 80% Large-bore and 20% Small-bore

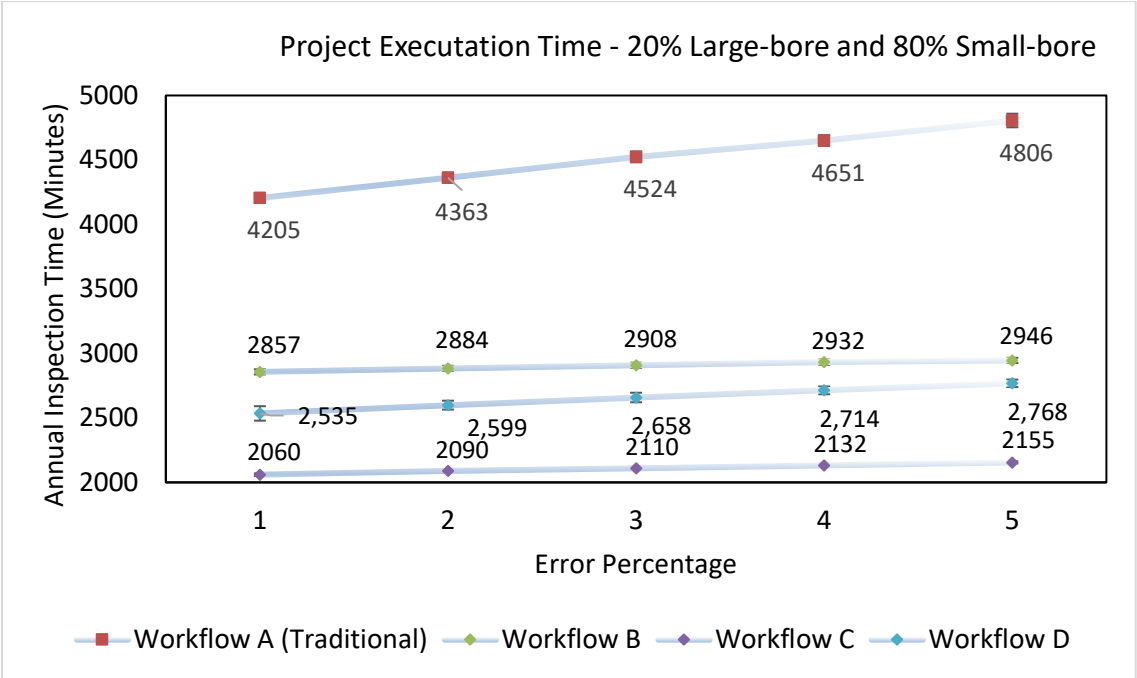

Figure 3-19. Simulated project execution time - 20% Large-bore and 80% Small-bore

3.7.1 Cost Benefit Analysis

In an effort to assess the economic impact of utilizing and integrating laser scanners and/or SLAM-based scanners into the existing workflows, a cost benefit analysis was also carried out in order to understand the investment needed to set up the proposed workflows and potential recurring savings and expenses, as well as to appreciate the advantage for an industry shop to implement this approach. Therefore, the analysis was carried out for Workflow B, C, and D, as they are compared against Workflow A (traditional workflow). The first-year startup costs and the annual costs are summarized in Table 3-10.

Table 3-10. Costs for each proposed workflow

		Workflow B		Workflow C		Workflow D	
	Unite Rate	Unit	Cost	Unit	Cost	Unit	Cost
First Year Cost							
Hardware (SLAM)	$5,000	0	-	3	$15,000	3	$15,000
Hardware (LS)	$50,000	2	$100,000	2	$100,000	0	-
Startup IT Integration	$20,000	1	$20,000	1	$20,000	1	$20,000
Annual Cost							
Maintenance (SLAM)	$500	0	-	3	$1,500	3	$1,500
Maintenance (LS)	$2,000	2	$4,000	2	$4,000	0	-
Scan vs BIM Training	$2,000	1	$2,000	1	$2,000	1	$2,000

The worker composition in this analysis consists of 25 fitters and 3 receivers. The benefit in this analysis is the time savings in applying the proposed workflows compared to traditional work process (Workflow A). Therefore, the experimental study results from Table 3-11 are used in the calculation of cost reduction associated with reduced time during receiving, with an assumption of $65/hour for each worker (a conservative estimate provided by the partner fabrication shop). Table 3-11 below summarizes the time reduction and associated cost savings.

Table 3-11. Benefits for each proposed workflow

	Workflow A	Workflow B	Workflow C	Workflow D
Simulated Average Work Completion Time (Minutes)	7,239	3,891	3,329	5,842
Time Reduction from Workflow A (schedule Minutes)	-	3,349	3,911	1,398
Annual Cost Savings	-	$101,553	$118,505	$70,994

Aggregating the costs and benefits for the proposed workflows, the payback period can be calculated, in an effort to assess the value in investing and maintaining the technologies required. The cumulative net benefit in the next five years using each workflow is shown in Figure 3-20 and can be calculated as:

$$Cumulative\ net\ benefit\ in\ year\ i = \left(\sum Startup\ costs + \sum_{n=o}^{n=i} Annual\ cost\ in\ year\ n\right) - \left(\sum_{n=o}^{n=i} (Time\ saved\ in\ year\ n\ \times hourly\ labour\ cost)\right)$$

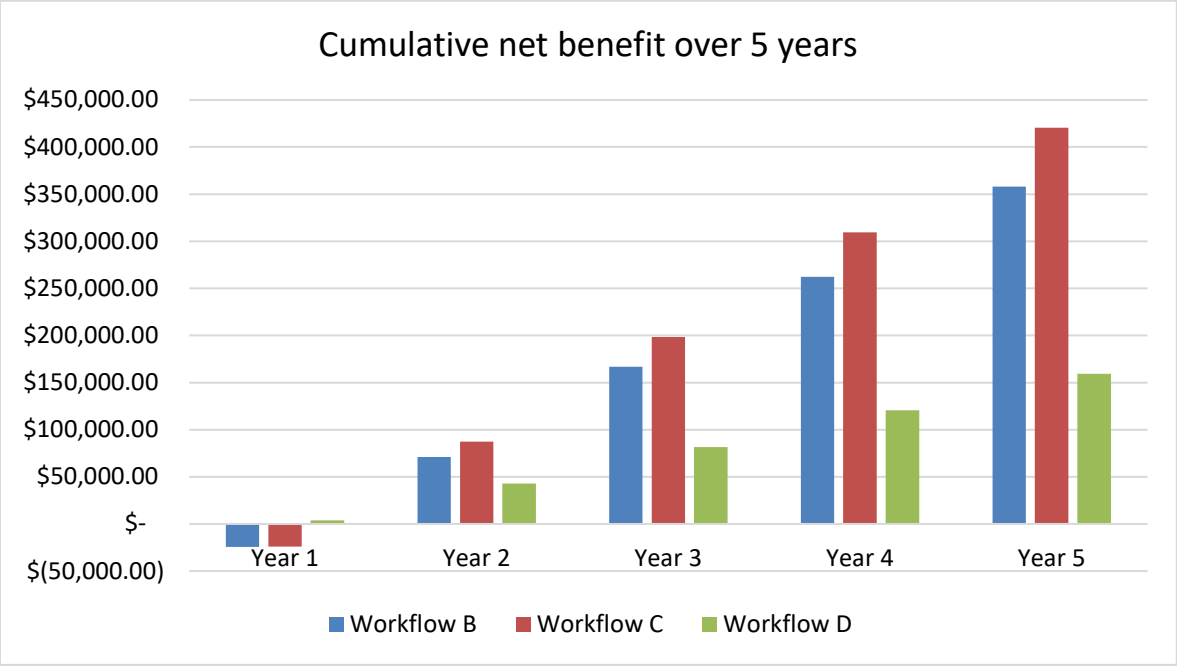

Figure 3-20. Cumulative net benefit of implementing Workflow B, C, and D over 5 years.

With the implementation of Workflows B, C, and D, their payback periods are 1.3, 1.2, and 0.9 years, respectively, for the estimated startup cost. It should be noted that payback period was chosen as an example metric to evaluate the economic justification for investment in 3D quality control methods, other methods could have been used as well, such as NPV (net present value), ROR (rate of return)

coupled with MARR (minimum attractive rate of return). Furthermore, the interest rates were low when this study was carried and that the company would use payback period for its decisions and not do a NPV analysis typically for investments of this size and uncertainty. While the scanner part of this cost is fixed, the software and library costs could be substantially lower, if this became a widely available product itself. It is important to also note the calculated payback period analysis in this section is based on the experiment's part composition (43% large-bore and 57% small-bore).

3.8 Conclusions

This chapter explored the utilization of 3D quality control systems in construction prefabrication, specifically, for the quality control process in obtaining assembly geometric information and quantifying the errors with respect to required tolerances for piping parts. The developed framework for generating 3D digital templates is used to facilitate scan-vs-3D-model, by superimposing as-built point clouds of completed assemblies onto their 3D design models (parsed from the developed 3D digital template library). By leveraging the library of 3D piping components during the receiving stage of the fabrication cycle, workflow steps involving the receivers and fitters are fundamentally altered, and this provides an opportunity to further improve the overall productivity involving 3D scanning technology and the proposed method. The proposed method has the following benefits for fabrication shops and projects:

1. Improved measurement accuracy and speed by using a 3D scan-vs-3D-model based approach
2. Reduced project risk by enabling earlier detection of mistakes by checker at the receiving stage

The case study applied the framework with two types of 3D data acquisition scanners, and inspection was conducted on both large-bore and small-bore parts. It was found that large-bore and small-bore had 4.2% and 4.8% of geometric issues, respectively. Furthermore, their inspection times were compiled to understand the potential time savings against traditional manual inspection. These parameters were applied to a simulation model, which examined combinations of technology and framework deployment scenarios, namely: (A) traditional workflow, (B) laser scanner and 3D scan-vs-3D-model application for all receiving parts, (C) SLAM-based scanner for small-bore parts and laser scanner for large-bore parts, and (D) SLAM-based scanner for small-bore parts and traditional workflow for large-bore parts. It was found that the combinations of proposed workflows

had an improvement over traditional workflow of between 46% and 54% in receiving inspection time. This result suggests that if the framework of 3D scan-vs-3D-model is applied in the workflow, there would be substantial time savings during geometric quality control.

To acknowledge different potential ratios of large and small-bore parts, as well as their error rate, a sensitivity analysis was conducted to understand the relationship and impact of these parameters on the overall receiving inspection time. This analysis is important, because fabrication shops often have a specialty in the assemblies that they fabricate. This means that some fabrication shops are often involved with projects dealing with large-bore items and some fabrication shops are more specialized on more complex and smaller size parts.

While the three workflows that utilized the proposed framework saw marginal increase in time under all three composition ratios and increasing error rate, the biggest change occurred in the traditional workflow, which saw from 1% to 5% error rate a 10% increase in equal ratio of receiving parts, 9% increase in 80% large-bore and 20% small-bore parts ratio, and 14% increase in 20% large-bore and 80% small-bore parts ratio. The impact is exacerbated by the time required to conduct quality control during fabrication receiving, as it takes more effort than the proposed framework to measure, compare, document, and process the out-of-tolerance materials.

A cost-benefit analysis was also carried out using the experimental study data and part composition to understand the economic justification of investing in the framework and its associated technology for full operation. While each fabrication shop would see different types of projects with varying levels of geometric complexity, if the proposed framework and the revised workflow are applied, the expected payback period would be less than two years. This means that taking into consideration the initial cost required to set up the framework and recurring annual expense, the cumulative annual benefit in time savings compared to the traditional workflow would outweigh the cumulative cost during the second year of full implementation.

It is important to note that while all three alternatives have about the same payback periods, Workflows B and C can provide significantly higher savings in terms of the absolute dollar amount saved. On the other hand, while Workflow D consistently underperforms in comparison to workflows B and C, its implementation may still be attractive to fabrication shops (especially in cases

where the fabrication shop is mostly dealing with small-bore parts). This is because the implementation of this workflow requires significantly less upfront capital, allowing the fabrication shops to more easily adopt the proposed frameworks.

Comparing the implementation of Workflow B and C, another factor to consider is that while the projected savings of Workflow C is higher in all cases, fabrication shops may find the implementation of Workflow B still more attractive, especially in cases where fabrication shops are mostly dealing with large-bore parts. This is because operationally working, integrating, and training on one type of 3D acquisition technology is easier and more feasible for many fabrication shops.

3.9 Discussions and Limitations

The framework developed in this research can be extended to include a wide range of fabrication parts with various general and specific attributes, including structural steel. The developed framework in this study was focused on piping parts due to their complexity and frequency of use. However, the same framework can be applied for generation of various beam types in structural steel fabrication.

Even though the simulation results in Figure 3-17, Figure 3-18, Figure 3-19 and are mostly linear, the use of the discrete-event-simulation is helpful because:

1. While fabrication and receiving activities are serial, they are not sequential (once an assembly is received it is stored in an inventory and then used in the fabrication process). This means that there is usually a lot more time to inspect and reject assemblies when they are in the receiving docs.
2. The number of resources that a shop has in their receiving stage vs. fabrication impacts the results of the project time (typically there is plenty of time at the receiving stage whereas fabrication and fitters are on the critical path). The simulation allows for change in the resources and to evaluate how they affect the wait times in bottlenecks, akin to sensitivity analysis.
3. The flow of activities is not linear for workflow D and a hybrid workflow is used. This means that for small-bore parts there is one set of activities and for large-bore parts there is a sperate set of activities.

4. By considering activity process times as probability distributions, the variations in final results can be easily captured through simulation.

The limitation of this research is that the developed framework can only be applied at the receiving stage for incoming parts. On a high level, the actual fabrication process can be broken down into 3 major steps, (1) receiving, (2) fabrication (fitting and welding), and (3) final QC and Shipping. While the developed framework addresses the issue with the lack of 3D models in the receiving stage, the other two stages are not addressed. Also, an economic justification has been done to investigate the payback period for investing in the implementation of 3D dimensional control systems. While the work attempts to cover various project types and scenarios, the analysis still may not be applicable to all fabrication shops. Fabrication is a highly fragmented market; different shops use different workflows and have different sets of requirements and constraints in place. Additionally, the economic justification analysis assumes same volume of work in each year. However, the volume of work in each year can be highly different depending on general market conditions. More work can be done to cover other types of fabrication shops, focusing on different industrial sectors to better understand the value of implementing 3D dimensional control systems in the broader market.

Another avenue for future research in this study is the determination of the minimum required shop size to make the required investment justified. This should be investigated in terms of the total assemblies per year, shop's square foot, project types, and materials. This investigation can be further elaborated by factoring environmental costs of scrap and rework.

In the first stage of the defined evolution stages, this chapter focused on the value of scan-vs-3D-model at the receiving stage. To demonstrate the potential value of implementing scan-vs-3D-model quality control in other sections of the fabrication life cycle (fabrication and final QC), next chapter provides two cases studies demonstrating potential use cases and value gained by the fabricator and the project owner.

Chapter 4
Utilization of Rapid Scan-vs-3D-BIM for Design and Quality Control of Assemblies; Two Case Studies

4.1 Chapter Summary and Contribution Statement

This Chapter includes two case studies that were conducted during the presented research. These case studies were conducted to investigate the value of using simple scan-vs-BIM analysis for fabrication shops. The context for each case study is presented as well as the results of using the scan-vs-BIM process in the fabrication process in each case. Some preliminary benefits analysis has also been completed.

In this Chapter, all data collection, processing, and communication to project participants were done by the author. In section 4.2 Geoffrey Cann provided editorial assistance to the parts of the manuscript for clarity. Sydney Bang (employee of the fabricator) facilitated the site visits as well as reviewing the disclosed costs in the manuscript for accuracy, explained in section 4.2.5. In section 4.3, all data collection, processing, and communication to project participants, as well as writing the manuscript, was done by me. Robert Albee (Engineering at the project owner) reviewed disclosed numbers for accuracy. Dr. Haas reviewed the manuscript and has provided editorial input to the manuscript in this Chapter.

4.2 Replacing Brownfield Assets Using Scan-vs-BIM; Case Study 1

4.2.1 Introduction

A food processing company (the Customer of the fabrication shop) needed to replace one of their storage tanks. The tank was 3 meters in diameter and 6 meters high, made of plastic and was going to be replaced by a new tank made with stainless steel. The tank was housed inside a confined building adjacent to the main plant, where they store raw materials used in the manufacturing process. The tank was old and was leaking fluid. The owners had decided that the tank was beyond the point where simple repairs or maintenance could bring it back to productive capacity. To begin the replacement process, the company had informed the fabricator that only old engineering shop diagrams about the tank's configuration, fittings, flanges, and footings existed.

The tank was at a height and was attached via connector piping directly through the exterior wall of the building. The company could not easily retrofit the fittings or the input/output pipe due to the placement and cost. Ideally, the new tank had to be an exact replica of the existing one. The replacement process was time-sensitive since the company could not afford for the tank to be offline for too long or to fail. Without the tank in operation, the plant did not function, and there was no feasible alternative. As the plant employs a few thousand staff, an unplanned shutdown was very costly.

The Customer contracted the fabricator to measure the old tank, design the replica, procure the steel, contract any subcomponents, build the replacement, and install the replacement at the plant. Initially, the fabricator intended to rely on the original design documents of the old tank to build the replica (the traditional process). If the measurements were incorrect or the diagrams were inaccurate, then the replica would not fit in the place of the old tank, fittings would be off, and the plant operations would be at risk. The consequences to the Fabricator and the plant were extremely high (a possible two-day downtime to correct the replica).

4.2.2 Objectives

The objectives of the fabricator were as follows:

- Build an exact replica of the existing tank
- Minimize rework and waste in the fabrication process.
- Complete rebuild and connect to existing piping within time and budget constraints.

4.2.3 Challenges To Consider

The challenges faced by the fabricator were as follows:

- Limited engineering time
- Constraints of resources and build time
- Accuracy was impeded; cannot rely on documentation and traditional measurement tools
- The asset was 6 meters off the ground with various occlusions; difficult to reach
- The factory needed to be in operation
- Limited acceptable downtime

4.2.4 The Approach

The Fabricator was assisted in using a laser scanner to scan the existing tank, capture its design in a digital format, and validate the fabricated replica with the original tank. The onsite scanning process was about 2 hours.

To achieve the highest possible accuracy, scan registration spheres were used. Also, to capture all surfaces, the laser scanner was placed on a 10-step platform rolling ladder and thus was able to scan the top of the tank, which was about 6 meters high. Once the point cloud was captured, the Fabricator then used the obtained point cloud to validate the 3D design model built by their design team.

In this case, the scan-vs-BIM comparison revealed a surprising feature on the tank (Figure **4**-**1**). A nozzle had been added to the tank at some point, but it was not reflected in the shop diagrams and the subsequent 3D model. The nozzle was at height and was overlooked by the conventional measurement team working on ladders and scaffolding.

The utilization of the scan-vs-BIM to validate the original design model allowed the fabricator to have confidence in the design. The model's accuracy eliminated the risk of rework and remediation at the site. The risk to the Customer of a potential unplanned multi-day downtime event was avoided.

Figure 4-1. (a) Initial design model. (b) The completed site scan of the tank. (c) The scan-vs-BIM reveals a missed nozzle at the back. The blue object is the 3D design model's point cloud and the gray object is the scan point cloud. (d) The missed nozzle was added to the design model. (e) The back nozzle on the existing tank to be replaced by the new tank. (f) Top view of the tank to be replaced. (g) Top view of the tank to be replaced.

4.2.5 Impact Analysis

A review of this scenario reveals the qualitative and quantitative benefits to the Fabricator and the Customer, summarized in Table 4-1.

Table 4-1. Qualitative Impacts

		Fabricator	Customer
Benefits	**Direct**	Accurate measurements completed faster	Delivery of tank replica completed on time
		Measurements are complete	Disturbance to site was minimized
	Indirect	Unplanned site remediation[1] was avoided because the nozzle was detected	Avoided a 2-day unplanned interruption[2] to operations
		Brand as a high-quality supplier was enhanced	Engineering and shop documents were updated to reflect the new tank

1 Without an exact replica of the original tank delivered to the site, the fabricator would have been obliged to dispatch 4 workers at the prevailing hourly rate to the factory to remediate the replica, a task lasting up to 3 days, at a cost ranging from $4800 to $14,400 per day (4 workers * $50 to $150/hour * 24 hours). Additional fabrication materials (steel parts) would be shipped as well for an incremental cost of $3000. The Fabricator typically absorbs this cost, which in this 1 case was estimated at between $7,800 and $17,400.

2 The factory avoids 1-2 days of reduced production capacity. The hourly cost for idled labor in addition to the lost revenue would have been between $5M-10$M.

4.2.6 Conclusions

The scan-vs-BIM process helped both the fabricator and the Customer avoid significant costs. Errors are reduced through using 3D dimensional control processes, eliminating drawing or measurement errors. The fabricator's reputation benefitted from the fast turnaround and accurate work. The Customer avoided an unplanned shutdown of their business. The Customer also now possesses correct engineering and as-built documents.

4.3 Utilization of Scan-vs-BIM for Final Quality Control; Case Study 2

4.3.1 Introduction

In this case, the project owner was a global company that designs and sells powerful magnetic filtration units to the oil and gas industry. The company sells and ships the pressure vessel assemblies along with their filtration systems to allow their clients to integrate their systems into their existing pipelines. The pressure vessel is shipped separately from the magnetic separator array; therefore, the fabrication of the pressure vessel must be accurate in order for the magnetic separator array to be successfully fit into the vessel at or near the final installation site, typically in another country and continent.

To ensure a proper fit between the design and the fabricated as-built, the company decided to use scan-vs-BIM at the end of their fabricator's process.

4.3.2 Technical Objective

To verify the design integrity and tolerances of three fabricated pressure vessels by using scan-vs-BIM techniques.
Assisted by the researcher, the following dimensions were checked and verified on three pressure vessels:

1. Inspection of the Overall exterior geometry
2. Verification of location of diverters

4.3.3 Check 1: Exterior Geometry

It was found that all three pressure vessels had out-of-tolerance deviations. The analysis is shown below (Figure **4**-**2**). For all three vessels, the top flange, the top of the vessel body and the side ID plates had a significant deviation from the design. This was likely caused by the weld connecting the bottom flange to the main body.

The blue object shown in the figure below is the 3D model, the green-yellow-red object is the deviation of the fabricated vessel (as scanned) from the model. The overlay shows a fit and perspective outlining deviations of up 2 CM at the top of the vessel.

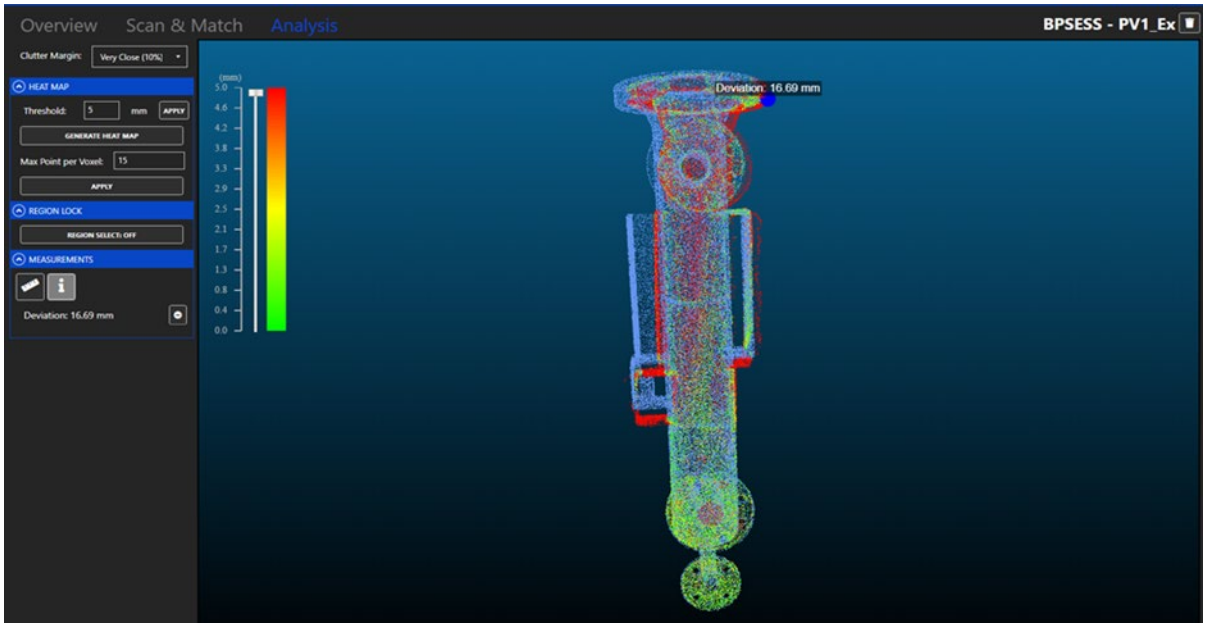

Figure 4-2. Scan-vs-BIM deviation analysis on one of the pressure vessels

4.3.4 Check 2: Diverter Analysis

The company had also requested the inspection of the location of diverters. As highlighted in Figure **4-3**, diverters are structures that are inside the pressure vessel designed to create turbulence in the flow. Due to the small diameter of the pressure vessels, it was not possible to use traditional tools to measure and verify the location of these diverters. That is why the company requested the verification of these structures using scan-vs-BIM.

While the external geometry had significant deviations, using scan-vs-BIM the research team was able to confirm compliance of the three diverters, as shown in Figure 4-3.

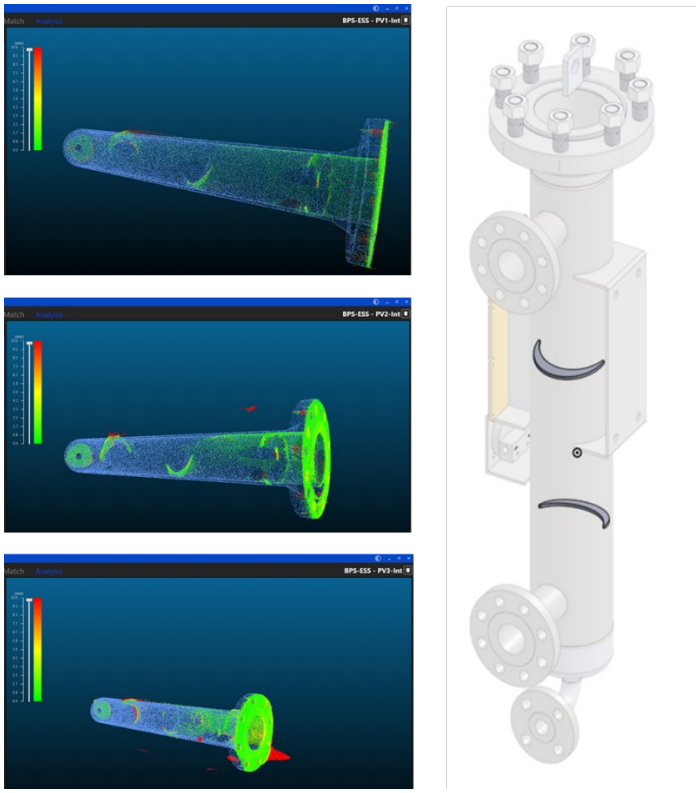

Figure 4-3. Location of three diverters confirmed. The diverters are highlighted in the model.

4.3.5 Impact Analysis and Conclusions

By performing the scan-vs-BIM analysis, the company was able to ensure a proper fit between their filtration systems and fabricated pressure vessel. The utilization of the scan-vs-BIM analysis allowed the company to have the fabricator fix the assemblies prior to shipping to the end-user. A review of this scenario reveals the qualitative and quantitative benefits to the fabricator and the customer, summarized in Table **4-2**.

Table 4-2. Qualitative Impacts

		Fabricator	Project Owner
Benefits	**Direct**	Accurate measurements completed faster	Delivery of pressure vessels was completed on time
		Measurements are complete	Disturbance to site was minimized
	Indirect	the shipping cost (return and resend) of three pressure vessels was avoided[1]	Avoided managing a dispute with their client and their fabricator [2]
		Brand as a high-quality supplier was enhanced	Accurate as-built documentation exists for future projects

[1] Without the early detection of issues, the Fabricator would have sent all 3 faulty pressure vessels to the respective clients, located in Texas, U.S.A. Due to the quality issues, the fabricator would have then been responsible for all remediation costs, including shipping costs from Texas to Ontario and shipping the fixed ones back to Texas again. The shipping cost is estimated to be $5,000 per pressure vessel. As such, the fabricator would have had to absorb $15,000 of cost. To replace this loss to the business, the Fabricator needs to find the equivalent in margin through incremental sales, or $75,000 in new sales (calculated based on a $20% margin).

[2] Each time that an erroneous assembly is shipped, the project owner needs to manage the dispute between their customer and their fabricator. Based on interviews, managing these disputes on average takes between 4 hours of two of the company's engineers ($60-$100/hr) as well as 4 hours of the customer success representative ($30-$50/hr). This means that for the three pressure vessels, the project owner avoided a cost ranging from $1,800 to $3,000. Additionally, depending on the contract, the project owner may be liable for delays as well. This calculation does not reflect the impact of such disputes on the project owner's brand and the potential additional sales, which was the main concern of the project owner in this case.

4.3.6 Conclusions

The scan-vs-BIM process helped both the fabricator and the project owner avoid significant costs. Errors are reduced through using LIDAR technology, eliminating the possibility of shipping incorrect assemblies. The Fabricator's and the project owner's reputation benefitted from the fast turnaround and accurate work.

This chapter (chapter 4) and the previous chapter (chapter 3) were both part of the first stage of the defined evolution stages. Both chapters focus on the value of implementing simple, and rapid quality control checks based on existing scan-vs-3D-model methods. In chapter 3, a new method was provided to allow fabricators that do not have the 3D model to participate in this type of quality control. This chapter covered the case where the 3D model is available and how it can be leveraged throughout the fabrication life cycle.

The next chapter is the beginning of the work done in the second stage of the evolution. In the upcoming chapter, we have defined a formal approach to identify and classify termination points for cases where the 3D model is available. This formalization allows for development of scalable solutions that can take advantage of 3D acquisition tools and techniques while being consistent with existing shop floor processes and required information types.

Chapter 5
Using Termination Points and 3D Visualization for Dimensional Control in Prefabrication

5.1 Chapter Summary and Contribution Statement

This chapter is based on the work published in the journal of Automation in Construction in September, 2021, with the same title (https://doi.org/10.1016/j.autcon.2021.103998). Minor changes are made to some parts of the article to be more consistent with the body of the thesis. Thus, the content of this chapter is not exactly the same as the paper.

I have written the entire manuscript, oversaw and conducted parts of the data collection and processing, facilitated access to the fabrication shop for data collection and helped with the programing of the algorithms. The data collected in this study, along with the data in Chapters 4, and 7 are the result of a 6-month data collection at the partner's fabrication facility in Cambridge, Ontario. Abdullah Majid, Miring Hung, were onsite full time and Steve Chuo and I trained and assisted them with the data collection during their employment. Sidy Ndiongue and Caleb T-Seng Tham assisted with the programming under my direction. In addition, I received editorial advice, feedback, and contributions for the manuscript from Prof. Carl Haas.

To increase productivity, quality, and safety, heavy industrial construction projects are increasingly adopting prefabrication and modularization techniques. This shift, in turn, has resulted in fabrication shops fabricating more complex assemblies with tighter tolerances. However, most measurement in these shops is conducted using manual hand measurement tools, which can be costly and is known to cause significant rework due to geometric noncompliance of termination points in particular. Termination points are defined as the coordinate system points where assemblies connect or are constrained. Automated, 3D-scanning measurement and visualization systems can potentially be accurate, repeatable, and objective sources of termination point data. In this chapter, a new framework for classification and calculation of termination points is presented that is based on automated, 3D-scanning measurement and visualization. The utilization of the framework enables fabrication shops and project owners to adopt effective 3D measurement solutions. To investigate the usefulness of the defined framework, a termination-point-based scan-vs-BIM method is

developed for objects with circular cross sections, such as pipe spool assemblies. The method was validated in an industrial-scale experimental study. The study demonstrated that the new framework could be used to develop applications that are more accurate and provide superior visualization to craft workers during fabrication, and thus potentially improve productivity and reduce rework.

5.2 Introduction

5.2.1 Prefabrication

Use of prefabrication is increasing. In fact, the global modular and prefabricated building market, which accounted for US$ 149.7 billion in 2019, is estimated to grow to US$ 287.2 billion by 2029, and is anticipated to register a Compound Annual Growth Rate (CAGR) of 6.8% [121,122]. This is largely because prefabrication allows more work to be completed in a controlled fabrication shop environment with lower labor costs and more automation, as opposed to a construction site. Adoption of prefabrication also reduces rework [4,61-64], and reducing rework helps projects to reach their schedule and budget targets [68] and to improve quality and productivity [65-67]. Currently, reported rework accounts for 6% to 12% of the cost of a typical construction project [69,70].

However, reducing rework for complicated assemblies and modules is hard; neither conventional methods, nor methods to use highly sophisticated surveying grade measurement systems are reliable enough in practice to control the compliance and mating of termination points. They tend to be ad hoc and not well formalized, and thus their integration as part of the fabrication process is challenging. For complicated assemblies and modules, a formal framework and methods are required to achieve the tighter tolerances that are required to fabricate assemblies offsite accurately, with respect to their termination points, so that the assemblies fit onsite and with each other. Otherwise, the traditional "custom-cut and fit at the job site" approach used in "stick-build" construction must be used along with its attendant delays and costs [29,30]. Formalizing these concepts requires further definition.

5.2.2 Termination Points

The expression "Termination Point" is often used in fabrication shops and on modular and prefabrication projects. We define termination points as the coordinate system points where assemblies connect or are constrained. Termination points are most often the points of connection in

global or local coordinates; they may also serve as critical fabrication control points on an assembly for which dimensional accuracy is important. The most critical issue from a geometric compliance standpoint, when prefabricating assemblies, is to make sure that the relevant measured surface and control points on the assembly are within tolerance with respect to the termination points and that there are no mating issues at termination points. The geometry of the intermediate areas is of secondary importance. An example of a termination point is illustrated in three ways in Figure 5-1. To solve the termination problem, assemblies have to meet at those termination points with the correct orientation as well. This is because, for assemblies to fit in practice, the connection surfaces (for example, flange faces) on both ends of the connecting assemblies must meet each other at the same location with the same orientation, that is they must be "flush" with each other. Otherwise, the fitting and mating work becomes fraught with difficulties and rework.

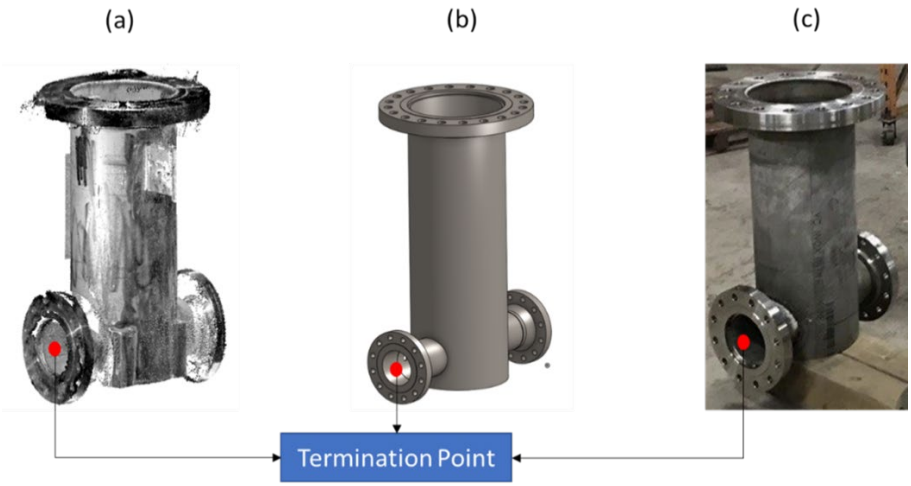

Figure 5-1. Termination point on a pressure vessel assembly: (a) the termination point is shown in the scan (as-built) point cloud, (b) the termination point is shown in the model (as-designed), and (c) the termination point is shown in the as-built photo

5.2.3 Existing Methods for Measurement of Termination Points

In In order to develop a framework and methods for controlling termination points, it is important to understand how measurement is currently done by craft workers in fabrication shops. In fabrication shops, currently, two general approaches exist for the measurement of termination points: (1) manual measurement with bubble levels, squares, straight edges, laser pointers, and tape measures, and (2) semi-automated, highly complex surveying methods (i.e., laser trackers and total stations). Both these

methods are similar in their use of discrete points located on structures and assemblies to verify the length and orientation of assemblies. Those points are located with varying degrees of manual dexterity, human observation, application of geometry and mathematics, use of workflows, and manual transcription of information, all of which can be subject to complexity, confusion and error. The lengths (using centerlines) and the orientation (using termination points, levels, or centerlines) are then calculated with methods that are subject to similar sources of error and compared against the allowable tolerance. An example of the type of verification report, common in current practice that attempts to communicate the results acquired by either of these two approaches is presented in Figure 5-2. Each length has been verified independently.

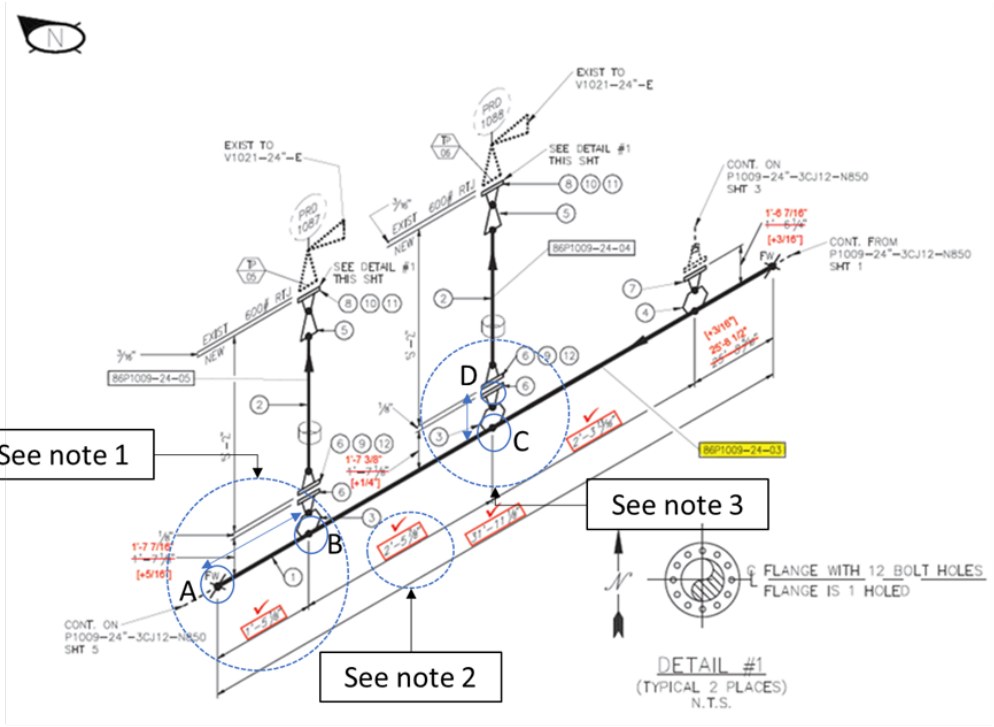

Note 1: The distance between termination point A (which is a field weld) and termination point B is verified. It is shown that both the design and the as-built measurements are 1' – 5/16'' (312 mm)

Note 2: The distance between termination point B and termination point C is verified. The as-built measurement indicates the exact requested measurement on the design as 2'-11/16'' (627 mm)

Note 3: The distances between termination point C and termination point D (center of flange face) is measured and there is a ¼'' (6.35mm) deviation. The designed distance was 1' – 1/8'' and the measurement was 1' – 3/8''

Figure 5-2. An example of a dimensional quality control drawing. The red checkmarks show where the lengths are acceptable.

After calculating lengths and orientations, a dimensional error (noncompliance) is established when the resulting value exceeds the specified (designed or field surveyed) value by $\pm$ the allowable tolerance. Once an error has occurred, the assembly must be reworked. The major shortcomings of the existing approaches are as follows:

1. Lack of visualization. Because of the way measurements are done (lack of dense 3D data); it can be difficult to interpret the results and plan the next steps. In other words, once an error is detected, it is difficult to understand the source(s) of the error(s) and then come to a solution.
2. The current approaches (especially manual methods) fail to account for the interplay between deviations at different points. This can result in undesirable accumulation (or "stacking") of tolerance errors on assemblies.
3. There are inherent inaccuracies in the existing methods that often go unnoticed. Most notably, it is with laser trackers and total stations. Laser trackers are known to be able to provide sub-millimetre accuracies. However, the accuracy index that the device manufacturer claims relates to the calculation of the coordinates between the device and a target. There is no guarantee that the manual placement of the target is done with the same level of accuracy.
4. In the case of Total Stations and Laser Trackers, the setup, acquisition, and post-processing are complicated and time-consuming, thus the turn-around-time between the time of acquisition and reporting of the potential error(s) leads to costly delays (a few days to a week).
5. The process of using tape measures is highly manual, and it can be error-prone in many situations.

   For example, to measure the distance between two bends on a pipe spool, centerlines are hand-drawn more-or-less accurately using a marker on the two straight pipes attached to the two ends of one bend. Once the centerlines are drawn (which is tedious and time-consuming), two squares are placed on the centerlines; the intersection of the squares will

provide the measurement point (commonly referred to as center of the bend) for one bend (two workers are required to hold the two squares). The same process must be applied for the other bend (another two workers are required). Once the centers of the bends have been determined, a fifth worker places and tensions a tape measure between the two centers, and a manual reading is attempted, assuming no-one's hold has slipped (at least five workers required for one reading for one assembly – this is highly inefficient). When sequential pairs of bends are not on the same plane, the spool must be rotated and levelled before it can be measured. Each step involved can introduce an error in the reading or transcription of values. Figure 5-3 shows the relationship between the center bends and pipe centerlines, as well as a group of workers using manual measurement tools for calculation and verification of the distance between the two bends.

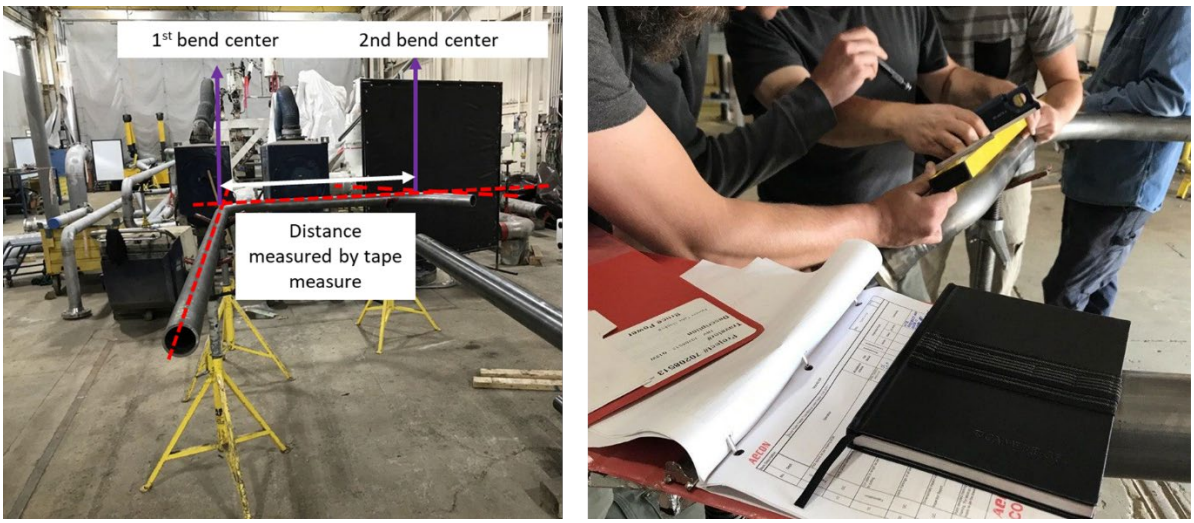

Figure 5-3. An example of measurement with tape measure

5.2.4 Research Motivation – Feeder Tube Fabrication

Hundreds of nuclear reactors around the world are entering the stage of their life where they must be refurbished or decommissioned. The CANDU (CANada Deuterium Uranium) reactors used in Canada are a good example for refurbishment. Each CANDU reactor consists of an array of 480 tubes containing reactor fuel in bundles and coolant that passes through a large horizontal cylindrical vessel called the calandria. At each side of the calandria, there are 480 feeder tubes (totalling at 960 feeder tubes per reactor). Replacement of these feeder tubes (essentially complex pipe spools) comprises the majority of the cost of refurbishment, which can reach close to $300M

per reactor. An example where managing termination points becomes a critical problem can be found in these refurbishment projects. This is because of additional risks engendered by working in a radiated reactor environment, where it is critical to use the best fabrication methods to manage and control tolerances to reduce worker dosage exposure. In these projects, slight distortion in the header from cutting and installing tubes (caused by the heating, cooling and shrinkage related to all forms of welding) will create a displacement and an orientation error at the target termination point. As a result, even feeder tubes that comply with the design (which typically does not get adjusted for the incurred displacement at the target) can experience substantial installation issues. This type of onsite rework event can cause significant financial damage, typically on the order of $100K per error (an estimate provided by a senior executive at a large construction company). Similar fitting and welding related problems emerge in complex and even relatively simple assemblies before they leave the fabrication shop.

5.3 Literature Review

To perform required dimensional quality assurance, researchers have been working on developing tools and techniques superior to manual hand measurement tools. Most developed methods are built on top of data acquired from two types of data input: (1) discreet point-based data collection by laser trackers and total stations, and (2) large and dense 3D data provided by various 3D data acquisition tools. In the following sections, the developed methods using the two types of data as input, as well as their applications, are reviewed. Once existing applications are explored, the knowledge gap for this research is described.

5.3.1 Discrete Point Based Data Collection

The first set of tools to be discussed is the use of optical tools that can produce single data points at each acquisition attempt. These devices are commonly referred to as total stations or laser trackers. Total Stations can read slope and distance from the instrument to a point (target or reflector). The process of capturing points with a total station starts by establishing the initial location of the total station in the world using a GPS (Global Positioning System) or using a benchmark point. The next step is to level the device. Once the global coordinates of the reference point are recorded and the device is levelled, the next step is to define the grid system by siting a second point with a known coordinate. This operation is called "back sighting." After the initial setup (none of these steps are

required with a laser scanner), the total station can be used to record coordinates of single points by having an operator point its telescopic lens and shoot an infrared laser beam towards the target connected physically (with varying degrees of accuracy and precision) to the intended measurement point. Total stations can also directly measure the distance to a point on an object that is reasonably reflective and refractive, within the field of view, and up to a few hundreds of meters away, without a reflector. A high-quality total station is typically claimed to be able to measure distances with an accuracy of about 1.5 millimetres over a distance of 1,500 meters [71]. Researchers have used these devices in a variety of applications. Afeni et al. used total stations recursively to monitor slope instability during mining operations [123]. Other researchers have applied high-frequency measurement using total stations for bridge vibration detection [124], short-span railway deflections [125], and bridge dynamic deformation assessment [126]. McPherron et al. [127] have developed a new measurement process using total stations to measure the artifact orientation measurement for optimized site formation.

As it relates to fabrication dimensional quality assurance (DQA), total stations and laser trackers are seldom used. This is because the acquisition process with a total station has manual elements that make it prone to errors, requires a highly trained operator, and has a high turnaround time to deliver the final inspection report. Furthermore, laying out points in advance to fabricate or build a design is substantially more complex, as geometric calculations of angles and distances are required. Offsets are often required as well. Finally, a target or reflector must be iteratively and manually tracked to each point.

5.3.2 3D-Scanning Data and Measurement

3D-scanning measurement systems are a potentially palatable solution for dimensional control related to termination points, because the data acquisition step is more automated and less time-consuming compared to laser trackers, and their output is visually easier to understand. In addition, Kwiatek et al. have shown that providing feedback in 3D enables faster interpretation of data and faster rectification when rework is necessary [128]. 3D scanning is the activity of collecting 3D data of the as-built environment. This data is often referred to as a point cloud which in its simplest form can be represented as a $3\times n$ matrix where all points are described in a shared global coordinate system. This type of point cloud is also referred to as unordered point cloud, where the order to

which the coordinates of points are recorded in the final array does not change the final result and visualization [129]. Point clouds can also be ordered where each row and column describe a specific point. Ordered point clouds are often described in standardized formats like **.E57 [130]. The utilization of ordered point clouds facilitates various types of rapid and accurate post-processing, such as edge detection using RANSAC [131] and normalized downsampling [132].

3D point clouds can be obtained with a variety of technologies such as photogrammetry [133], Simultaneous Localization and Mapping [80], and Laser Scanning [134]. The applications of 3D point clouds for dimensional quality verification (regardless of how they are obtained) can be viewed in two broad categories: (1) applications relying on the 3D designed model (Scan-vs-BIM), (2) applications without relying on the original design model (Scan-to-BIM).

When the 3D design model is available, the goal of different methods is to compare the two data sets. In its simplest form, the Euclidean distances between points on the scan data are compared against the points on the model for geometric compliance verification [92,93]. More advanced methods are also developed. Nahangi et al. [53] posit that in the case of pipe spool fabrication, assemblies and modules are analogous to robotic systems and, as such, propose the use of forward kinematic analysis to compare the two systems (the scan data vs. the design data) for detection of any discrepancies. Kalasapudi et al. [54] use graph theory to account for the accumulation of errors in assemblies. Both these methods are similar in their systematic inspection, where each assembly is assumed to be a system with the subassemblies and components being treated as members of those systems. These approaches assume that if the compliance of the scan and model as a system is sufficient, the deviations on single elements are of secondary importance.

Other methods rely on extracting features on the scan data with the assistance of BIM. The attributes of the detected features are then compared against the model for verification and dimensional control. For example, centerlines have been used by researchers as an important attribute. Guo et al. [135] used centerlines in piping elements. They achieved a 3.78 mm accuracy in their detection algorithm. This method was initially limited to simple and straight components. Nahangi et al. [73] then improved that method by creating nodes at each joint, which was the center point at those cross-sections parsed from the model to construct the skeletal model on the scanned data. The skeletal model would then be compared against the design model for final dimensional

control. Other methods include detection of location and orientation at the centers of assemblies with circular cross-sections. Maalek et al. [49] used Pratt's circle fitting algorithm and the squared Mahalanobis distance computation.

In cases where the 3D design model does not exist, it becomes more difficult and computationally expensive to perform dimensional quality control. In these cases, the raw data is used to detect parametric features and objects using various methods. The attributes of those features can then be compared against quality control requirements (communicated in 2D format). Dimitrov et al. [48] have developed a generalizable approach to reconstruct elements' geometry using NURBS (Non-Uniform Rational B-Splines). Wang et al. [47] focused on cylindrical objects and used Density-Based Spatial Clustering (DBScan) to help generate parametric models from 3D point clouds. Ahmed et al. [45] used the Hough Transform on cross-sectional slices of pipe assemblies to extract the radius of pipe assemblies. The major shortcoming of their approach was that it assumed the orientation of the pipe spools would be parallel or perpendicular to the scanner's Z-axis. While the described methods in this section are powerful and solve important problems, their use in fabrication shops is very limited. The reasons for this are further explored in the next section.

5.3.3 Knowledge Gap

While there are several advantages in using 3D-scanning measurement systems, fabrication shops have been slow to adopt them. This is largely because existing (industrially accepted) shop methods are predicated on discrete (point-based) measurement techniques. Laser trackers and tape measures are used to make measurements from one feature to another feature on a piece or an assembly, both of which are idealized as points (i.e. whether the point accurately locates the intended feature is subject to the error sources described earlier) with a measured distance between them. Limitations exist with this approach; In the case of a tape measure, the location of both points in space is not known, nor is the orientation of the line between them. In the case of a laser tracker, location of the features in space is known, and orientation of the line can be calculated, but relationship to the assembly of which they are a part or to features in their vicinity can only be visualized by the surveyor and are only partially recorded. Most information is lost and therefore cannot be used in the subsequent processes such as communication with welding and fitting crew members.

In contrast, 3D-scanning captures millions of points on the assembly, but their relationship to relevant features as well as information such as line length and orientation, needs to be post-calculated with algorithms. Increasingly, the post-processing can happen in real time, the results can be displayed in 3D (and in mixed reality, juxtaposed with the model), and the information can be preserved for subsequent processes or for revisiting. However, these capabilities are only now emerging commercially. Furthermore, the slow adoption of 3D scanning systems for dimensional quality control can be explained by the disconnect between the level of abstraction provided by existing 3D scanning and shop methods. Existing 3D scanning methods are sophisticated and have a high level of abstraction. Tolerances are viewed and managed in 3D and features are accurately detected with respect to the assembly. This high level of abstraction, while theoretically superior, fails to accommodate existing expectations from quality control personnel in fabrication shops. On the other hand, manual tools and discrete point-based devices have a very low level of abstraction. Single points are collected and the distances and angles between them are calculated. Figure 5-4 attempts to show the knowledge gap between existing fabrication requirements and advanced 3D scanning-based tools.

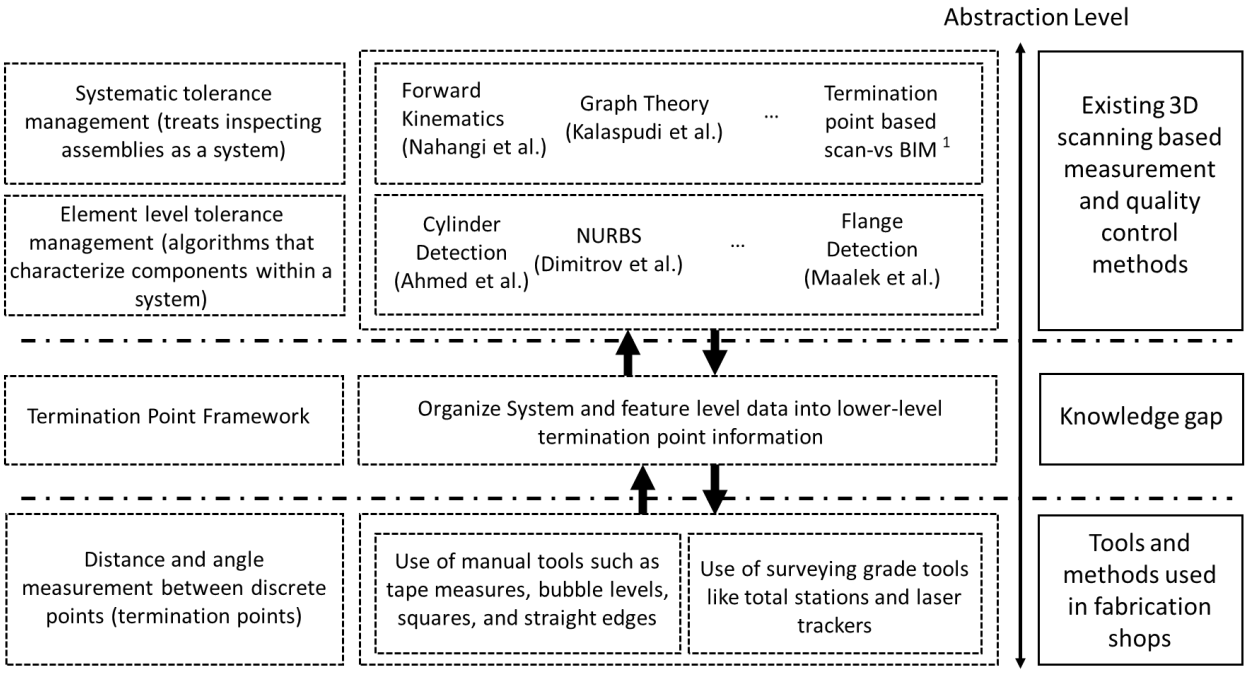

[1] The developed and validated application in this article to demonstrate the usefulness of the termination point framework

Figure 5-4. Visual demonstration of knowledge gap in this research

A framework for managing and calculating termination points needs to be developed to address the knowledge gap described above. The lack of a formalized framework and methods for measurement and management of termination points has resulted in: (1) expensive, inadequate solutions delivered by surveying and engineering teams in the form of complex technology and workflows, and (2) unnecessarily limited use of 3D-scanning measurement and visualization systems in fabrication shops. The development of such a framework has the potential to bridge the gap between existing quality control expectations and advanced 3D scanning methods, thus paving the way towards implementation of automated and 3D measurement tools in fabrication shops' day-to-day processes.

5.4 Framework and Methodology

The methodology section of this research can be broken down into two major parts. First, a framework is defined for measuring and calculating termination points and related assembly object points (in design and as-built space). The defined model allows for generating useful and accurate

termination point information. Second, to demonstrate the application of the defined model, a termination-point-based scan-vs-BIM fitting optimization method for assemblies with circular cross-sections (such as pipes) using 3D laser scanned data as an input is described.

5.4.1 Termination Point Framework

All dimensional quality control measures (manual or 3D scanning based) serve two major goals: (1) build occurs so that critical measurements are within tolerance, and (2) assemblies and modules correctly mate at their designed locations. In doing so, fabricators and project owners can assure the elimination of rework due to geometry misalignment of various assemblies and components. Termination points were broadly defined earlier as the coordinate system points where assemblies connect or are constrained. Termination point(s) are normally point(s) of connection for: (1) module to module, (2) assembly to module, and (3) assembly to assembly (we can consider a module a complex assembly so that the simpler definition holds). To support building a generalized framework and simplify the language around assemblies and modules, we define a system as a set of assemblies and subassemblies where the members of that system create a unified physical structure that is going to be attached to another physical structure (i.e., system). In this definition, a pipe spool can be a system just as a complicated module can be a system, as long as they are going to be connected to another system of assemblies. With this definition of a system and earlier definition of termination points, the problem of controlling critical dimensions as well as multiple assemblies and modules mating can be described as the interface of multiple systems at their termination points. In the process of installing multiple systems, mating at one or many termination points may be required. Also, in the installation process, there always is at least one reference system and at least one connecting system. The reference system is the system to which connecting system(s) will be added. The reference system can be onsite where additional systems are added. Figure 5-5 below shows an example to demonstrate different relationships between termination points, reference systems, and connecting systems.

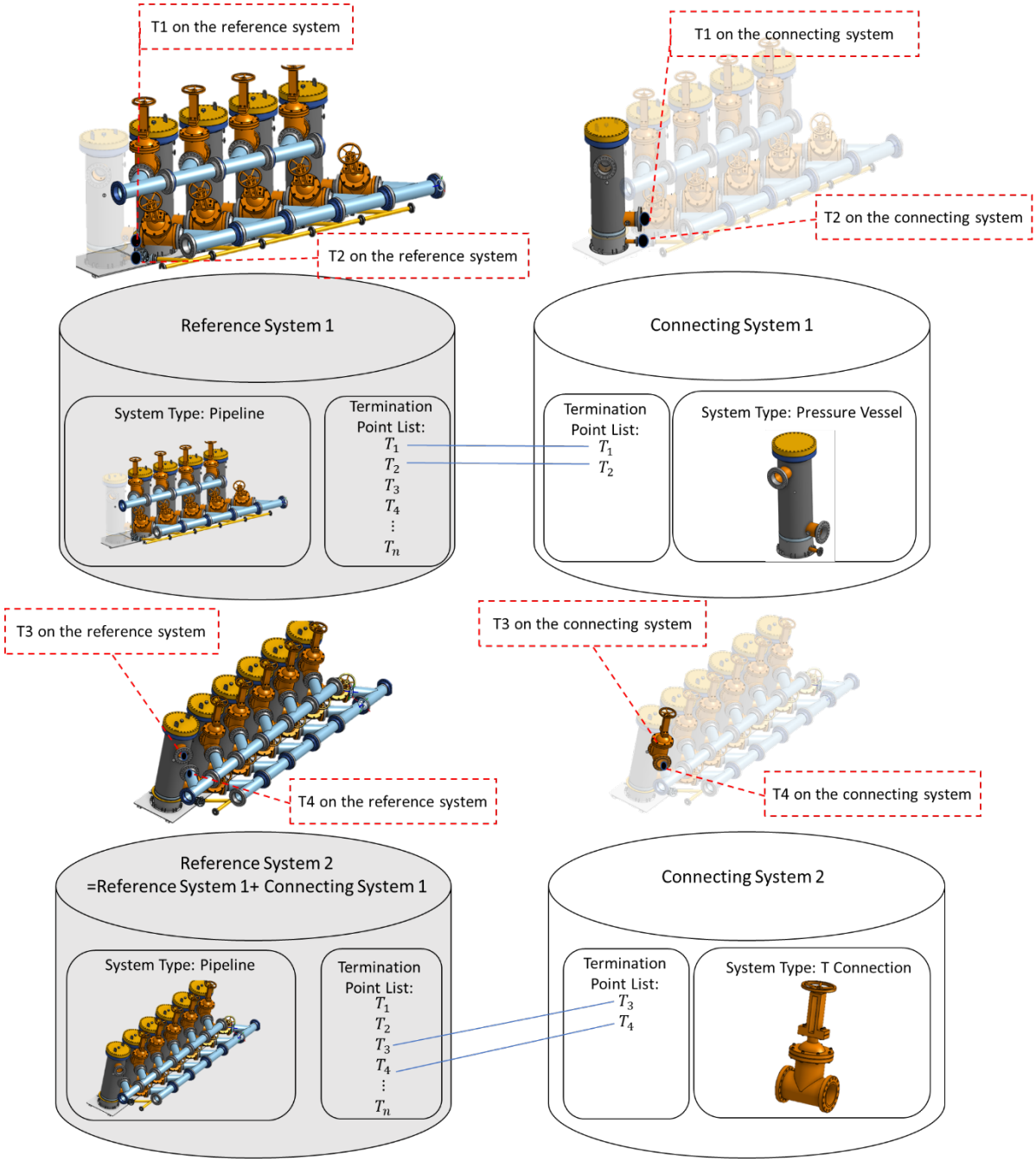

Figure 5-5. Demonstration of various system types and their relationship with various industrial assembly types

To describe the above system of assemblies and modules, we have defined ten classes of termination points and vectors to support all connection scenarios. The classes exist in two spaces: (1) the 3D-model space (designated with subscript *m*), in which the designed locations and

orientations of termination points are defined, and (2) the as-built space (designated with subscript *s*), in which the measured (using the methods previously described) coordinates of features in the as-built assembly are defined, that are then used to calculate estimated locations and orientations of termination points. The classes are defined in Table 5-1 and Table 5-2, and they are illustrated in Figure 5-6.

Table 5-1. Termination point classes in the 3D-model and As-built spaces

Termination Point Class	3D-model	As-built
(A): Origin termination point	A_m	A_s
(B): Destination termination point	B_m	B_s
(C): Assembly mate-to-origin termination point	C_m	C_s
(D): Assembly mate-to-destination termination point	D_m	D_s
(E): Assembly non-mate termination point	E_m	E_s

Table 5-2. Termination vector classes in the 3D-model and As-built spaces

Termination Vector Class	3D-model	As-built
(F): Normal-to-origin termination plane	$\overrightarrow{F_m}$	$\overrightarrow{F_s}$
(G): Normal-to-destination termination plane	$\overrightarrow{G_m}$	$\overrightarrow{G_s}$
(H): Normal-to-assembly mate-to-origin plane	$\overrightarrow{H_m}$	$\overrightarrow{H_s}$
(I): Normal-to-assembly mate-to-destination plane	$\overrightarrow{I_m}$	$\overrightarrow{I_s}$
(J): Normal-to-assembly non-mate termination plane	$\overrightarrow{J_m}$	$\overrightarrow{J_s}$

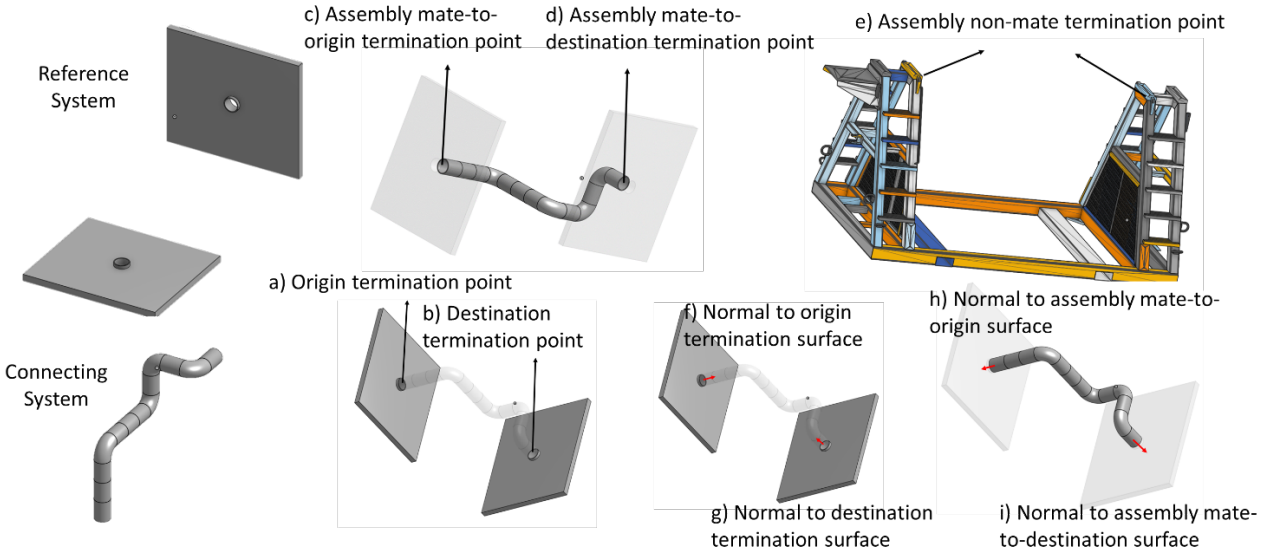

Figure 5-6. Visualization of different termination point classes in the model space. A simple reference system and the connecting system are shown.

An example connecting system is a feeder tube fabricated in a fabrication shop. In this example, the reference assembly is the header in the nuclear reactor vault, where all fabricated feeder tubes will be installed. Termination point classes A and B and termination vector classes F and G all relate to the connecting system. Termination point classes C and D and termination vector classes H and I all relate to the reference system. Termination point class E and termination vector class I can exist on any assembly regardless of the status of their system. These termination classes relate to any critical measurement and termination point that is not a mating location to another assembly.

The origin termination point and normal-to-origin termination plane (classes A and F on the connecting system) are defined as the point and a plane orientation to which the installation of an assembly is initially attempted. Similarly, the assembly mate-to-origin termination point and normal-to-assembly mate-to-origin plane are defined (classes C and H) as the point, and surface orientation on the reference system that are the mating locations to termination classes A and F. Conceptually, termination point classes A and C and their respective normal vectors share the same coordinate and orientation in any defined global coordinate system. The only difference is that classes A and F are defined on the connecting system, and classes C and H are defined on the reference system.

The destination termination point and normal-to-destination termination plane (classes B and G on the connecting assembly) are defined as the point, and plane orientation to which mating is attempted after mating has occurred at the origin termination point. In other words, once termination point class A is co-located (either virtually or physically) with termination point class C and their normal vectors are aligned, the installation of the remaining termination points can be attempted. The distinction between the origin and destination termination point classes is important since, in practice, the installation (fitting and welding or bolting) is always done one termination point at a time. This implies that workers cannot attempt simultaneous installation at various termination points. Similarly, the assembly mate-to-destination termination point and normal-to-assembly mate-to-destination plane (classes D and I on the reference system) are defined as the point and normal vector to which their termination classes B and G have to mate. Conceptually, termination point classes B and D and their respective normal vectors share the same coordinate and orientation. The only difference is that termination point classes B and G are defined

on the connecting system, and termination point classes D and I are defined on the reference system.

This classification and nomenclature supports the generation of methods and applications for quality control of combinations of termination points. More importantly, it enables 3D-scanning measurement systems to be utilized as a primary source of input data. To demonstrate the usefulness of this classification system, a novel method is provided in the following sections that enables users to visualize fabrication errors from the perspective of termination points. Such a perspective is critical in practice.

5.4.2 Termination-Point-Based Scan-vs-BIM Fitting Optimization and Visualization

An extensive body of knowledge exists to use scan-vs-BIM methods as a way to calculate and visualize discrepancies between a 3D scan of an as-built object and its 3D design model [55]. Existing methods assume that all points on the scan point cloud (once the clutter is removed and the object of interest is extracted from the scan point cloud data), and the 3D model are of equal importance. Thus, these methods rely on global fit algorithms such as Principal Component Analysis and then refine the overlay by employing localized optimization in all or selective regions using methods such as Iterative Closest Point. However, in reality, not all points on the model and on the scan are of the same importance. As described earlier, termination points have greater importance to fabricators and quality control personnel. This is due to the fact that: (1) most quality control data is calculated and communicated based on termination points, and (2) typically, tighter tolerances are required by project owners around these termination points.

To address this shortcoming and to use the developed framework, a method is developed that incorporates the termination points and normal vectors in the calculation and visualization of the overlay between a scan and a model. The details of the steps involved in the developed method are described in Algorithm 1. The algorithm starts by superimposing the two data sets (scan point cloud and model point cloud) using traditional algorithms such PCA (Principal Component Analysis) and ICP (Iterative Closest Point). The initial overlay is then updated such that the termination point classes $A_m \; and \; A_s$ are overlaid, and their normal vectors' orientations are aligned ($\overrightarrow{F_m} \; and \; \overrightarrow{F_s}$ are made parallel), as demonstrated in Figure 5-7 on an example pipe spool assembly. This updating

step can be described as locking the overlay around the origin termination point. The described algorithm was programmed by the research team using the C# programming language. The prototype application was used for site testing and validation.

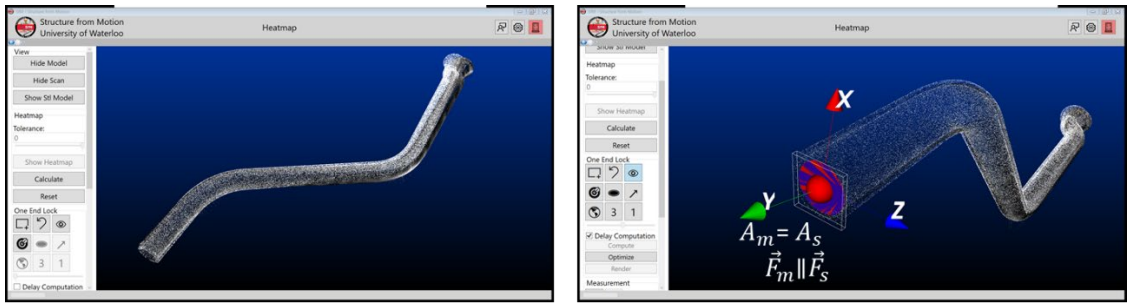

(a) (b)

Figure 5-7. Updating the overlay between scan and model point cloud using the origin termination point and normal to origin termination vector: (a) The initial overlay between the two data sets (PCA + ICP), (b) overlay updated based on origin termination point class A information.

Locking to one termination point can potentially exacerbate the fit error at the destination termination point. There are acceptable rotations around the origin termination point that can reduce the deviation at the destination termination point B. In other words, the normal-to-origin termination plane class (F) between the model and scan space can have small rotational adjustments to minimize location and relative orientation deviation on the destination termination point. An optimization algorithm is implemented to solve this problem and inform fabrication workers of remedial actions that they can consider to minimize the deviation at the destination termination point class B.

To adjust the overlay, such that the deviation between the destination termination points of the model and the as-built $[B_m, B_s]$ is minimized, an optimization algorithm was developed that allows for user-defined rotation around the origin termination points $[A_m, A_s]$ (virtually, and then in reality, if acceptable). The algorithm applies rotation increments in each direction and calculates the root mean square error between the scan point cloud and the model point cloud in the selected region. As soon as the root mean square error in an increment is increased compared to its previous step, the application will accept the previously calculated rotation matrix as the optimized rotation angle and moves onto rotation possibilities in the other axis until searches are completed about all three axes. Finally, using the calculated rotations, the scan point cloud is adjusted, the deviation analysis

colormap (heatmap) is updated, and the minimized distance between the destination termination points is illustrated to ease visualization and understanding. The optimization algorithm is summarized below, and Figure 5-8 shows the result of applying the optimization algorithm.

Algorithm 5.1: Adjusted termination point based scan-vs-BIM for minimization of deviation at the destination termination point

Input: 3D point cloud of as-built assembly $\{S\}$ and $[A_s, B_s, \overrightarrow{F_s} \in \{S\}]$, Initial 3D model point cloud $\{M_p\}$ and $[A_m, B_m, F_m, \in \{M_p\}]$, and $[\propto= (\propto_x, \propto_y, \propto_z)]^*$

Output: Deviation point cloud $\{S'\}$ such that: $|A_s - A_m| = 0, \measuredangle \overrightarrow{F_s, F_m} < \alpha, and\ minize\ f(B_s, B_m) = |B_s - B_m|$

Null $\{Pt_{B_m}\}$:$\emptyset \rightarrow \{Pt_{B_m}\}$

Null $\{Pt_{B_s}\}$:$\emptyset \rightarrow \{Pt_{B_s}\}$

Region Selection

Select a region that contains B_s and B_m

$\{Pt_{B_m}\} = All\ P_i\ such\ that\ P_i \in \{M_p\}\ and\ P_i \in \{selected\ region\}$

$\{Pt_{B_s}\} = All\ P_i\ such\ that\ P_i \in \{S\}\ and\ P_i \in \{selected\ region\}$

Hill climbing X direction

For i=1 to 100

$\propto_{x_i} = i * \frac{\propto_x}{100}$

$Rotate\ \{S\}$ around A_s by $\propto_{x_i}$

$RMSE_i = RMSE\ between\ \{Pt_{B_m}\}\ and\ \{Pt_{B_{s_{Transformed}}}\}$

If $RMSE_i < RMSE_{i-1}$ then i=i+1

If not

$\propto_{x_{optimized}} = \propto_{x_{i-1}}$

End for

Apply hill climbing in Y direction

Apply hill climbing in Z direction

$\{S_{optimized}\}$ =Rotate {S} by $\propto (\propto_{x_{i-1}}, \propto_{y_{i-1}}, \propto_{z_{i-1}})$

Deviation Map

Calculate discrepancy between $\{S_{optimized}\}$ and {M}

Report Deviation at B_M and B_s, and α

Visualize adjusted deviation colormap

* Allowable rotation angle in each direction at the origin termination point.

Figure 5-8 demonstrates the results before and after applying the proposed optimization to the scan-vs-BIM termination points dimensional analysis. Initially, after adjusting the overlay to lock the origin termination point classes ($\mathrm{A_s}\ and\ \mathrm{A_m}$) and aligning their respective normal vectors ($\mathrm{F_s}\ and\ \mathrm{F_m}$), the discrepancy at the destination point is calculated and visualized (Figure 5-8-a). The proposed optimization is then used to calculate a rotation angle around the origin termination point to minimize the discrepancy at the destination termination point (class B). This process is akin to installing one end of the pipe spool and applying rotations by the workers to get the destination point into place. Depending on the material of the assembly and site's condition, the allowable rotation around the termination point may vary. As such, the allowable rotation around each axis is set to be a user input.

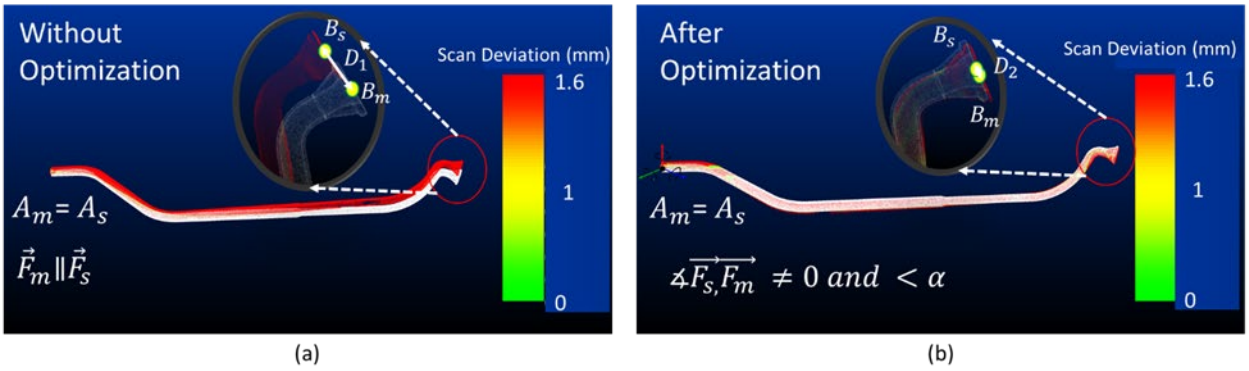

Figure 5-8. (a) color-map after transforming the scan point cloud such that $\boldsymbol{A_s = A_m}$ and $\vec{\boldsymbol{F}}_{\boldsymbol{s}} \parallel \vec{\boldsymbol{F}}_{\boldsymbol{m}}$ (results of section 4.2). (b) The overlay between scan and model is adjusted for $\propto = (\boldsymbol{-1.256^{\circ}, 0.009^{\circ}, -0.296^{\circ}})\ \boldsymbol{and\ D_2 < D_1}$

5.5 Experimental Results

The developed application was tested during the fabrication of 30 feeder tubes. As explained in (section 5.5), feeder tubes are pipe spool assemblies with complex geometry that later need to fit in into a tightly constrained (low tolerance, precise dimensions required) space in the nuclear reactor vault. As such, a fabrication tolerance of $\frac{1}{16}''$ was requested by the project owner. Termination points' normal vector tolerances were not specified in this case. The reason is likely the practical inability of the conventional dimensional tolerance control approaches to measure normal vectors.

The bending of the feeder tubes was subcontracted to a bending company in Ontario, and the partner fabrication shop had the responsibility of fitting and welding different parts of the feeder tubes together. Each feeder tube can be comprised of one to four welding locations (one to four tacking and welding iterations per assembly). See examples in Figure 5-9 and Figure 5-10.

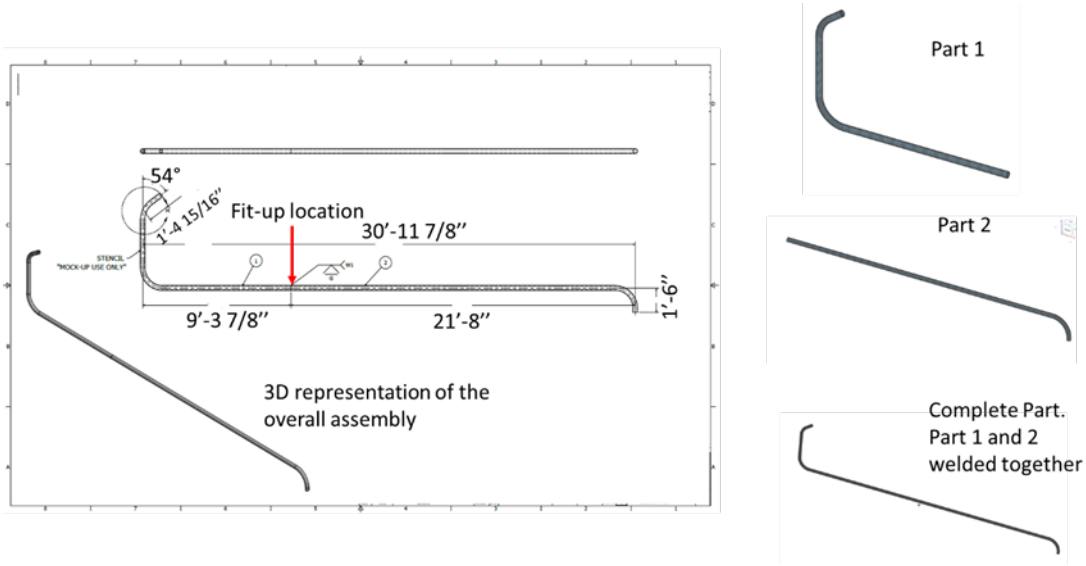

Figure 5-9. An example feeder tube comprised of two parts and one fit-up location.

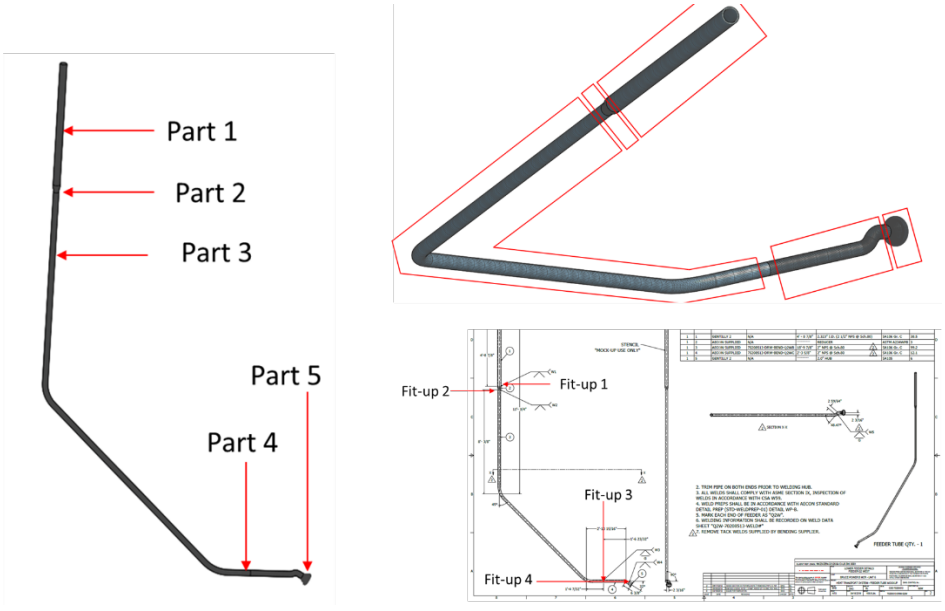

Figure 5-10. An example feeder tube comprised of 5 parts and four fit-up locations.

Each incoming part was inspected by a 3rd party quality control contractor to make sure that all the bending and forming was within tolerance. During fabrication (after initial QC of subcontracted parts), each feeder tube would go through several quality control steps. A summary of all required dimensional quality control steps for the fabrication of feeder tubes follows:

1. Initial check: before the first tack weld, all components are dimensionally checked against design.
2. After tack weld: once a tack weld is completed by the fitters, the relative orientation of attaching parts is inspected.
3. After weld: once a weld is completed, the dimensions are checked again.
4. Before shipment: as the last step, once all the welds are completed and the assembly is ready, the feeder tubes are checked again.

The developed method in this study was tested in conjunction with existing manual tools for more than 400 QC checks as part of the fabrication of 30 feeder tubes. The diameter of the feeder tubes in this project varied between 70 mm to 100 mm, and the principal length varied between 0.5m up to 5m. Two Co-op students were hired and were responsible for data acquisition during fabrication. To obtain the expected accuracy in this project, laser scanning was chosen as the method for 3D as-built acquisition. The laser scanner model used in this study was a FARO Focus M70 (see Table 5-3 for detail). The resolution of the scanner was set to $\frac{1}{5}$ and the quality was set to 4X.

Table 5-3. FARO Focus M70 specifications

Factor	Value
Range error	± 3mm at 25m
Scanning range	0.6m – 70m
Acquisition speed	488,000 points/sec
Weight	4.2 KG

To scan all components, two scanners were used at the same time. On average, three scans were acquired per inspection per assembly. Figure 5-11 shows an example of a feeder tube being scanned in the fabrication shop environment.

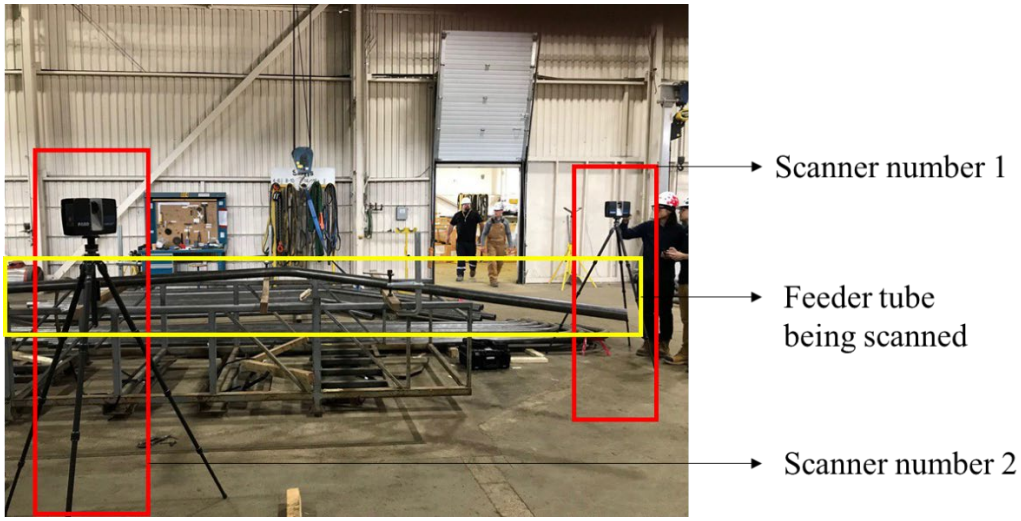

Figure 5-11. An example feeder tube being scanned.

5.5.1 Validation

To validate whether the developed application works correctly, the application was used in parallel to existing industrially accepted methods. In this project, of all 400-dimensional QC steps, the developed method was used on 141 steps. This means that the research team was not able to scan all pipe spools in all of their stages of fabrication (this was because of the fast pace of the fabrication where workers were hired to work on the weekend as well as night shifts). The research team made sure that all 60 feeder tubes were inspected at least once with some of the feeder tubes inspected multiple times (totaling to 141 inspections during the fabrication project) using the developed application software. During the 141 QC checks done using the developed application, 7 fit-ups were flagged as noncompliant. All 7 flagged assemblies were later checked and confirmed by QC personnel as incorrect and had to be reworked. Table 5-4 and Figure 5-12 summarizes the results of the experiments using the developed method in conjunction with existing hand measurement tools.

Table 5-4. Summary of the functional demonstration of the developed framework

Number of feeder tubes	Total manual QC checks	Total QC checks with the new method	Total number of scans acquired	Using the method, the number of detected noncompliant assembles	Number approved flags by QC
60	400	141	500	7	7

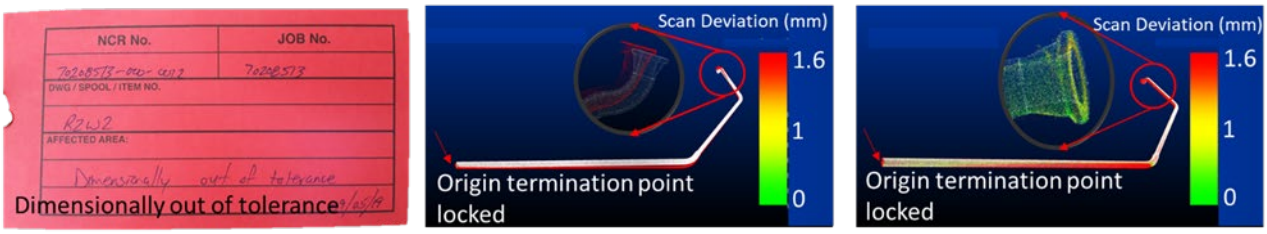

(a) (b) (c)

Figure 5-12. (a) An example NCR (non-compliance report) of a feeder tube with a dimensional error. (b) The error was detected in the developed method, and the results were communicated to the QC personnel. (c) The assembly was reworked and accepted by the application and the QC personnel.

5.6 Discussion and Conclusion

The The growth in prefabrication and modular projects requires fabrication shops to re-evaluate their existing measurement and quality control processes. Existing measurement processes rely heavily on manual hand measurement tools, or highly complex surveying-grade measurement systems, which are often either not reliable, or too expensive, or both. Because of uncertainties related to manual measurement tools and the increasing complexity of designed assemblies, project owners and designers require tighter tolerances and more frequent QC steps to reduce the risk of dimensional noncompliance issues. Dimensional noncompliance causes increased project completion times, increased rework costs, and fabrication worker frustration. To help solve this problem and to equip fabrication workers with easier to use and accurate measurement and visualization tools, 3D scanning and measurement systems can potentially be deployed.

In this chapter, a framework for naming, detecting, and measuring termination points and for their use in dimensional control is presented. The framework can be used to develop useful and accurate measurement applications with 3D data. Applications of the defined framework could potentially even help dimensional control that uses traditional measurement methods, as it provides a standard and a new clarity for specification and communication that does not exist in practice.

Using the developed framework, a termination-point-based scan-vs-BIM optimization and visualization method was developed, and it was validated using functional demonstration based on experiments conducted in a fabrication shop environment. Relying on the method and associated graphic functions to visualize key discrepancies in 3D, quality control personnel made critical QC decisions in practice. The developed method was able to detect and flag 7 fit-up configurations as

noncompliant, which was later verified by the quality control personnel for cross-validation purposes. As discussed in the results section, the results of the analysis were approved by the QC personnel, and flagged assemblies were all reworked. This demonstrated that (1): the developed application based on the developed framework can be used by QC personnel as part of the fabrication process, and (2) the developed algorithm works correctly and can detect incorrect assemblies before they are shipped to the site. Further, the importance of improved visualization of quality control through the use of 3D data and analysis was echoed by plant engineers, "visualizing and discussing errors with the quality control team is a lot easier with this method," said one plant engineer reviewing the presented scan-vs-BIM analysis.

While the developed method is an important contribution of this research chapter, the more significant contribution is the definition of termination point classes and the related dimensional control framework. The developed framework will allow future solutions leveraging 3D scanning to be built compatible with existing quality control and measurement frameworks accepted by the industry. Currently, termination-point-based solutions exist only primarily in the form of fitters' and welders' intrinsic knowledge (unwritten "know-how") and in complex workflows understood only by highly trained surveyors and expert software users. Utilization of the proposed framework can be used as a foundation for many other applications using 3D data that can be used by craft workers and be used as part of the fabrication process.

5.7 Limitations and Future Work

The main limitation of the developed algorithm in this study was the lack of integration with the 3D scanner and software's graphical user interface. The developed application requires the 3D scan point cloud of the built assembly as an input and cannot directly import and register scans from the laser scanner. This in effect creates a two-step process where the scanning and analysis are two sets of activities, which adds time and prevents the application from being used as an in-process application. Due to this lack of integration, the research team had to compensate by hiring extra personnel for the scanning activity, resulting in missing some of the inspection steps. Furthermore, many improvements can be made in the next iterations of the application software to make it more user-friendly, so that fabrication shop workers can easily use it as part of the application process.

For the future, the developed framework should be used to test with other types of assemblies such as structural steel, skids, and complex modules.

Finally, for future related research, the 3D data delivery and communication across different stakeholders can be improved using Augmented Reality. Creating correspondence between a color-map deviation point cloud and the fabricated assembly may be cumbersome on large symmetrical shapes. Superimposing deviation maps onto built assemblies can potentially save time in data interpretation and communication. Additionally, 3D models can be projected onto assemblies as an active guidance system for welders and fitters as they are building assemblies. The active guidance system will be the foundation for a fully autonomous robotic system for the fabrication of complex assemblies. These concepts are further explored in Chapter 8.

This chapter provided a generalized framework to identify and classify termination points. The work carried out was the first part of the second phased of the fabrication evolution stages. Next chapter provides a method and a physical design for determining termination points for cases where the detection is difficult using existing machine vision methods. Existing machine vision methods can calculate termination points on parametric objects (e.g. center point on a circle such a bolt-hole or a flange, planes, and cylinders). However, these methods struggle to detect points on non-parametric surfaces (imagine a random location on a pressure vessel). The next chapter defines a physical structure that can be used to detect termination points on acquired point clouds.

Chapter 6
Development of a Fixture for Automated Detection of Nonparametric Termination Points

6.1 Chapter Summary and Contribution Statement

In this chapter, a method for locating termination points with a marker apparatus and a 3D scanner is described. The method and the marker can be used for detecting termination points on non-parametric surfaced and works within the defined framework in the previous chapter. The defined method replaces the need for purpose-built surveying and marking systems that require a trained surveyor to operate and can be integrated with laser scanners.

This chapter is based on the work published by World Intellectual Property Organization on November 18 , 2021, with the title "System and Method for Discrete Point Coordination and Orientation Detection in 3D Point Clouds". Minor changes are made on some parts of the document to be more consistent with the body of the thesis. Thus, the content of this chapter is not exactly the same as the patent filing.

I have written all of the manuscript, developed the original idea, produced the initial design of the target, and done the initial prototyping. Additionally, I have conducted the test cases that are later explained in this chapter. Wilson Li has helped with the programing for the detection part in the point clouds. I received editorial advice, feedback, and contributions for the manuscript from Prof. Carl Haas and Mark Pecen.

6.2 Overview

Two general types of physical fixture and required post-processing methods are developed that allow for the detection of coordinates and orientation of termination points in a point cloud representing an assembly. The first type leverages a special geometric configuration to allow for automatic detection of the target's reference points' (defined below) coordinates and orientations. The second type uses unique features such as edge detection, feature detection, and Machine Learning based detection to find the coordinates and orientation of the target's reference points. The calculation of termination points is a critical activity, since existing measurement approaches

rely on the accurate calculation of these points on assemblies, as explained in the previous chapter. The utilization of the proposed targets in conjunction with 3D data acquisition units provides a net new measurement method as an intermediary solution between manual tools (i.e., tape measure) and surveying grade tools, such as Total Stations and Laser Trackers.

6.3 Definitions

6.3.1 Reference Points

Each target has at least one reference point. Once a target is detected, the coordinate and orientation of the reference point(s) (in the global coordinate system) related to the target can be obtained. Also, the normal vector of the target at each reference point can be calculated. Note that the reference point may or may not be the center point of a target. This depends on how the reference point is defined with respect to a target.

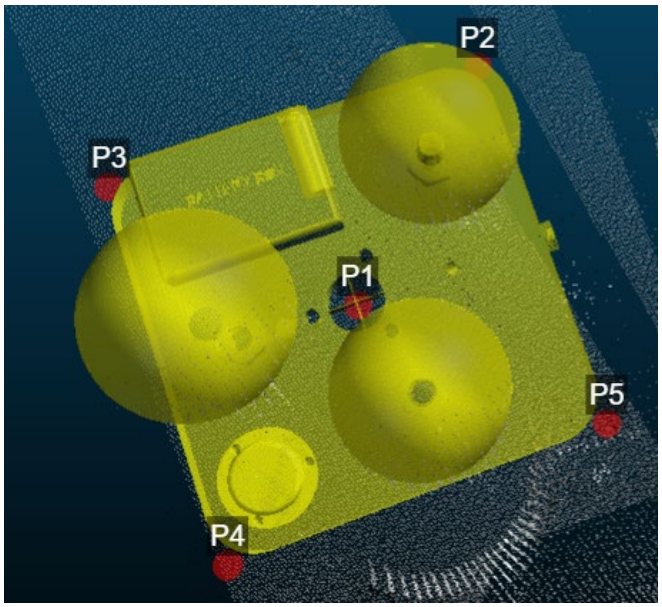

Figure 6-1. Example target with 5 reference points (P1 to P5)

6.3.2 Termination Target

Termination Target is a physical fixture. By installing the reference point(s) of a Termination Target onto a termination point, the coordinate and orientation of that termination point can be obtained. Two general types of Termination Targets exist:

(1) Using specific geometry to calculate the coordinate and orientation of reference points.

(2) Using unique patterns that can be detected by a 3D acquisition unit. Various methods can be used to detect each target, including machine vision-based approaches such as pattern recognition, edge detection, and RANSAC. Some example targets that can be used are shown below.

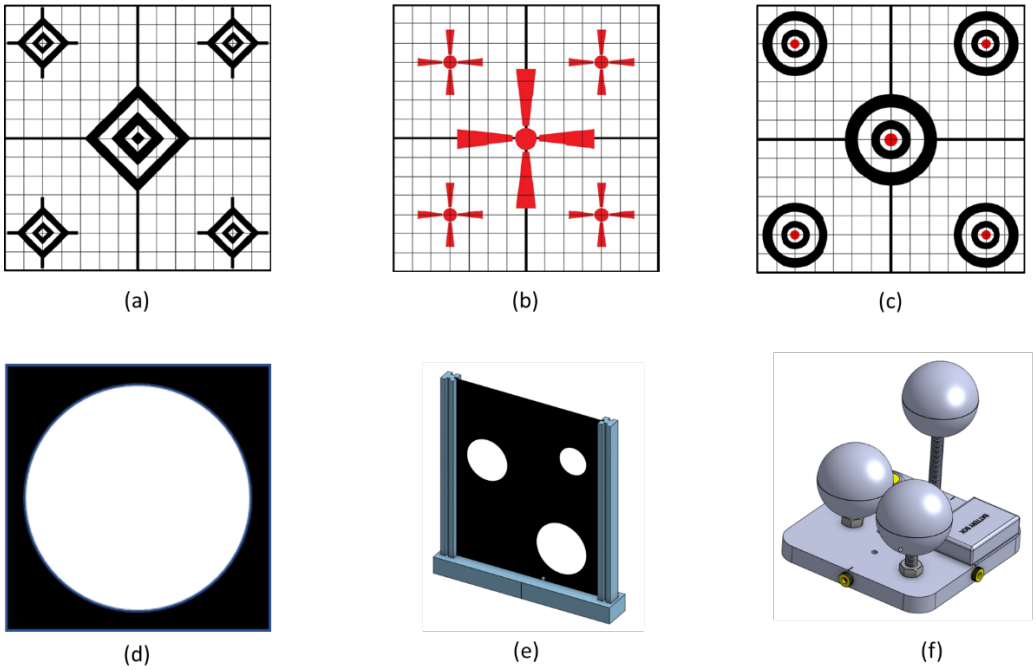

Figure 6-2. Example targets that can be detected via 3D acquisition unit. (a), (b), and (c) example targets leveraging pattern recognition for detection. (d) edge detection combined with RANSAC. (e) Edge detection combined with RANSAC and optimization based on geometry. (f) RANSAC and geometry-based optimization.

6.4 Knowledge Gap and Problem Statement

The problem addressed by the device described in this chapter is the detection of coordinates and orientation of termination points on 3D objects in their corresponding 3D point cloud. This is accomplished by placing reference points of Termination Targets onto termination points of interest. The developed algorithms can then accurately detect the location of such termination points. As described in the previous chapter, currently, termination-point-based solutions exist only primarily in the form of fitters' and welders' intrinsic knowledge (unwritten "know-how") and in

complex workflows understood only by highly trained surveyors and expert software users. The proposed device can be used in conjunction with laser scanners to allow fabrication workers access termination point based solutions that are easy to use.

Regardless of the technology that is used to capture an object (laser scanning, SLAM, or photogrammetry), the result will always be a 3D point cloud where the object is represented by series of points with known coordinate measurements.

The challenge that this chapter addresses is the ability to draw an accurate and one-to-one relationship between a point on an object and a point on a point cloud. For example, Figure 6-3 shows a case where the fabricator is interested in knowing the distance between points A and B. As shown in Figure 6-3-(d) and Figure 6-3-(e), there are several hundred points in each region, and rapidly finding the correct point accurately and repeatably is not possible using existing approaches. Complex best fitting algorithms need to be used, which are time-consuming and too complex for implementation in fabrication shop environments. The incorrect selection of points A and B on the point cloud can result in erroneous confirmation or rejection of the assembly. It should be noted that A and B are points of intersection between the panels on the assembly and their location can easily be visualized by an operator on the actual physical structure. However, their location cannot be easily determined in the as-built point cloud without the use of the proposed target in this chapter.

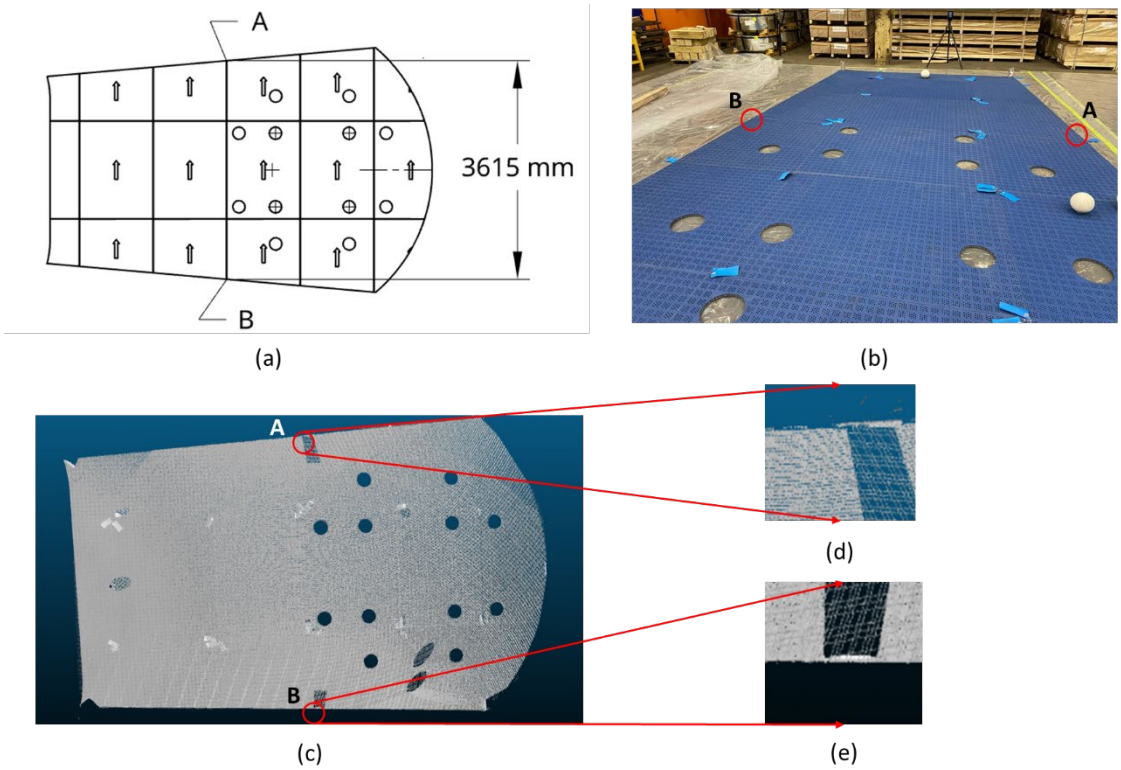

Figure 6-3. The challenge in finding correspondence between specific points on the object and the 3D as-built point cloud of the object. (a) requested distance measurement on the design drawing. (b) points A and B on the as-built assembly. (c) the as-built point cloud. (d) points on the point A's neighborhood that can be potentially selected as point A by a user. (e) points on the point B's neighborhood that can be potentially selected as point B by a user.

Due to this challenge (the inability to rapidly find correspondence between a termination point on an object to the termination point in the point cloud), 3D point clouds are rarely used for control and verification of reference points in assemblies, structures, or manufacturing parts.

Currently, alternative acquisition technologies with different underlying methods are being used for the detection and verification of reference points on built objects. These approaches were extensively discussed in the previous chapter.

6.5 Method and Framework

To solve the problem described in Section 6.4, a 3D mobile fixture was designed (hereinafter called "Termination Target") for assisting in the detection of any termination point in 3D the as-built point cloud. To find correspondence between an object and the 3D point cloud, the Termination Target should be installed on the point of inspection. After positioning the Termination Target on the point of interest on an object, the problem of finding a specific point in an assembly from a 3D point cloud can then be translated into finding the reference point on the Termination Target within the 3D point cloud (the required offsets can be post-calculated). Two types of Termination Targets are defined, within each type various methods and designs can be employed to calculate the reference points. The rest of this section explains the overall methodology, the workflow for using the targets, and the target types and some examples.

6.5.1 Methodology

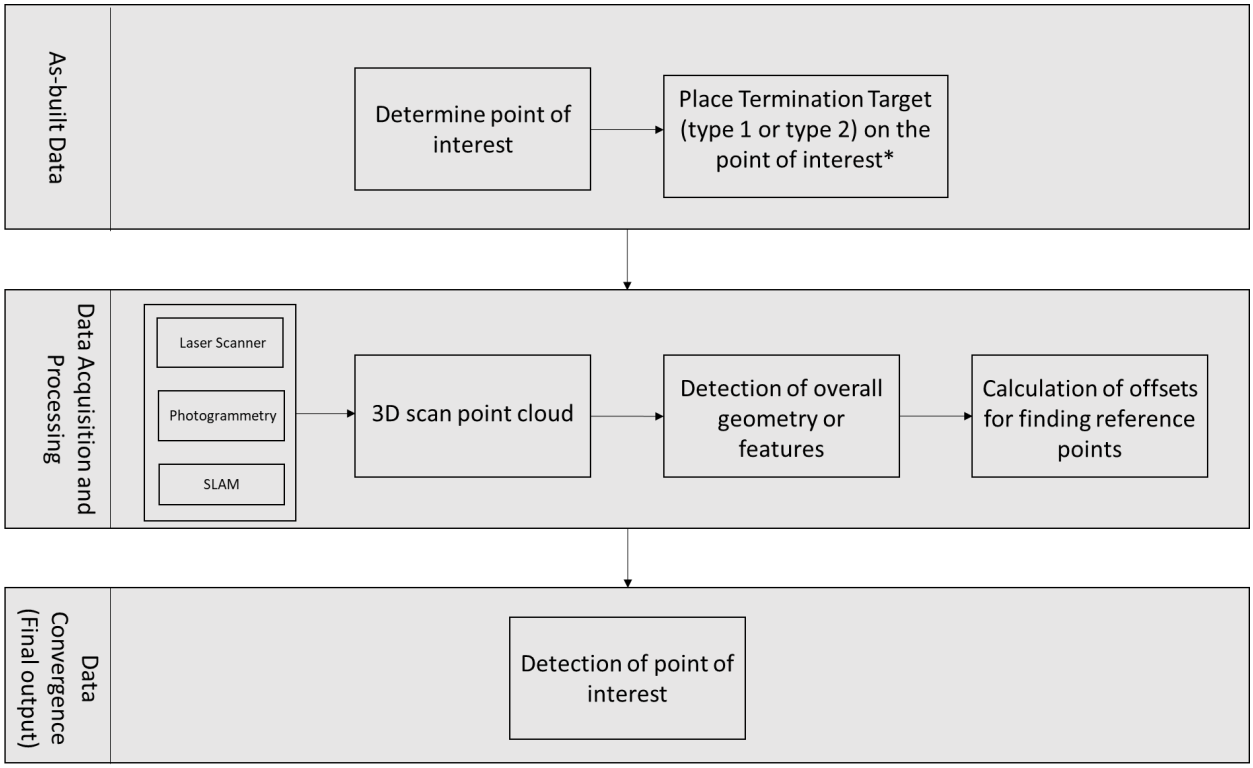

Figure 6-4. Methodology description for detection of termination points using developed fixture.

Figure 6-4 shows the methodology for detecting termination points on objects in 3D scan point clouds, regardless of the source of acquisition and the type of termination point (parametric vs. nonparametric). The methods used in the two types of Termination Target are based on using RANSAC (RANdom SAmple Consensus), spatial geometry, pattern recognition, feature detection, and deep learning. The utilization of this methodology can result in rapid and accurate detection of termination points in assemblies and structures. Two types of targets and methods have been discussed.

The detection module works in principle by synthesizing the information of the point cloud subset scanned on the target into a precise representative point and vector geometrically related to it in space. Thus, a relatively sparse and accurate point cloud subset acts as geometric survey that is processed statistically to define an arbitrary and precise point in space near it that would likely be missed by the scanner otherwise.

6.5.2 The Workflow

The workflow for the detection of specific points on objects within 3D point cloud is as follows:

1. Determination of the point of interest
2. Placement of Termination Target on the point of interest
3. Acquisition of a 3D point cloud
4. Detection of the point of interest

Example placement of a Termination Target to obtain the required measurement in Figure 6-3 is show in Figure 6-5.

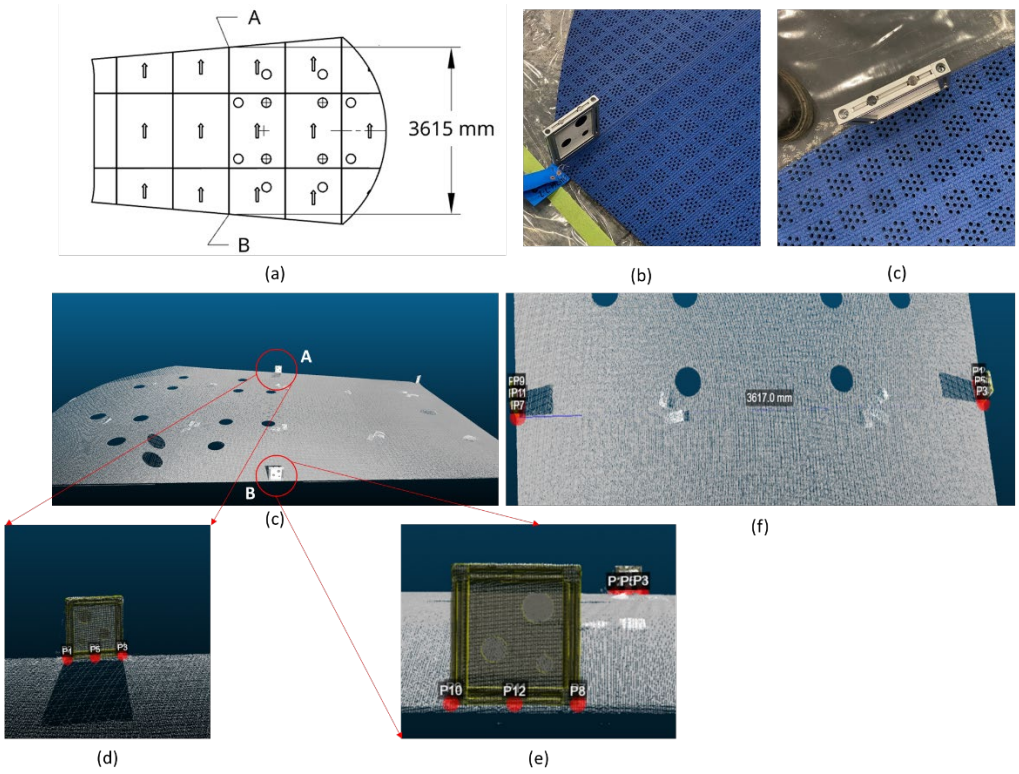

Figure 6-5. The point of interest detected on the object and 3D model. Termination Target is then placed on the point of interest to find correspondence between the point of interest and the 3D point cloud. (a) The required distance from A to B derived from the design drawing. (b) Placement of termination target on point A. (c) Placement of termination target on point B. (d) Detection of the first termination target and the associated reference points. (e) Detection of the second termination target and the associated reference points. (f) Calculating the distance between termination points detected by the targets.

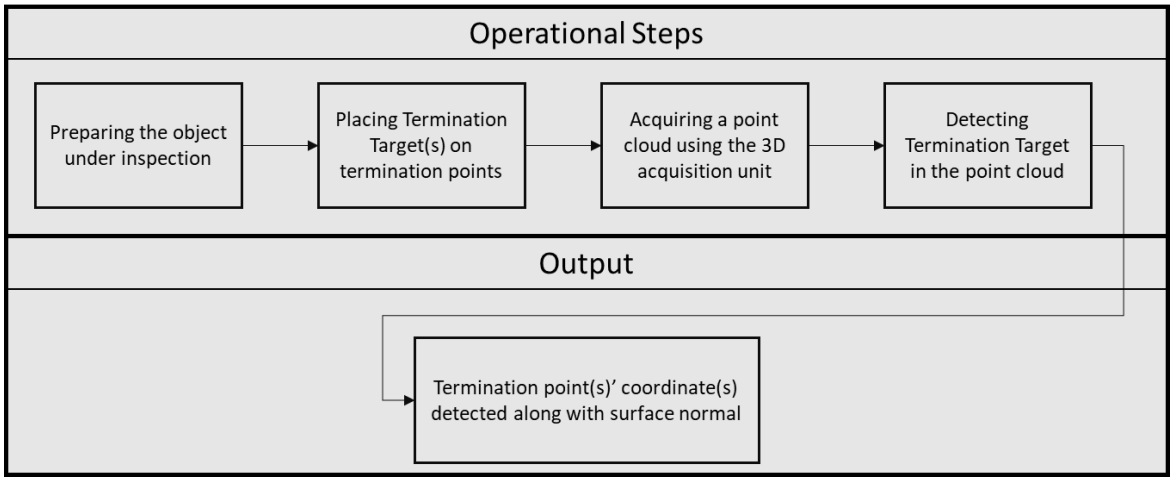

Figure 6-6. Steps involved in using Termination Target.

6.6 Termination Target Type 1

The first Type of Termination Targets are ones comprised of targets that their geometry allows for accurate detection of reference points coordinate and orientation. In this section, two examples are shown. However, depending on the application and geometric constraints, other geometric configurations may be utilized.

6.6.1 Example 1:

The drawing below shows the parametric relationship and dimensions of Termination Target components. The described Termination Target is comprised of a main base, a magnetic layer (this layer is in the bottom to allow for the target to easily attach itself to stainless-steel structures), 3 spheres (at least), and 3 shafts connecting the spheres to the base. Figure 6-7 provides a front view, a top view, a bottom view, and a perspective view of the Termination Target.

The dimensions on the drawings can be explained as follows:

- D1, D2, and D3 are the diameters of the three spheres.
- L1, L2, and L3 are the lengths of the connecting shafts.
- A1, A2, and A3 are the diameters of the shafts (the shafts can be any shape and do not have to be cylindrical)
- Db is the diameter of the main base (the base can be any shape and does not have to be cylindrical)
- R1, R2, and R3 are the distances of the shafts base to the reference point.

The reference point was defined as the point to which that should be placed onto the Termination Target of interest. In other words, the reference point on the Termination Target is the point of interest on the object of interest. Calculating the location of the reference point provides the correspondence between the scan point cloud and the termination point of interest.

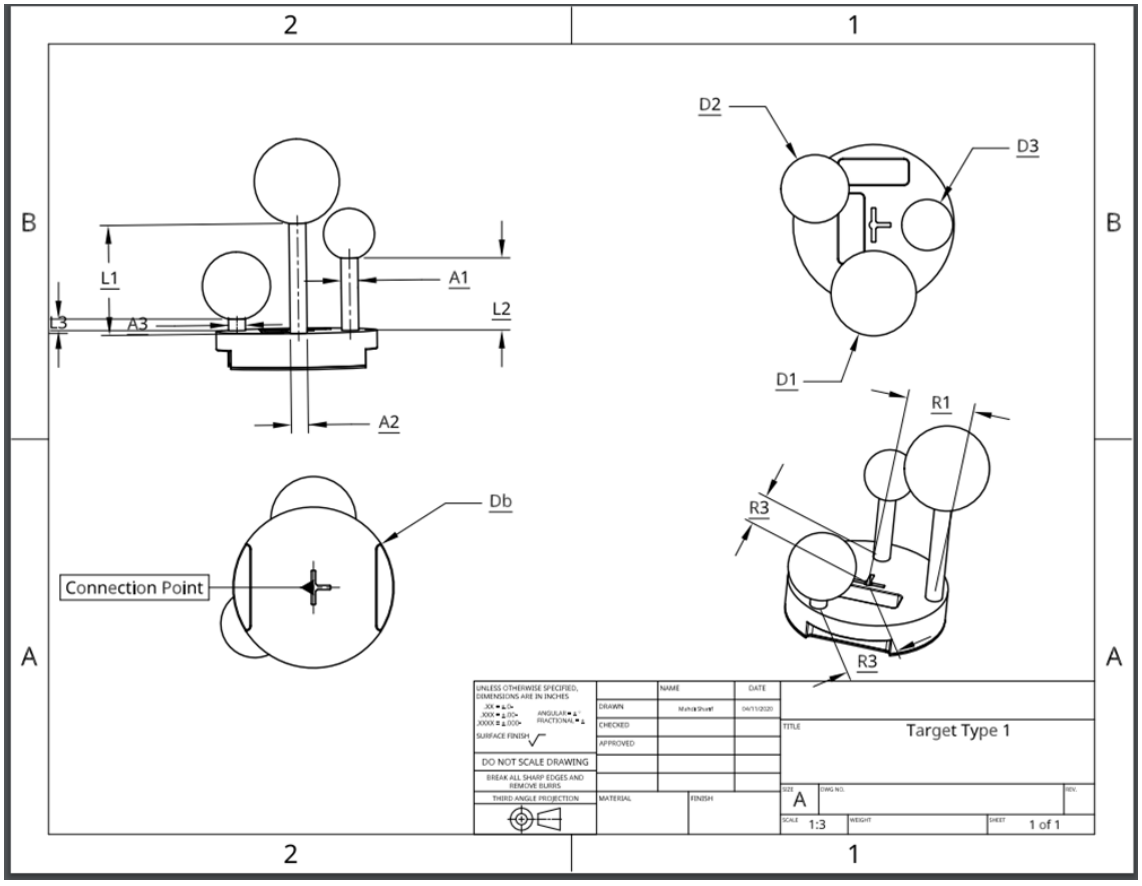

Figure 6-7. Drawing of Termination Target Type 1

The problem of finding a termination point (a point of interest) on an assembly from a 3D point cloud can be translated into finding the reference point on the Termination Target using a 3D point cloud. Figure 6-8 shows the methodology used to find a termination point using Termination Target. Each section is explained herein.

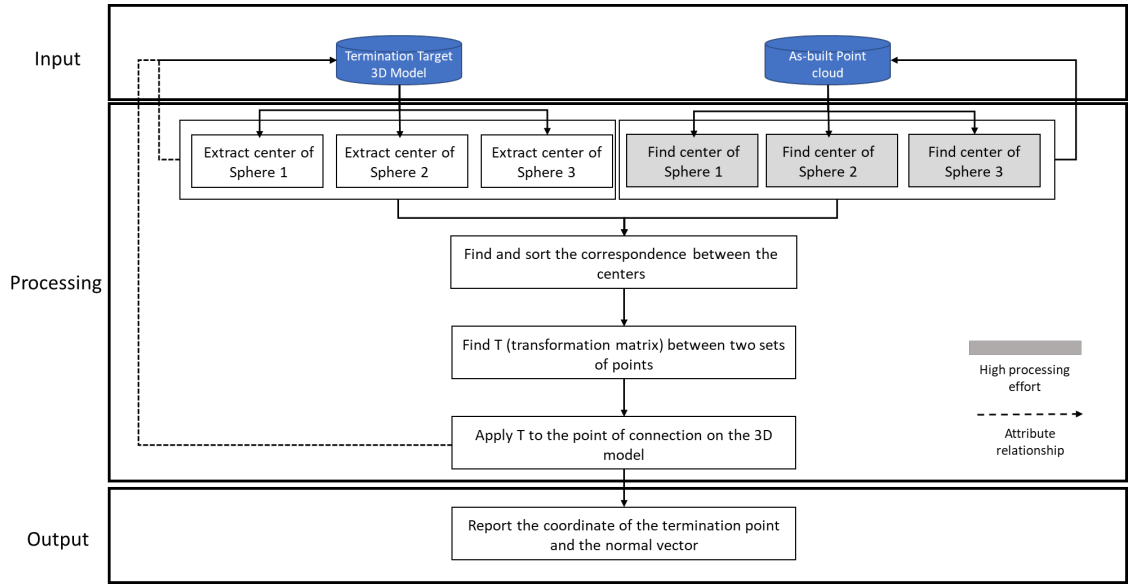

Figure 6-8. Overall methodology explained for finding termination points using Termination Target.

Input

The inputs are the 3D model of the Termination Target and a point cloud of the scene that includes a Termination Target placed on a termination point. The centers of three spheres and the point of connection are attributes of the design, and the coordinates of these are known from the 3D model. These known attributes are as follows:

- The coordinate of the center of Sphere 1 (R1= D1/2): $C_A = (X_A, Y_A, Z_A)$
- The coordinate of the center of Sphere 2 (R2=D2/2): $C_B = (X_B, Y_B, Z_B)$
- The coordinate of the center of Sphere 3 (R3=D3/3): $C_C = (X_C, Y_C, Z_C)$
- The coordinate of the reference point: $C_D = (X_D, Y_D, Z_D)$
- The normal vector (orientation) at of the reference point: $N_{C_D} = (N_{X_D}, N_{Y_D}, N_{Z_D})$

It is important to understand that the relationship between the center of the spheres and the reference point is known since they are a characteristic of the design model.

The second input is a point cloud of the scene including a Termination Target that has been placed on a termination point or any point of interest. An example point cloud of Termination Target is

shown below. Note that depending on the line of sight and the geometry of the termination point, a different point cloud representation may be obtained. The developed methodology will work regardless of the line of sight, as long as the 3 spheres are visible.

The coordinates of the spheres in the point cloud are unknown, which will be calculated in the next step. Let's name the center of the spheres as follows:

- The coordinate of the center of Sphere 1 (R1= D1/2): $C_{A'} = (X_{A'}, Y_{A'}, Z_{A'})$
- The coordinate of the center of Sphere 2 (R2= D2/2): $C_{B'} = (X_{B'}, Y_{B'}, Z_{B'})$
- The coordinate of the center of Sphere 3 (R3= D3/2): $C_{C'} = (X_{C'}, Y_{C'}, Z_{C'})$

Processing Methods

Two methods, automated and semi-automated, are suggested that can be used for finding the spheres in the 3D scan point cloud.

Automated:

The first step is to find the center of the spheres in the point cloud. To do this (finding 3 spheres in the space), an octree data structure is implemented to structure the data points.

Octree

An octree is used to structure the data in a way that the closest points to an arbitrary point are searchable. Implementation of Octree allows for compartmentalization of points into neighbourhoods based on their Euclidean distances. The Octree method allows for stopping the subdivision based on the number of points inside a bin. The information regarding the neighbouring bins also becomes accessible.

After dividing the space into bins where the principal length of each bin is 2*Db, RANSAC (RANdom SAmple Consensus) is used to search for spheres in each bin. Note that the input parameter of the RANSAC algorithm is the radius of the sphere that is being searched for and the level of confidence, which is a measure that controls how strict or easy the acceptance threshold is. Given that the manufacturing of the Termination Target can be obtained with 0.005'' accuracy, a high confidence level can be assigned to avoid false positives.

Applying the Octree and RANSAC will allow finding the center of the spheres in the space, hence the coordinates of $C_{A'}, C_{B'}, C_{c'}$ are known in the coordinate system of the scan point cloud.

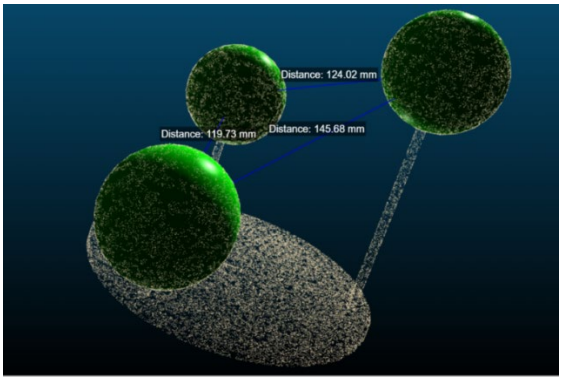

Figure 6-9. Three spheres found in the scanned point cloud using Octree and RANSAC

Semi-Automated:

The semi-automated approach to find $C_{A'}, C_{B'}, C_{c'}$ includes a manual initiation point for the RANSAC method. This means that a user will be asked to provide a point on Sphere 1 in the scan point cloud. Using that point, the best sphere will be fitted to Sphere 1 and the coordinate of C_A, will be determined. Knowing $C_{A'}$, D1, D2, D3, R1, R2, and R3, the potential candidates for finding the center of sphere 2 will be limited to the circumference of a sphere whereby the radius is the distance between the C_A and C_B. Now that the potential answer space has been substantially reduced, the RANSAC algorithm can find the center of Sphere 2. A similar method can be applied for the 3rd sphere to find $C_{C'}$. In the end, $C_{A'}, C_{B'}, C_{c'}$ are found.

The next step is to map $C_{A'}, C_{B'}, C_{c'}, \mathrm{C_A}, \mathrm{C_B}, \mathrm{C_C}$ which are expressed in a different coordinate system to the coordinate system of the point cloud. In other words, the transformation matrix T has to be found that overlays set of points related to the model ($P_m = \{C_A, C_B, C_C\}$) to another set of points related to the scan point cloud ($P_s = \{C_{A'}, C_{B'}, C_{C'}\}$)

To do this, initially, a sorting algorithm is applied to find the correct correspondence between spheres (to map the sphere 1 (R1=D1/2) in the model to the sphere 1 (R1=D1/2) to the sphere in the scan).

After sorting, Principal Component Analysis (PCA) is used to find the transformation matrix (T).

Output

Once T is found, the coordinate of a termination of an assembly can be calculated as follows:

$$Coordinate\ of\ the\ termination\ point = T \times C_D$$

Additionally, the normal vector at the termination point can also be calculated as follows:

$$Normal\ vector\ at\ the\ termination\ point = T \times \vec{n}_D$$

Where $\vec{n}_D$ is the normal vector at the reference point in the design model of the Termination Target

6.6.2 Example 2:

The drawing below shows the parametric relationship and dimensions of the second example the embodiment type 1 of a Termination Target and its components.

In this embodiment, the Termination Target includes a main base, a magnetic layer, 2 spheres (at least) stacked on top of each other, and 2 shafts connecting the spheres to the base.

The dimensions on the drawings can be explained as follows:

- D1, and D2 are the diameters of the two spheres.
- L1, and L2 are the lengths of the connecting shafts.
- A1, A2, and A3 are the dimensions of the base, The base can be cylindrical as well or any other shape.

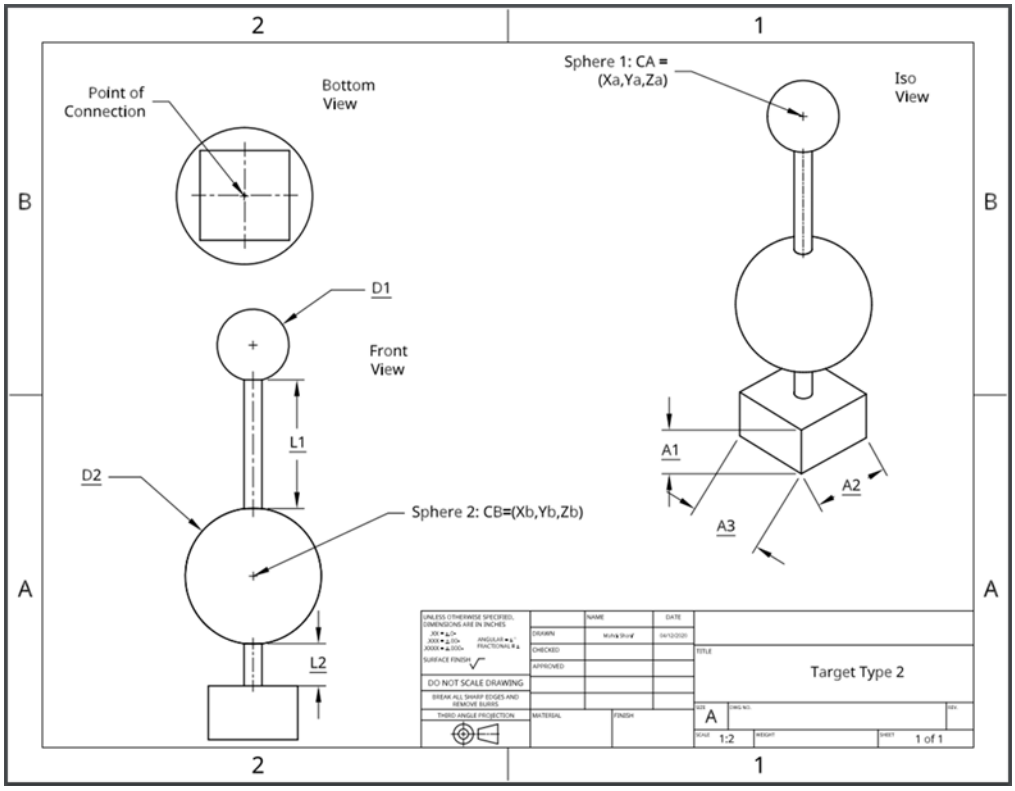

Figure 6-10. Drawing of Termination Target Type 1, second example

The below figure shows the methodology used to find the reference point's coordinate in a scan point cloud using the second design of Termination Target type 1.

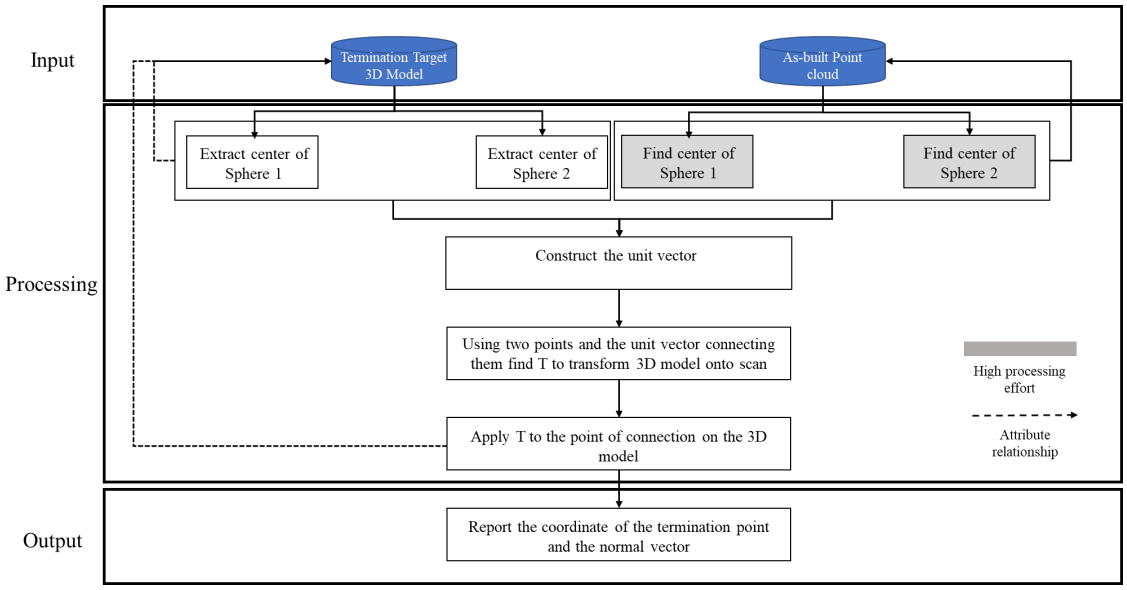

Figure 6-11. The overall methodology for finding correspondence between an object and the 3D point cloud scan

Input

The coordinates of the spheres in the Termination Target model is as follows:

Sphere 1: $C_A = (X_a, Y_a, Z_a)$

Sphere 1: $C_B = (X_b, Y_b, Z_b)$

Also assign the coordinate of the point of connections as:

Point of Connection: $C_c = (X_c, Y_c, Z_c)$

Let's assign the coordinates of the centre of the spheres and the point of connection in the scan point cloud as:

Sphere 1: $C_{A'} = (X_{a'}, Y_{a'}, Z_{a'})$

Sphere 1: $C_{B'} = (X_{b'}, Y_{b'}, Z_{b'})$

Point of Connection: $C_{c'} = (X_{c'}, Y_{c'}, Z_{c'})$

The problem of finding correspondence between an object and a scan point cloud can now be expressed as finding the coordinates of $C_{c'}$.

Processing

Similar to the previous example for finding the centre of spheres, two approaches can be used:

Automated

The first step in the processing workflow is to find the center of the spheres in the point cloud. To do this (finding 2 spheres in the space), an octree data structure is implemented to structure the data points.

After dividing the space into bins where the principal length of each bin is $2*({A_1}^2 + {A_2}^2 + {A_3}^2)^{0.5}$, RANSAC (RANdom SAmple Consensus) (note that the principal length of the bins can be changed) is used to search for spheres in each bin. It is important to note that the input parameter of the RANSAC algorithm is the radius of the sphere that is being searched for and the level of confidence which is a measure that controls how strict or easy the acceptance threshold is. Given the manufacturing of the Termination Target is with 0.005'' accuracy, a high confidence level will be assigned to avoid false positives.

Applying the Octree and RANSAC will allow finding the center of the sphere in the space, hence the coordinates of $C_{A'}, \text{and } C_{B'}$ are known in the coordinate system of the point cloud.

Semi-Automated

Another approach to find $C_{A'}, \text{and } C_{B'}$ is to include an initiation point for the RANSAC method. This means that the user would be asked to provide a point on Sphere 1 in the scan point cloud. Using that point, the best sphere will be fitted to Sphere 1 and the coordinate of C_A, will be determined. Knowing $C_{A'}$, and L1, the potential candidates for finding the center of sphere 2 will be limited to the circumference of a sphere whereby the radius is L1. Now that the potential answer space has been substantially reduced, the RANSAC algorithm can find the center of Sphere 2 and hence $C_{A'}, and\ C_{B'}$ are found.

Knowing the coordinates of $C_{A'}, and\ C_{B'}$ the unit vector connecting the spheres and the direction of the normal vector can be calculated. The unit vector can be calculated as follows:

$$\vec{U} = \frac{C_{A'} - C_{B'}}{|C_{A'} - C_{B'}|}$$

The relationship between the unit vector with the normal vector at the connection point and centre of spheres is shown figure below.

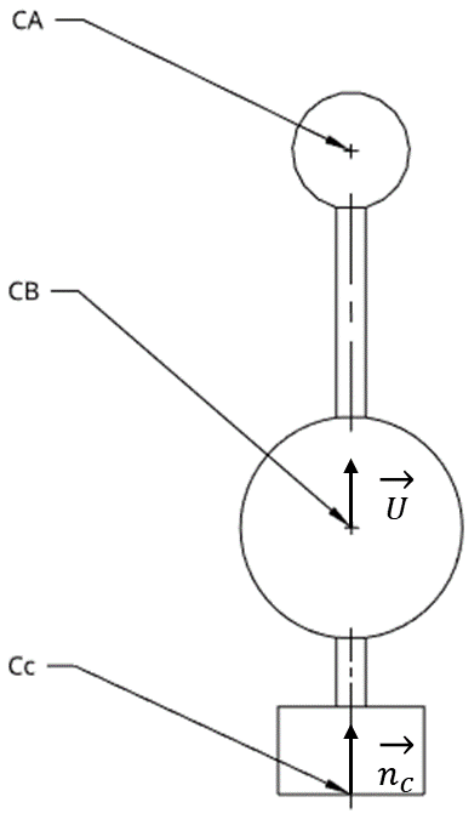

Figure 6-12. Relationship between the center of spheres and the unit vector

Output

Once $\vec{U}$ and CB' is known, the coordinate of $C_{c'}$ can be calculated as follows:

$$C_{c'} = \overrightarrow{C_{B'}} \times (L_2 + A_1)$$

And the normal vector at the connection point can be calculated as:

6.7 Termination Target Type 2

In this type, various pattern recognition algorithms can be used to determine the relationship between Target's features to its reference points (as opposed to using parametric geometric shapes such as spheres). An example of this type of Termination Target is shown below:

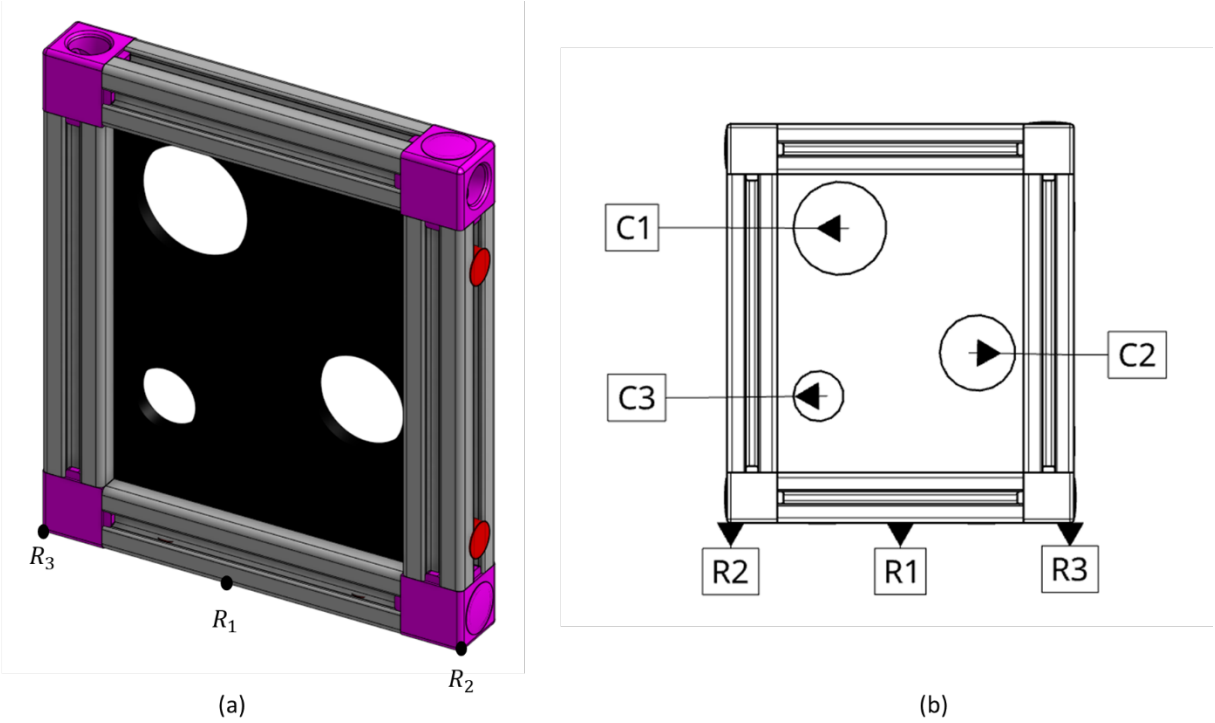

Figure 6-13. Termination Target Type 2, using edge detection for reference point calculation (R1, R2, and R3).

In this example, once the target is scanned, using the color difference, an edge detection algorithm is used to detect the three centers. Figure 6-14 shows the methodology used to calculate reference points using this target type.

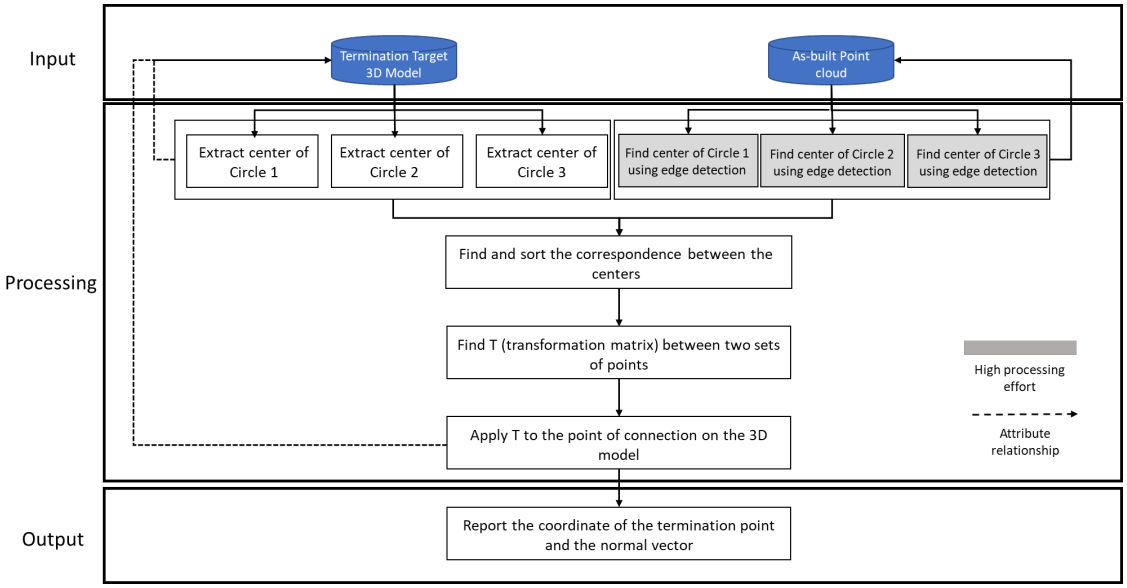

Figure 6-14. Methodology to detect reference points in example Termination Target type 2.

Input

The inputs are the 3D model of the Termination Target and a point cloud of a scene, including at least one Termination Target placed on a termination point. The centers of the three circles and the reference points are known from the 3D model and are as follows:

- The coordinate of the center of Circle 1 (R1= D1/2): $C_1 = (X_1, Y_1, Z_1)$
- The coordinate of the center of Circle 2 (R2=D2/2): $C_2 = (X_2, Y_2, Z_2)$
- The coordinate of the center of Circle 3 (R3=D3/3): $C_3 = (X_3, Y_3, Z_3)$
- The coordinate of the reference Point 1: $R_1 = (X_{R1}, Y_{R1}, Z_{R1})$
- The orientation of the reference point 1: $N_{R_1} = (N_{X_{R1}}, N_{Y_{R1}}, N_{Z_{R1}})$
- The coordinate of the reference Point 2: $R_2 = (X_{R2}, Y_{R2}, Z_{R2})$
- The orientation of reference point 2: $N_{R_2} = (N_{X_{R2}}, N_{Y_{R2}}, N_{Z_{R2}})$
- The coordinate of reference Point 3: $R_2 = (X_{R3}, Y_{R3}, Z_{R3})$
- The orientation of reference point 3: $N_{R_3} = (N_{X_{R3}}, N_{Y_{R3}}, N_{Z_{R3}})$

It is important to understand that the relationship between the center of the circles and the reference points are known since the characteristic of the design is known.

The second input is a point cloud that includes at least one Termination Target that has been placed on a termination point or any point of interest. The developed methodology will work regardless of the line of sight, as long as the 3 circles are visible.

The coordinates of the circles in the point cloud are unknown, which will be calculated in the next step. Let's name the center of the circles as:

- The coordinate of the center of Circle 1 (R1= D1/2): $C_{A'} = (X_{A'}, Y_{A'}, Z_{A'})$
- The coordinate of the center of Circle 2 (R2= D2/2): $C_{B'} = (X_{B'}, Y_{B'}, Z_{B'})$
- The coordinate of the center of Circle 3 (R3= D3/2): $C_{C'} = (X_{C'}, Y_{C'}, Z_{C'})$

Processing Methods

Two methods, automated and semi-automated, are suggested that can be used for finding the circles in the 3D scan point cloud. The framework for implementing the automated and semi-automated circle finding is similar to the methods described earlier for target type 1.

To calculate the location of the reference points, the first step is to find the center of the circles in the point cloud. To do this (finding 3 circle centers in the space), an edge detection algorithm is used. Once the edge image is produced (based on different intensity values between black and white pixels), RANSAC will be used to best fit circles to the edge image. Knowing the three circles' relative location and diameter, the RANSAC algorithm will find the three centers in the space. Using the 3 centers, a unique transformation will be calculated to transform the 3D model of the Termination Target on the point cloud. The transformed location of reference points will be taken as the coordinate and orientation of termination points.

Output

Once T is found, the coordinate of a termination of an assembly can be calculated as follows:

$$Coordinate\ of\ the\ termination\ point = T \times C_D$$

Additionally, the normal vector at the termination point can also be calculated as follows:

$$Normal\ vector\ at\ the\ termination\ point = T \times \vec{n}_D$$

Where $\vec{n}_D$ is the normal vector at the connection point in the design model of the Termination Target. The following pseudo code provides more details on the sequence of mathematic operations.

Algorithm 6.1: Glove Target Detection in a Point Cloud

Input: 3D point cloud of as-built assembly which contains a Glove Target $\{S\}$ and Point $P_s \; and \;\; P_s \in \{S \; and \; Glove \; Target\}$], Initial 3D model of the termination target $\{M_T\}$

Output: Termination point coordinate in the scan's coordinate system $\{T_s\}$ and normal vector at termination point $\{N_T\}$

From $\{M_T\}$ extract the following information:

$C_{1_m} = \left(X_{C_{1_m}}, Y_{C_{1_m}}, Z_{C_{1_m}}\right) \; and \; D_{C_1}$, coordinate of the first circle on the target in the model coordinate system

$C_{2_m} = \left(X_{C_{2_m}}, Y_{C_{2_m}}, Z_{C_{2_m}}\right) \; and \; D_{C_2}$, coordinate of the second circle on the target in the model coordinate system

$C_{3_m} = \left(X_{C_{3_m}}, Y_{C_{3_m}}, Z_{C_{3_m}}\right) \; and \; D_{C_3}$, coordinate of the third circle on the target in the model coordinate system

$R_1 = \left(X_{R_1}, Y_{R_1}, Z_{R_1}\right)$, coordinate of a reference point on the target in the model coordinate system

$N_{R_1} = (N_{X_{R_1}}, N_{X_{R_1}}, N_{X_{R_1}})$, normal vector at reference point in the model coordinate system

$$\| \; C_1 - C_2 \; \| = \propto_1$$
$$\| \; C_1 - C_3 \; \| = \propto_2$$
$$\| \; C_3 - C_2 \; \| = \propto_3$$

Region Selection

Select a region in the vicinity of P_s such that only points within D_T (target's principal length) are kept:

For i=1:n

If $X_{p_i} > X_{P_s} \times D$

Delete P_i

Else

If $Y_{p_i} > Y_{P_s} \times D$

Delete P_i

If $Z_{p_i} > Z_{P_s} \times D$

Delete Z_i

End if

End for

Update {S}

Run edge detection {S}

Run RANSAC on the edge image

Find candidates for the first circle: $\{C_{1_{C_1}}, C_{1_2}, \cdots, C_{1_{C_n}}\}$

Find candidates for the second circle: $\{C_{2_{C_1}}, C_{2_{C_2}}, \cdots, C_{2_{C_n}}\}$

Find candidates for the third circle: $\{C_{3_{C_1}}, C_{3_{C_2}}, \cdots, C_{3_{C_n}}\}$

Multiple candidates found per circle

Run distance check between candidates

$$\| C_{2_{C_1}} - C_{1_{C_1}} \| = \propto_1 \pm \varepsilon\ (scanner's\ error)$$
$$\| C_{3_{C_1}} - C_{1_{C_1}} \| = \propto_2 \pm \varepsilon\ (scanner's\ error)$$
$$\| C_{2_{C_1}} - C_{3_{C_1}} \| = \propto_3 \pm \varepsilon\ (scanner's\ error)$$

Find circles coordinates in the in the scan's coordinate system

$$C_{1_s} = \left(X_{C_{1_s}}, Y_{C_{1_s}}, Z_{C_{1_s}}\right)$$
$$C_{2_s} = \left(X_{C_{2_s}}, Y_{C_{2_s}}, Z_{C_{2_s}}\right)$$
$$C_{3_s} = \left(X_{C_{3_s}}, Y_{C_{3_s}}, Z_{C_{3_s}}\right)$$

Calculate T such that $\{C_{1_m}, C_{2_m}, C_{3_m}\}$ is transformed onto $\{C_{1_s}, C_{2_s}, C_{3_s}\}$

Calculate Termination point and normal using T

$$Coordinate\ of\ the\ termination\ point\colon\ T_s = T \times R_1$$

$$Normal\ vector\ at\ the\ termination\ point\colon N_s = T \times \vec{n}_{R_1}$$

Report T_s and N_s

6.8 Example Application

6.8.1 Objective

A collaborating fabricator in Ontario wanted to verify the distance from center to center between two flanges on a pressure vessel and share the results with their project owner. Normally this objective would have been fulfilled by using tape measure by the owner's inspector at the fabrication facility. However, due to the COVID19 pandemic and lockdown measures in the Ontario province, the fabricator and the project owner wanted to explore ways and methods to inspect this measurement in a remote and unbiased way.

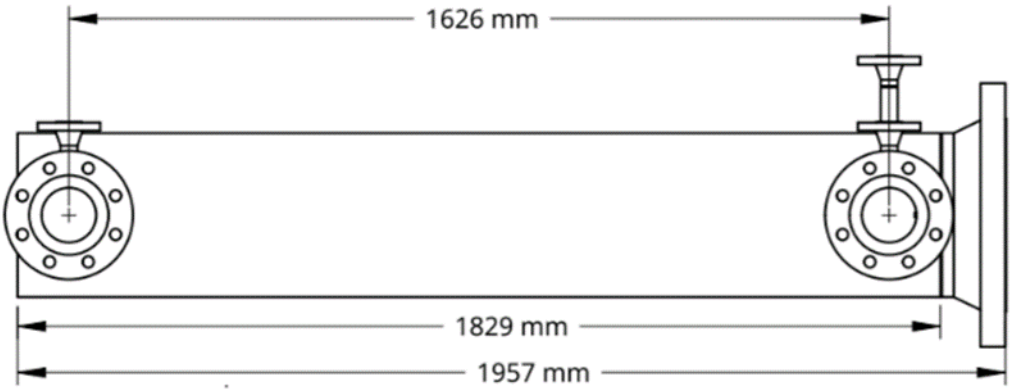

Figure 6-15. The center-to-center measurement between two flanges on a pressure vessel assembly

6.8.2 The Approach

To solve the challenge, the fabricator decided to use Termination Targets along with a laser scanner. In this way, the human errors (biases) of using the manual measurement tools were eliminated. In other words, it was irrelevant which inspector (owner's or fabricator's) runs the scanner since the results would always be the same. Also, once the data was captured, it was shared with the owner for final review and approval. Figure 6-16 shows the process of using the Termination Targets.

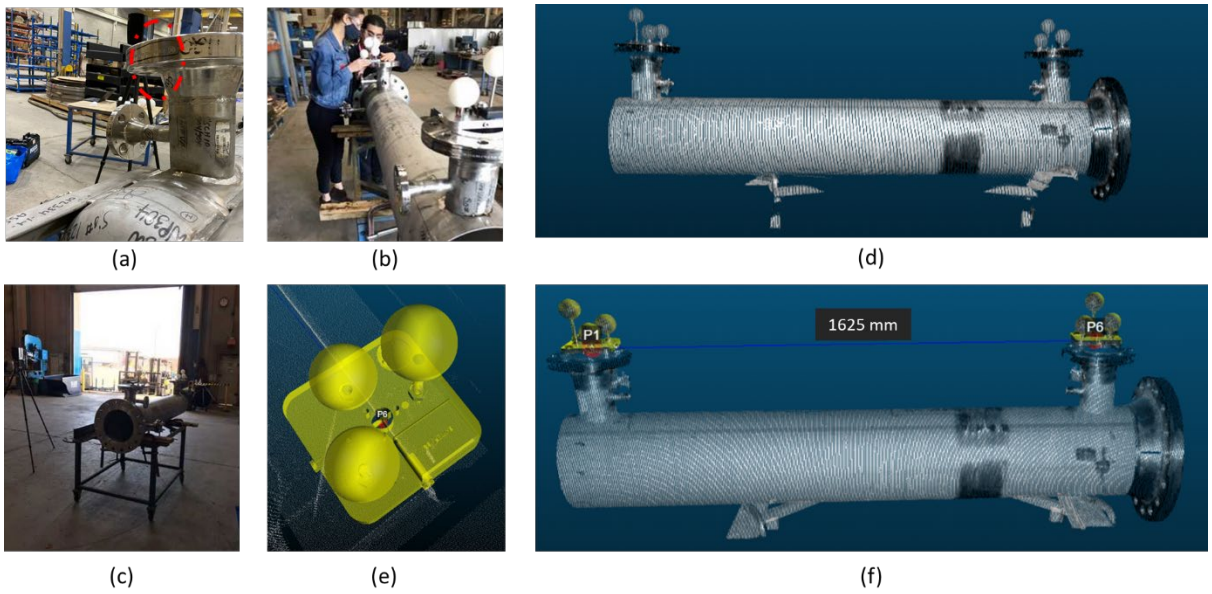

Figure 6-16. Steps in using Termination Targets to verify fabrication quality.

Steps in using Termination Targets:

a) The center line on the flange was detected and chalk was used to outline the calculated centerline

b) The reference point of the Termination Targets was placed onto the centerline and tangent to the hole in the flange. This was done by fabricator's quality control team

c) The laser scanner was used to collect a point cloud. The laser scanner is positioned such that both Termination Targets are visible.

d) The resulting point cloud was reviewed. Termination Targets were captured and visible.

e) The Termination Target was found using the semi-automatic approach.

f) The distance between the termination points was calculated (the Euclidean distance between the reference points of the two targets)

6.8.3 The Result

Using the Termination Targets the fabricator in this case was able to verify the distance between the flanges' center points. This approach was especially desirable due to the COVID19 restrictions on workers' mobility. The distance measurement confirmed that the distance between flanges was within tolerance. The researcher later confirmed that the pressure vessel was sent to the site, and there were no reported issues.

6.8.4 The limitation

The Termination Target automates several steps in the measurement process, however, the process of finding termination points on assemblies is still left to human operators with manual tools. This is an acceptable limitation, since all other advanced measurement approaches (Total stations or Laser Trackers) suffer from the same limitation. Methods and frameworks of potentially eliminating this limitation are further discussed in the next two chapters.

Chapter 7
Using 3D Scanning for Accurate Estimation of Termination Points for Dimensional Quality Assurance in Pipe Spool Fabrication

7.1 Chapter Summary and Contribution Statement

Previous chapter demonstrated how a physical target can be used and integrated as part of the scanning process to detect and calculate the coordinate and orientation of termination points on scanned point clouds. This chapter focuses on metrics and methods to calculate and articulate the accuracy of calculating termination points in a way that is consistent with existing methods for calculation and expression of accuracy. Additionally, this chapter develops a net new method for detecting termination points without the use of the target and using machine vision-based methods.

This chapter is based on work published in the Internal Journal of Industrialized Construction in September, 2021, with the same title (https://doi.org/http://doi.org/10.29173/ijic253). Minor changes are made to some parts of the article to be more consistent with the body of the thesis. Thus, the content of this chapter is not exactly the same as the paper.

I have written the manuscript, overseen and conducted part of data collection and processing, facilitated access to the fabrication shop for data collection and helped with the programing of the algorithms. The data collected in this study was the result of a 6-month data collection at the partner's fabrication facility in Cambridge, Ontario. Jackie Bai was onsite full time, and Steve Chuo and I trained and assisted him with the data collection during his employment. Sidy Ndiongue and Caleb T-Seng Tham assisted with the programming under my direction. Chris Rausch contributed to the background section as well as editorial contribution to the manuscript for clarity. In addition, I received editorial advice, feedback, and contributions for the manuscript from Prof. Carl Haas.

7.2 Abstract

Increased prefabrication and modularization have resulted in fabrication shops producing more complex assemblies with tighter tolerances. Most measurements in fabrication shops are still done using manual tools that are not accurate enough for engineering tolerance specifications, which can lead to rework. 3D scanning and measurement systems can provide increased accuracy and digital

integration capabilities. The utilization of existing 3D scanning methods does not sufficiently support fast and accurate Dimensional Quality Assurance (DQA) of pipe spool fabrication. This is because no DQA methods to date have focused solely on termination points for pipe spool assemblies. In this thesis chapter, a new scan-vs-BIM method is developed to accurately estimate termination points for 3D scanned cylindrical object assemblies. This method relies on statistically fitting circular features at termination points and thus eliminating conventional issues with target placement for laser trackers and measurement readings for tape measures. The method is tested in an industrial-scale experiment, where 30 pipe spool assemblies were fabricated and more than 400 quality control steps completed. The accuracy of termination point detection was benchmarked against results from a laser tracker and compared against commercial scan-to-BIM software. Results show that the developed method has an average accuracy of 1.01mm and is significantly better than the scan-to-BIM software with an average accuracy of 4.75mm.

7.3 Introduction

The increased adoption of modularization and prefabrication has allowed for enhanced quality of the final built product. While these trends also allow for automated and controlled processes to increase quality, safety, and productivity [36,66,67,136], the continued existence of onsite rework remains a significant cost and schedule impediment for these types of projects [137]. This is especially true in complex pipe spool fabrication projects, where the geometry of assemblies is typically bespoke and intricate. Depending on the type of project and enumeration approach, rework can amount to 3% to 10% of a project's cost [11,14]. Rework manifests itself in a variety of forms in piping projects, and only some of it is documented by project participants. Examples of costly rework scenarios that can be avoided by improved measurement and data communication tools include modules not mating due to error in one or more termination points onsite, bolt-hole misalignment in flange connections, re-cutting and re-welding of assemblies due to design misinterpretation, delayed approval and shipment of assemblies due to QC (quality control) processes becoming a bottleneck, fabrication worker confusion due to design changes, and repetitive measurement due to tight tolerances and lack of utilization of fit-for-purpose tools. In general, the use of Dimensional Quality Assurance (DQA) tools has the primary objective to increase and maintain an adequate level of quality. As a by-product, DQA tools also have the potential to

save project costs by avoiding rework, material waste, and increasing productivity. Conventional measurement tool kits can be divided into two groups: (1) manual hand measurement tools such as tape measures, bubble levels, and straight edges, and (2) advanced surveying grade tools such as total stations and laser trackers. To perform the required quality control measurements, both of these methods are similar in their use of termination points. Termination points are identifiable parametric features on assemblies that are idealized by points. The distance and angle between termination points on assemblies are calculated and compared with the allowable tolerance value. While they are accurate, surveying-grade tools are seldom used in fabrication shops due to their complexity and high cost of operation. As such, fabrication workers use manual measurement tools for most of their measurements. The lack of an advanced, accurate, and integrated measurement approach in fabrication shops is one of the main root causes of geometric rework incidents [138].

7.3.1 Research Scope and Problem Definition

This research focuses on improving the dimensional quality of piping element fabrication, since this can amount to 50% of the total cost of an industrial construction project [24]. The range of materials used, coupled with the extensive hands-on time from craft workers, makes the piping portion of projects costly and time-consuming. Furthermore, incorporating automated dimensional quality assurance processes into the piping industry is challenging yet necessary, because most components in a piping project are bespoke. Most measurement is still conducted using manual hand measurement tools such as tape measures, bubble levels, squares, and straight edges.

This research proposes a new measurement method that utilizes 3D scan data and can deliver rapid dimensional quality control data based on termination points. The utilization of 3D scan data is advantageous over existing tools, since 3D scan data can provide superior visualization and can be integrated as part of the fabrication process, as shown by [36]. The delivery of information based on termination points is critical for two reasons: (1) the abstraction of termination points allows for the development of a computationally efficient and accurate approach, and (2) the utilization of termination points in delivering the quality control information would allow for seamless integration into fabrication shops' processes without extensive training or process changes, since existing QC frameworks rely on measurement and communication of tolerances using termination points.

The challenges being addressed in this research are that existing methods for DQA of pipe spool fabrication are often too time-consuming for efficient deployment, provide non-structured or inadequately abstracted information, and often sacrifice accuracy at termination points to achieve overall minimum average error reduction. These challenges are overcome using a new framework and algorithms that efficiently provide accurate information of termination points. While the level of required accuracy remains high for pipe spool DQA, as the cost of 3D scanners continues to decrease, efficient processing of point cloud data will have a significant role in complex infrastructure projects.

7.4 Dimensional Quality Assurance for Pipe Spool Fabrication using 3D Point Clouds

The use of 3D point clouds for dimensional quality assurance (DQA) of pipe spool fabrication has existed in a range of research projects for well over the past decade. While other digitization approaches have also been explored, such as 2D image analysis, they often have fundamental challenges for inspection of pipe spool assemblies within a fabrication facility such as featureless pipe surfaces, lighting issues from weld flashes, and the dynamic setup requirements for complex pipe spools which cannot guarantee consistent camera pose between setups [139,140]. An example of infrastructure projects with complex pipe spool fabrication process is the refurbishment of existing nuclear reactors. Due to the high accuracy requirements for these types of infrastructure projects, laser scanners are uniquely positioned among other types of digitization devices for conducting DQA. The ranging error of laser scanners can be as low as 1mm (ranging error for the scanner used in this study is defined as a systematic measurement error at around 10m and 25m) and have the ability for rapid data collection.

Researchers have adopted the use of 3D point cloud approaches to circumvent many of the conventional challenges associated with other digitization approaches. In general, there are two main ways to instantiate such DQA processes: with or without an existing as-designed 3D model [135]. Such approaches are summarized in Figure 1 and reviewed in detail in the subsequent sections.

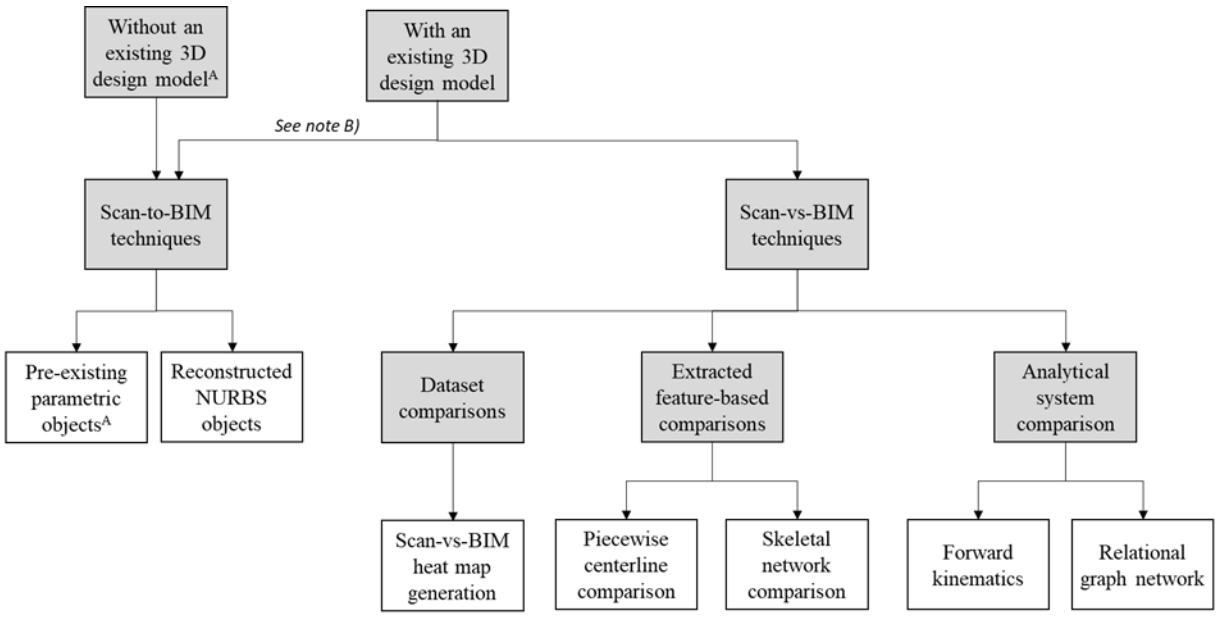

A) "3D design model" refers to the distinct model of the pipe spool assembly being fabricated, whereas "pre-existing parametric objects" refers to a library of potential parametric pipe spool objects

B) A 3D model produced through Scan-to-BIM can be compared with as-designed BIM for DQA. Such comparison is likely to be indirect (e.g., comparing the termination points of an assembly from the as-designed 3D model with those produced from the scan-to-BIM model).

Figure 7-1. Overview of existing methods for dimensional quality assurance for prefabricated pipe spool assemblies using 3D point cloud data.

7.4.1 Dimensional Quality Assurance without a 3D design model

In many instances fabrication shops do not have access to the 3D design model of the assemblies they need to build. This happens because of multiple reasons including: (1) interoperability issues between various software, (2) lack of contractual obligations to transfer the 3D model, (3) 3D models usually correspond to engineering ISO drawings not fabrication shop drawings. As such, in these cases, Scan-to-BIM methods are used in these instances. When an existing 3D design model of the pipe spool being fabricated is not available, feature detection algorithms can be used to extract curvature-based features in a point cloud and compared with information contained in 2D drawings. These methods can be categorized under prevailing work described as "scan-to-BIM", where a 3D model is re-created from a point cloud. Previously, Ahmed et al. [45] used Hough Transform on cross-sectional slices of pipe assemblies to extract pipe radii of known sizes. A shortcoming of the method described by Ahmed is that it assumes the orientation of the pipe spools is parallel or

perpendicular to the scanner's Z-axis. Son et al. [46] used curvature feature extraction from local surface patches at known locations prescribed on piping and instrumentation diagrams (P&IDs) and subsequently fit non-uniform rational basis spline (NURBS) geometry to generate pipe spool model elements. Wang et al. [47] used Density-Based Spatial Clustering of Applications with Noise (DBScan) to help generate complete pipe spool assembly models from 3D point clouds. While these algorithms may rely on a set of pre-existing parametric objects (oftentimes of set sizes) to fit to a segmented point cloud, other methods have also been developed which reconstruct model elements using more granular geometric techniques to minimize discrepancies with the as-built conditions. For instance, Dimitrov et al. [48] developed a generalizable technique that fits NURBS geometry to constructed elements that do not need to conform to strict parametric assumptions (e.g., a pipe must be perfectly straight). The significance of techniques like this is that they avoid the errors accrued by trying to best-fit straight pipe elements to as-built features which may have non-negligible deformation such as from welding distortion. However, the downside of these approaches is that inferring discrete errors between as-built and as-designed states (represented by drawings) is hard, and relies on tedious, timely analyses.

Across existing scan-to-BIM methods for pipe spool fabrication, perhaps the most useful (and recent) technique has been developed by Maalek et al. [49]. Their method extracts the center and orientation of key pipe flanges on assemblies using algorithms such as the Pratt's circle fitting algorithm and the squared Mahalanobis distance computation. While the most conducive to pipe spool fabrication DQA, this method still requires a subsequent comparison of as-built features (i.e., flange centers and plane orientations) with as-designed information, which can be tedious and time-consuming. Additionally, many commercially available software packages rely on human operators to manually find objects and to best-fit parametric objects into point clouds. In their recent work, Essnashary et al. [50] have investigated the resulting fundamental imprecisions when human operators are involved in scan-to-BIM methods.

7.4.2 Dimensional Quality Assurance with a design model

While notable works have emerged to help conduct DQA when an existing model is not available or developed to a suitable level of detail, far more suitable methods have been developed for directly comparing 3D point clouds with existing as-designed models (i.e., “scan-vs-BIM”). Not only does this approach circumvent extensive subsequent evaluations to understand and abstract information for DQA, but these processes do not strictly require a semantically rich BIM for engendering full automation. Often, a “semantically sparse” CAD model (e.g., stereolithography format) is suitable, as this chapter later posits and defends. Upon surveying existing methods for DQA within scan-vs-BIM, there are three distinct sub-categories: (1) direct dataset comparisons, (2) extracted feature-based comparisons, and (3) analytical system comparisons.

7.4.3 Direct dataset comparisons

The most basic, yet perhaps pervasive scan-vs-BIM method is directly overlaying a scan on a model and depicting deviations using a heat-map. This method can be used to visualize overall Euclidean distance-based deviations between an as-built and as-designed state. However, the challenge of using this method for DQA in pipe spool fabrication is that not all deviations can be directly inferred by Euclidean distances, for instance, if a pipe is shifted along its principal axis, deviations may not be appropriately displayed (in contrast to a case where a pipe is rotated about that same axis, whereby a linear propagation in a heat-map would be displayed). Given the limitations of direct heat-map comparison, researchers have adopted more advanced methods such as the use of random sample consensus (RANSAC) to extract pipe segments and perform deviation analysis using orientation comparisons of pipes [51].

7.4.4 Extracted feature-based comparisons

Since direct dataset comparisons do not capture all of the types of discrepancies that can exist for pipe spool fabrication, researchers have used extracted feature-based comparisons for improved DQA. The most basic form of this involves extracting the centreline of pipes (including start and end nodes) and comparing this data with similar features from an as-designed model. Since the model does not need to be semantically rich, this method is efficient and robust. In their work, Guo et al. [8] use this form of centerline comparison after extracting straight pipe segments in MEP modules. While their method achieves a suitable accuracy (3.78 mm), it cannot be directly used for more

complex assemblies which have various angles and joints. This is where other techniques such as comparing skeleton networks as posited by Nahangi et al. [52] may be more suitable. In this method, the point cloud is converted into a skeletal model by extracting cross-sections of objects and fitting lines through the centre of each cross-section. An input BIM is also used to instantiate the skeletal candidates (i.e., radius of pipe at key locations), and to infer the deviation of the as-built status to the design intent. This is then carried out for an entire pipe assembly. In general, the use of extracted feature-based comparison may be useful for understanding potential realignment measures, these methods involve more computation than strictly required for an initial DQA assessment of termination points on pipe spool assemblies. Furthermore, occlusions in point cloud data lead to challenges when generating centerlines through an assembly.

7.4.5 Analytical system comparison

A final way to utilize an as-designed model for DQA in pipe spool fabrication is the use of advanced analytical system comparisons. Such techniques are related to extracted features yet assume or represent pipe spools as analogous analytical systems. In their work, Nahangi et al. [53] use the analogy of kinematic chains to identify errors and posit realignment measures. First, forward kinematics is used to compute the discrepancy between as-built and as-planned pipe spool segments. Such computation relies on the assumption that pipes can be modelled and behave similarly to joints in robotics systems (i.e., rotations and translations about joints). This method, while powerful for potentially providing near real-time feedback on how to correct defective assemblies, relies on having sufficient point cloud coverage of pipe spools. Furthermore, the results of this method are currently not conducive for quick termination point checking (i.e., centre points and alignment of pipe flanges). Other analytical systems comparisons have involved the use of graph theory to abstract and track the accumulation of error in pipes. This technique, as outlined by Kalasapudi et al. [54], requires establishing a comprehensive tolerance network associated with each pipe element and subsequently quantifying and comparing the errors of each associated pipe element. In summary, while several innovative techniques can be used to abstract errors in pipe spool assemblies, oftentimes, these approaches are far too comprehensive to adopt for real-time DQA of termination points.

7.4.6 Knowledge gap and research contribution

While existing methods for DQA of pipe spool fabrication using 3D point clouds have several value-adding capabilities, in general, they have the following limitations which this chapter aims to address:

- Primitive fitting techniques often sacrifice accuracy at termination points in order to achieve an overall minimum average error reduction.
- Pipe spool termination features are often regularly shaped primitives, which do not require the same level of complexity or sophistication to process and analyze as irregularly shaped primitives – whereby potentially more efficient algorithms can be used to decrease computational cost/time.
- No methods to date have delivered approaches for efficient DQA of termination points on pipe spool assemblies, which continues to be an essential (yet rudimentary) requirement for prefabricated project execution.

Finally, while a range of devices can be used to generate a 3D point clouds (such as projector-camera systems, photogrammetry, range cameras, laser vision sensors, etc.) [139,141,142], the use of 3D laser scanners is targeted in this work, given their widespread adoption and proven reliability in industry for high accuracy, speed, insensitivity to lighting conditions, range and high density – all of which are highly conducive to pipe fabrication in offsite facilities as demonstrated by Guo et al. [143]

7.5 Methodology

The methodology section of this research is broken into two main sections. Initially, the required definitions and classification of termination points are provided based on the classification discussed in Chapter 5. Secondly, the method for developing a termination point based scan-vs-BIM is explained. The method was used as part of the fabrication of 30 pipe spool fabrication. The results of using the method are explained in section 7.6.

7.5.1 Termination Point Definition and Classes

As defined in Chapter 5, termination points are defined as local coordinate systems where assemblies are connected or constraints. Furthermore, termination points are identifiable parametric features on assemblies that are idealized by points. The detection of termination points is part of the fabrication process. For example, the center point of flanges is often used as a termination point. As seen in Figure 7-2, a fabrication worker is using manual measurement tools to

draw the centerlines on the flanges of a pressure vessel to allow subsequent quality control measurements.

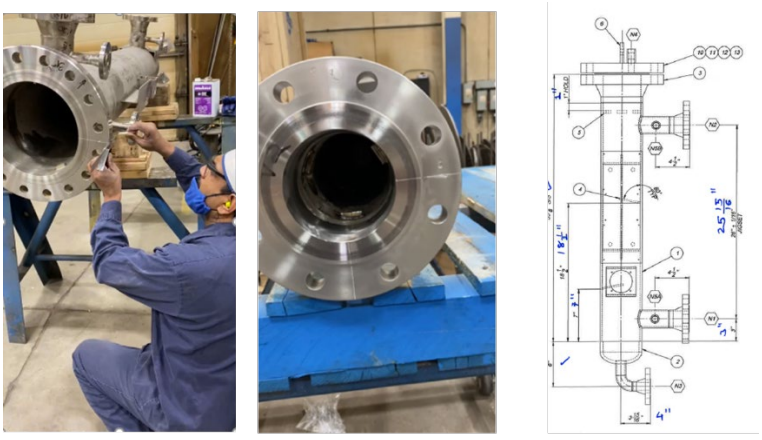

(a) (b) (c)

Figure 7-2. The use of termination points as part of the fabrication process. (a) A fabrication worker using manual measurement tools to detect the centerline on a flange. (b) the centerline marked on the flange using chalk. (c) the required QC measurements using termination points

To allow for the development of a comprehensive framework, the same classification discussed in Chapter 5 was used. For ease of comprehension for the reader, this classification is reiterated in this section. These classes were defined as follows:

Table 7-1. Termination point classes in the 3D-model and As-built spaces

Termination Point Class	3D-model	As-built
(A): Origin termination point	A_m	A_s
(B): Destination termination point	B_m	B_s
(C): Assembly mate-to-origin termination point	C_m	C_s
(D): Assembly mate-to-destination termination point	D_m	D_s
(E): Assembly non-mate termination point	E_m	E_s

Table 7-2. Termination vector classes in the 3D-model and As-built spaces

Termination Vector Class	3D-model	As-built
(F): Normal-to-origin termination plane	$\overrightarrow{F_m}$	$\overrightarrow{F_s}$
(G): Normal-to-destination termination plane	$\overrightarrow{G_m}$	$\overrightarrow{G_s}$
(H): Normal-to-assembly mate-to-origin plane	$\overrightarrow{H_m}$	$\overrightarrow{H_s}$
(I): Normal-to-assembly mate-to-destination plane	$\overrightarrow{I_m}$	$\overrightarrow{I_s}$
(J): Normal-to-assembly non-mate termination plane	$\overrightarrow{J_m}$	$\overrightarrow{J_s}$

Table 7-1 provides the definition for termination point coordinates in the 3D model space (subscripted by m) and 3D scan space (subscripted by s). Table 7-2 has definitions related to the orientation of termination points in the scan and the 3D model spaces. The definitions of the classes in Table 7-1 and Table 7-2 are available in Chapter 5 more extensively. Here is a summary:

- Class A: The point to which the installation process is first attempted.
- Class B: The point(s) to which the installation process is attempted once the origin termination point has been locked into place.
- Class C: The point to which the receiving assembly (or site location) is mating with the origin termination point.
- Class D: The point to which the receiving assembly (or site location) is mating with the destination termination point.
- Class E: A point that is not mating with another assembly but is still important to measure from or to.
- Class F: The orientation of the origin termination point.
- Class G: The orientation of the destination termination point(s).
- Class H: Orientation of the mating location of the receiving assembly or site location to the origin termination point.
- Class I: Orientation of the mating location of the receiving assembly or site location to the destination termination point(s).
- Class J: Orientation of the none mate termination point(s).

7.5.2 Termination Point Based Scan-vs-BIM for Pipe Spool Assemblies

In the described method in this section, fabrication errors are visualized by providing a comparison between a 3D-scanned point cloud of an as-built assembly and its corresponding 3D-model (as-designed) point cloud. The described method uses termination points to provide the overlay comparison between the scanned point cloud and the model point cloud. Utilization of the detected termination points in providing the comparison is critical for fabrication dimensional quality assurance processes because the current quality control requirements dictate the measurements from and to termination points. Additionally, the tolerance requirements on termination points are often tighter than other fabrication tolerances (since they are the mating

locations between different assemblies), and fabrication workers need exact geometric data for these points. The required steps for the termination-point-based overlay comparison are summarized in Algorithm 1.

Algorithm 1: Termination Point Based Scan-vs-BIM

Input: 3D point cloud of as-built assembly $\{S\}$, and 3D model {M} in STL format

Output: Deviation point cloud $\{S'\}$ such that: $|A_s - A_m| = 0, \measuredangle\overrightarrow{F_s,F_m} \cong 0$

Null $\{S'\}$:$\emptyset \rightarrow \{S'\}$

Initial Positioning

Select 3 points on scan point cloud $\{P_s\} = \{P_1, P_2, P_3\}\ and\ \{P_s\} \subset \{S\}$

Create Model point cloud from the STL file $\{M_p\}$

Select 3 points on model point cloud $\{P_M\} = \{P'_1, P'_2, P'_3\}\ and\ \{P_M\} \subset \{M_p\}$

Apply PCA between $\{P_M\}\ and\ \{P_s\}$

Transform $\{S\}$ onto $\{M_p\} \therefore \{S\} \rightarrow \{S_{T_1}\}$

Select region $\{R\}$ such that $\{A_s\ and\ A_m\} \in \{R\}$

$\{M_R\} = \{M_p\} \Cap \{R\}$

$\{S_R\} = \{S\} \Cap \{R\}$

Apply ICP between $\{S_R\}$ and $\{M_R\}$

Apply Transformation to $\{S_{T_1}\} \therefore \{S_{T_1}\} \rightarrow \{S_{T_2}\}$

Model

Calculate $[A_m, \overrightarrow{F_m}, R_{A_m}]^*$

Scan

Using $[A_m, \overrightarrow{F_m}]$ estimate $[A_s, \overrightarrow{F_s}, R_{A_s}]^{**}$

Deviation Map

Transform $\{S_{T_2}\}$ such that:

1. $|A_s - A_m| = 0$
2. $\measuredangle\overrightarrow{F_s,F_m} = 0$

$\therefore \{S_{T_2}\} \rightarrow \{S_{T_3}\}$

$\{S'\} =$ Calculate discrepancy between $\{S_{T_3}\}$ and {M}

Report $(A_m, \overrightarrow{F_m}, R_{A_m}), (A_s, \overrightarrow{F_s}, R_{A_s})$

Visualize $\{S'\}$

* R_{A_m} denotes to the radius of the cross-section containing A_m

** R_{A_s} denotes to the radius of the cross − section containing A_s

7.5.3 STereoLithography format (STL)

Many design firms consider their specific CAD format proprietary and refrain from sharing them with the fabricators. To accommodate this limitation and to develop a generalized method, this study relies on an STL format of the model. This format stores the model data by tessellating the surfaces in triangles and storing the normal vector for each triangle (it has no other property and thus, design firms are more willing to share this data type). The definition of a mesh is provided in the next section. Figure 7-3 shows the difference in various model representations.

7.5.4 Generation of 3D model point cloud from the mesh

In order to create the point cloud of the 3D model, the first step is to convert the CAD design (where the assembly is defined parametrically) into a mesh object. A mesh is defined as a collection of vertices, triangles, quadrilaterals (quads), or other simple convex polygons (n-gons) that define the shape of a polyhedral object. Most commercial design packages allow for the export of the mesh object from the CAD model. The common formats for storing mesh files are *.STL and *.obj. Figure 7-3 shows the difference in various model representations.

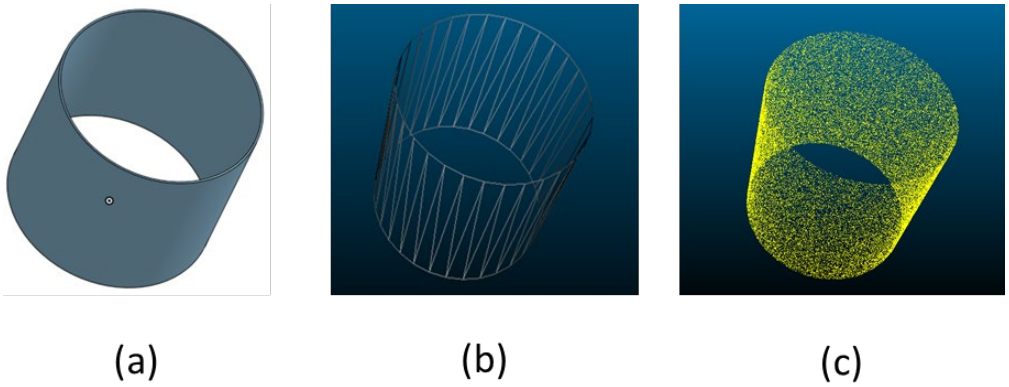

Figure 7-3. (a) CAD model representation of a simple cylinder. (b) Mesh representation of the model. (c) Point cloud representation of the model.

To generate a point cloud representation of the model from the input *.STL, the following steps are taken:

1. Parse the STL file by extracting every triangle and performing the following:
    a. Calculate the area covered by each triangle.
    b. Store each triangle into a list.

2. Calculate a list of the weighted probability that a randomly chosen point will be located on a given triangle. This is done by dividing a triangle given area by the total area.
3. Convert the list of weighted probabilities to a cumulative list of probabilities.
4. Generate a random number from 0 to 1 and find the first number in the cumulative list with a value greater or equal to the selected number. Repeat this process, depending on how many sample points are needed. This will provide a list of the indices of repeating triangles to choose from.
5. For each triangle in the list created in the previous step, generate a point on the triangle's surface.

7.5.5 Finding the global optimum between scan and model

This method uses the scan point cloud and the 3D model object as the two inputs. To overlay a scan point cloud on a model point cloud, Principal Component Analysis (PCA) is used for coarse alignment between the two point clouds. Three corresponding points are required as input for this calculation. After obtaining the rough alignment, an Iterative Closest Point (ICP) optimization is implemented to improve the overlay results.

7.5.6 Finding the local optimum between scan and model

The next step is to select a region that contains the origin termination points in the scan and model point cloud ($\text{classes } A_s \text{ and } A_m$). Once a region is selected, the ICP algorithm is applied to that specific region. The local optimization will result in an improved overlay in the area containing $\{A_{m,}\ \overrightarrow{F_m}, A_s, \overrightarrow{F_s}\}$. Figure 7-4 shows how the region selection is implemented and the final result after updating the overlay.

Figure 7-4. (a) The overlay after applying the matching step described in section 7.5.5. The area of interest is selected and outlined by the dotted red square. (b) The result after locally applying ICP to the region of interest. (c) As shown, the local optimization aligns the normal-to-origin termination planes on the 3D model point cloud and as-built point cloud ($\overrightarrow{\boldsymbol{F_m}} \parallel \overrightarrow{\boldsymbol{F_s}}$).

7.5.7 Finding the origin termination point on the model point cloud (A_m)

The information of the model's center-point can be theoretically extracted from the CAD file. However, as stated earlier, in many situations, the parametric CAD file is not made available to fabrication shops. As such, the objective in this step is to find the center point on a circular cross-section on the 3D model point cloud (without relying on the original CAD format) and to capture it's coordinate (A_m) in the global coordinate system. The implemented approach requires a user to seed an algorithm that finds A_m by selecting a point (via an interactive graphical user interface) on the plane which contains $A_m = (A_{mx}, A_{my}, A_{mz})$, and for which the normal vector is parallel with $\vec{F}_m = (F_{mx}, F_{my}, F_{mz})$. The selection takes place on the mesh object point cloud (where only the vertices are visible to the user); this allows the user to easily visualize the plane containing A_m. This plane (P_{A_m}) can be defined as follows:

$$P_{A_m}:$$
$$F_{mx}X + F_{my}Y + F_{mz}Z - \left[F_{mx}A_{mx} + F_{my}A_{my} + F_{mz}A_{mz}\right] = 0 \quad \text{[Eqn. 7.1]}$$

Once the initial point is selected by the user (on the mesh), an algorithm is developed and described in the following paragraphs to calculate A_m and $\vec{F}_m$.

Assign $A_m = (A_{mx}, A_{my}, A_{mz})$ to be the center point on the 3D model point cloud in the global coordinate system. The next step is to structure the vertices on the mesh object in a way that the closest point to an arbitrary point is indexed and searchable. To do this, octree-based data segmentation is used, which allows for the compartmentalization of points into neighbourhoods based on their Euclidean distances. The Octree method divides the 3D space into bins (the bins may or may not be equal in size depending on the method), allows for stopping the subdivision based on the number of points inside a bin (its key advantage in this application over kd-tree), and the information regarding the neighbouring bins can also be accessed [144]. Once a point on the plane P_{A_m} is selected, two neighbouring points with the shortest Euclidean distance to the selected point are retrieved from the octree data structure. The two calculated points, along with the selected point, are used to define a plane and a circle. Using the three points, a center point, radius, and the normal vector are calculated.

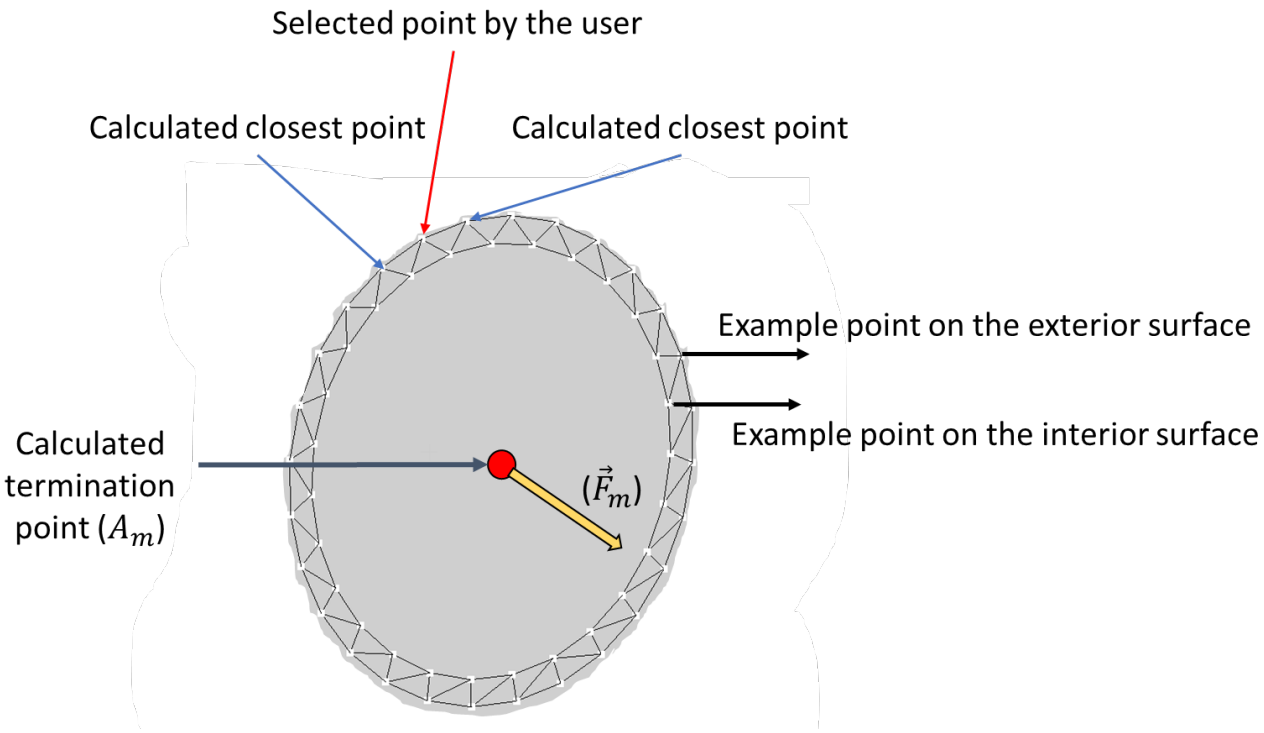

Figure 7-5. Plane $\boldsymbol{P_{A_m}}$(shown in the mesh representation) is calculated using the mesh object and a user-selected point. The termination point $\boldsymbol{A_m}$ and normal-to-origin termination plane ($\boldsymbol{\vec{F}_m}$) is calculated.

In fabrication projects, the pipe thickness is typically detailed in CAD models, this means that in the mesh object, there will be points corresponding to the exterior surface, and there will be points corresponding to the interior surface of an object (pipe or any other object with circular cross-section). There are cases where even though the user selects a point on the exterior surface, the next closest points lay on the interior surface, or the user inadvertently selects a point on the interior surface. As such, the defined circle by the two closest points to a selected point by the user would be incorrect and would not correspond to the center point of the cross-section. In other words, the center of the defined circle does not yield A_m due to incorrect points used to construct the circle. To address this issue, an outlier removal method was implemented. As previously described, after selecting a point, the two nearest points to the selected point are calculated. Using the three points, a circle with the termination point as its center and a calculated radius are hypothesized. The hypothesized circle can be described as:

$$C_{A_mH}: (A_{mH}, R_{A_mH}) \quad \text{[Eqn. 7.2]}$$

where C_{A_mH} denotes to the hypothesized circle at the origin termination point in the model space, A_{mH} denotes to the hypothesized origin termination point coordinate in the 3D model (hypothesized circle's center), and R_{A_mH} denotes to the radius of the hypothesized circle. Once the circle is hypothesized, a puck volume is constructed such that the center is A_{mH}, the radius is $R_{Puck} = R_{A_mH} + \varepsilon_1$, the height of $H_{Puck} = \varepsilon_2$, and where ε_1 and ε_2 are small values used as padding. Once the puck object is defined, the points encompassed by the volume of the puck are counted. If the number of points captured exceeds the predefined limit, the hypothesized center is accepted as the termination point of that section A_m. If the number of points is lower than the limit, the next closest point is selected, and all possible circles are constructed. The algorithm will stop when the number of encompassed points exceeds the limit. Figure 7-6 shows an example where the initial hypothesized circle is incorrect, and the outlier removal algorithm rejects it and finds the correct circle and termination point.

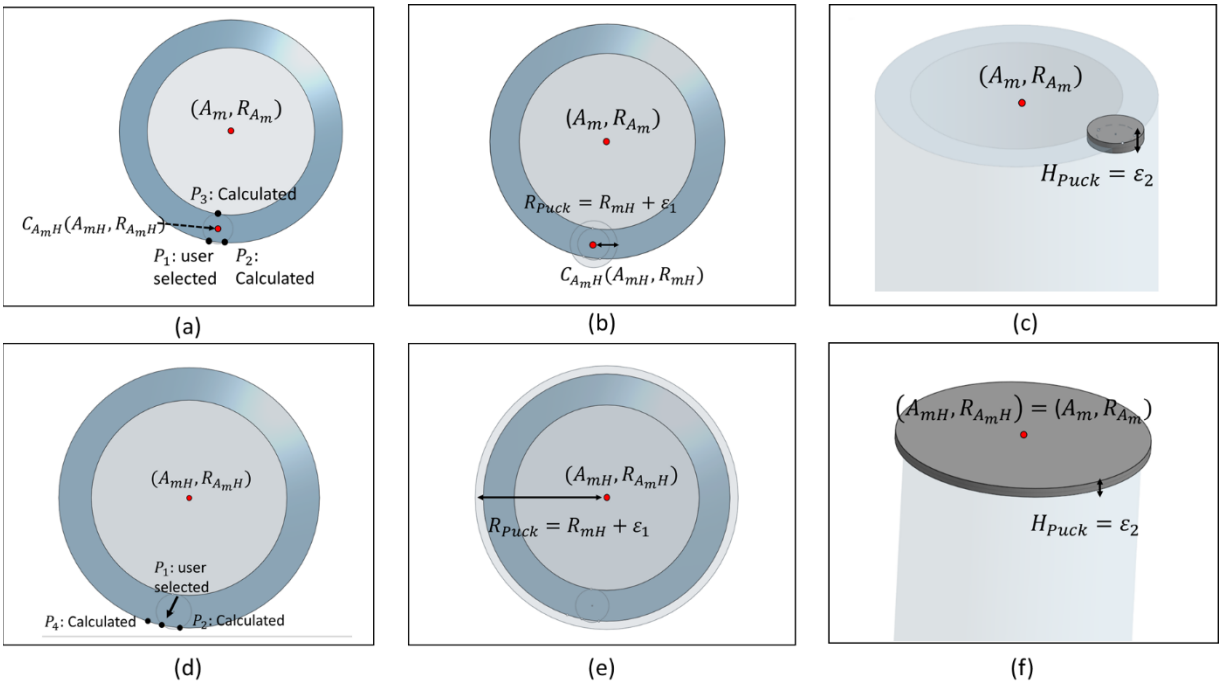

Figure 7-6. (a) Top view of the plane $\boldsymbol{P_{A_m}}$. $\boldsymbol{P_1}$ selected by the user. Existence of $\boldsymbol{P_3}$ in the initial set of closest points results in an erroneous cross-section termination point detection. (b) Creation of the puck volume. (c) The number of points encompassed by the created puck is lower than the predefined limit. (d) The next closest point is selected. (e) creation of the puck object. (f) the volume encompassed by the puck object exceeds the limit, and the hypothesized circle is accepted.

7.5.8 Finding the origin termination point in scan point cloud (A_s)

Based on calculations in the previous section, the coordinate of the termination point class A_m $[A_m = (A_{mx}, A_{my}, A_{mz})]$, the normal-to-origin termination vector class $\vec{F}_m$ $[\vec{F}_m = (F_{mx}, F_{my}, F_{mz})]$, and the radius R_{A_m} are known in the global coordinate system. These attributes are used to seed a search; the objective is to detect the termination point class A_s along with the radius of the end plane R_{A_s} on the as-built point cloud. Note that it is assumed that the normal-to-origin termination point vector classes are parallel between the scan and model. In other words, it is assumed that after applying the local ICP (Section 7.5.6) $\vec{F}_m \parallel \vec{F}_s$. The following diagram (Figure 7-7) describes the implementation process for finding the termination point in the scan point cloud (A_s).

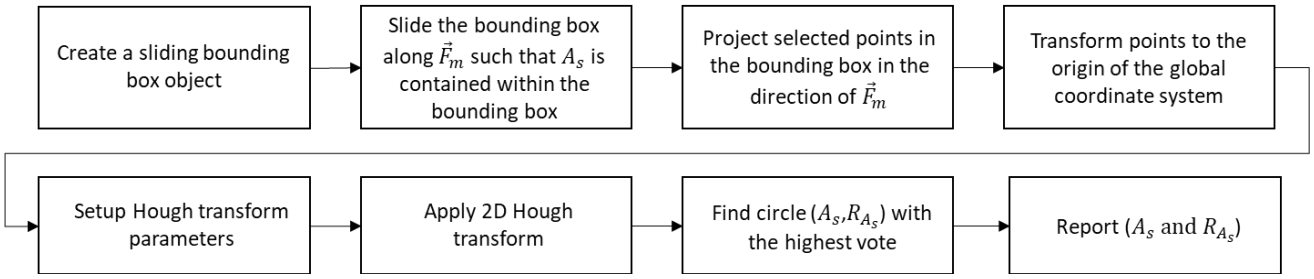

Figure 7-7. The implementation process for finding the termination point class A_s and the radius of the section R_{A_s}

7.5.9 Creating the bounding box object

A bounding box object can be created in the global coordinate system by using a six-element array with elements corresponding to $(x_{min}, x_{max}, y_{min}, y_{max}, z_{min}, z_{max})$

$$\text{Bounding box dimensions} = \begin{cases} -r + increment \times BoundingBoxIndex \\ -r + increment \times (BoundingBoxIndex + 1) \\ -r \times width \\ r \times width \\ -r \times height/2 \\ r \times height/2 \end{cases} \quad \text{[Eqn. 7.3]}$$

The $BoundingBoxIndex$ is a user-controlled value. The *BoundingBoxIndex* is a method to allow users to select the bounding box that includes the termination point class A_s in the scan point cloud.

7.5.10 Finding the bounding box that contains the termination point class A_s

To find the bounding box that contains the termination point A_s, the defined bounding box needs to be aligned with the calculated $\vec{F}_m$.The objective is to align the vector created by $[\text{BoundingBoxDimensions}[1] - \text{BoundingBoxDimensions}[0]]$ with $\vec{F}_m$ (the principal axis of the component that contains the termination point A_s). To align an arbitrary vector ($\vec{u}$) with an arbitrary vector ($\vec{v}$), Rodriguez's rotation formula is used [145]:

$$\vec{k} = \vec{u} \times \vec{v} \quad \text{[Eqn. 7.4]}$$

$$K = \begin{bmatrix} 0 & -k_y & k_y \\ k_z & 0 & -k_x \\ -k_y & k_x & 0 \end{bmatrix} \quad \text{[Eqn. 7.5]}$$

$$\boldsymbol{R} = \boldsymbol{I} + (sin\theta)\boldsymbol{K} + (1 - cos\theta)\boldsymbol{K^2} \quad \text{[Eqn. 7.6]}$$

$$\boldsymbol{T} = \begin{bmatrix} R_{(1,1)} & R_{(1,2)} & R_{(1,3)} & c_x \\ R_{(2,1)} & R_{(2,2)} & R_{(2,3)} & c_y \\ R_{(3,1)} & R_{(3,2)} & R_{(3,3)} & c_z \\ 0 & 0 & 0 & 1 \end{bmatrix} \quad \text{[Eqn. 7.7]}$$

$\vec{F}_m$ should be substituted in the above equation by $\vec{v}$ to align the bounding box object with the termination plane. Once the rotation has been determined, the bounding box is transformed to the correct location. This is done by applying the rotation matrix that was determined in the previous step and then translating to where the termination point class A_m is located (calculated in section 7.5.7). Figure 7-8 shows an example illustrating how the bounding box is aligned with $\vec{F}_m$ and the contained points by the bounding box are highlighted.

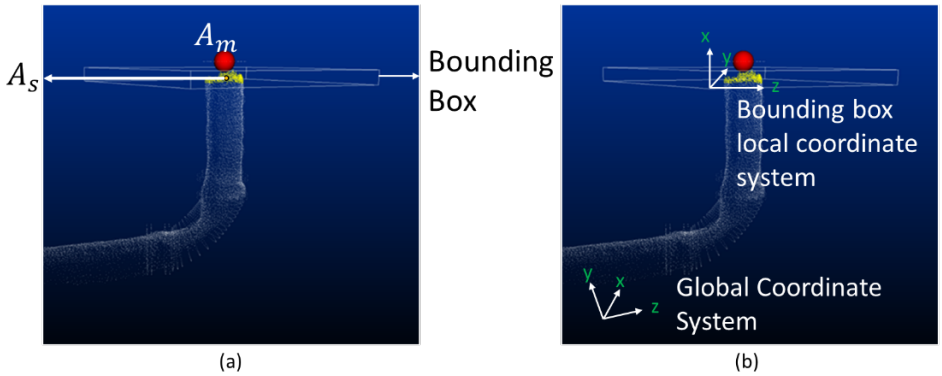

Figure 7-8. (a) The bounding box object is created and transformed. A_s is included in the bounding box. The points contained in the bounding box object are highlighted. (b) The local coordinate system of the bounding box and the global coordinate system are shown.

7.5.11 Projecting points within the bounding box onto a plane

Once the bounding box is created and transformed, the points inside the bounding box can then be selected. The next step is to find the center point using the selected subset of points. The bounding box center point is required when projecting points.

$$BoundingBoxPoint_1 = \begin{bmatrix} BoundingBoxDimesions[0] \\ BoundingBoxDimesions\ 1] \\ BoundingBoxDimesions\ 2] \end{bmatrix} \quad \text{[Eqn. 7.8]}$$

$$BoundingBoxPoint_2 = \begin{bmatrix} BoundingBoxDimesions[3] \\ BoundingBoxDimesions[4] \\ BoundingBoxDimesions[5] \end{bmatrix} \quad \text{[Eqn.7.9]}$$

$$BoundingBoxCenter_{beforeTransform} = \frac{BoundingBoxPoint_1 + BoundingBoxPoint_{2_2}}{2} \quad \text{[Eqn. 7.10]}$$

$$bbc = Bounding\ Box\ Center\ = \boldsymbol{T} * BoundingBoxCenter_{beforeTransform} \quad \text{[Eqn. 7.11]}$$

The coordinates of the selected points (scan point cloud) are described in the global coordinate system. To project along $\vec{F}_m$(the principal axis of the bounding box). The coordinates must be described in the local coordinate system of the Bounding box (Figure 7-8-(b)). Let's name the coordinate of the bounding box center (described in the global coordinate system) as *bbc*= (bbc_x, bbc_y, bc_z). Given that the R for rotating from the global coordinate to the local coordinate system is calculated (section 7.5.10), applying the following transformation will transform all selected points within the bounding box to the local coordinate system of the bounding box. Once the selected points are transformed to the origin of the local coordinate system, the points within the bounding box can now be projected onto the plane with $\vec{n} = \vec{F}_m$:

$$T_{Global\ to\ Local} = \begin{bmatrix} R_{(1,1)} & R_{(1,2)} & R_{(1,3)} & bbc_x \\ R_{(2,1)} & R_{(2,2)} & R_{(2,3)} & bbc_y \\ R_{(3,1)} & R_{(3,2)} & R_{(3,3)} & bbc_z \\ 0 & 0 & 0 & 1 \end{bmatrix}^{-1} \quad \text{[Eqn. 7.12]}$$

A column vector is then created, representing each point, and then each point is multiplied by $T_{Global\ to\ Local}$

$$Point\ in\ Bounding\ Box\ Coordinate\ System = \begin{bmatrix} R_{(1,1)} & R_{(1,2)} & R_{(1,3)} & bbc_x \\ R_{(2,1)} & R_{(2,2)} & R_{(2,3)} & bbc_y \\ R_{(3,1)} & R_{(3,2)} & R_{(3,3)} & bbc_z \\ 0 & 0 & 0 & 1 \end{bmatrix}^{-1} \times \begin{bmatrix} x_i \\ y_i \\ z_i \\ 1 \end{bmatrix} = \begin{bmatrix} x'_i \\ y'_i \\ z'_i \\ 1 \end{bmatrix}$$

[Eqn. 7.13]

After performing the multiplication, the points contained in the bounding box can be described in the bounding box's coordinate system. To project the points within the bounding box, the x' element has to be suppressed (X direction of the coordinate system is aligned with $\vec{F}_m$). The depiction of Y' and Z' values for each point in a Cartesian 2D coordinate system would then represent the projection of the points within the bounding box onto the plane P_{A_s} with the normal vector equal to $\vec{F}_s$. Figure 7-9 shows a plot of the section in the Z' and Y' axis.

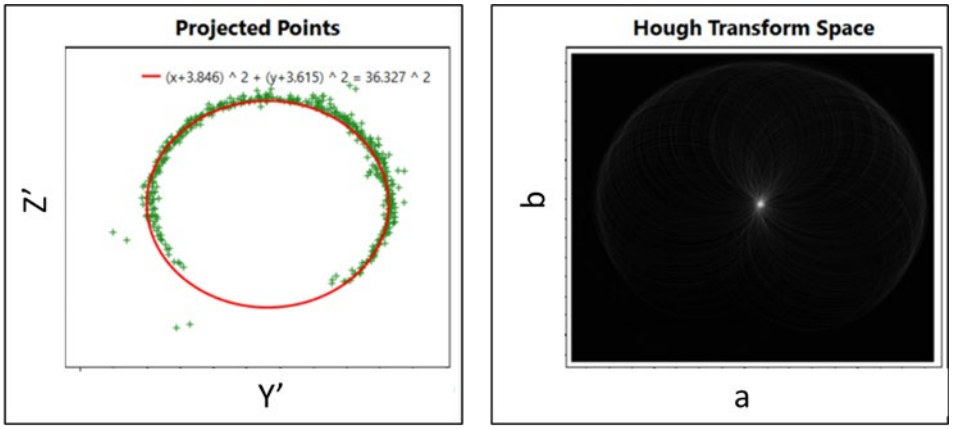

Figure 7-9. Detection of $\boldsymbol{A_s}$ and $\boldsymbol{D_{A_s}}$ using Hough transform.

7.5.12 Circle Hough transform to detect A_s and R_{A_s}

A guided Hough transform is used to best-fit a circle to the projected data points. The circle Hough transform is a voting algorithm that allows for the calculation of the diameter ($D_{A_s} = 2 \times R_{A_s}$) and center of a circle (A_s) [146].

In the implementation of the Hough transform, there are three important parameters that will impact its performance:

1. **Radius Guess**: the search for finding the highest vote needs a starting point. In the suggested workflow in this research, R_{A_m} (calculated in the step described in section 7.5.7) is used as the initial radius guess.
2. **Radius Tolerance**: determines the search space as a multiplier of the radius guess.
3. **Radius Resolution**: determines the number of intervals within the search space.

7.5.13 Final transformation and discrepancy analysis

Once the coordinates of A_s and A_m are known (in the global coordinate system), the initial overlay between the scan and model point clouds (step described in 7.5.5) can be updated such that A_s is overlaid onto A_m and the orientation of the end planes between the scan and model are aligned ($\vec{F}_m \parallel \vec{F}_s$). This process can be best described as a digital 3D jig, where one end is locked, and the deviation on the other end is calculated. Once the overlay between the scan and model is updated,

a discrepancy analysis can be done between the two data sets outlining the out-of-alignment areas. This can be done by calculating the deviation of each point in the scan point cloud to the closest point on the model point cloud. The results of the discrepancy analysis can be shown in the form of a colour map where points exceeding the tolerance threshold are coloured in red and points below the tolerance threshold are coloured in green. Figure 7-10 summarizes the steps explained in section 7.5.

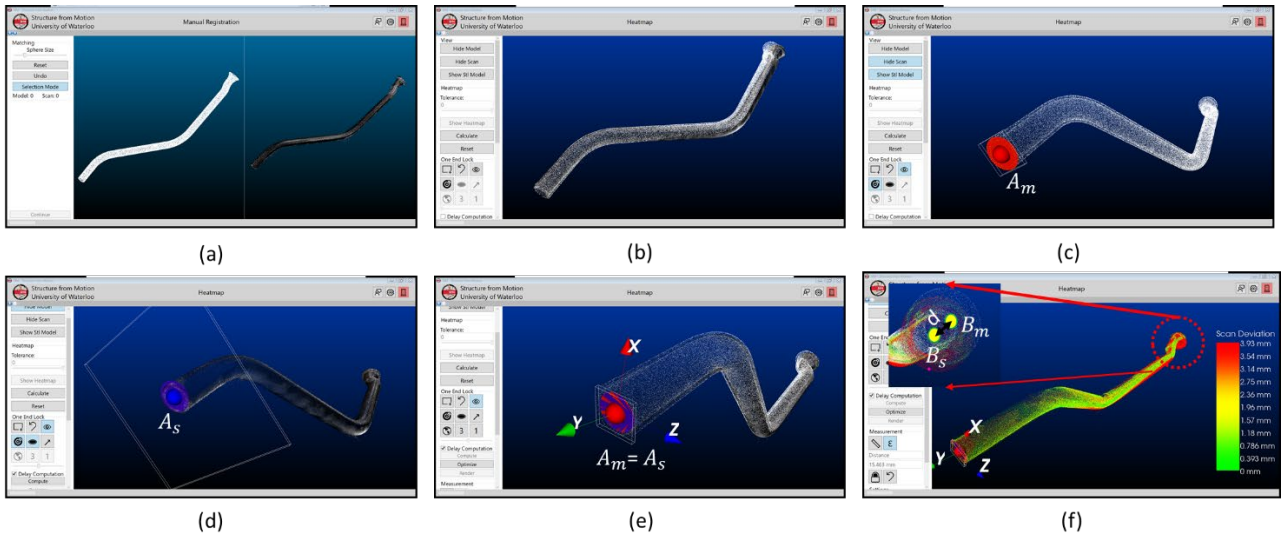

Figure 7-10. (a) The model (as-designed) point cloud next to the scanned (as-built) point cloud of a pipe spool. (b) The initial positioning (PCA+ICP, described in 7.5.5). (c) The model origin termination point is detected (section 7.5.7). (d) the scan origin termination point is calculated (section 7.5.8). (e) the scan point cloud is transposed such that the scan origin termination point is overlaid on the model origin termination point (7.5.13). (f) The colormap is generated, and the deviation at the destination termination points between model and scan is calculated (7.5.13)

7.6 Results

To validate the accuracy of calculated termination points by the described method, the results of the method were compared against the reports provided by a third-party quality inspection firm. For the inspection of incoming pipe spools, a hand-held laser scanner arm device (0.05 mm accuracy at 100 mm distance [147]) was used. The fabricator then provided access to the verification reports to the research team, where the diameter at the termination points on the as-built objects was calculated and reported. Since this method is regarded as the industrially accepted method for measuring termination points and their corresponding diameter, these values are used as ground truth. A snapshot of one such report is provided in Figure 7-11. Additionally, the results of the FARO

Arm were cross-checked by using a calibrated caliper. The results of validating the FARO Arm results are described in section 7.6.1.

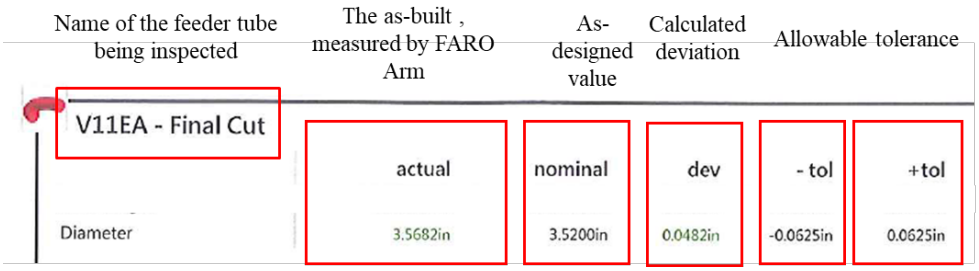

Figure 7-11. Verification report provided by the third-party company. The allowable tolerance is 1.58 mm. All feeder tubes have a verification report.

The dataset collected in this research was also used to find the termination points using a commercial scan-to-BIM software package. The accuracy results of the commercial package were then compared with the developed method (both were benchmarked against FARO Arm) in section 7.6.5.

7.6.1 FARO Arm Verification

To verify that the provided data by the FARO Arm scanner (which the fabricator had hired a surveying crew to measure with) was accurate, a calibrated manual caliper was used to cross-check the provided data.

On average, the difference (between caliper and FARO Arm) in the measured diameters was 0.07 mm, with the maximum difference being 0.39 mm. Since the maximum difference between the caliper readings and the scanner arm was less than the required tolerance on this project (1.58 mm or 1/16''), the readings of the arm scanner were accepted as the ground truth (baseline) for the comparison and benchmarking of the developed method. The absolute point-by-point difference between the caliper's readings and the FARO Arm's readings is illustrated in Figure 7-12.

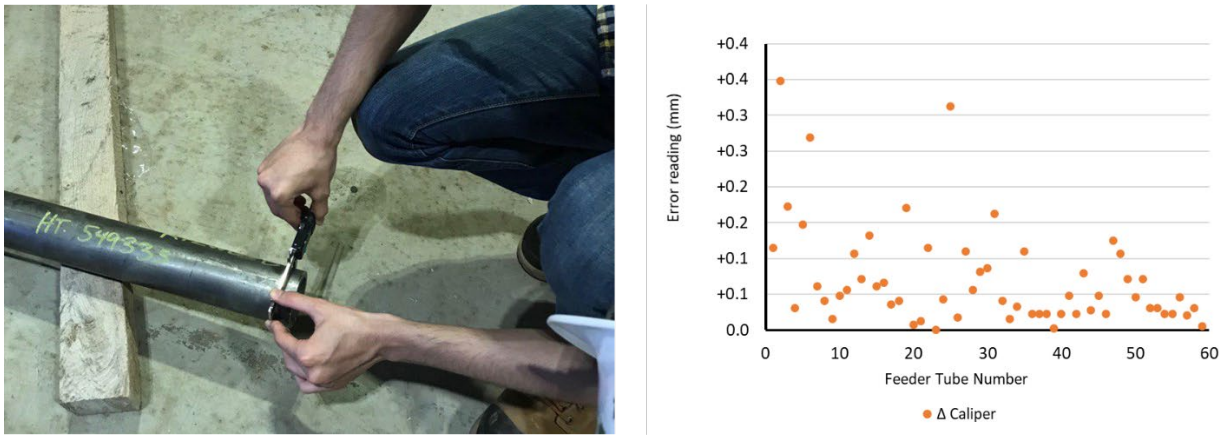

Figure 7-12. The difference between calliper readings and the FARO Arm

7.6.2 Accuracy in Calculation of Model and Scan Origin Termination Points $[A_s \text{ and } A_m]$

To estimate the accuracy of the calculated coordinates for the origin termination points in the scan and model (A_s and A_m) the calculated diameter at the plane in which these points are included is used (D_{A_m} is the calculated diameter at the plane containing A_m and D_{A_s} is the calculated diameter at the plane containing A_s). The comparison of diameters will provide a reasonable estimation since both methods (developed method and measuring with the scanner arm) rely on circle fitting algorithms using points captured on the perimeter of the cross-section. Hence, inaccurate diameter calculation will result in inaccurate coordinate estimation, and accurate diameter calculation is conducive to an accurate coordinate calculation for the termination points.

7.6.3 Diameter Accuracy at the Model Origin Termination Plane (D_{A_m})

As explained in section 7.5.4, a polygon mesh format is used for model representation, which uses triangles to represent objects. The process of converting CAD models into a mesh object may cause inaccuracies, which is a function of the settings to generate the mesh file. Additionally, rounding error is inevitable in the process of unit conversation (the models were designed in inches, and all calculations were done in mm). Finally, the developed method may also cause some minor errors in estimating the model termination point. As such, the calculated diameter for the model (D_{A_m}) was compared with its nominal CAD value for all feeder tubes, and the error is reported in Figure 7-13.

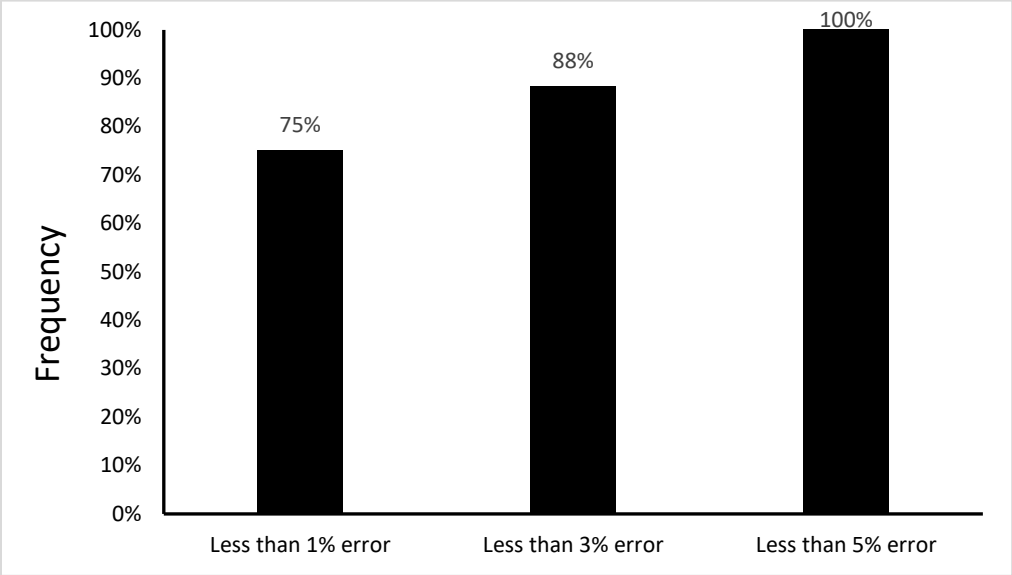

Figure 7-13. Error in calculating $\boldsymbol{D_{A_m}}$

7.6.4 Diameter Accuracy at the Scan Origin Termination Plane (D_{A_s}) Using Laser Scanner Data Input

The point clouds of 30 feeder tubes (each with two termination points) and a total of 60 termination points were captured and analyzed. After the initial acquisition by the laser scanner, the point clouds were registered together to create a complete point cloud representation of the as-built objects (multiple scans were acquired and stitched together). The D_{A_s} was then calculated using the method described in section 7.5.8. As explained earlier, to determine the D_{A_s}, the Hough Transform requires three input parameters. The initial radius guess is the calculated D_{A_m} (section 7.5.7) since the allowable tolerance for this project was 1.5 mm. The minimum radius tolerance was determined such that the search space would never get smaller than the allowable tolerance. As such, the minimum radius tolerance was set to 2% (radius tolerance is a proportional metric). Meaning, for the smallest test case with a diameter of 70 mm, the search space would be 1.4 mm. To see the impact of radius tolerance and radius resolution, nine value pairs were tested for all captured data to evaluate which value pair provides the best estimation for calculating D_{A_s}. It should be noted that both the radius tolerance and radius resolution are unitless parameters. For example, when the value pair is set to [radius tolerance=10% and radius resolution=200] for a feeder tube with a nominal diameter of 100 mm, to estimate D_{A_s} , the algorithm would start with the initial radius

guess of 100mm and continues its search with steps equal to $\frac{100\times0.1}{200}$mm (radius resolution). In this example, the boundary of the neighbourhood in which the search is conducted would be $100mm \pm (100 \times 0.1)mm$ (radius resolution). Table 7-3 shows different value pair combinations for performance evaluation.

Table 7-3. Different parameters tested in the developed framework

Parameter	Value pairs								
Radius Resolution	50	50	50	100	100	100	200	200	200
Radius Tolerance	2%	10%	50%	2%	10%	50%	2%	10%	50%

As shown in Figure 7-14, the best performance for the laser scanned data with an average absolute error of 1.01 mm (average accuracy as a percent is equal to 1.18%) and standard deviation of 0.62 was obtained when the radius resolution was set to 2% and the radius tolerance was set to 200. Additionally, when set to [2%, 200] value pair, the maximum error as an absolute value was 2.76 mm, the maximum error as a percent was 3.05%, the absolute minimum error was 0.09 mm, and the minimum error as a percent was 0.2%.

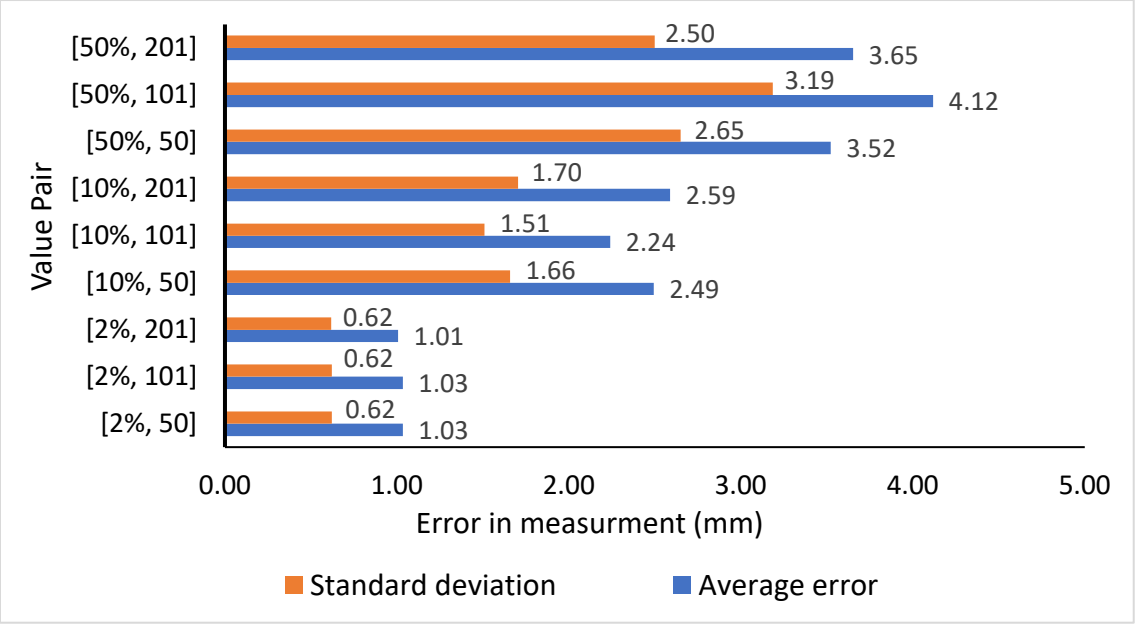

Figure 7-14. Evaluation of best value pair for Hough Transform based on laser scanned data input

Finally, using the optimized value pair, the frequency-error calculations for all termination points were calculated and are shown below.

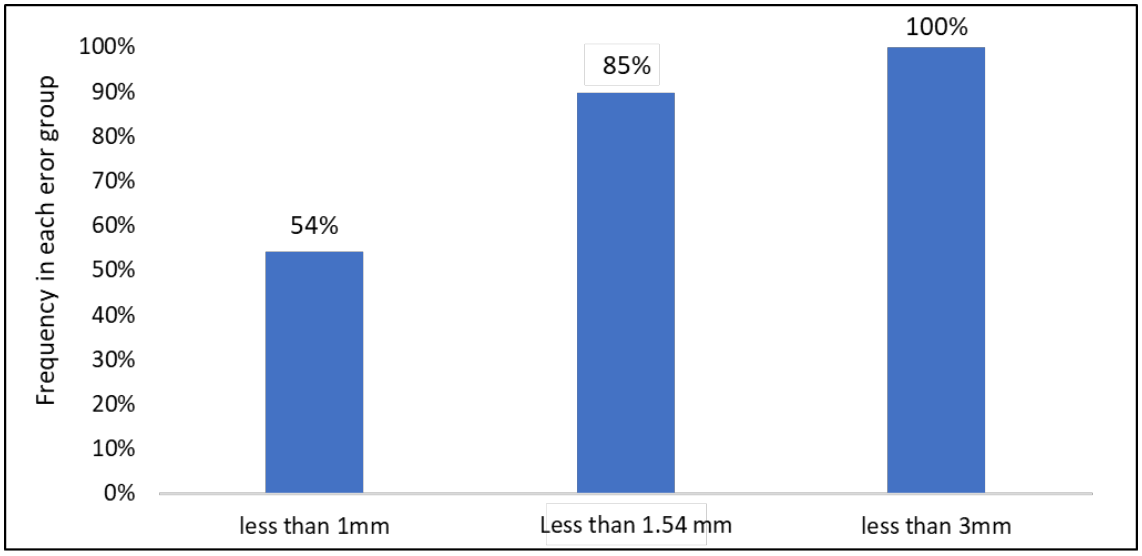

Figure 7-15. The frequency of error based on absolute error

7.6.5 Comparison with Commercial Scan-to-BIM

In addition to testing the method with different parameters, the obtained point clouds were used to measure the accuracy of utilizing a commercial software package for converting the scan point clouds to BIM objects. In this study, Edgewise® was used to convert the obtained as-built point clouds to BIM objects. The diameter of the feeder tube was then extracted as an attribute of the BIM object. The extracted diameter was compared against the ground truth, and the performance was compared against the developed method.

Using the laser scanner data provided improved accuracy in 91% of the cases. The developed method has an average error of 1.01 mm, a standard deviation of 0.62, a maximum error of 2.76 mm, and a minimum error of 0.09 mm. Comparatively, the Edgewise software solution has an average error of 4.01 mm, a standard deviation of 4.75, a maximum error of 22.3 mm, and the minimum error being 0.02 mm. The results are further illustrated in Table 7-4 and Figure 7-16.

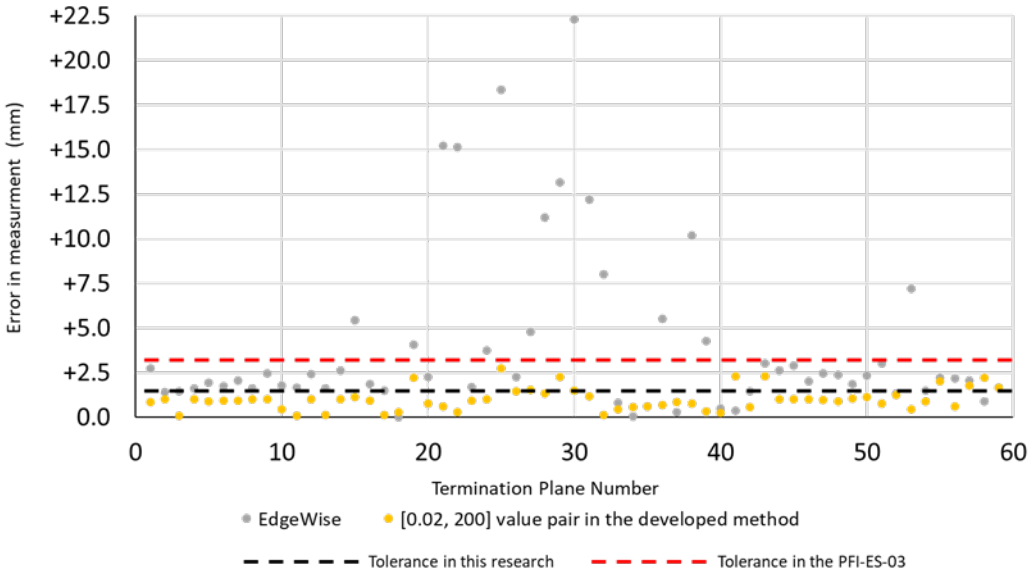

Figure 7-16. The measurement error in using both methods has been shown with a laser scanner as their data input source. The reference measurement is data collected by the probing unit.

Table 7-4. Performance comparison results with the laser scanner as the data input source

Method	Edgewise	Developed method
Average error (mm)	+4.01	1.01
Standard deviation	4.75	0.62
Maximum error (mm)	22.3	2.76
Minimum error (mm)	0.02	0.09

In 15% of the cases, the error of the developed method is more than the required accuracy. This is due to (1) the used laser scanner, and (2) the used method for registration of the scans. The laser scanner used in this study is a lower-tier scanner with an average accuracy of 3 mm; as such, since the input data in the method doesn't necessarily have the required accuracy, the developed method fails to completely compensate. Additionally, due to the fast pace of fabrication, in this study, two laser scanners were used at the same time and targetless registration methods were used. The utilization of these methods while facilitating faster scanning time, can add additional inaccuracies for the input data. Finally, while the developed method does not have sufficient accuracy in 15% of the cases, it has sufficient accuracy for all the cases under the requirements by PFI-ES-03. This is important, since most piping projects follow the requirements suggested by this standard. While the

algorithm described may be complex, its use as a function called by an interactive user interface can be made quite simple, intuitive and appropriate for an untrained technician or for a pipe fitter or QC person.

7.7 Conclusions and Recommendations

The recent growth in prefabrication and modular projects requires fabrication shops to re-evaluate their existing measurement and quality control processes. Existing measurement processes rely heavily on manual hand measurement tools, which often yield deficient accuracy. Aware of uncertainties with manual measurement tool based methods and with the increased complexity of assemblies, project owners and designers require more frequent QC steps to reduce the risk of dimensional issues, which in turn causes increased project completion time, increased rework cost, and fabrication worker frustration. To solve this problem and equip fabrication workers with an advanced measurement tool, 3D measurement systems can potentially be deployed. In this paper, a method for accurate detection and measurement of termination points was provided.

To determine the accuracy of detecting termination points in the scan and model point clouds, the calculated diameter in the circle fitting algorithm was used as an approximation. The final registered point cloud was used for the measurement of point cloud accuracy. This is important, since the hardware equipment can only certify an average accuracy in each scan and does not account for errors in the registration step. In the developed method, the calculated diameter in the model space is used to seed a search and to approximate the diameter in the scan space. Thus, the developed method provided an improved accuracy using the laser scanner compared to the method described by Nahangi et al. [141].

The developed method in this research was used in conjunction with traditional quality control tools for the fabrication of feeder tubes. As part of this research project, the method detected 7 non-compliant pipe spools, which was later confirmed by the QC team upon further investigation.

It should be noted that while only 85% of detected termination points had an accuracy below the required tolerance in this project (1.54 mm), all termination points had an accuracy below 3 mm. The 3 mm threshold is important since most projects follow the tolerance requirements

recommended by PFI-ES-03 [148] which has a 3 mm tolerance recommendation on most angles and distances.

Laser scanners also proved to be a reliable and accurate source of 3D data. While their utilization is less mobile and more time-consuming compared to SLAM scanners, their use may be required based on the required accuracy. Furthermore, to reduce the time required with a laser scanner, in this paper, multiple laser scanners were used at the same. Additionally, existing commercial software can be used to streamline and automate the data acquisition and point cloud registration aspect of laser scanners.

In future work, data communication across different stakeholders can be improved using Augmented Reality. Creating correspondence between a colour map deviation point cloud and the fabricated assembly may be cumbersome on large symmetrical shapes. Superimposing deviation maps onto built assemblies can potentially save time in data interpretation and communication. Additionally, 3D models can be projected onto assemblies that are being built as an indication for the next steps and guiding welders and fitters as they are building assemblies. However, improved productivity by better communication and real-time guidance through Augmented Reality has to be extensively researched and investigated.

Chapter 8
Final Stage of Fabrication Evolution and Advanced Visualization Tools

8.1 Chapter Summary and Contribution Statement

This Chapter provides a framework for potential improvements in the third stage of fabrication shops' evolution. The framework has four parts, (1) Collaboration and supply chain visibility through cloud technology, (2) Advanced control systems, (3) Measurement and comparison technologies, and (4) Improved visualization. The concepts in this stage are abstract and serve as a framework for future research and development. Lastly, the concept of improved visualization (as an example) is further explored, and some preliminary results of a developed application are reported.

The improved visualization section of this chapter is based on the work submitted to the United States Patent and Trademark Office on February 18, 2021, with the title "Accurate Overlaying of Holograms using Targets for Objects with Ambiguous Orientation for Mixed Reality and Augmented Reality Applications." Minor changes are made on some parts of the document to be more consistent with the body of the thesis. Thus, the content of this chapter is not exactly the same as the patent filing.

I have written the entire manuscript in this Chapter. Vishvam Mazumdar has provided assistance for implementing the developed algorithms on Microsoft HoloLens. I received editorial advice, feedback, and contributions for the manuscript from Prof. Carl Haas and Mark Pecen.

8.2 Collaboration and Supply Chain Visibility Through Cloud Technologies

The resurgence in applications using cloud technology has unlocked several new potentials. Companies are now able to access almost unlimited computing resources through their smart phones, tablets, or computer browsers. The growth in applications built on the cloud is not only important because of the computing power they can provide to users but also solving many interoperability and versioning issues. For example, companies are now increasingly using cloud based software applications for their design processes. This allows them to have a unique and up-to-

date design model that can be accessed by everyone from everywhere with internet access. Version control has been made easier, and true real-time collaboration is now feasible.

While the use of cloud technologies is gaining rapid adoption in the design stage, their use is still fairly limited to capture fabrication data. This is because the fabrication data is still logged manually on paper and stored on computers as PDF documents. The most advanced tools allow for those PDF documents to be viewed and commented on by various project stakeholders.

Integration of advanced 3D inspection systems can bring about a new era of collaboration based on 3D as-built data. Project stakeholders can remotely visualize and measure assemblies while assemblies and modules are in the fabrication shop and being fabricated. The as-built data can then be stored as part of the digital twin, and asset owners can have accurate true as-built data alongside their physical assets. The integration of cloud-based technologies also enables remote inspection and approval workflows. Project owners can request fabricators to only ship assemblies once they have been approved by their inspectors. Furthermore, disputes can be resolved quicker by everyone accessing the same set of data that is captured by an indiscriminate device.

8.3 Advanced Control Systems

All of the tools and methods described in Stages 1&2 assume the human operator as the controller in the feedback loop process. The development of the termination point framework can enable the development of human-robotic systems. The development of such systems allows for gradually changing the controller from human operators to robots supervised by expert craft workers. The development of robotic systems capable of the fitting process would require investigation and development in the following areas:

- Accurate detection of termination points in crowded scenes
- Accurate handling and positioning of assemblies
- Systems for measurement post-welding (this would require years of research as the impact of welding on assembly distortion is highly dependent on the type of weld and welding operator)
- Realignment and correction of assemblies

8.4 Measurement and Comparison Technologies

Existing measurement and quality control frameworks are built based on access to traditional and manual tools. The ability to capture full, accurate, dense 3D data unlocks two important opportunities:

1. Interaction between as-built assembly tolerances can be visualized.

As described in the earlier chapters in this thesis, scan-vs-BIM approaches are all rendered useless if the accurate design model is not available. Unfortunately, this is the case in many instances. Fabricators either do not have access to the 3D model, or the 3D model itself does not reflect the latest changes in the design. Additionally, in cases that there is an accurate and up-to-date 3D model, there are instances that accumulation of within tolerance can create onsite fit-up issues.

To solve this problem, as-built data against as-built should be leveraged. In other words, as long as assemblies are not experiencing mating issues at their termination points, their compliance with the original design is of secondary importance. Since 3D data can capture assemblies completely, they can enable project participants to visualize the fit-up prior to shipping assemblies. Any issue can be detected early on and can be remediated in the fabrication shop. So, in future, fabrication shops not only can use scan-vs-BIM methods to control their fabrication, but they can also manage complex multi assembly installations by using scan-vs-scan algorithms.

2. A complete quality control analysis can be done using a single point cloud.

Once an accurate point cloud is captured, many measurements can be made on the digital representations. This is a fundamental change in measurement capabilities by fabrication shops. Existing measurement requirements are based on few critical measurements. To reduce their risk, designers in turn, ask for tight tolerances on those specific measurements. However, these requests create many rework instances in fabrication shops since they do not have the right measurement tools for the requested measurement. This inefficiency increases the cost of the fabrication which the project owner in many cases ends up paying for.

This inefficiency can be avoided by utilizing 3D dimensional control systems. More lax tolerances can be demanded because a single point cloud acquisition is conducive to many quality checks. As such,

the requirement for a few critical measurements with tight tolerances can be substituted by many measurements with laxer tolerance that can ensure onsite fit.

8.5 Improved Visualization Tools

There has been a resurgence in various immersive Augmented Reality visualization tools. Big tech companies such as Amazon, Microsoft, Google, and Facebook have all invested in their own version of these devices. In addition to their application and use cases in the general consumer market and gaming, these tools can be utilized in the context of improving the fabrication and installation of industrial assemblies. The main concern when it comes to using these tools for fabrication control is their accuracy. That means both properly articulating the accuracy and whether it is sufficient.

In this section, some preliminary work (that was later patented) to improve the accuracy of these devices using the developed termination point framework is explained.

8.5.1 Abstract

A method is developed to establish a relationship between a 3D model and a scene viewed by an Augmented Reality/Mixed Reality unit where the relationship between the model and the object in the scene is ambiguous. The method uses targets (paper or fixture) placed on points in the scene that correspond to points on the model. The cartesian coordinate of the targets is detected by the AR/MR device. Using the coordinates of the target points in the 3D model and the detected points in the scene, the hologram is superimposed in a way that the corresponding points are overlayed, and the orientation of the hologram is adjusted. The accuracy of the overlay is then improved by minimizing the difference between the similarity index between the 3D model and scene points. Applications of the developed method include but are not limited to: (1) guidance system for fabrication of assemblies, (2) quality control of built objects, (3) fit-up assurance between multiple connecting units.

8.5.2 The Problem

In the domain of AR/MR a challenge exists to accurately and robustly superimpose holograms onto their corresponding locations in a scene viewed by an AR/MR device (this can be a Microsoft HoloLens, iPhone, iPad, or any other AR/MR enabled device) [149,150]. This is due to the fact that the coordinate system of the 3D model is different than the coordinate system of the AR/MR unit.

Additionally, the relationship between the object of interest and the AR/MR unit is unknown. Currently, two general approaches exist to overlay a hologram onto a scene. The first approach is using common features between a model and a scene. The shortcomings of this approach are: (1) that there are not always enough distinguishing features that exist on the object; in other words, the performance depends on the geometry of the model that is intended to be viewed, (2) long computation time, which impairs real-time visualization, (3) the fit between the hologram and the scene is a general fit between two parametric objects, however, in quality control applications, the fit needs to be based on termination points so that deviations can be properly interpreted and reported. The second approach used by applications such as Vuforia [151] is using Machine Learning algorithms to train a model to detect a type of object. For example, a CNN (Convolutional Neural Network) can be trained to detect a specific 20'' flange. This approach is only effective if the same object is manufactured multiple times. However, this assumption may not always be attainable. For example, in fabrication applications, parts are non-recurring and often custom-made.

8.5.3 The Solution

A method and an apparatus are developed that allows users to select a plurality of corresponding points (at least two) between a 3D model and a scene. The detection of points in the scene is done by placing targets on those points. The detection of the targets in the scene allows for creating a correspondence between the hologram and the as-built environment. Depending on how points are selected between a model and a scene, a 3D model can supplement an object, or it can be overlaid onto a corresponding object. The developed method has the following advantages:

1. The performance does not depend on the geometry.
2. The workflow is simple and fast (it takes few minutes to complete and visualize a hologram)
3. The developed method is potentially accurate because of its use of termination points and the implemented optimization.
4. The utilization of termination points in providing the overlay is useful in fabrication quality control processes.

8.5.4 Prior Art

The closest prior art to the method described in this chapter is what is specified by Schlumberger Technology Corp [152] for Applying Augmented Reality to an Object, as per [1 – 10] below.

1. Identify components of a physical object
2. Identify a point of interest of component
3. Obtain captured images of the component
4. Estimate viewing direction
5. Obtain planar model of the component
6. Identify the difference between obtained captured image
7. Identify passing criteria of point of interest
8. Compare difference to passing criteria
9. Produce discrepancy report
10. Recommend remedial action

8.5.5 The difference from prior art:

The present invention differs from the identified prior art in the following ways:

1. The developed method does not use planar images of the preexisting 3D model. Rather, the relationship between model and scene is established using termination points and installed targets.
2. Unlike the prior art, the developed method does not rely on estimating a viewing direction between the device and a selected point in a scene.
3. The developed method improves accuracy by establishing a relationship between detected points in the scene and the 3D model

How this invention goes beyond the existing body of knowledge:

1. This invention enables the overlaying of holograms through a mathematic deterministic approach. Utilization of this approach will guarantee a correct overlay between a hologram and a scene regardless of common features and without having to train a machine learning model.
2. This invention enables the overlaying to be based on specific points between the 3D model and the scene. This approach (as opposed to a global best fit) would allow for useful quality control data interpretation by checking datum points on an object in the manufacturing and fabrication industries.
3. This invention can compensate for inherent errors in the AR/MR unit. This invention can increase the accuracy to which a hologram is overlayed by leveraging the priori knowledge of the relationship between termination points in the model and the detected relationships

in the scene. A similarity index is defined and is maximized to update the coordinate of detected points, and the overlay is adjusted.

Other relevant prior art includes:

- Apparatus and method for providing augmented reality for maintenance applications [153]
- Operating and monitoring system utilizing augmented reality technology [154]
- Augmented reality with direct user interaction [155]

As explained earlier, none of the aforementioned prior arts use target detection as a method for creating a correspondence between a 3D model and a scene.

8.5.6 Definitions

Hologram

A hologram is defined as a three-dimensional image formed by the interference of light beams from a laser or other coherent light source. In the context of this invention, a hologram is referred to as the 3D object that is superimposed onto the scene and that can be viewed by the AR/MR unit.

Target

A target is an object with a unique pattern or geometry that can be detected by the AR/MR's camera. Various methods can be used to detect each individual target, including machine vision-based approaches such as pattern recognition, edge detection, and RANSAC. Some example targets that can be used are shown below.

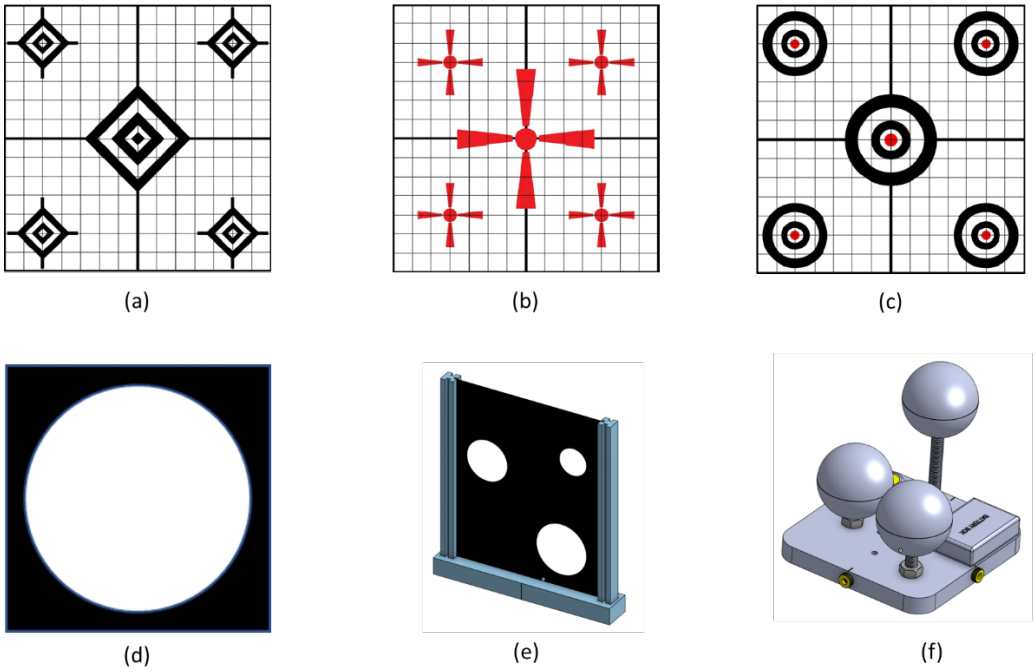

Figure 8-1. Example targets that can be detected via an AR/MR unit. (a), (b), and (c) example targets leveraging pattern recognition for detection. (d) edge detection combined with RANSAC. (e) Edge detection combined with RANSAC and optimization based on geometry. (f) RANSAC and geometry optimization.

Reference Point

Each target has at least one reference point. Once a target is detected, the coordinate of the reference point (in the AR/MR unit's coordinate system) related to the target can be obtained. Also, the normal vector of the target can be calculated. Note that the reference point may or may not be the center point of a target. This depends on how the reference point is defined with respect to the target.

Supplementing a Hologram

Supplementing a hologram refers to cases where the 3D object has components that do not already exist in the scene viewed by the AR/MR unit. An example of this is shown in Figure 8-3, where the 3D object is a magnetic array that has been added onto the scene to provide additional information.

Overlaying a Hologram

Overlaying a hologram is referred to cases where all components of the 3D model already exist in the scene. The objective here is accurately superimposing the 3D model onto its corresponding object in the scene. The main application of this is quality control to detect deviations on the as-built from the 3D model.

8.5.7 Detailed Description (input apparatus)

The workflow for superimposing holograms using termination points is shown in Figure 8-2 (an example where the hologram is overlaid onto the object) and Figure 8-3 (an example where the hologram is supplementing the scene). The process starts with identifying two or more distinct points on the 3D model (the minimum number of required points depends on the method used for calculating the transformation matrix to transform the hologram onto the object of interest). The selected points should exist in both model and scene spaces. Once the points are selected in the model space, the user would need to place targets to corresponding points in the scene. The placement needs to be such that the reference point of the target is superimposed onto the selected point of the object as accurately as possible. After obtaining the two sets of data in the model coordinate system and AR/MR unit's coordinate system, the hologram can be transformed and visualized to a user.

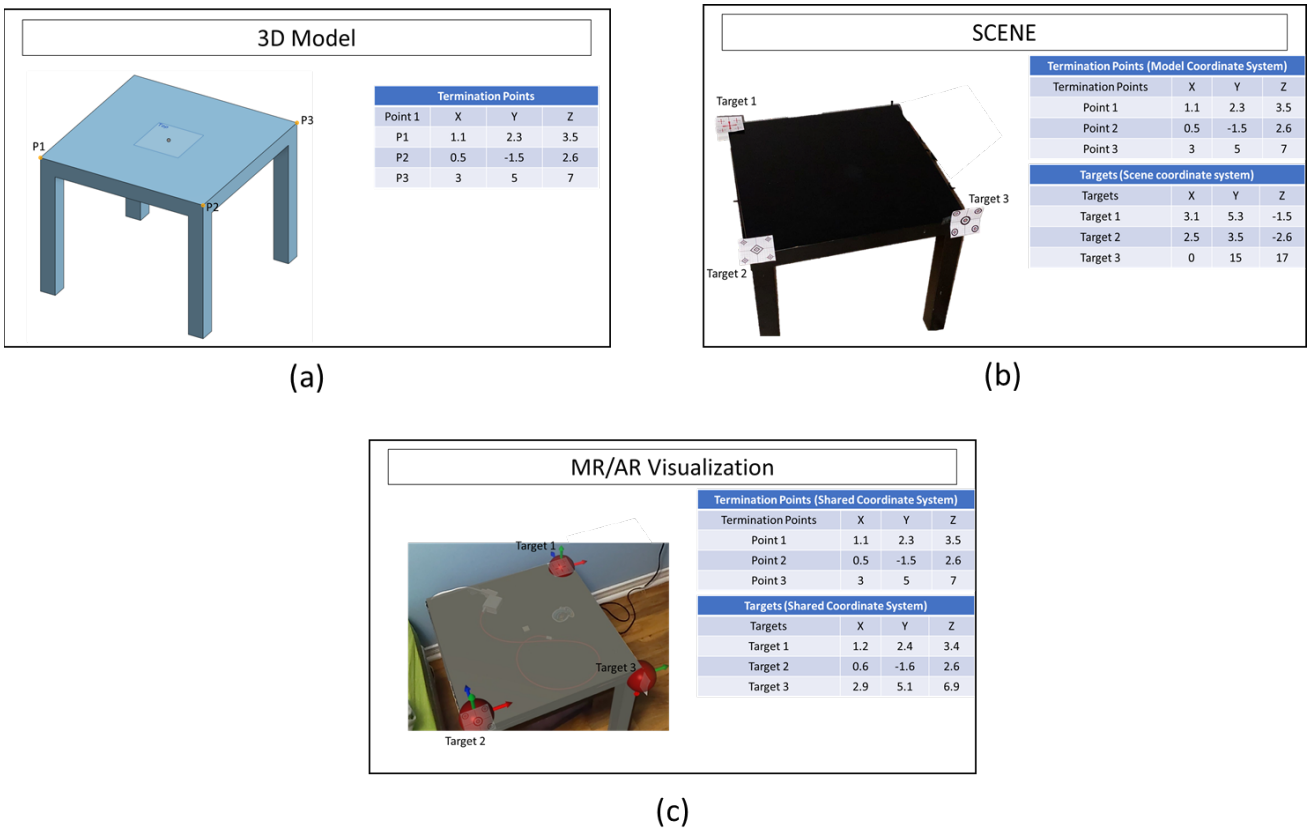

Figure 8-2. The workflow that is enabled by the described method. A case where the hologram is overlaid on a scene is shown in this example. (a) three points on the 3D model are selected. The coordinates of these points are described in the model's coordinate system. (b) Paper targets are placed onto points in the physical space such that their location corresponds to those points selected in the 3D model. Reference points of these targets are detected by the AR/MR unit, and their coordinate is obtained in the AR/MR unit's coordinate system. (c) having the two data sets, the hologram can be transformed onto the scene

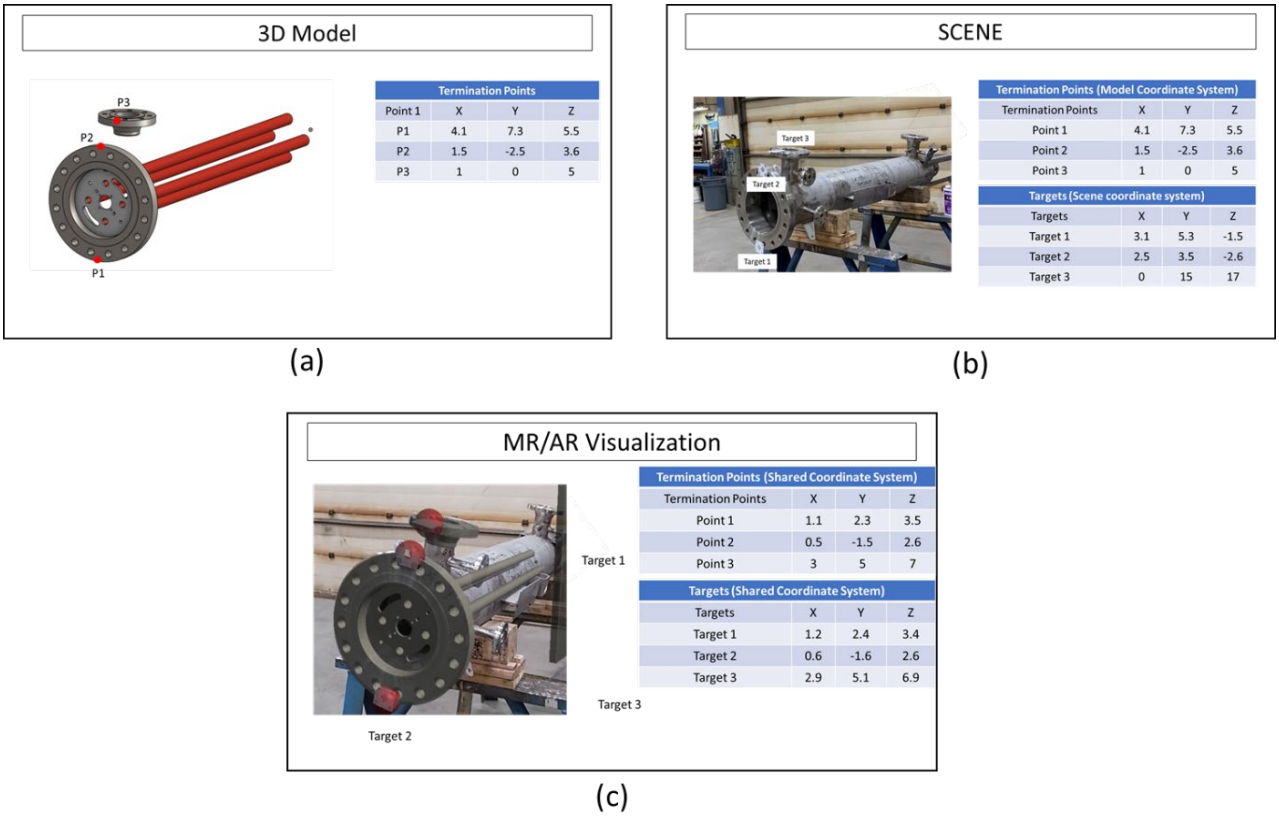

Figure 8-3. The workflow that is enabled by the described method. A case where the hologram is supplementing a scene is shown in this example. (a) three termination points on the 3D model are selected. The coordinates of these points are described in the model's coordinate system. (b) Paper targets are placed onto physical space such that their location corresponds to those points selected in the 3D model. Reference points of these targets are detected by the AR/MR unit, and their coordinate is obtained in the AR/MR unit's coordinate system. (c) having the two data sets, the hologram can be transformed onto the scene

8.5.8 Apparatus

Figure 8-4 describes the proposed apparatus in this chapter. The method is comprised of an input apparatus described earlier and a processing apparatus described hereinafter.

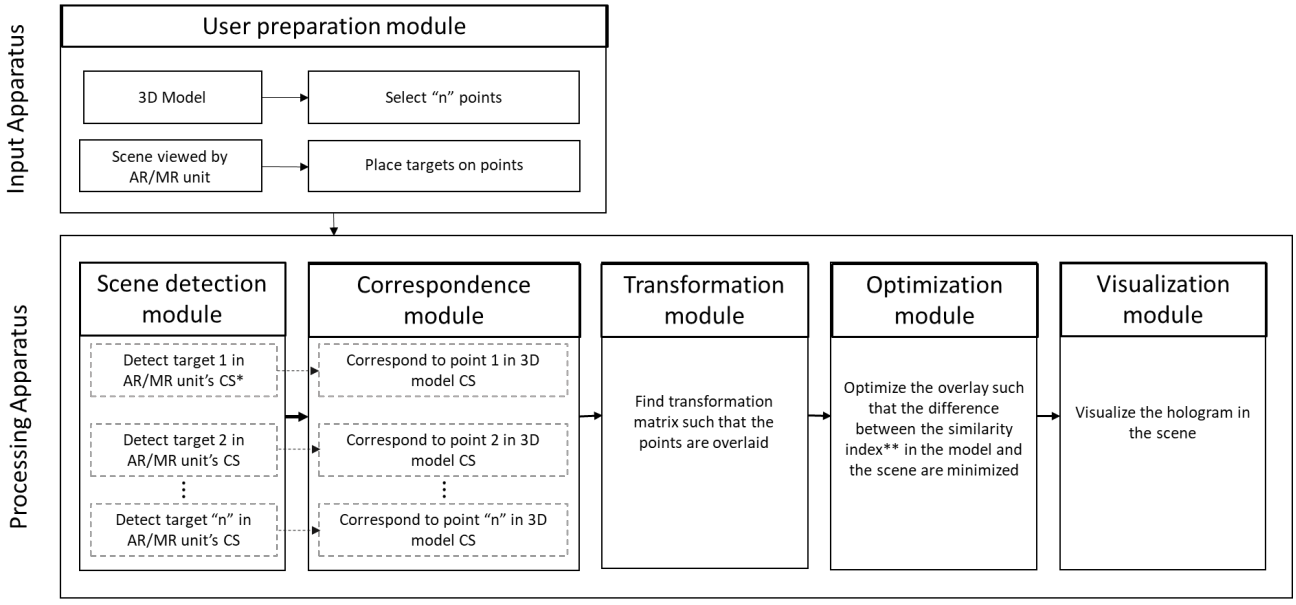

* CS is short for Coordinate System
** The definition of the similarity index is provided in the optimization section

Figure 8-4. Described apparatus.

The input apparatus requires a user to select a plurality of termination points on the 3D model and place targets onto corresponding points.

8.5.9 Scene detection module

The scene detection module is where the reference points on targets are detected. Each target has a reference point and a normal vector associated with the reference point.

8.5.10 Correspondence module

Detected points from the previous step are sorted such that the correspondence between detected points in the scene and points in the 3D model is established.

8.5.11 Transformation module

Let's name the set of points detected in the 3D model and the scene as follows:

Points in the 3D model:

$$P_m = [[P_{m_1}], [P_{m_2}], \dots, [P_{m_n}]]$$

Target Points in the scene (AR/MR unit's coordinate system):

$$P_s = [[P_{s_1}], [P_{s_2}], \dots, [P_{s_n}]]$$

In the transformation module, a transformation matrix T is calculated such that P_m is transformed onto P_s. In other words, the objective in this section is to find rotation matrix R and translation matrix T such that:

$$P_s = R \times P_m + T$$

8.5.12 Method #1 – Principal Component Analysis

In this method, at least three corresponding points between the model and scene are required (three or more targets should be used). Once the 3 points on the model and 3 points in the scene are established, the PCA method described here can be used to calculate a transformation matrix [152]. This method is well established and is already used by many researchers and commercial software packages.

8.5.13 Method #2 – Cross Product

This method requires exactly three corresponding points between the model and the scene (three targets should be used). Let the name of points in the model space be $A_m, B_m, \text{and } C_m$ (the subscript "m" is for points on the 3D model). Similarly, let the detected points in the scene viewed by the AR/MR unit be $A_s, B_s, \text{and } C_s$ (subscript "s" refers to the point in the scene).

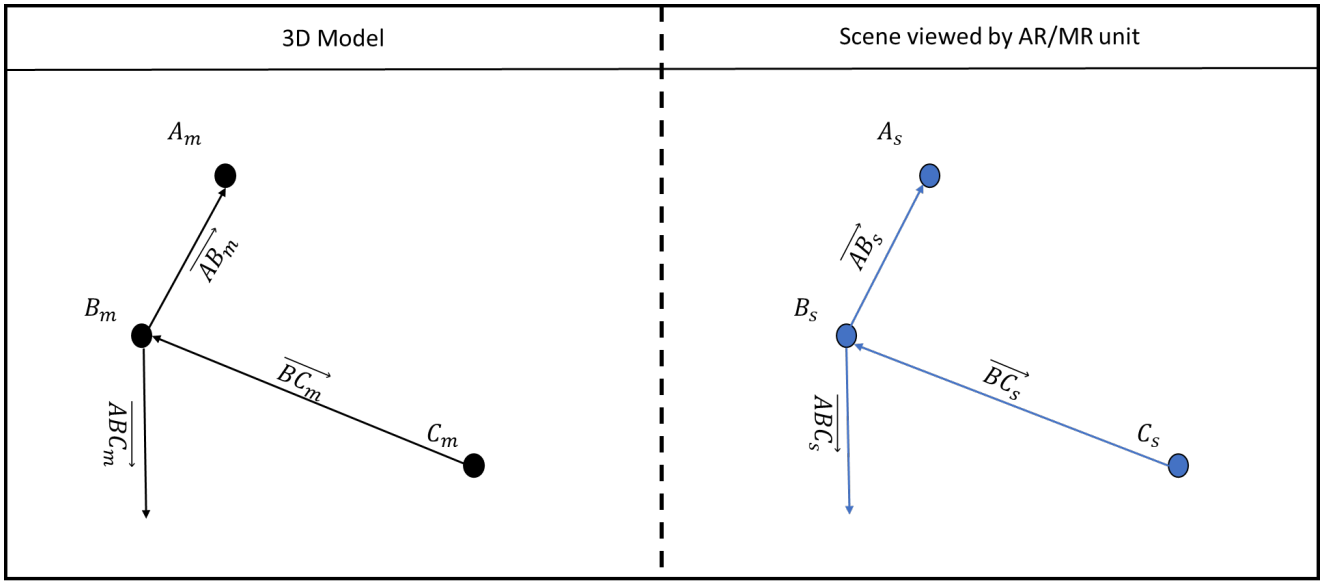

Figure 8-5. An example representation of selected points in the 3D model and the corresponding points detected by the AR/MR unit.

In the model:

$$\overrightarrow{BC_m} = B_m - C_m$$
$$\overrightarrow{AB_m} = A_m - B_m$$
$$\overrightarrow{ABC_m} = \overrightarrow{BC_m} \times \overrightarrow{AB_m}$$

In the scene:

$$\overrightarrow{BC_s} = B_s - C_s$$
$$\overrightarrow{AB_s} = A_s - B_s$$
$$\overrightarrow{ABC_s} = \overrightarrow{BC_s} \times \overrightarrow{AB_s}$$

The rotation matrix can be calculated as follows:

$$R = [\overrightarrow{BC_m}, \overrightarrow{ABC_m}, \overrightarrow{AB_m}].[\overrightarrow{BC_s}, \overrightarrow{ABC_s}, \overrightarrow{AB_s}]^T$$

And the translation can be calculated as:

$$T = A_m - A_s$$
$$or$$
$$T = B_m - B_s$$
$$Or$$

$$T = C_m - C_s$$

8.5.14 Optimization Module

When superimposing the hologram, three sources of error exist:

(1) Errors in drawing and finding termination points on the object (in the scene)
(2) Errors in placing the targets onto those termination points
(3) Errors in the detection of termination points by the AR/MR unit

To improve the accuracy of the calculated transformation matrix and hence the fit between the hologram and the physical scene, an optimization module is proposed. The optimization module is based on maximizing a similarity index (function) between the detected points in the scene and the points in the model. In other words, by assuming the termination points as the object's datum points, the geometric relationship between the detected points should resemble the geometric relationship between those points in the 3D model. By maximizing the similarity between the relationship of points in the scene, the captured coordinates will be adjusted, and a new/more accurate transformation matrix will be calculated. Additionally, the overlay result is more meaningful from the quality control perspective since the datum points are known and predetermined (as opposed to a global fit between the hologram and the object). Figure 8-6 demonstrates the parameters of the problem with 3 points.

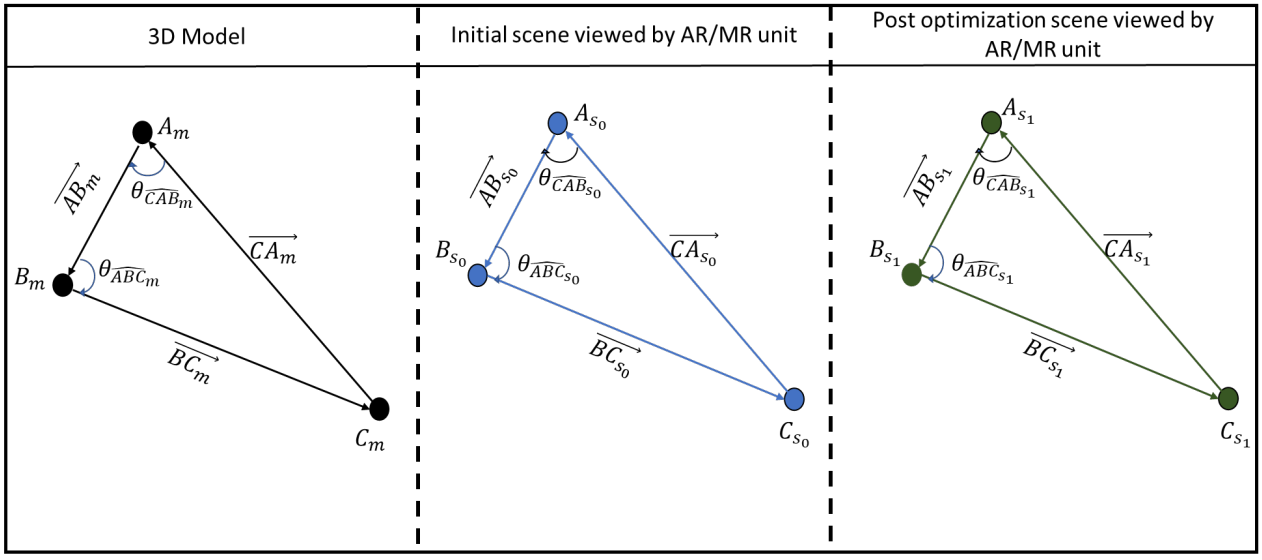

Figure 8-6. Parametric representation of the problem with 3 termination points. The notation can scale with more termination points.

Parameter definitions:

A_m: First termination point's coordinate in the model space

B_m: Second termination point's coordinate in the model space

C_m: Third termination point's coordinate in the model space

$\overrightarrow{AB_m} = B_m - A_m$, $\overrightarrow{BC_m} = C_m - B_m$, $\overrightarrow{CA_m} = A_m - C_m$

$\theta_{\widehat{CAB}_m}$: Angle created by vectors $\overrightarrow{CA_m}$ and $\overrightarrow{AB_m}$ (the first and last vectors)

$\theta_{\widehat{ABC}_m}$: Angle created by vectors $\overrightarrow{AB_m}$ and $\overrightarrow{BC_m}$ (the second and third vectors)

A_{s_0}: First termination point's coordinate detected by the AR/MR unit in the scene.

B_{s_0}: Second termination point's coordinate detected by the AR/MR unit in the scene.

C_{s_0}: Third termination point's coordinate detected by the AR/MR unit in the scene.

$\overrightarrow{AB_{s_0}} = B_{s_0} - A_{s_0}$, $\overrightarrow{BC_{s_0}} = C_{s_0} - B_{s_0}$, $\overrightarrow{CA_{s_0}} = A_{s_0} - C_{s_0}$

$\theta_{\widehat{CAB}_{s_0}}$: Angle created by vectors $\overrightarrow{CA_{s_0}}$ and $\overrightarrow{AB_{s_0}}$ (the first and last vectors)

$\theta_{\widehat{ABC}_{s_0}}$: Angle created by vectors $\overrightarrow{AB_{s_0}}$ and $\overrightarrow{BC_{s_0}}$ (the second and third vectors)

A_{s_1}: First termination point's coordinate is updated after the optimization.

B_{s_1}: Second termination point's coordinate is updated after the optimization.

C_{s_1}: Third termination point's coordinate is updated after the optimization.

$\overrightarrow{AB_{s_1}} = B_{s_1} - A_{s_1}$, $\overrightarrow{BC_{s_1}} = C_{s_1} - B_{s_1}$, $\overrightarrow{CA_{s_1}} = A_{s_1} - C_{s_1}$

$\theta_{\widehat{CAB}_{s_1}}$: Angle created by vectors $\overrightarrow{CA_{s_1}}$ and $\overrightarrow{AB_{s_1}}$ (the first and last vectors)

$\theta_{\widehat{ABC}_{s_1}}$: Angle created by vectors $\overrightarrow{AB_{s_1}}$ and $\overrightarrow{BC_{s_1}}$ (the second and third vectors)

Constraints:

The optimization should not change the coordinate of initially detected points more than the accuracy of the AR/MR unit. To deploy this condition, the following constraints are suggested. μ is used as a parametric representation of the total Euclidean value of the inaccuracy of the AR/MR unit. ($X_{A_{s_1}}$ denotes to the X direction of the point A_{s_1})

$$X_{A_{s_1}} - \mu < X_{A_{s_1}} < X_{A_{s_1}} + \mu$$

$$Y_{A_{s_1}} - \mu < Y_{A_{s_1}} < Y_{A_{s_1}} + \mu$$

$$Z_{A_{s_1}} - \mu < Z_{A_{s_1}} < Z_{A_{s_1}} + \mu$$

$$X_{B_{s_1}} - \mu < X_{B_{s_1}} < X_{B_{s_1}} + \mu$$
$$Y_{B_{s_1}} - \mu < Y_{B_{s_1}} < Y_{B_{s_1}} + \mu$$
$$Z_{B_{s_1}} - \mu < Z_{B_{s_1}} < Z_{B_{s_1}} + \mu$$
$$X_{C_{s_1}} - \mu < X_{C_{s_1}} < X_{C_{s_1}} + \mu$$
$$Y_{C_{s_1}} - \mu < Y_{C_{s_1}} < Y_{C_{s_1}} + \mu$$
$$Z_{C_{s_1}} - \mu < Z_{C_{s_1}} < Z_{C_{s_1}} + \mu$$

Objective:

The objective can be visually defined as making the triangle (or hexagon in the case where more than 3 termination points are detected) detected in the scene more similar to the triangle created by termination points in the scene.

Maximize:

$$f\left(X_{A_{s_1}}, Y_{A_{s_1}}, Z_{A_{s_1}}, X_{B_{s_1}}, Y_{B_{s_1}}, Z_{B_{s_1}}, X_{C_{s_1}}, Y_{C_{s_1}}, Z_{C_{s_1}}\right)$$
$$= \frac{\left|1 - \frac{\overrightarrow{AB_m}}{\overrightarrow{AB_{s_0}}}\right| + 1}{\left|1 - \frac{\overrightarrow{AB_m}}{\overrightarrow{AB_{s_1}}}\right| + 1} \times \frac{\left|1 - \frac{\overrightarrow{CA_m}}{\overrightarrow{CA_{s_0}}}\right| + 1}{\left|1 - \frac{\overrightarrow{CA_m}}{\overrightarrow{CA_{s_1}}}\right| + 1} \times \frac{\left|1 - \frac{\overrightarrow{BC_m}}{\overrightarrow{BC_{s_0}}}\right| + 1}{\left|1 - \frac{\overrightarrow{BC_m}}{\overrightarrow{BC_{s_1}}}\right| + 1} \times \frac{\left|1 - \frac{\theta_{\widehat{CAB}_m}}{\theta_{\widehat{CAB}_{s_0}}}\right| + 1}{\left|1 - \frac{\theta_{\widehat{CAB}_m}}{\theta_{\widehat{CAB}_{s_1}}}\right| + 1} \times \frac{\left|1 - \frac{\theta_{\widehat{ABC}_m}}{\theta_{\widehat{ABC}_{s_0}}}\right| + 1}{\left|1 - \frac{\theta_{\widehat{ABC}_m}}{\theta_{\widehat{ABC}_{s_1}}}\right| + 1}$$

Once the objective function is defined, various constrained multi-variable optimization methods can be used. These methods include but are not limited to: (1) Trust-Region Constrained Algorithm [156], (2) Sequential Least Squares Programming (SLSQP) Algorithm [157], and (3) Genetic algorithm [158]. By performing the suggested optimization algorithm, the Cartesian location of detected termination points can be updated, and the described error sources causing the inaccuracies can be compensated for.

Solving the proposed optimization would result in updated reference points coordinates. Upon updating these coordinates, the overlay is adjusted to compensate for errors in the placement of targets and the error in the detection of reference points.

Following figures and videos show a use case of the AR headset in a fabrication shop environment. In this case, the fabricator, fabricates the pressure vessel that will be housing a magnetic array inside itself. The magnetic array is manufactured by another and will be shipped separately to the client. The fabricator used the AR headset to visualize how the array will fit inside the pressure vessel. The length of the array was verified against the pressure vessel.

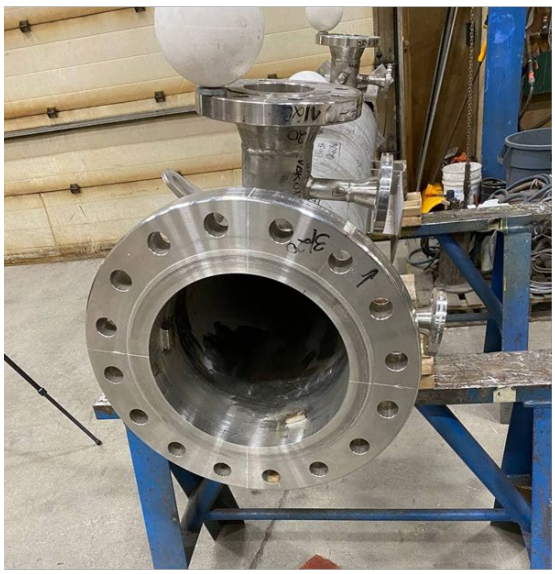

Fabricated in Ontario

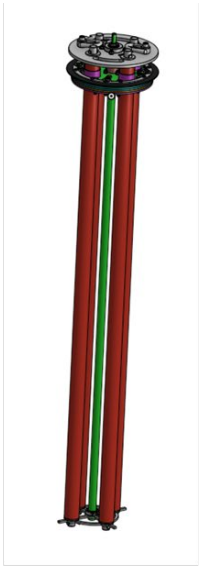

Manufactured in Alberta

Figure 8-7. Fabricated pressure vessel to be check by the fabricator to make sure the magnetic array (manufactured by another vendor) will fit in

Figure 8-8. Fabrication worker visualizing the fit using an AR headset

Figure 8-9. AR view

8.6 Conclusions

In this chapter, four potential paths for improvement and development for fabrication shops were defined. These improvement avenues include: (1) Collaboration and supply chain visibility through cloud technology, (2) Advanced control systems, (3) Measurement and comparison technologies, and (4) Improved visualization. Improved visualization was further explored as an example improvement avenue to demonstrate the type of applications and challenges that fabrication shops and technology providers face.

Chapter 9
Summary, Limitations, Research Contributions, and Future Research

9.1 Thesis Summary

A framework and methods were presented in this thesis to support integration of 3D feedback control systems to improve dimensional conformance during fabrication of engineered assemblies such as process piping, structural steel, vessels, valves, and associated instrumentation for industrial construction projects. It was explained that typically, fab shops do not use 3D feedback control systems in their measurement and quality control processes. Instead, most measurements are done using manual tools such as tape measures, callipers, bubble levels, straight edges, and squares. Inefficiency and errors ensue, costing the industry tens of billions of dollars per year globally. Improvement is impeded by a complex fabrication industry system dependent on deeply embedded existing processes, inflexible supply chains, and siloed information environments. This thesis aimed to address these impediments by developing and validating a new implementation framework including several specific methods.

To accomplish this goal, several research objectives were defined and pursued:

1. Determine if 3D dimensional control methods are possible for fab shops that do not have access to 3D models corresponding to shop drawings, thus serving as a step toward deploying more integrated, sophisticated and higher performing control systems.
2. Discover ways to solve incompatibility between requested information from fabrication workers and the output information delivered by state-of-the-art 3D inspection systems.
3. Conduct a credible cost-benefit analysis to understand the benefits required to justify the implementation costs, such as training, process change management, and capital expenditures for 3D data acquisition units for fab shops.
4. Investigate ways to compare quality and accuracy of dimensional control data sourced from modern point cloud processing methods, conventional surveying methods, and hand tools.

Methodologies used in this research included: (1) an initial literature review to understand the knowledge gaps coupled with informal interviews of practitioners from industrial research partners, and this was revisited throughout the development of the dissertation, (2) development of a conceptual framework for 3D fabrication control based on 3D imaging, (3) development and validation of algorithms to address key impediments to implementation of the framework, (4) experiments in the fab shop environment to validate elements of the framework, (5) analysis to develop conclusions, identify weaknesses in the research, understand its contributions, and make recommendations.

By developing and testing the preceding framework, it was discovered that three stages of evolution are necessary for implementation. These stages are:

1. Utilization of 3D digital templates to enable simple scan-vs-3D-model workflows for shops without access to 3D design models.
2. Development of a new language and framework for dimensional control through current ways of thinking and communication of quality control information.
3. Redefining quality control processes based on state-of-the-art tools and technologies, including automated dimensional control systems.

Each of these evolution stages were explained. Developments in each chapter pertained to a specific evolution stage. Specifically, Chapters 3 and 4 focused on the first stage. Chapters 5,6, and 7, focused on the second stage. Chapter 8 focused on the last stage of the evolution. Algorithms, methods, workflows, and frameworks were developed for each stage. The developments were tested, and some case studies were conducted, and the results were reported.

Most of the test data in this thesis were collected at the Aecon Group's fabrication facilities in Sherwood Park, Alberta, and Cambridge, Ontario. Some of the case studies were also implemented in other fabrication shops in Ontario.

The rest of this chapter focuses on contributions and conclusions in each evolution stage and each thesis chapter, as well as, explaining limitations with the presented research.

9.1.1 Stage 1: Utilization of 3D Digital Templates for Fabrication Control

Fabrication shops' lack of access to 3D models along with the perceived high capital cost of scanning equipment, was further investigated in Chapter 3 to explain why many fabrication shops cannot integrate 3D dimensional inspection systems. It was explained that many fabrication shops' existing supply chains and information environments do not demand and cannot generate 3D models corresponding to cutsheet drawings.

To address this limitation, a framework for developing 3D digital template models was developed for inspecting received parts. The framework was used for developing a library of 600 3D models of piping parts. The library was leveraged to deploy a 3D quality control system that was then tested in an industrial-scale case study. The results of the case study were used to develop a discrete event simulation model. The simulation results from the model and subsequent cost-benefit analysis show that investment in integrating the scan-vs-3D-model quality control systems can have significant cost savings and provide a payback period of less than two years.

9.1.2 Stage 2: Development of a new language and framework for dimensional control

In Chapters 5, 6, and 7 it was explained that existing measurement and control processes in fabrication shops all rely on the detection of discrete points on assemblies. These points often represent a parametric feature such as the center of a flange (circular section) or the centerline of a pipe (a cylinder object). It was also explained that both surveying grade tools and manual measurement tools were similar in that they enabled fabrication workers to assess the geometric compliance of their assemblies using these specific points and develop reports corresponding to the requested information. 3D acquisition units on the other hand, do not readily provide this information. 3D acquisition units provide a complete, accurate, 3D digital representation of an assembly that can be compared against a 3D model. In these chapters, it was explained that even though comparing the scanned object against its 3D model is an acceptable method for detecting errors and deviations (and in many cases it is a more complete and holistic method compared to existing approaches where only a few critical measurements are evaluated), fabricators are still hesitant to use them. It was explained that this is not because scan-to-BIM approaches are inaccurate. It was explained that existing quality control processes are defined based on traditional tools. Implementation of 3D inspection tools requires redefining quality control processes. In this

paradigm shift, fabricators no longer need to perform only a few critical measurements rather to inspect the complete structure using 3D scanners and scan-vs-BIM methods.

To bridge the gap between what 3D inspection systems can offer and what is expected by the fabrication workers, a transition stage was defined. In this transitional stage, fabricators can take full advantage of 3D dimensional control systems as well as fulfilling their existing requirements for providing measurements between specific points and features.

To develop the required tools and methods for this stage, the concept of Termination Points was further defined and a framework for measuring and classifying them was developed. The framework was used to developed applications and tools based on the provided set of definitions. Those applications and tools were further analyzed, and the results were reported in each chapter.

9.1.3 Stage 3: Automated Inspection Systems and Fabrication Processes

The last stage in transitioning fabrication shops from manual and 2-dimensional processes to automated and advanced control processes was discussed in Chapter 8. Four main areas for improvement and advancements were identified. These four areas included: (1) Collaboration through cloud technology, (2) Advanced control systems, (3) Measurement and comparison technologies, and (4) Improved visualization. Interestingly, much of the existing literature focuses on this stage and how improved tools and functions can be developed in fabrication shops. Advanced Visualization tools were further explored as an example area for future development. The fabrication shop of the future can be envisioned as a shop that has these tools integrated.

9.2 Contributions

The key contributions and respective conclusions for thesis are summarized below.

9.2.1 Utilization of 3D Digital Templates

A generalized framework for developing libraries of various industrial parts was developed. The developed framework can be used as a way for fabricators to integrate scan-vs-BIM 3D inspection systems at the receiving stage of their workflow.

To demonstrate the usefulness of the framework, a library of more than 600 piping parts was developed. The developed library was integrated into a scan-vs-3D-model software application and

was tested at the research partner's fabrication facility in Cambridge, Ontario. The results of the implementation showed that enabling 3D dimensional inspection at the receiving stage can reduce risks of project delays by earlier detection of issues.

The results of the case study and data from existing fabrication flow and processes were used to develop a discrete event simulation model. The model was used to simulate the cost of integrating such systems under various scenarios and using various scanning technologies. It was demonstrated that the fastest payback period could be accomplished by using a hybrid model for scanning technologies. Additionally, it was demonstrated that regardless of the project type or the choice in scanning technology, a payback period of under 3 years can be accomplished.

9.2.2 Utilization of Simple Scan-vs-3D-Model for Design and Fabrication Verification

Two case studies were carried out to demonstrate the value of performing rapid and simple scan-vs-BIM analysis. These case studies focused on two different stages of the supply chain. In one case study, it was shown that how scan-vs-3D-model can be used in cases where a retrofit is required, and the design data of existing assets is either is not available, or they are inaccurate. The second case study focused on the value of utilizing scan-vs-3D-model at the final stage of fabrication to confirm the quality of fabricated items. It was demonstrated with a 2hour investment in scan-vs-3D-model, weeks of delays and disputes were avoided.

9.2.3 Using Termination Points and 3D Visualization for Dimensional Quality Control

A definition and a framework for classifying termination points was provided. The framework was developed to allow advanced 3D dimensional control solutions to be developed in a way that is consistent with current ways of thinking. The utilization of the developed framework is critical for future applications to consider since existing supply chains and data workflows rely on quality control information to be reported with respect to termination points.

To demonstrate the usefulness of the framework and the set of definitions, a scan-vs-BIM optimization and visualization application was developed. The application was tested as part of a large industrial-scale case study, which included the fabrication of more than 30 feeder tubes with more than 400 quality control checks. The developed application flagged 7 feeders with having a

geometric issue. All 7 assemblies were later confirmed by the quality control department to have had an issue.

9.2.4 Development of a Fixture for Detection of Termination Points

To make applications and solutions accessible to fabrication workers, it is important to deliver them in a simple and understandable way. However, detection of termination points, especially on nonparametric surfaces can be a highly complex task with many steps involved. To allow for detection and calculation of termination points along with maintaining simplicity, a hardware fixture was designed and built. The developed fixture can be installed on any point of interest on any given assembly and the location and orientation of the termination point can be calculated as long as the device is visible to a scanner. Additionally, the practice of installing optical targets onto specific points on structures is a familiar and existing process when advanced surveying tools such as laser trackers are used. The developed device provides the same set of capabilities that can be accomplished by a laser tracker. This is an important distinction since running 3D scanners is a far more automated and simpler process compared to laser trackers and total stations. Also, the provided data is in 3D, which enables other scan-vs-BIM and scan-to-BIM workflows and applications.

9.2.5 Dimensional Quality Assurance for Pipe Spool Verification

To further explore the potential of the developed termination point framework, a semi-automated approach for accurately detecting termination points with circular cross-section was developed. The developed application was used as part of the fabrication of feeder tubes. The accuracy of the method was later measured and benchmarked against quality control checks done by a 3rd party inspection firm. The experiments were done using data from laser scanners. The resulted accuracy from the developed method was superior to some of the existing and recent methods in the literature. An important contribution of this work was reporting the accuracy of point cloud data based on their accuracy to capture termination points. Exiting certificates and calibration documents all report the accuracy as an average error across all points in a captured point cloud. This is not useful information because:

1. The reported accuracy measure does not include the errors in the registration process.

2. Not all points in a point cloud have the same level of importance

In other words, for 3D inspection systems to be used by fabricators, it is critical to articulate the accuracy based on their ability to measure termination points on a final resulting point cloud. The work in this chapter attempts to address this concern by providing accuracy measures based on termination point calculation.

9.3 Limitations

One of the limitations in Stage 1 of this research is that the developed framework can only be applied at the receiving stage for incoming parts. On a high level, the actual fabrication process can be broken down into three major steps, (1) receiving, (2) fabrication (fitting and welding), and (3) final QC and shipping. While the developed framework addresses the issue with the lack of 3D models in the receiving stage, the other two stages are not addressed. Also, an economic justification has been done to investigate the payback period for investing in the implementation of 3D dimensional control systems. While the work attempts to cover various project types and scenarios, the analysis still may not be applicable to all fabrication shops. Fabrication is a highly fragmented market; different shops use different workflows and have a different set of requirements and constraints in place. More work can be done to cover other types of fabrication shops, focusing on different industrial sectors to better understand the value of implementing 3D dimensional control systems in the broader market.

The other limitation in Stage 2 of this research is that the developed applications and experiments all include the minimum (only 2) termination points on assemblies. While this is what often happens and is required in piping systems, many other applications and assemblies have multiple termination points connecting to a multitude of termination points on another assembly. In these cases, more advanced systematic tolerance checking is required, as some of the termination points may be more critical than the others. For example, an assembly may be connecting to another assembly at five termination points. However, two of the termination points have field weld and the other three must be exactly in the designed location as they would be mating with other prefabricated termination points. In this case, the system for managing deviations at the termination points needs to be able to prioritize the fit of the three of the termination points over the fit of the other two. An example assembly with eleven termination points is shown in Figure 9-1.

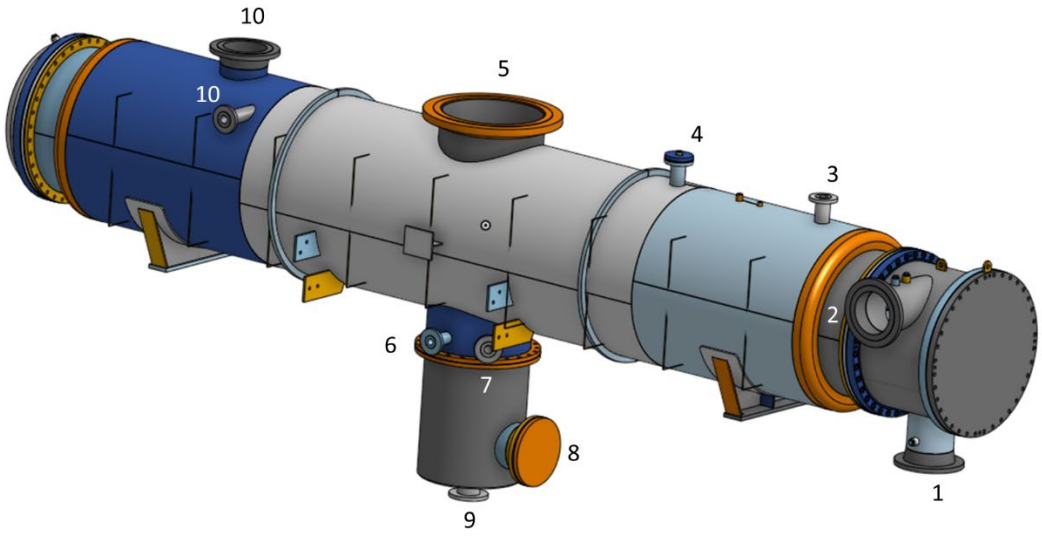

Figure 9-1. Requirement for managing a system of termination points for more complex structures.

The other limitation of this research in Stage 2 is that the developed applications all require low-level models (**.STL). This is both an advantage and a limitation. From a practical perspective, fabrication shops have a better chance to acquire STL models, so in this research the author chose to use them as a basis to develop the applications. However, using the low-level model introduces inaccuracies and additional steps in getting the information regarding the geometry of the assembly. If higher-level model file types are used, the information regarding termination points can simply be parsed as an object property.

Finally, the required methods in this work all rely on an accurate 3D design model to be available. However, from a practical standpoint, there are times that changes in the design drawings do not get reflected into the 3D model (at least not in real-time). This issue will become irrelevant by implementing the framework explained in Chapter 8, by using as-built data against as-built data. Compliance against original design is irrelevant if there is a way for fabricators and project owners to verify fit between site conditions against their shop assemblies. Implementation of such systems requires fundamental changes in the way projects and fabricators conduct their quality control.

9.4 Future Work

In this section some avenues for extending the conducted research in this thesis are provided.

9.4.1 Measurement Automation

Fabrication shops do not use 3D dimensional control systems. This offers technology providers and researchers a great opportunity. However, any solution and new approach have to be simple to use and easy to implement in fabrication shop environments. As such, an avenue for future research is automating some of the manual steps required in performing methods introduced in this research as well as other methods available in the literature. One of the areas that still requires manual input and can be counter-intuitive for fabrication users is the registration process of multiple point clouds. Existing methods are either manual or require large scanning areas with a high mutual coverage rate [159]. To automate this process, deep learning (DL) algorithms can potentially be leveraged. DL can be used because in the context of fabrication control, it is known that in the scanning area there will always be a target object with a known 3D model. Additionally, since small scan areas are desirable (to reduce scanning time) the noise rate is low compared to other applications.

The other important aspect of Measurement Automation is the further integration of the control feedback loop concept that was introduced earlier in this thesis. The termination framework provides a basis to integrate the feedback loop system into the measurement paradigm.

9.4.2 Integration with Digital Twins and Supply Chain Visibility

Implementation of 3D inspection systems can facilitate the integration of fabrication data in the Digital Twins and provide supply chain visibility. Currently, fabrication data is only recorded on PDF documents and are shared using Email or ERP (Enterprise Resource Planning) systems. 3D data can be collected, and the data can be uploaded to client or cloud servers, where they can be accessible to all project stakeholders. This also facilitates collaboration and additional workflows between project stakeholders. Assemblies can be remotely inspected and approved prior to shipping. Accurate and up-to-date models can be made based on the point cloud data.

9.4.3 Utilization of Immersive Visualization Tools

As explained in the previous chapter, the developed termination point framework can be used to build Augmented Reality based applications with sufficient accuracy. The potential for these applications can be explored in three main domains:

1. Visualization of the fit between site condition and assemblies in fabrication shops

Once an assembly is scanned, the digital hologram of the assembly can be used to visualize the fit between the hologram (of the assembly in the fabrication shop) and the site condition. Termination points between the assembly in the shop and the site condition can be used to provide a fit between the hologram and the site assembly. The fabrication worker can visualize the fit condition prior to shipping and verify if there are any issues.

2. Active fitter guidance during the fabrication process

This is especially useful on large symmetrical objects. Existing research indicates that providing the 3D model during the fabrication process will improve productivity. The delivery of these 3D models so far has been using computer screens or 2-sided isos [24]. It would be interesting to investigate the impact of immersive visualization tools to bolster workers' visualization ability. An analogy for this would be laser projectors. Augmented Reality devices can project the full 3D model onto the assembly and guide the fitter as they are positioning the next pieces to their assembly.

3. Control of Fabricated Assemblies

Instead of scanning and comparing the scan against the 3D model, the model can be superimposed onto the object itself. Discrepancies can be visualized to the worker. This approach has three main advantages over traditional scanning and comparing against the model.

(1) The cost of AR headsets is significantly lower than laser scanners.

(2) The time for visualizing the overlay is substantially lower.

(3) Many steps are automated including registration of the data.

While there are many advantages to this approach, the feasibility and the accuracy of these tools need to be further investigated and documented.

9.4.4 Connection Verification Between Multiple Assemblies

The last component of the future for this research focuses on frameworks to ensure fit-up between assemblies without relying on the design data. As was explained in this thesis, the design data in many cases is not available or is not up to date. Furthermore, compliance to the original design is of less importance compared to assemblies fitting together onsite. The ultimate goal of quality control measurements and processes is to avoid expensive site rework. This can be theoretically accomplished by fitting the as-built data from the construction site to the as-built data from the fabrication shop. Termination points can be detected, and the mating conditions can be calculated before shipping assemblies to the construction site. Development of such a framework and tool requires significant algorithmic development as well as a level of readiness from the industry for such solutions.

9.4.5 Advanced Tolerance Management Systems

Enabling all project stakeholders to see deviations in near real-time and in 3D has the potential to make designers and owners re-think existing tolerance requirements from fabricators. Currently, very strict and tight tolerances are required from fabricators. These requirements are predicated on the fact that owners could have enforced QC checks on a limited set of dimensions. As such, strict tolerances are enforced at those critical locations. However, 3D dimensional inspection offers an opportunity to fully and comprehensively inspect all dimensions of an assembly, quickly and cost effectively. This in-turn can allow owners to allow more relaxed tolerances at those specific points and enforce the required tolerance over the whole assembly. This would be beneficial to all parties as enforcing strict tolerances is costly to all parties.

9.5 Publications

9.5.1 Published Journal Articles

- Sharif, M. M., Haas, C., & Walbridge, S. (2022). Using termination points and 3D visualization for dimensional control in prefabrication. Automation in Construction, 133, 103998. https://doi.org/10.1016/j.autcon.2021.103998

- M.M. Sharif, C. Rausch, S. Ndiounge, C. Haas, S. Walbridge, Using 3D Scanning for Accurate Estimation of Termination Points for Dimensional Quality Assurance in Pipe Spool Fabrication, International Journal of Industrialized Construction. (2021) , pp.30-45. https://doi.org/http://doi.org/10.29173/ijic253.
- M. Sharif, M. Nahangi, C. Haas, J. West, Automated Model-Based Finding of 3D Objects in Cluttered Construction Point Cloud Models, Computer-Aided Civil and Infrastructure Engineering. 32 (2017) , pp.893-908. https://doi.org/10.1111/mice.12306.
- N. Jeanclos, M. Sharif, S.K. Li, C. Kwiatek, C. Haas, Derivation of Minimum Required Model for Augmented Reality Based Stepwise Construction Assembly Control, in: Anonymous Advanced Computing Strategies for Engineering, Springer International Publishing, Cham, 2018, pp. 336-358.
- C. Kwiatek, M. Sharif, S. Li, C. Haas, S. Walbridge, Impact of Augmented Reality and Spatial Cognition on Assembly in Construction, Automation in Construction. 108 (2019) , pp.102935. https://doi.org/10.1016/j.autcon.2019.102935.
- M.E. Esfahani, C. Rausch, M.M. Sharif, Q. Chen, C. Haas, B.T. Adey, Quantitative Investigation on the Accuracy and Precision of Scan-to-BIM Under Different Modelling Scenarios, Automation in Construction. 126 (2021) , pp.103686. https://doi.org/10.1016/j.autcon.2021.103686..

9.5.2 Submitted Journal Articles

- M.M. Sharif, S. Chuo, C. Haas, S. Walbridge, A 3D Digital Templates Framework for Rapid 3D Quality Control in Prefabrication, Automation in construction. Under Review. Date of Submission:30/7/2021

9.5.3 Conference Papers

- M.M. Sharif, S. Chuo, A. Majid, M. Hung, C. Haas, (2021), Utilization of Low Pass Filters for the Calculation of Termination Points for 3D fabrication control of Pipe Spools, International Conference on Computing in Civil Engineering

- Esfahani, M. E., Eray, E., Chuo, S., Sharif, M. M., & Haas, C. (2019). Using Scan-to-BIM Techniques to Find Optimal Modeling Effort, A Methodology for Adaptive Reuse Projects. In ISARC. Proceedings of the International Symposium on Automation and Robotics in Construction (Vol. 36, pp. 772-779). IAARC Publications.
- Kwiatek, C., Li, S. K., Sharif, M. M., Jeanclos, N., Haas, C. T., & Walbridge, S. (2018). Facilitating the Communication of Rework Information to Craft Workers Using an Augmented Reality Process. In ISARC. Proceedings of the International Symposium on Automation and Robotics in Construction (Vol. 35, pp. 1-8). IAARC Publications.

9.5.4 Published Patent

- M.M. Sharif, S. Li, C. Haas, M. Pecen, (2021), System and Method for Discrete Point Coordinate and Orientation Detection in 3d Point Clouds, Application Reference Number: K8002217WO,

9.5.5 Filed Patent

- M.M. Sharif, V. Mazumdar, C. Haas, M. Pecen, (2021), Accurate Overlaying of Holograms using Targets for Objects with Ambiguous Orientation for Mixed Reality and Augmented Reality Applications, Application Reference Number: 63/150,720

References

[1] Industrial Info Resources, Industrial Capital and Maintenance Project Coverage, (2021), https://www.industrialinfo.com/index.jsp,.

[2] FMI, Regional Prefabrication Assessment , (2019).

[3] C.T. Haas, W.R. Fagerlund, Preliminary Research on Prefabrication, Pre-Assembly, Modularization and Off-Site Fabrication in Construction, , 2002.

[4] X. Li, G.Q. Shen, P. Wu, T. Yue, Integrating Building Information Modeling and Prefabrication Housing Production, Automation in Construction. 100 (2019) , pp.46-60. https://doi.org/10.1016/j.autcon.2018.12.024.

[5] S. Mostafa, K.P. Kim, V.W.Y. Tam, P. Rahnamayiezekavat, Exploring the Status, Benefits, Barriers and Opportunities of using BIM for Advancing Prefabrication Practice, International Journal of Construction Management. 20 (2018) , pp.146-156. https://doi.org/10.1080/15623599.2018.1484555.

[6] A.G.F. Gibb, Off-Site Fabrication: Prefabrication, Pre-Assembly and Modularisation, Whittles, 1999. ISBN187032577X.

[7] L. Jaillon, C. Poon, Y.H. Chiang, Quantifying the Waste Reduction Potential of using Prefabrication in Building Construction in Hong Kong, Waste Management. 29 (2009) , pp.309-320.

[8] J. Guo, Q. Wang, J. Park, Geometric Quality Inspection of Prefabricated MEP Modules with 3D Laser Scanning, Automation in Construction. 111 (2020) , pp.103053. https://doi.org/10.1016/j.autcon.2019.103053.

[9] S. Jang, G. Lee, Process, Productivity, and Economic Analyses of BIM–based Multi-Trade prefabrication—A Case Study, Automation in Construction. 89 (2018) , pp.86-98.

[10] H. Said, Prefabrication Best Practices and Improvement Opportunities for Electrical Construction, Journal of Construction Engineering and Management. 141 (2015) , pp.04015045.

[11] P.E.D. Love, D.J. Edwards, H. Watson, P. Davis, Rework in Civil Infrastructure Projects: Determination of Cost Predictors, Journal of Construction Engineering and Management. 136 (2010) , pp.275-282. https://doi.org/10.1061/(ASCE)CO.1943-7862.0000136.

[12] P.E.D. Love, Influence of Project Type and Procurement Method on Rework Costs in Building Construction Projects, Journal of Construction Engineering and Management. 128 (2002) , pp.18-29. https://doi.org/10.1061/(ASCE)0733-9364(2002)128:1(18).

[13] A. Mills, P.E. Love, P. Williams, Defect Costs in Residential Construction, Journal of Construction Engineering and Management. 135 (2009) , pp.12-16. https://doi.org/10.1061/(ASCE)0733-9364(2009)135:1(12).

[14] J.B.H. Yap, P.L. Low, C. Wang, Rework in Malaysian Building Construction: Impacts, Causes and Potential Solutions, Journal of Engineering, Design and Technology. (2017).

[15] B. Hwang, S.R. Thomas, C.T. Haas, C.H. Caldas, Measuring the Impact of Rework on Construction Cost Performance, Journal of Construction Engineering and Management. 135 (2009) , pp.187-198. https://doi.org/10.1061/(ASCE)0733-9364(2009)135:3(187).

[16] G. Ye, Z. Jin, B. Xia, M. Skitmore, Analyzing Causes for Reworks in Construction Projects in China, Journal of Management in Engineering. 31 (2015) , pp.4014097. https://doi.org/10.1061/(ASCE)ME.1943-5479.0000347.

[17] C. Kwiatek, Impact of Spatial Cognitive Abilities on the Effectiveness of Augmented Reality in Construction and Fabrication,.

[18] S. Chuo, Simulation Modelling and Analysis of Impact of 3D Feedback Workflow on Prefabrication of Industrial Construction, (2020).

[19] C. Rausch, Algorithms for Geometric Optimization and Enrichment in Industrialized Building Construction, (2021).

[20] C. Rausch, R. Lu, S. Talebi, C. Haas, Deploying 3D Scanning Based Geometric Digital Twins during Fabrication and Assembly in Offsite Manufacturing, International Journal of Construction Management. (2021) , pp.1-14.

[21] M. Nahangi, C. Rausch, C.T. Haas, J. West, Dimensional Variability Analysis of Construction Assemblies using Kinematics Chains and Building Information Models,ISARC. Proceedings of the International Symposium on Automation and Robotics in Construction 34 (2017).

[22] C. Kwiatek, M. Sharif, S. Li, C. Haas, S. Walbridge, Impact of Augmented Reality and Spatial Cognition on Assembly in Construction, Automation in Construction. 108 (2019) , pp.102935. https://doi.org/10.1016/j.autcon.2019.102935.

[23] M.E. Esfahani, E. Eray, S. Chuo, M.M. Sharif, C. Haas, Using Scan-to-BIM Techniques to Find Optimal Modeling Effort; A Methodology for Adaptive Reuse Projects,ISARC. Proceedings of the International Symposium on Automation and Robotics in Construction 36 (2019), pp. 772-779.

[24] P.M. Goodrum, J. Miller, J. Sweany, O. Alruwaythi, Influence of the Format of Engineering Information and Spatial Cognition on Craft-Worker Performance, Journal of Construction Engineering and Management. 142 (2016) , pp.04016043.

[25] M. Lawson, R. Ogden, C. Goodier, Design in Modular Construction, CRC Press, Boca Raton ; London ; New York, 2014. ISBN0415554500. https://doi.org/10.1201/b16607.

[26] L.S. Sieden, Buckminster Fuller's Universe, 2. print. ed., Plenum Press, New York, NY <>, 1990. ISBN9780306431784.

[27] R. Sacks, L. Koskela, B.A. Dave, R. Owen, Interaction of Lean and Building Information Modeling in Construction, Journal of Construction Engineering and Management. 136 (2010) , pp.968-980.

[28] W. Nadim, J.S. Goulding, Offsite Production in the UK: The Way Forward? A UK Construction Industry Perspective, Construction Innovation. 10 (2010) , pp.181-202.

[29] A. Gibb, F. Isack, Re-Engineering through Pre-Assembly: Client Expectations and Drivers, Building Research & Information. 31 (2010) , pp.146-160. https://doi.org/10.1080/09613210302000.

[30] C. Milberg, Tolerance Considerations in Work Structuring,International Group of Lean Construction 15 (2007), pp. 233-243.

[31] Y. Shahtaheri, C. Rausch, J. West, C. Haas, M. Nahangi, Risk Mitigation through Tolerance Strategies for Design in Modularization, Modular and Offsite Construction (MOC) Summit Proceedings. (2015).

[32] G. Henzold, Geometrical Dimensioning and Tolerancing for Design, Manufacturing and Inspection, (2006).

[33] Y.S. Hong, T.C. Chang, A Comprehensive Review of Tolerancing Research, International Journal of Production Research. 40 (2002) , pp.2425-2459.

[34] H. Johnsson, J.H. Meiling, Defects in Offsite Construction: Timber Module Prefabrication, Construction Management and Economics. 27 (2009) , pp.667-681.

[35] C. Milberg, I.D. Tommelein, T. Alves, Improving Design Fitness through Tolerance Analysis and Tolerance Allocation,Proc., 3rd Int. Conf. on Concurrent Engineering in Construction (2002).

[36] C. Kwiatek, M. Sharif, S. Li, C. Haas, S. Walbridge, Impact of Augmented Reality and Spatial Cognition on Assembly in Construction, Automation in Construction. 108 (2019) , pp.102935. https://doi.org/10.1016/j.autcon.2019.102935.

[37] Y. Shahtaheri, C. Rausch, J. West, C. Haas, M. Nahangi, Managing Risk in Modular Construction using Dimensional and Geometric Tolerance Strategies, Automation in Construction. 83 (2017) , pp.303-315.

[38] C. Rausch, M. Nahangi, M. Perreault, C.T. Haas, J. West, Optimum Assembly Planning for Modular Construction Components, Journal of Computing in Civil Engineering. 31 (2016) , pp.04016039.

[39] M. Sharif, Construction Scene Point Cloud Acquisition, Object Finding and Clutter Removal in Real Time, (2017).

[40] M. Nahangi, C.T. Haas, J. West, S. Walbridge, Automatic Realignment of Defective Assemblies using an Inverse Kinematics Analogy, Journal of Computing in Civil Engineering. 30 (2015) , pp.04015008.

[41] T. Hartmann, M. Fischer, Applications of BIM and Hurdles for Widespread Adoption of BIM, 2007 AISC-ACCL eConstruction Roundtable Event Rep. (2008).

[42] D. Bryde, M. Broquetas, J.M. Volm, The Project Benefits of Building Information Modelling (BIM), International Journal of Project Management. 31 (2013) , pp.971-980.

[43] J.S. Goulding, F.P. Rahimian, X. Wang, Virtual Reality-Based Cloud BIM Platform for Integrated AEC Projects, Journal of Information Technology in Construction. 19 (2014) , pp.308-325.

[44] C. Park, D. Lee, O. Kwon, X. Wang, A Framework for Proactive Construction Defect Management using BIM, Augmented Reality and Ontology-Based Data Collection Template, Automation in Construction. 33 (2013) , pp.61-71.

[45] M.F. Ahmed, C.T. Haas, R. Haas, Automatic Detection of Cylindrical Objects in Built Facilities, Journal of Computing in Civil Engineering. 28 (2014) , pp.4014009. https://doi.org/10.1061/(ASCE)CP.1943-5487.0000329.

[46] H. Son, C. Kim, C. Kim, Fully Automated as-Built 3D Pipeline Extraction Method from Laser-Scanned Data Based on Curvature Computation, Journal of Computing in Civil Engineering. 29 (2015). https://doi.org/10.1061/(ASCE)CP.1943-5487.0000401.

[47] B. Wang, C. Yin, H. Luo, J.C.P. Cheng, Q. Wang, Fully Automated Generation of Parametric BIM for MEP Scenes Based on Terrestrial Laser Scanning Data, Automation in Construction. 125 (2021) , pp.103615. https://doi.org/10.1016/j.autcon.2021.103615.

[48] A. Dimitrov, R. Gu, M. Golparvar-Fard, Non-Uniform B-Spline Surface Fitting from Unordered 3D Point Clouds for as-Built Modeling, Computer-Aided Civil and Infrastructure Engineering. 31 (2016) , pp.483-498. https://doi.org/10.1111/mice.12192.

[49] R. Maalek, D.D. Lichti, R. Walker, A. Bhavnani, J.Y. Ruwanpura, Extraction of Pipes and Flanges from Point Clouds for Automated Verification of Pre-Fabricated Modules in Oil and Gas Refinery Projects, Automation in Construction. 103 (2019) , pp.150-167. https://doi.org/10.1016/j.autcon.2019.03.013.

[50] M.E. Esfahani, C. Rausch, M.M. Sharif, Q. Chen, C. Haas, B.T. Adey, Quantitative Investigation on the Accuracy and Precision of Scan-to-BIM Under Different Modelling Scenarios, Automation in Construction. 126 (2021) , pp.103686. https://doi.org/10.1016/j.autcon.2021.103686.

[51] C.H.P. Nguyen, Y. Choi, Comparison of Point Cloud Data and 3D CAD Data for on-Site Dimensional Inspection of Industrial Plant Piping Systems, Automation in Construction. 91 (2018) , pp.44-52. https://doi.org/10.1016/j.autcon.2018.03.008.

[52] M. Nahangi, C.T. Haas, Skeleton-Based Discrepancy Feedback for Automated Realignment of Industrial Assemblies, Automation in Construction. 61 (2016) , pp.147-161. https://doi.org/10.1016/j.autcon.2015.10.014.

[53] M. Nahangi, J. Yeung, C.T. Haas, S. Walbridge, J. West, Automated Assembly Discrepancy Feedback using 3D Imaging and Forward Kinematics, Automation in Construction. 56 (2015) , pp.36-46. https://doi.org/10.1016/j.autcon.2015.04.005.

[54] V.S. Kalasapudi, P. Tang, Y. Turkan, Computationally Efficient Change Analysis of Piece-Wise Cylindrical Building Elements for Proactive Project Control, Automation in Construction. 81 (2017) , pp.300-312. https://doi.org/10.1016/j.autcon.2017.04.001.

[55] I. Brilakis, C.T. Michael Haas, Infrastructure Computer Vision, Elsevier Science & Technology, San Diego, 2019. ISBN9780128155035.

[56] C. Rausch, R. Lu, S. Talebi, C. Haas, Deploying 3D Scanning Based Geometric Digital Twins during Fabrication and Assembly in Offsite Manufacturing, International Journal of Construction Management. (2021) , pp.1-14.

[57] J.J. Lin, A. Ibrahim, S. Sarwade, M. Golparvar-Fard, Bridge Inspection with Aerial Robots: Automating the Entire Pipeline of Visual Data Capture, 3D Mapping, Defect Detection, Analysis, and Reporting, Journal of Computing in Civil Engineering. 35 (2021) , pp.04020064.

[58] M. Sharif, M. Nahangi, C. Haas, J. West, M. Ibrahim, Resilient Infrastructure, (2016).

[59] M. Sharif, M. Nahangi, C. Haas, J. West, Automated Model-Based Finding of 3D Objects in Cluttered Construction Point Cloud Models, Computer-Aided Civil and Infrastructure Engineering. 32 (2017) , pp.893-908. https://doi.org/10.1111/mice.12306.

[60] Statistics Canada, Table 36-10-0480-01: Labour Productivity and Related Measures by Business Sector Industry and by Non-Commercial Activity Consistent with the Industry Accounts. (2020), https://doi.org/10.25318/3610048001-eng,.

[61] Q. Chen, D.M. Hall, B.T. Adey, C.T. Haas, Identifying Enablers for Coordination Across Construction Supply Chain Processes: A Systematic Literature Review, Engineering, Construction,

and Architectural Management. ahead-of-print (2020) , pp.11-21. https://doi.org/10.1108/ECAM-05-2020-0299.

[62] T. Bock, Construction Automation and Robotics, Robotics and Automation in Construction, 2008, pp.21-42. https://doi.org/10.5772/5861.

[63] M. Pan, T. Linner, W. Pan, H. Cheng, T. Bock, A Framework of Indicators for Assessing Construction Automation and Robotics in the Sustainability Context, Journal of Cleaner Production. 182 (2018) , pp.82-95. https://doi.org/10.1016/j.jclepro.2018.02.053.

[64] M. Sharif, M. Nahangi, C. Haas, J. West, Automated Model-Based Finding of 3D Objects in Cluttered Construction Point Cloud Models, Computer-Aided Civil and Infrastructure Engineering. 32 (2017) , pp.893-908. https://doi.org/10.1111/mice.12306.

[65] L. Sveikauskas, S. Rowe, J. Mildenberger, J. Price, A. Young, Measuring Productivity Growth in Construction, Monthly Labor Review. (2018) , pp.1-34. https://doi.org/10.21916/mlr.2018.1.

[66] M.F. Tchidi, Z. He, Y.B. Li, Process and Quality Improvement using Six Sigma in Construction Industry, Journal of Civil Engineering and Management. 18 (2012) , pp.158-172. https://doi.org/10.3846/13923730.2012.657411.

[67] M. Noguchi, The Effect of the Quality-Oriented Production Approach on the Delivery of Prefabricated Homes in Japan, Journal of Housing and the Built Environment. 18 (2003) , pp.353-364. https://doi.org/10.1023/b:joho.0000005759.07212.00.

[68] D. Zhang, C.T. Haas, P.M. Goodrum, C.H. Caldas, R. Granger, Construction Small-Projects Rework Reduction for Capital Facilities, Journal of Construction Engineering and Management. 138 (2012) , pp.1377-1385. https://doi.org/10.1061/(ASCE)CO.1943-7862.0000552.

[69] P.E.D. Love, D.J. Edwards, Forensic Project Management: The Underlying Causes of Rework in Construction Projects, Civil Engineering and Environmental Systems. 21 (2004) , pp.207-228. https://doi.org/10.1080/10286600412331295955.

[70] B. Akinci, F. Boukamp, C. Gordon, D. Huber, C. Lyons, K. Park, A Formalism for Utilization of Sensor Systems and Integrated Project Models for Active Construction Quality Control, Automation in Construction. 15 (2006) , pp.124-138. https://doi.org/10.1016/j.autcon.2005.01.008.

[71] Leica, Leica FlexLine TS10, (2021), https://leica-geosystems.com/products/total-stations/manual-total-stations/leica-flexline-ts10,September 17, 2021.

[72] HardHat Engineer, Elbow Manufacturing Process - Pipe Fittings, (2017).

[73] M. Nahangi, C.T. Haas, Skeleton-Based Discrepancy Feedback for Automated Realignment of Industrial Assemblies, Automation in Construction. 61 (2016) , pp.147-161. https://doi.org/10.1016/j.autcon.2015.10.014.

[74] B. Hwang, S.R. Thomas, C.T. Haas, C.H. Caldas, Measuring the Impact of Rework on Construction Cost Performance, Journal of Construction Engineering and Management. 135 (2009) , pp.187-198. https://doi.org/10.1061/(ASCE)0733-9364(2009)135:3(187).

[75] D. Zhang, C.T. Haas, P.M. Goodrum, C.H. Caldas, R. Granger, Construction Small-Projects Rework Reduction for Capital Facilities, Journal of Construction Engineering and Management. 138 (2012) , pp.1377-1385. https://doi.org/10.1061/(ASCE)CO.1943-7862.0000552.

[76] L. Klein, N. Li, B. Becerik-Gerber, Imaged-Based Verification of as-Built Documentation of Operational Buildings, Automation in Construction. 21 (2012) , pp.161-171. https://doi.org/10.1016/j.autcon.2011.05.023.

[77] H. Son, C. Kim, Y. Turkan, Scan-to-BIM - an Overview of the Current State of the Art and a Look Ahead, (Jun 18, 2015). https://doi.org/10.22260/isarc2015/0050.

[78] Z. Zhu, I. Brilakis, Comparison of Optical Sensor-Based Spatial Data Collection Techniques for Civil Infrastructure Modeling, Journal of Computing in Civil Engineering. 23 (2009) , pp.170-177. https://doi.org/10.1061/(ASCE)0887-3801(2009)23:3(170).

[79] T. Bailey, H. Durrant-Whyte, Simultaneous Localization and Mapping (SLAM): Part II, IEEE Robotics & Automation Magazine. 13 (2006) , pp.108-117. https://doi.org/10.1109/MRA.2006.1678144.

[80] C. Cadena, L. Carlone, H. Carrillo, Y. Latif, D. Scaramuzza, J. Neira, I. Reid, J.J. Leonard, Past, Present, and Future of Simultaneous Localization and Mapping: Toward the Robust-Perception Age, IEEE Transactions on Robotics. 32 (2016) , pp.1309-1332. https://doi.org/10.1109/TRO.2016.2624754.

[81] M. Golparvar-Fard, J. Bohn, J. Teizer, S. Savarese, F. Peña-Mora, Evaluation of Image-Based Modeling and Laser Scanning Accuracy for Emerging Automated Performance Monitoring Techniques, Automation in Construction. 20 (2011) , pp.1143-1155. https://doi.org/10.1016/j.autcon.2011.04.016.

[82] P. Tang, D. Huber, B. Akinci, R. Lipman, A. Lytle, Automatic Reconstruction of as-Built Building Information Models from Laser-Scanned Point Clouds: A Review of Related Techniques, Automation in Construction. 19 (2010) , pp.829-843. https://doi.org/10.1016/j.autcon.2010.06.007.

[83] X. Xiong, A. Adan, B. Akinci, D. Huber, Automatic Creation of Semantically Rich 3D Building Models from Laser Scanner Data, Automation in Construction. 31 (2013) , pp.325-337. https://doi.org/10.1016/j.autcon.2012.10.006.

[84] C. Kim, C.T. Haas, K.A. Liapi, Rapid, on-Site Spatial Information Acquisition and its use for Infrastructure Operation and Maintenance, Automation in Construction. 14 (2005) , pp.666-684. https://doi.org/10.1016/j.autcon.2005.02.002.

[85] J. Huang, D. Millman, M. Quigley, D. Stavens, S. Thrun, A. Aggarwal, Efficient, Generalized Indoor WiFi GraphSLAM, 2011 IEEE International Conference on Robotics and Automation. (May 2011), pp. 1038-1043. https://doi.org/10.1109/icra.2011.5979643.

[86] G. Grisettiyz, C. Stachniss, W. Burgard, Improving Grid-Based SLAM with Rao-Blackwellized Particle Filters by Adaptive Proposals and Selective Resampling, Proceedings of the 2005 IEEE International Conference on Robotics and Automation. (2005), pp. 2432-2437. https://doi.org/10.1109/ROBOT.2005.1570477.

[87] Shoudong Huang, Gamini Dissanayake, Convergence and Consistency Analysis for Extended Kalman Filter Based SLAM, IEEE Transactions on Robotics. 23 (2007) , pp.1036-1049. https://doi.org/10.1109/TRO.2007.903811.

[88] P. Kim, J. Chen, Y.K. Cho, SLAM-Driven Robotic Mapping and Registration of 3D Point Clouds, Automation in Construction. 89 (2018) , pp.38-48. https://doi.org/10.1016/j.autcon.2018.01.009.

[89] T. Pribanić, S. Mrvoš, J. Salvi, Efficient Multiple Phase Shift Patterns for Dense 3D Acquisition in Structured Light Scanning, Image and Vision Computing. 28 (2010) , pp.1255-1266. https://doi.org/10.1016/j.imavis.2010.01.003.

[90] O.A. Hall-Holt, S.M. Rusinkiewicz, Real-time structured light range scanning of moving scenes, (2004).

[91] C. Kwiatek, M. Sharif, S. Li, C. Haas, S. Walbridge, Impact of Augmented Reality and Spatial Cognition on Assembly in Construction, Automation in Construction. 108 (2019) , pp.102935. https://doi.org/10.1016/j.autcon.2019.102935.

[92] F. Bosché, A. Guillemet, Y. Turkan, C.T. Haas, R. Haas, Tracking the Built Status of MEP Works: Assessing the Value of a Scan-Vs-BIM System, Journal of Computing in Civil Engineering. 28 (2014) , pp.05014004. https://doi.org/10.1061/(ASCE)CP.1943-5487.0000343.

[93] J. Wang, W. Sun, W. Shou, X. Wang, C. Wu, H. Chong, Y. Liu, C. Sun, Integrating BIM and LiDAR for Real-Time Construction Quality Control, Journal of Intelligent & Robotic Systems. 79 (2014) , pp.417-432. https://doi.org/10.1007/s10846-014-0116-8.

[94] P. Tang, E.B. Anil, B. Akinci, D. Huber, Efficient and Effective Quality Assessment of As-Is Building Information Models and 3D Laser-Scanned Data, in: Anonymous Computing in Civil Engineering (2011), , 2011, pp. 486-493.

[95] Y. Turkan, F. Bosche, C.T. Haas, R. Haas, Automated Progress Tracking using 4D Schedule and 3D Sensing Technologies, Automation in Construction. 22 (2012) , pp.414-421. https://doi.org/10.1016/j.autcon.2011.10.003.

[96] R. Maalek, D.D. Lichti, J.Y. Ruwanpura, Automatic Recognition of Common Structural Elements from Point Clouds for Automated Progress Monitoring and Dimensional Quality Control in Reinforced Concrete Construction, Remote Sensing (Basel, Switzerland). 11 (2019) , pp.1102. https://doi.org/10.3390/rs11091102.

[97] M. Bassier, S. Vincke, H. De Winter, M. Vergauwen, Drift Invariant Metric Quality Control of Construction Sites using BIM and Point Cloud Data, ISPRS International Journal of Geo-Information. 9 (2020) , pp.545. https://doi.org/10.3390/ijgi9090545.

[98] H. Qin, D.A. Peak, V. Prybutok, A Virtual Market in Your Pocket: How does Mobile Augmented Reality (MAR) Influence Consumer Decision Making? Journal of Retailing and Consumer Services. 58 (2021). https://doi.org/10.1016/j.jretconser.2020.102337.

[99] J. Bodner, F. Augustin, H. Wykypiel, J. Fish, G. Muehlmann, G. Wetscher, T. Schmid, The Da Vinci Robotic System for General Surgical Applications: A Critical Interim Appraisal, Swiss Medical Weekly. 135 (2005) , pp.674-678.

[100] I. Hacmun, D. Regev, R. Salomon, The Principles of Art Therapy in Virtual Reality, Frontiers in Psychology. 9 (2018) , pp.2082. https://doi.org/10.3389/fpsyg.2018.02082.

[101] J. Forren, M. Ramadan, S. Sarrazin, Action over form: combining off-loom weaving and augmented reality in a non-specification model of design, in: Anonymous Virtual Aesthetics in Architecture, Routledge, 2021, pp. 107-113.

[102] Y. Zhou, H. Luo, Y. Yang, Implementation of Augmented Reality for Segment Displacement Inspection during Tunneling Construction, Automation in Construction. 82 (2017) , pp.112-121. https://doi.org/10.1016/j.autcon.2017.02.007.

[103] D. Mitterberger, K. Dörfler, T. Sandy, F. Salveridou, M. Hutter, F. Gramazio, M. Kohler, Augmented Bricklaying, Construction Robotics (Online). 4 (2020) , pp.151-161. https://doi.org/10.1007/s41693-020-00035-8.

[104] G. Betti, S. Aziz, G. Ron, Pop Up Factory: Collaborative Design in Mixed Rality-Interactive Live Installation for the makeCity Festival, 2018 Berlin,In Proceedings: CUMINCAD (2019).

[105] B. Lafreniere, T. Grossman, F. Anderson, J. Matejka, H. Kerrick, D. Nagy, L. Vasey, E. Atherton, N. Beirne, M. Coelho, N. Cote, S. Li, A. Nogueira, L. Nguyen, T. Schwinn, J. Stoddart, D. Thomasson, R. Wang, T. White, D. Benjamin, M. Conti, A. Menges, G. Fitzmaurice, Crowdsourced Fabrication, Proceedings of the 29th Annual Symposium on User Interface Software and Technology. (Oct 16, 2016), pp. 15-28. https://doi.org/10.1145/2984511.2984553.

[106] G. Jahn, C. Newnham, M. Beanland, Making in Mixed Reality. Holographic Design, Fabrication, Assembly and Analysis of Woven Steel Structures,In: Proceeding of 2018 ACADIA (2018).

[107] G. Jahn, A. Wit, J.P. Samara, BENT: Holographic Handcraft in Large-Scale Steam-Bent Timber Structures,Acadia 2019 Acadia 2019. (2019), pp. 1-11.

[108] Y. Song, R. Koeck, S. Luo, Review and Analysis of Augmented Reality (AR) Literature for Digital Fabrication in Architecture, Automation in Construction. 128 (2021) , pp.103762. https://doi.org/10.1016/j.autcon.2021.103762.

[109] T. Tawfeek, Study the Influence of Gas Metal Arc Welding Parameters on the Weld Metal and Heat Affected Zone Microstructures of Low Carbon Steel, International Journal of Engineering and Technology (IJET). 9 (2017) , pp.2013-2019.

[110] Metalica Metals, Socket Weld ,2021date of last access:December 17,.

[111] Explore the World of Piping, Definition and Details of Threaded Fittings ASME B16.11,2021date of last access:December 17,.

[112] Piping Resources Inc., Technical Resources for Piping ,2021date of last access:December 17,.

[113] Allied Group, Cap Technical Sheet,2021date of last access:December 17,.

[114] MD Exports LLP, Highly Acclaimed Manufacturer & Exporter Presents Best Offer Ever on ANSI/ASME B16.9 90° Short Radius Elbow,.

[115] Stattin Stainless, Stainless Steel Sch10 90° Long Radius Pipe Elbows,.

[116] WELLGROW INDUSTRIES CORP, Stainless & Carbon Steel Butt-Welding Fittings ,2021date of last access:December 17,.

[117] BHSVIK Tube Corporation, Stainless Steel Long Radius Elbow ,2021date of last access:December 17,.

[118] Piping Study, Piping Study Tee ,.

[119] Atlas Steels, Stainless Steel Pipe, Fittings & Flanges ,.

[120] FlexSim, Our History , (2020).

[121] PMI, Global Modular and Prefabricated Building Market is Expected to Drive due to Rising Growth in Construction Spending, (2020), https://www.globenewswire.com/news-

release/2020/06/25/2053535/0/en/Global-Modular-and-Prefabricated-Building-Market-is-expected-to-drive-due-to-rising-growth-in-construction-spending-PMI.html,September 17, 2021.

[122] Slowey, Kim, Cowin, Laurie, Beeton, Joe, Beeton, Brown, Katheleen, 7 Trends that Will Shape Commercial Construction in 2019, (2019), https://www.constructiondive.com/news/7-trends-that-will-shape-commercial-construction-in-2019/543978/,September 17, 2021.

[123] T. Afeni, F. Cawood, Slope Monitoring using Total Station: What are the Challenges and how should these be Mitigated? South African Journal of Geomatics. (2014).

[124] W. Lienhart, M. Ehrhart, M. Grick, High Frequent Total Station Measurements for the Monitoring of Bridge Vibrations, Journal of Applied Geodesy. 11 (2017) , pp.1-8. https://doi.org/10.1515/jag-2016-0028.

[125] P.A. Psimoulis, S.C. Stiros, Measuring Deflections of a Short-Span Railway Bridge using a Robotic Total Station, Journal of Bridge Engineering. 18 (2013) , pp.182-185. https://doi.org/10.1061/(ASCE)BE.1943-5592.0000334.

[126] P.A. Psimoulis, S.C. Stiros, Measuring Deflections of a Short-Span Railway Bridge using a Robotic Total Station, Journal of Bridge Engineering. 18 (2013) , pp.182-185. https://doi.org/10.1061/(ASCE)BE.1943-5592.0000334.

[127] S.J.P. McPherron, Artifact Orientations and Site Formation Processes from Total Station Proveniences, Journal of Archaeological Science. 32 (2005) , pp.1003-1014. https://doi.org/10.1016/j.jas.2005.01.015.

[128] C. Kwiatek, M. Sharif, S. Li, C. Haas, S. Walbridge, Impact of Augmented Reality and Spatial Cognition on Assembly in Construction, Automation in Construction. 108 (2019) , pp.102935. https://doi.org/10.1016/j.autcon.2019.102935.

[129] T. Weber, R. Hänsch, O. Hellwich, Automatic Registration of Unordered Point Clouds Acquired by Kinect Sensors using an Overlap Heuristic, ISPRS Journal of Photogrammetry and Remote Sensing. 102 (2015) , pp.96-109. https://doi.org/10.1016/j.isprsjprs.2014.12.014.

[130] D. Huber, The ASTM E57 File Format for 3D Imaging Data Exchange, Proceedings of SPIE. 7864 (Mar 10, 2011), pp. 78640A-9. https://doi.org/10.1117/12.876555.

[131] H. Ni, X. Lin, X. Ning, J. Zhang, Edge Detection and Feature Line Tracing in 3D-Point Clouds by Analyzing Geometric Properties of Neighborhoods, Remote Sensing (Basel, Switzerland). 8 (2016) , pp.710. https://doi.org/10.3390/rs8090710.

[132] Y. Lin, R.R. Benziger, A. Habib, Planar-Based Adaptive Down-Sampling of Point Clouds, Photogrammetric Engineering and Remote Sensing. 82 (2016) , pp.955-966. https://doi.org/10.14358/PERS.82.12.955.

[133] R. Burtch, History of Photogrammetry, Notes of the Center for Photogrammetric Training. (2004).

[134] R. Staiger, Terrestrial Laser Scanning Technology, Systems and Applications,2nd FIG Regional Conference Marrakech, Morocco 1 (2003).

[135] J. Guo, Q. Wang, J. Park, Geometric Quality Inspection of Prefabricated MEP Modules with 3D Laser Scanning, Automation in Construction. 111 (2020) , pp.103053. https://doi.org/10.1016/j.autcon.2019.103053.

[136] J. Irizarry, M. Gheisari, B.N. Walker, Usability Assessment of Drone Technology as Safety Inspection Tools, Journal of Information Technology in Construction (ITcon). 17 (2012) , pp.194-212.

[137] McKinsey & Company, The Next Normal in Construction, (2020), https://www.mckinsey.com/~/media/McKinsey/Industries/Capital%20Projects%20and%20Infrastructure/Our%20Insights/The%20next%20normal%20in%20construction/executive-summary_the-next-normal-in-construction.pdf,.

[138] S. Chuo, Simulation Modelling and Analysis of Impact of 3D Feedback Workflow on Prefabrication of Industrial Construction, (2020).

[139] J. Bae, S. Han, Vision-Based Inspection Approach using a Projector-Camera System for Off-Site Quality Control in Modular Construction: Experimental Investigation on Operational Conditions, Journal of Computing in Civil Engineering. 35 (2021) , pp.04021012.

[140] M. Safa, A. Shahi, M. Nahangi, C. Haas, H. Noori, Automating Measurement Process to Improve Quality Management for Piping Fabrication,Structures 3 (2015), pp. 71-80.

[141] M. Nahangi, T. Czerniawski, C.T. Haas, S. Walbridge, Pipe Radius Estimation using Kinect Range Cameras, Automation in Construction. 99 (2019) , pp.197-205. https://doi.org/10.1016/j.autcon.2018.12.015.

[142] B.A. Abu-Nabah, A.O. ElSoussi, Al Alami, Abed ElRahman K, Virtual Laser Vision Sensor Environment Assessment for Surface Profiling Applications, Measurement. 113 (2018) , pp.148-160.

[143] J. Guo, Q. Wang, J. Park, Geometric Quality Inspection of Prefabricated MEP Modules with 3D Laser Scanning, Automation in Construction. 111 (2020) , pp.103053.

[144] I. Carlbom, I. Chakravarty, D. Vanderschel, A Hierarchical Data Structure for Representing the Spatial Decomposition of 3-D Objects, IEEE Computer Graphics and Applications. 5 (1985), pp.24-31https://doi.org/10.1109/MCG.1985.276454.

[145] K.K. Liang, Efficient Conversion from Rotating Matrix to Rotation Axis and Angle by Extending Rodrigues' Formula, arXiv Preprint arXiv:1810.02999. (2018).

[146] D. Ioannou, W. Huda, A.F. Laine, Circle Recognition through a 2D Hough Transform and Radius Histogramming, Image and Vision Computing. 17 (1999) , pp.15-26.

[147] FARO, Accuracy Specifications for the Gage Arm, (2017), https://knowledge.faro.com/Hardware/Legacy-Hardware/Gage/Accuracy_Specifications_for_the_Gage_Arm,.

[148] Pipe Fabrication Institute, Fabricating Tolerances , (2000), https://fdocuments.net/document/pfi-es-03-2000.html,.

[149] M. Al-Adhami, S. Wu, L. Ma, Extended Reality Approach for Construction Quality Control, (2019).

[150] Y. Zhou, H. Luo, Y. Yang, Implementation of Augmented Reality for Segment Displacement Inspection during Tunneling Construction, Automation in Construction. 82 (2017) , pp.112-121.

[151] PTC, Vuforia: Market-Leading Enterprise AR,.

[152] S. Wold, K. Esbensen, P. Geladi, Principal Component Analysis, Chemometrics and Intelligent Laboratory Systems. 2 (1987) , pp.37-52.

[153] Kevin J Conner, Santosh Mathan, Apparatus and method for providing augmented reality for maintenance applications, (2015).

[154] Wolfgang Friedrich, Wolfgang Wohlgemuth, Operating and monitoring system utilizing augmented reality technology, (2000).

[155] Otmar Hilliges, David Kim, Shahram Izadi, David Moiyneaux, Stephen Edward Hodges, David Alexander Butler, Augmented reality with direct user interaction, (2017).

[156] R.H. Byrd, R.B. Schnabel, G.A. Shultz, A Trust Region Algorithm for Nonlinearly Constrained Optimization, SIAM Journal on Numerical Analysis. 24 (1987) , pp.1152-1170.

[157] Z. Xuan, G. Wei, Z. Ni, J. Zhang, Decoupling Offloading Decision and Resource Allocation Via Deep Reinforcement Learning and Sequential Least Squares Programming,International Conference on Communications and Networking in China (2020), pp. 554-566.

[158] J.H. Holland, Genetic Algorithms, Scientific American. 267 (1992) , pp.66-73.

[159] J. Fan, L. Ma, Z. Zou, A Registration Method of Point Cloud to CAD Model Based on Edge Matching, Optik. 219 (2020) , pp.165223.